TRANSPORTATION RESEARCH

RECORD

No. 1343

Soils, Geology, and Foundations

Rockfall Prediction and Control and Landslide Case Histories

A peer-reviewed publication of the Transportation Research Board

TRANSPORTATION RESEARCH BOARD
NATIONAL RESEARCH COUNCIL

NATIONAL ACADEMY PRESS
WASHINGTON, D.C. 1992

Transportation Research Record 1343
Price: $24.00

Subscriber Category
IIIA soils, geology, and foundations

TRB Publications Staff
Director of Publications: Nancy A. Ackerman
Senior Editor: Naomi C. Kassabian
Associate Editor: Alison G. Tobias
Assistant Editors: Luanne Crayton, Norman Solomon, Susan E. Gober
Production Coordinator: Karen W. McClain
Office Manager: Phyllis D. Barber
Production Assistant: Betty L. Hawkins

Printed in the United States of America

Library of Congress Cataloging-in-Publication Data
National Research Council. Transportation Research Board.

Rockfall prediction and control and landslide case histories.
p. cm. — (Transportation research record, ISSN 0361-1981; no. 1343)
ISBN 0-309-05206-8
1. Rockslides. 2. Landslides. I. Series.
TE7.H5 no. 1343
[QE599]
388 s—dc20
[551.3'07] 92-24222
CIP

Sponsorship of Transportation Research Record 1343

GROUP 2—DESIGN AND CONSTRUCTION OF TRANSPORTATION FACILITIES
Chairman: Charles T. Edson, New Jersey Department of Transportation

Soil Mechanics Section
Chairman: Michael G. Katona, Air Force Engineering and Service Center, Tyndall AFB

Committee on Soils and Rock Instrumentation
Chairman: John L. Walkinshaw, Federal Highway Administration, U.S. Department of Transportation
Loren R. Anderson, Richard J. Bathurst, Harold E. Beeston, Douglas A. Blankenship, Joseph A. Caliendo, Barry R. Christopher, Brian J. Dawes, Charles N. Easton, David J. Elton, Neil F. Hawks, Kenneth A. Jackura, W. Allen Marr, P. Erik Mikkelsen, Anthony Minnitti, Soheil Nazarian, Dawit Negussey, John L. Nieber, Garry W. Rhodes, A. J. Simmonds, Thomas C. Tonkins, Duncan C. Wyllie

Geology and Properties of Earth Materials Section
Chairman, Robert D. Holtz, University of Washington

Committee on Engineering Geology
Chairman: Jeffrey R. Keaton, Sergent Hauskins & Beckwith
Robert K. Barrett, William D. Bingham, Scott F. Burns, Jerome V. De Graff, Carol J. Hammond, Steve M. Lowell, Stanley M. Miller, Harry L. Moore, Stephen F. Obermeier, A. Keith Turner, Duncan C. Wyllie

Study Committee on Landslides: Analysis and Control
Chairman: A. Keith Turner, Colorado School of Mines
David M. Cruden, J. Michael Duncan, Robert D. Holtz, Jeffrey R. Keaton, Verne C. McGuffey, Victor A. Modeer, Jr., Robert L. Schuster, Tien H. Wu, Duncan C. Wyllie

FHWA Liaison Representative: John L. Walkinshaw
NRC Liaison Representative: Riley M. Chung

G. P. Jayaprakash, Transportation Research Board staff

Sponsorship is indicated by a footnote at the end of each paper. The organizational units, officers, and members are as of December 31, 1991.

Transportation Research Record 1343

Contents

Foreword

Rockfalls and landslides are responsible for significant damage to transportation facilities worldwide. In the United States alone, the damage to public and private facilities by landslides is estimated to be in the range of $1 billion to $2 billion a year. Methods of investigation, prediction, management, and control are therefore of major concern to engineers and geologists.

The papers included in this Record are based on results of recent studies on rockfalls and landslides which were conducted by researchers from state and federal agencies, academia, and the private sector. The first portion focuses on rockfall prediction and control and the second portion describes landslide case histories and includes discussions on environmental, socioeconomic, and technical aspects.

Abridgment

Reliability of Slopes: Incorporating Qualitative Information

J. C. SANTAMARINA, A. G. ALTSCHAEFFL, AND J. L. CHAMEAU

The transition from theoretical results to real results is often the critical step in the decisionmaking process of a geotechical engineer. The proposed method for the reliability analysis of slopes calculates the theoretical solution and then modifies it to account for qualitative information. The first step involves calculation of the probability of failure on the basis of available information from the idealized geotechnical structure. This theoretical probability is then modified by a quality factor to yield an actual probability of failure. Qualitative aspects are represented by verbal statements that are translated to belief/importance factors in the form of membership functions; the processing of this information is based on fuzzy logic. The results of corrected probabilities of failure are compared with experience-based predictions made by Lambe in his Terzaghi Oration at the Eleventh Conference of the International Society for Soil Mechanics and Foundation Engineering. Data from sociological studies and questionnaire-based measurements of risk acceptance are presented. The corrected probability of failure is then compared with the membership function of the acceptable risk to establish a measure of the urgency of repairs. The approach is implemented in a computerized decision support system incorporating extensive support information and recommendations.

In his Terzaghi Oration given at the Eleventh International Conference, Lambe presented a figure that relates probability of failure to factor of safety (*1*). It is not based on calculations, but a numerical representation of engineering judgment. It incorporates qualitative factors that relate to design, analysis, construction, and performance of a geotechnical system, such as the Amuay Project.

A method to incorporate qualitative information in the standard reliability analysis of slopes is presented. The approach separates the theoretical solution based on probability theory from the practical one, obtained from the theoretical solution by incorporating qualitative information by means of fuzzy set theory.

THEORETICAL SOLUTION

Nominal Factor of Safety

In common practice, the value of resistance selected for the analysis is lower than the mean resistance, whereas the reverse is true for the load. The selected values are not absolute lower and upper bounds, respectively, however; they are conservative estimates based on experience.

The conservative estimation of design parameters results in the calculation of a nominal factor of safety, FS_{nom}, which is smaller than the mean factor of safety FS_μ. Assuming normal distribution for the load L and resistance R, the relation between FS_μ and FS_{nom} is

$$FS_{nom} = FS_\mu \left(\frac{1 - \delta_R V_R}{1 + \delta_L V_L} \right) \quad (1)$$

where

V = coefficient of variation, and
δ = the standardized value that allows for a certain percentile under the curve (e.g., for the 90th-percentile load and resistance, $\delta_R = \delta_L = 1.3$).

The coefficient of variation for the resistance is about 0.2 when effective stress analysis is applied to a slope in homogeneous media and it is higher for soils with some cementation. The coefficient of variation for the resistance varies between 0.15 and 0.25 for normal load conditions. On the basis of this equation, the ratio between the two factors of safety is about 1.5 to 2.0 in common slope stability practice.

Theoretical Probability of Failure

If the safety margin, SM, is defined as the difference between resistance R and load L, the probability of failure p_f is the probability of $SM \leqq 0$. Assuming normal distributions for both R and L, p_f is

$$p_f = \Phi \left(\frac{FS_\mu - 1}{V_R^2 FS_\mu^2 + V_L^2} \right) \quad (2)$$

where Φ = the standard normal distribution. Other distributions may be assumed without affecting the rest of the analysis.

ADJUSTED PROBABILITY OF FAILURE

The consideration of variables not included in the theoretical analysis is usually viewed with apprehension because of their vague and qualitative nature. To circumvent this problem,

J. C. Santamarina, Department of Civil Engineering, University of Waterloo, Waterloo, Ontario N21 3G1, Canada. A. G. Altschaeffl, Department of Civil Engineering, Purdue University, West Lafayette, Ind. 47907. J. L. Chameau, Department of Civil Engineering, Georgia Institute of Technology, Atlanta, Ga. 30332.

qualitative information is included in the analysis by means of fuzzy sets (*2*). Although this is not the only possible method to incorporate qualitative information, it was found convenient for the problem considered.

Qualitative aspects are represented by verbal statements that are transformed to belief/importance factors on a selected scale. The result of this analysis is a fuzzy adjusted probability. If the result of the theoretical probability of failure is expressed as

$$p_f = 10^{-\beta} \tag{3}$$

then the adjusted value may be given in the form (*3*)

$$p_f^c = 10^{-\beta\alpha} \tag{4}$$

where α is a correction factor of qualitative parameters not considered in the theoretical analysis. When qualitative aspects indicate very poor conditions of the project, α may be a small number. In the extreme case, $\alpha = 0$, and the system has an adjusted probability of failure of 1.0. In the opposite case, when all aspects of the project are extremely good, α approaches 1.0 and the adjusted probability of failure p_f^c remains equal to the theoretical value p_f.

Fuzzy Set Representation

The α correction factor is evaluated using fuzzy sets (*4*). A unique representation called supportless fuzzy sets is used in this analysis. It consists of a list of membership values defined at discrete points.

Stacks of Fuzzy Constraints

Six categories were selected to represent the possible levels for quality of the project: excellent operation, sound operation, intermediate operation, approximate operation, no-rational operation, and very good service conditions. The last category allows for the compensatory effect of very good performance and maintenance on the lesser quality of other parameters.

Each category is defined as a group of constraints that restrict the conditions of a project must have to belong to such a category. These dimensions and their constraints result in a data structure referred to as the stack of contraints. The stack of constraints for very good service conditions follows:

Qualifications of the engineer-designer
(0.4 0.8 1.0 0.9 0.4 0.2 0.1)
Extent/quality of geologic assessment
(0.4 0.8 1.0 0.9 0.4 0.2 0.1)
Quality of available data
(0.2 0.8 1.0 0.9 0.2 0.1 0.0)
Quality of design method
(0.4 0.8 1.0 0.9 0.4 0.2 0.1)
Completeness of the design of the structure
(0.0 0.1 0.2 0.7 1.0 1.0 1.0)
Importance of design errors or emissions
(0.2 0.8 1.0 0.9 0.2 0.1 0.0)
Contractor's prior record
(0.4 0.8 1.0 0.9 .04 0.2 0.1)
Supervision during construction
(0.2 0.8 1.0 0.9 0.2 0.1 0.0)
Quality of field controls during construction
(0.4 0.8 1.0 0.9 0.4 0.2 0.1)
Importance of construction errors
(0.2 0.8 1.0 0.9 0.2 0.1 0.0)
Difficulties during construction
(0.4 0.8 1.0 0.9 0.4 0.2 0.1)
Monitoring program
(0.0 0.0 0.0 0.2 0.5 0.8 1.0)
In-service inspection
(0.0 0.0 0.0 0.2 0.5 0.8 1.0)
Manfunctions during the life of the structure
(0.0 0.0 0.0 0.2 0.5 0.8 1.0)
Maintenance program
(0.0 0.0 0.0 0.2 0.5 0.8 1.0)

To determine the similarity between a given Category A and the project, the characteristics of the project are compared with those constraints that represent Category A. Comparison at the level of each dimension i is based on the filtering operation, which results in a similarity value s_i (*5*),

$$S_i^A = \frac{\text{Cardinality } (mf_i^{proj} \cap mf_i^A)}{\text{Cardinality } (mf_i^{proj})} \tag{5}$$

where mf = membership function. The overall similarity between the project and Category A is the minimum of all individual similarities S_i^A.

ACCEPTABLE PROBABILITY OF FAILURE

The following parameters were found to determine the level of acceptable risk in the context of slope stability (*6–8*):

- Loss of human life,
- Potential economic loss,
- Relative cost of lowering the probability of failure (certain) with respect to the expected cost of postfailure repairs (probable),
- Technical and economic capacity to implement repairs,
- Unique structure, or one of a group,
- Existing or to-be-constructed structure,
- Temporary or permanent,
- Remaining service life,
- Type and importance of service, and,
- Effect on lifelines.

Different sources of information were used to determine the levels of acceptable p_f for slopes. Table 1 summarizes the results of a questionnaire answered by the engineers involved in the reliability of existing slopes. These data support more general results obtained by the authors from two different groups of assessors, including professors and students from a variety of engineering branches. In Study 1, 22 assessors evaluated the acceptability of a generic failure (*4*), whereas in Study 2, 8 assessors evaluated the acceptability of the failure of temporal and permanent structures of either low or high

TABLE 1 SLOPE STABILITY—ACCEPTABLE PROBABILITY OF FAILURE

Conditions	P_f
Unacceptable in most cases	less than 10^{-1}
Temporary structures no potential life loss low repair cost	10^{-1}
Nil consequences of failure high cost to lower Pf i.e., bench slope, open pit mine	1 to 2 10^{-1}
Existing slope of riverbank at docks available alternative docks repairs can be promptly done do-nothing: attractive idea	5 10^{-2}
To-be-constructed; same condition	less than 5 10^{-2}
Slope of riverbank at docks no alternative docks pier shutdown threatens operations	1 to 2 10^{-2}
Low consequences of failure repairs can be done when time permits repair cost < cost to lower Pf	10^{-2}
Existing large cut interstate highway	1 to 2 10^{-2}
To-be-constructed; same condition	less than 10^{-2}
Acceptable in most cases except if lives may be lost	10^{-3}
Acceptable for all slopes	10^{-4}
Unnecessarily low	10^{-5} or lower

importance. The results of Study 2 show that temporal and low importance systems are represented by the same curve, as are the results for permanent and high importance systems. Membership functions from these two studies are shown in Figure 1. These results are in agreement with observations by Ashby in the environmental field (*9*).

THE PROGRAM SLOPE

SLOPE consists of seven blocks.

Block 1: Input of Preliminary Information

Block 2: Verification of the Calculated Factor of Safety

The purpose of this part of the program is to aid the user in assessing the validity of the stability analysis. In response, the system may recommend that the user review the analysis before proceeding. In this part, questions will address the following design decisions.

- Selection of strength parameters: short and long term, effective stress or total stress analysis, brittleness, heterogeneity and strain compatibility, in situ and induced pore pressure, variability of soil parameters, and tests' scale effects.
- Possibility of weak seams (historical evidence or resulting from in situ testing).
- Formation of tension cracks and buildup of pore pressure.
- Selection of failure surface.
- Potential effects of erosion.
- Other loads.

Block 3: Selection of Acceptable Risk

This section gathers external information about the project in order to determine the acceptable risk. The user's quali-

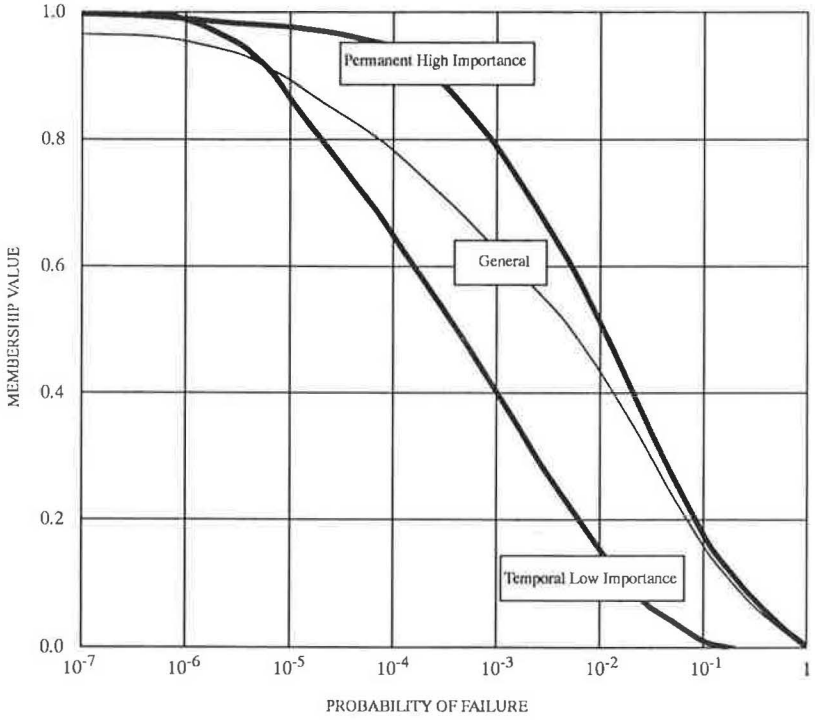

FIGURE 1 Membership functions for acceptable probability of failure.

tative answer is translated into a fuzzy set and compared with the corresponding constraint in three stacks. Each stack represents a different level of acceptable risk: very low, intermediate, and very high. There is a membership function for acceptable risk associated with each stack. Once the similarity between the project and each stack is established, S_i, the membership function for the acceptable risk, is calculated. The computational formula is shown in Equation 6.

$$\nu = \nu_{vl} * S_{vl}^2 + \nu_{in} * S_{in}^2 + \nu_{vh} * S_{vh}^2 \quad (6)$$

where

ν_{vl} = very low risk,
ν_{in} = intermediate risk, and
ν_{vh} = very high risk.

This approach allows for compensatory effects and gives emphasis to the best-matched category.

Block 4: Calculation of Theoretical Probability of Failure

The calculation of the mean factor of safety FS_μ follows Equation 1. The theoretical probability of failure is then calculated by means of a polynomial approximation.

Block 5: Selection of Membership Function for α Correction

The user's qualitative answers are translated into fuzzy sets and compared with the corresponding constraint in each of the stacks. Each stack or category has an associated membership function for the value of α (α ranges between 0.0 and 1.0, and is discretized every 0.1). The final similarity value of each category is used to calculate the membership function for the project, following the same approach used to determine the membership function for acceptable risk (Equation 6).

Blocks 6 and 7: Adjusted Probability of Failure and Urgency of Repairs

The adjusted p_f is obtained by the fuzzy multiplication of β and α, resulting in a non-crisp value p_f^c. Finally, p_f^c is filtered through the membership function for the acceptable risk to obtain a final acceptability index AI (a crisp number):

$$AI = \frac{\text{Cardinality } (mf_{\alpha\beta} \cap mf_{\text{risk}})}{\text{Cardinality } (mf\alpha\beta)} \quad (7)$$

The complement of Ai is a measure of the need for immediate repairs, in other words, an urgency index UI.

RESULTS AND OBSERVATIONS

Results obtained with this type of analysis were compared with corrections proposed by Lambe (*1*), observing very similar trends. Additional results that further support the importance of qualitative variables on performance and emphasize the need to design for low theoretical probability of failure are shown in Figure 2. For a particular design with a central factor of safety of 2.0 and a theoretical p_f less than 10^{-5}, a project of intermediate quality will bring the adjusted probability of failure to a value greater than 10^{-3} (note that low coefficients of variation are assumed). Social limits on the probability of failure fuzzified from Ashby (*9*) and membership values for acceptable probability of failure were added to Figure 2. It can be concluded that in order to obtain an

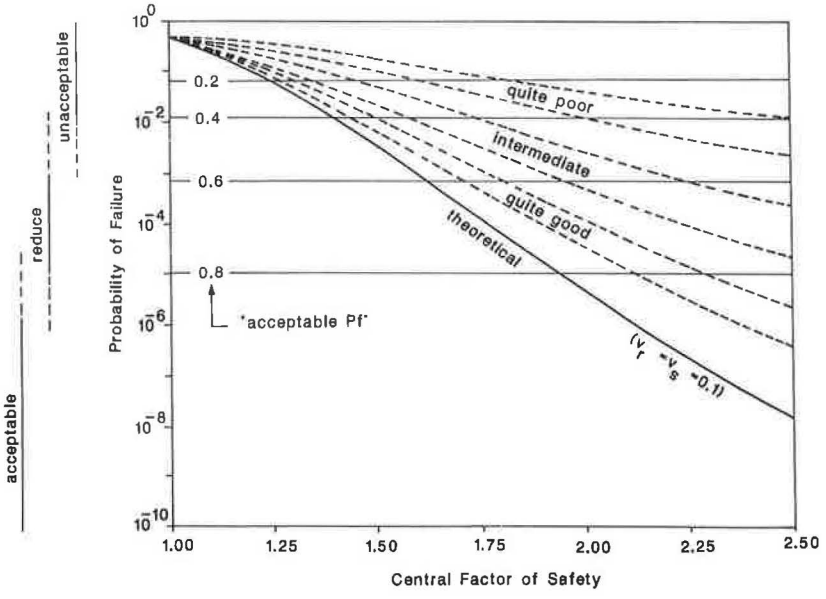

FIGURE 2 Results and implications.

adjusted probability of failure of about 10^{-4} with standard practice, a minimum common practice *FS* of about 1.6 to 1.7 is needed.

ACKNOWLEDGMENT

This study was supported in part by the EXXON Research and Engineering Company.

REFERENCES

1. W. T. Lambe. Amuay Landslides. *Proc., 11 ICSMFE*, San Francisco, Golden Jubilee Volume, 1985, pp. 137–158.
2. H.J. Zimmerman. *Fuzzy Sets Theory and Its Applications*. Kluwer-Nijhoff, 1985.
3. C.B. Brown. The Merging of Fuzzy and Crisp Information. *Journal of Engineering Mechanics Division*, ASCE, Vol. 106, 1980, pp. 123–133.
4. J. C. Santamarina and J. L. Chameau. Membership Functions II: Trends in Fuzziness and Implications. *International Journal of Approximate Reasoning*, Vol. 1, 1987, pp. 303–317.
5. J. C. Santamarina and J. L. Chameau. Fuzzy Windows and Classification System. *International Journal of Man Machine Studies*, Vol. 32, 1990, pp. 187–201.
6. A. Casagrande. Role of the Calculated Risk in Earthwork and Foundation Engineering. *Journal of Soil Mechanics Division*, ASCE, Vol. 91, 1965, pp. 1–40.
7. B. Fischhoff, S. Lichtenstyein, P. Slovic, S. L. Derby, and R. L. Keeney. *Acceptable Risk*. Cambridge University Press, 1981.
8. O. G. Ingles. The Perception of Risk by Australian Civil Engineers and Its Implication in Design. *Proc., Symposium on Risk Assessment in Geomechanics*, Institution of Civil Engineers, Australia, 1982.
9. L. Ashby. The Risk Equations—The Subjective Side of Assessing Risks. *New Scientist*, May 1977, pp. 398–400.

Publication of this paper sponsored by Committee on Engineering Geology.

Rockfall Hazard Rating System

LAWRENCE A. PIERSON

Many miles of highway pass through terrain with adjacent rock slopes that are subject to rockfall, which is due in part to construction practices in the past that relied on overly aggressive excavation techniques. Although these techniques facilitated removal of broken material, they commonly resulted in slopes more prone to rockfall. The Rockfall Hazard Rating System (RHRS) is intended to be a proactive tool that allows transportation agencies to rationally address their rockfall hazards instead of simply reacting to rockfall accidents. The RHRS provides a defensible, standardized way to spend the limited construction funds available by numerically differentiating the apparent risk at rockfall sites. The Oregon Department of Transportation (ODOT) began developing the RHRS in 1984. Funding from an FHWA-sponsored Highway Planning and Research (HPR) grant allowed ODOT to complete development of the system and test it at over 3,000 sites. Much of the RHRS's rating is subjective. Proper training in RHRS application is necessary to ensure the consistency of ratings between different raters. The responsibility for slope evaluations and design concepts should rest with experienced individuals. ODOT's staff of engineering geologists have demonstrated that reasonable and repeatable slope ratings can be achieved.

Transportation agencies are expected to provide a safe highway system for the public. This is not a simple task to accomplish, and it is made more difficult when highways pass through terrain requiring highway rock cuts. In mountainous states such as Oregon, many miles of roadway pass through steep terrain where rock slopes adjacent to the highway are common. Some of these man-made slopes are over 100 ft high and many are situated near the base of rugged natural slopes extending hundreds of feet further upslope, creating an inherent rockfall potential. This potential is compounded by the way our highway systems have evolved. Until recently, it was standard construction practice to use overly aggressive blasting and ripping techniques to construct rock slopes. This construction practice facilitated excavation and frequently resulted in slopes prone to rockfall. Where rockfall conditions exist, agencies are faced with the difficult task of reducing the risk of rockfall.

Oregon Department of Transportation (ODOT) management and legal counsel recognized the value of having a systematic way to set rockfall project priorities and allocate the limited repair funds. To be effective, the program would include an inspection of all rock slopes along the highway system to identify where rockfall would most likely affect the roadway. Once identified, these sections would be rated relative to each other by trained personnel to determine which ones presented the greatest risk. A rating system was needed to accomplish this.

Oregon Department of Transportation, Highway Division, 800 Airport Road, SE, Salem, Oreg. 97310

EVOLUTION OF ROCKFALL HAZARD RATING SYSTEM (RHRS)

Oregon began to discuss the need for an RHRS in 1984. As part of an initial literature search on the subject, a study by C. O. Brawner and Duncan Wyllie (*1*) was reviewed. It contained rating criteria and a scoring method that grouped rockfall sections into either A, B, C, D, or E categories based on the potential and expected effect of a rockfall event. ODOT adopted a similar assessment approach to the RHRS as part of the preliminary rating or rockfall areas.

In a subsequent study, Wyllie (*2*) outlined a more detailed rating procedure for prioritizing rockfall sites. Wyllie's method included specific categories for evaluation and scoring using an exponential scoring system. This became the prototype for Oregon's RHRS. The rating sheet format and the exponential scoring system were adopted. Some of the categories in the RHRS are similar, and others are new. All categories have been modified on the basis of experience in developing and applying the RHRS statewide over the past several years. Detailed narratives of the rating criteria were added to promote consistent application.

The final phase of RHRS development began in July 1989 when ODOT was selected to perform the HPR pooled-fund study. The principal objective of the study was to complete the development of an effective RHRS. Through full-state implementation, the RHRS was tested at over 3,000 sites. The narratives were finalized and forms and rating aids were developed. In order to streamline implementation of the system for other agencies, this information was documented in the RHRS User's Manual (*3*).

DESCRIPTION OF SYSTEM

The RHRS is a six-step process that allows agencies to actively manage the rock slopes along its highway system by providing a rational way to make informed decisions on where and how to spend construction funds. The process requires a greater commitment and focus on the rock slope issue than is commonly the case for many agencies. This commitment consists of additional working hours and dollars to complete the initial survey, to update the data base regularly, and to develop remedial programs aimed at reducing the rockfall risk at the worst sites. In addition, a properly trained and experienced staff is needed to perform the slope evaluations and to develop remedial designs.

The RHRS contains two phases of inspection: the preliminary rating phase, which is a part of the slope survey, and the detailed rating phase. This staged approach is the most efficient way to implement the RHRS in situations where an agency has responsibility for many slopes with a broad range of rockfall potential.

Slope Survey

The slope survey is an essential feature of the RHRS that allows an agency to accurately determine the number and location of its rockfall sites. The best way to approach the survey is without any preconceived notions of how many sites there are or where the most hazardous sites are located.

Accurate delineation of the rockfall section is important. For the RHRS, a rockfall section is defined as any uninterrupted slope along a highway where the level and occurring mode of rockfall are the same. Grouping separate cut slopes into one long section will diminish the value and the flexibility of the resulting data base. Grouping can occur later when project limits are defined during the project development process.

The maintenance person who is most knowledgeable about a section's rockfall history and the associated maintenance activities should accompany the rater because the past rockfall activity is an important indicator of what to expect in the future. As a better data base of rockfall occurrences is developed, more accurate conclusions for the rockfall potential can be made. It is important during this process to document the rockfall maintenance information, which is an important element of the preliminary rating.

Preliminary Rating

The purpose of the preliminary rating (Figure 1) is to group the rockfall sections inspected during the slope inventory into three broad, more manageable categories. Without this step, many additional hours would be spent applying the detailed rating at sites with only a low to moderate chance of producing a hazardous condition. This rating is a subjective evaluation of the rockfall potential and requires judgments by experienced, insightful personnel.

The RHRS is primarily concerned with the rockfall potential at a site. The criterion of the estimated potential for rock on the roadway is therefore the controlling element of this rating. Where clarification is needed, the historical rockfall activity is used as a modifier of the preliminary rating.

A C rating means either that it is unlikely that a rock will fall at this site or that if one should fall, it is unlikely that it will reach the roadway—the risk that a hazardous situation will occur is nonexistent to low. As the rating increases to a B, the risk ranges from low to moderate. For A-rated sections, the risk ranges from moderate to high. Little is gained by adding intermediate categories. Consistency is most important. The ability and the comfort level in making these decisions improve with experience. All rockfall sections that receive an A rating should be photographed. These photographic records are useful when preliminary design concepts are discussed and especially useful for discerning changes in the slope that occur between reviews.

CLASS / CRITERIA	A	B	C
ESTIMATED POTENTIAL FOR ROCK ON ROADWAY	HIGH	MODERATE	LOW
HISTORICAL ROCKFALL ACTIVITY	HIGH	MODERATE	LOW

FIGURE 1 Preliminary rating system.

The preliminary evaluation is a critical step in the RHRS process, especially when there are a large number of slopes to consider. Initially, only the A-rated sections should be evaluated with the detailed rating system. This will economize the effort while directing it toward the most critical areas. The B-rated sections should be evaluated as time and funding allow. The C-rated sections receive no further attention and therefore are not included in the RHRS data base.

Detailed Rating System

Detailed rating, shown in Figure 2, is the third step in the RHRS. The detailed rating includes 10 categories that, when evaluated, scored, and totaled, allow an agency to numerically differentiate rock slopes from the least to the most hazardous. Slopes with higher scores present the higher risk. These 10 categories represent the significant elements of a rockfall section that contribute to the overall hazard. The four columns of criteria on the right correspond to logical breaks in the increasing risk associated with each category. Accordingly, the scores above each column increase from left to right exponentially from 3 to 81 points. An exponential system provides a rapid increase in score that distinguishes the more hazardous sites. The set scores are representative of a continuum of points ranging from 1 to 100. Using a continuum of points instead of only the set points listed at the top of each column allows the rater flexibility in evaluating the relative impact of conditions that are extremely variable.

To assist with scoring, the RHRS User's Manual (*3*) includes a scoring graph for each category. A sample graph for slope height is shown in Figure 3. The curve on the graph is the plot of the function $y = 3^x$, which defines the exponential scoring system used for all categories. The graph relates the category evaluation to an appropriate score. Even with subjective categories such as ditch effectiveness, the graph is quite useful in assigning a score to a condition that falls somewhere between the described benchmarks. Exact scores can be tabulated for the measurable categories by calculating the value of the exponent x of the function $y = 3^x$. The formulas that yield the exponent values are presented in Table 1.

Before decisions can be made on how to score a rockfall section, the criteria for each category must be well understood and carefully considered. To aid in understanding, narratives for each category are included. These narratives are based on extensive field testing of the system. Some categories require a subjective evaluation, whereas others can be directly measured and then scored. Along with the following category descriptions, sample ratings are provided.

Slope Height

Slope height represents the vertical height of the slope, not the slope distance. Rocks on high slopes have more potential energy than those on lower slopes, and therefore present a greater hazard and receive a higher rating. This measurement, obtained using the relationships shown in Equation 1 (Figure

CATEGORY			RATING CRITERIA AND SCORE			
			POINTS 3	POINTS 9	POINTS 27	POINTS 81
SLOPE HEIGHT			25 FEET	50 FEET	75 FEET	100 FEET
DITCH EFFECTIVENESS			Good catchment	Moderate catchment	Limited catchment	No catchment
AVERAGE VEHICLE RISK			25% of the time	50% of the time	75% of the time	100% of the time
PERCENT OF DECISION SIGHT DISTANCE			Adequate sight distance, 100% of low design value	Moderate sight distance, 80% of low design value	Limited sight distance, 60% of low design value	Very limited sight distance 40% of low design value
ROADWAY WIDTH INCLUDING PAVED SHOULDERS			44 feet	36 feet	28 feet	20 feet
GEOLOGIC CHARACTER	CASE 1	STRUCTURAL CONDITION	Discontinuous joints, favorable orientation	Discontinuous joints, random orientation	Discontinuous joints, adverse orientation	Continuous joints, adverse orientation
		ROCK FRICTION	Rough, irregular	Undulating	Planar	Clay infilling, or slickensided
	CASE 2	STRUCTURAL CONDITION	Few differential erosion features	Occasional differential erosion features	Many differential erosion features	Major differential erosion features
		DIFFERENCE IN EROSION RATES	Small difference	Moderate difference	Large difference	Extreme difference
BLOCK SIZE / VOLUME OF ROCKFALL/EVENT			1 Foot / 3 cubic yards	2 Feet / 6 cubic yards	3 Feet / 9 cubic yards	4 Feet / 12 cubic yards
CLIMATE AND PRESENCE OF WATER ON SLOPE			Low to moderate precipitation; no freezing periods; no water on slope	Moderate precipitation or short freezing periods or intermittent water on slope	High precipitation or long freezing periods or continual water on slope	High precipitation and long freezing periods or continual water on slope and long freezing periods
ROCKFALL HISTORY			Few falls	Occasional falls	Many falls	Constant falls

FIGURE 2 Summary sheet of the Rockfall Hazard Rating System (RHRS).

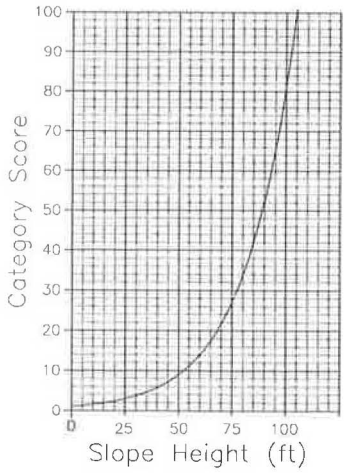

FIGURE 3 Sample scoring graph.

4), is to the highest point from which rockfall is expected, including the natural slope above the cut slope. The angles α and β and the distance X must be recorded. The angles can be measured with either a Brunton compass or a clinometer. Significant error can be introduced by careless measurement; averaging several measurements of these angles should minimize the problem. To further minimize error, the elevations of the points that define the distance X should be as equal as possible. The designation edge of pavement (EP) should be used only as a general guide. However, this measurement will also be useful in rating Category 5: Roadway Width.

Discussion The purpose of the 10 categories is to allow an agency to distinguish between rockfall sections with a relative rating. The slope height category is one that should be adjusted to fit local conditions in order to provide adequate score separation. In Oregon, all slopes that are 105 ft high or greater receive a score of 100 points.

TABLE 1 EXPONENT FORMULAS

Category	Formula (x)
Slope Height	$\frac{\text{Slope Ht. (ft.)}}{25}$
Average Vehicle Risk	$\frac{\%\ \text{Time}}{25}$
Sight Distance	$\frac{120 - \%\ \text{Decision Sight Dist.}}{20}$
Roadway Width	$\frac{52 - \text{Roadway Width (ft.)}}{8}$
Block Size	Block Size (ft.)
Volume	$\frac{\text{Volume (cu. ft.)}}{3}$

Sample The determined slope height is 40 ft. Using the scoring graph shown in Figure 3, this corresponds to a slope height score of 6 points.

Ditch Effectiveness

The effectiveness of a ditch is measured by its ability to restrict falling rock from reaching the roadway. The rater should consider several factors in estimating ditch effectiveness: (a) slope height and angle; (b) ditch width, depth, and shape; (c) anticipated volume of rockfall per event; and (d) impact of slope irregularities (launching features) on falling rocks. Evaluating the effect of slope irregularities is especially important because they can completely negate the benefits expected from a fallout area. Valuable information on ditch performance can be obtained from maintenance personnel. Scoring should be consistent with the following descriptions:

- **Good catchment, 3 points**—all or nearly all falling rocks are retained in the catch ditch.
- **Moderate catchment, 9 points**—falling rocks occasionally reach the roadway.
- **Limited catchment, 27 points**—falling rocks frequently reach the roadway.
- **No catchment, 81 points**—no ditch or totally ineffective ditch. All or nearly all falling rocks reach the roadway.

Sample The slope is 40 ft high and is cut on a 0.25:1 slope. The existing ditch is narrow, approximately 6 ft wide. Halfway up the slope is an irregular bench about 2 ½ ft wide that slopes toward the highway at about 60 degrees. The majority of the rockfall originates from the upper third of the slope. Falling rocks tend to stay in the ditch unless they hit the intermediate slope bench, which causes much of the rock to be directed onto the paved roadway. This is apparent from the distressed nature of the pavement that has been damaged by rockfall impacts. The maintenance person indicated that regular road patrols are necessary to keep the roadway clear. Because of the slope irregularity, the ditch provides limited catchment, and a score of 70 points is assigned.

Average Vehicle Risk (AVR)

AVR measures the percentage of time that a vehicle will be present in the rockfall hazard zone. The percentage is obtained by using a formula as shown in Equation 2, based on slope length, average daily traffic (ADT), and the posted speed limit at the site. A rating of 100 percent means that on average a car will be within the defined rockfall section 100 percent of the time. Where high ADTs or longer slope lengths exist, values greater than 100 percent will result and this means that at any particular time more than one car is present within the measured section. The result directly relates to the significance of the route and the potential hazard by approximating the likelihood of a vehicle's being present and thus being involved in a rockfall incident.

$$\frac{\text{ADT (cars/day)} \times \text{slope length (miles)} / 24\ \text{(hours/day)}}{\text{Posted speed limit (mph)}} \times 100\% = \text{AVR} \qquad (2)$$

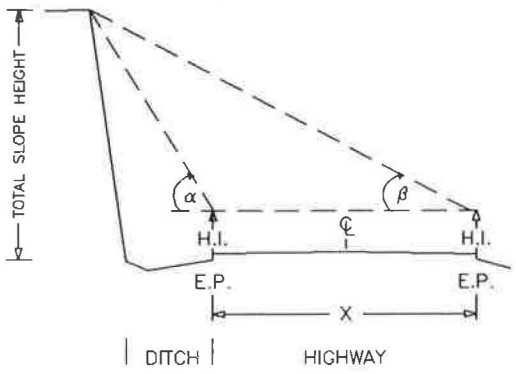

$$\text{TOTAL SLOPE HEIGHT} = \frac{(X)\ \sin\alpha \cdot \sin\beta}{\sin(\alpha - \beta)} + \text{H.I.} \qquad (1)$$

Where: X = distance between angle measurements.
H.I. = height of the instrument.

FIGURE 4 Slope height diagram.

Sample Based on an ADT of 5,200 vehicles per day, a slope length of 0.09 mil, and a posted speed limit of 30 mph, the calculated AVR is 65 percent. This correlates to a score of 17 points.

Percent of Decision Sight Distance

The decision sight distance (DSD) is the length of roadway (in feet) that a driver must have to make a complex or instantaneous decision. The DSD is critical when obstacles on the road are difficult to perceive or when unexpected or unusual maneuvers are required. Sight distance is the shortest distance along a roadway for which a 6-in. object is continuously visible to the driver. Normally an object will be most obscured when it is located just beyond the sharpest part of a curve. The sight distance can change appreciably throughout a rockfall section. Horizontal and vertical highway curves, along with obstructions such as rock outcrops and roadside vegetation, can severely limit a driver's ability to notice a rock in the road. The DSDs recommended by the American Association of State Highway and Transportation Officials (AASHTO) are presented in Table 2. The relationships between DSD and the posted speed limit were modified from Table III-3 of AASHTO's *Policy on Geometric Design of Highways and Streets* (*4*). The distances in Table 2 represent the low design value and the speed limit posted for the rockfall section should be used.

Once determined, these two values can be substituted into Equation 3 to calculate the percent of DSD:

$$\frac{\text{Actual sight distance}}{\text{Decision sight distance}} \times 100\% = \%\ \text{DSD} \qquad (3)$$

Sample The posted speed limit is 30 mph for a curved section of highway. The recommended sight distance for this speed is 450 ft. The actual sight distance is impaired by the rock slope on the inside of the curve in conjunction with a series of power poles and roadside vegetation. The measured sight distance is 315 ft. Substituting these values into the formula, the percent of DSD is 70, which correlates to a score of 16 points.

Roadway Width

Roadway width is measured perpendicular to the highway centerline from edge of pavement to edge of pavement (EP to EP). This measurement represents the available maneuvering room to avoid a rockfall, and should be the minimum width when roadway width is not constant. On divided roadways only the paved portion available to the driver should be measured.

TABLE 2 DECISION SIGHT DISTANCE

Posted Speed Limit (mph)	Decision Sight Distance (ft)
25	375
30	450
35	525
40	600
45	675
50	750
55	875
60	1,000
65	1,050

Sample The paved roadway includes two 12-ft lanes, a 2-ft shoulder adjacent to the cut slope, and a 4-ft shoulder on the opposite side for a total of 30 ft, which correlates to a score of 21 points.

Geologic Character

A slope's geologic conditions are evaluated with this category. Since the conditions that cause rockfall generally fit into two categories, Case 1 and Case 2 rating criteria have been developed. Case 1 is for slopes where joints, bedding planes, or other discontinuities are the dominant structural features. Case 2 is for slopes where differential erosion or oversteepening is the dominant condition. The rater should use the case that best fits the slope. If both situations are present and it is unclear which dominates, both are scored but only the worst case (highest score) is used in the rating.

Case 1: Structural Condition "Adverse" as used here involves considering such characteristics as rock friction angle, joint filling, and the effects of water, if present, as well as the joint's spatial relationship to the slope. Adverse joints are those that allow block, wedge, planar, or toppling failures. "Continuous" refers to joints longer than 10 ft.

- **Discontinuous joints, favorable orientation, 3 points**—slope contains jointed rock with no adversely oriented joints, bedding planes, etc.
- **Discontinuous joints, random orientation, 9 points**—slope contains randomly oriented joints creating a variable pattern. The slope is likely to have some scattered blocks with adversely oriented joints but no dominant adverse pattern is present.
- **Discontinuous joints, adverse orientation, 27 points**—rock slope exhibits a prominent joint pattern, bedding plane, or other discontinuity with an adverse orientation. These features have less than 10 ft of continuous length.
- **Continuous joints, adverse orientation, 81 points**—rock slopes exhibits a dominant joint pattern, bedding plane, or other discontinuity with an adverse orientation and more than 10 ft long.

Case 1: Rock Friction Rock friction directly affects the potential for a block to move relative to another. Friction along a joint, bedding plane, or other discontinuity is governed by the macro- and microroughness of the surfaces. Macroroughness is the degree of undulation of the joint relative to the direction of possible movement. Microroughness is the texture of the surface. The rockfall potential is greater in areas where joints contain highly weathered or hydrothermally altered products, where movement has occurred causing slickensides or fault gouge to form, where open joints dominate the slope, or where joints are water filled. Noting the

failure angles from previous rockfalls on a slope can aid in estimating general rock friction along discontinuities.

- **Rough, irregular, 3 points**—the surface of the joints is rough and the joint planes are irregular enough to cause interlocking. This macro- and microroughness provide an optimal friction situation.
- **Undulating, 9 points**—macroroughness but without the interlocking ability.
- **Planar, 27 points**—macrosmooth and microrough joint surfaces. Friction is derived strictly from the roughness of the rock surface.
- **Clay infilling, or slickensides, 81 points**—low-friction materials, such as clay and weathered rock, separate the rock surfaces, negating any micro- or macroroughness of the joint planes. Slickensided joints also have a very low friction angle and belong to this category.

Case 2: Structural Condition Case 2 is used for slopes in which differential erosion or oversteepening is the dominant condition leading to rockfall. Because rockfall is caused by a loss of support either locally or throughout the slope, erosion features such as oversteepened slopes, unsupported rock units, or exposed resistant rocks on a slope may eventually lead to a rockfall event. Common slopes that are susceptible to this loss of support are layered units containing easily weathered rock that erodes, undermining more durable rock; talus slopes; and highly variable units such as conglomerates, mudflows, rock/soil slopes, etc., that weather and allow resistant rocks and blocks to fall as the matrix material is eroded.

- **Few differential erosion features, 3 points**—minor differential erosion features that are not distributed throughout the slope.
- **Occasional erosion features, 9 points**—minor differential erosion features that are widely distributed throughout the slope.
- **Many erosion features, 27 points**—differential erosion features that are large and numerous throughout the slope.
- **Major erosion features, 81 points**—severe cases such as dangerous erosion-created overhangs or significantly oversteepened soil/rock slopes or talus slopes.

Difference in Erosion Rates The rate of erosion on a Case 2 slope directly relates to the potential for a future rockfall event. As erosion progresses, unsupported or oversteepened slope conditions develop. The impact of the common physical and chemical erosion processes, as well as the effects of human actions, should be considered. The degree of hazard caused by erosion and also the score given this category should reflect how quickly the erosion is occurring; the size of rocks, blocks, or units being exposed; the frequency of rockfall events; and the amount of material released during the event.

- **Small difference, 3 points**—erosion features take many years to develop. Slopes that are near equilibrium with their environment are covered in this category.
- **Moderate difference, 9 points**—the difference in erosion rates allows erosion features to develop over a few years.
- **Large difference, 27 points**—the difference in erosion rates is such that noticeable changes in the slope develop annually.
- **Extreme difference, 81 points**—the difference in erosion rates allows rapid and continuous development of erosion features.

Sample The slope consists of basalt and there is a greater density of natural joints and blast-induced fractures in the upper part of the slope. The joints and fractures are the dominant structural features of the slope and therefore a Case 1 condition exists. The fracture pattern is random and the joints are discontinuous. On this basis the slope receives a structural condition score of 9 points.

Extensive hydrothermal alteration has occurred along the natural joints leaving a ¼-in. clay coating on many surfaces. The surfaces of the blast-induced fractures are fresh and undulating. Failure of blocks along the clay coatings creates unsupported slope conditions leading to other block failures. Because not all surfaces are clay-coated, a score of less than 81 points is appropriate and a score of 60 points is assigned.

Block Size or Volume of Rockfall per Event

If individual blocks are typical of the rockfall, the block size should be used for scoring. If a mass of blocks tends to be the dominant type of rockfall, the volume per event should be used. A decision on which one to use can be determined from the maintenance history or estimated from observed conditions when no history is available. This measurement will also be beneficial in determining remedial measures.

Sample The rockfalls tend to be individual blocks. The block size is consistently in the 3½-ft size range. A block size score of 47 points is determined.

Climate and Presence of Water on Slope

Water and freeze-thaw cycles contribute to the weathering and movement of rock materials. If water is known to flow continually or intermittently from the slope, the slope is rated accordingly. Areas receiving less than 20 in. per year are low-precipitation areas. Areas receiving more than 50 in. per year are considered high-precipitation areas. The impact of freeze-thaw cycles can be interpreted from knowledge of the freezing conditions and their effects at the site.

The rater should note that the 27-point category is for sites with long freezing periods or water problems such as high precipitation or continually flowing water. The 81-point category is reserved for sites that have both long freezing periods and one of the two extreme water conditions.

Discussion Information on average temperatures and length of freezing periods can be obtained from National Oceanic and Atmospheric Administration (NOAA) climatological publications (5). The criteria used for this category should

be adjusted to fit local conditions to ensure proper score separation.

Sample This area receives 60 in. of precipitation annually and experiences severe winter conditions for 3 to 4 months per year. Water on the slope is not an issue. A score of 81 points is given because of the heavy rainfall and long freezing periods.

Rockfall History

Historical information is best obtained from the maintenance personnel responsible for the slope because they directly represent the known rockfall activity at the site. There may be no history available at newly constructed sites or where documentation practices are poor. The maintenance cost at a site may be the only information that reflects the rockfall activity. Historical information is an important check on the potential for future rockfalls. If the score given a section does not compare with the rockfall history, a review of the rating is advisable.

- **Few falls, 3 points**—rockfalls only occur a few times a year or less, or only during severe storms. This category is also used if no rockfall history data are available.
- **Occasional falls, 9 points**—rockfall occurs regularly and can be expected several times a year and during most storms.
- **Many falls, 27 points**—typically rockfall occurs frequently during a certain season, such as the winter or spring wet period, or the winter freeze-thaw, etc. This category is for sites where frequent rockfalls occur during a certain season and are not a significant problem during the rest of the year. This category may also be used where severe rockfall events have occurred.
- **Constant falls, 81 points**—rockfalls occur frequently throughout the year. This category is also used for sites where severe rockfall events are common.

Sample This area was identified by the maintenance personnel as being a seasonal rockfall problem. Road patrols are required daily during the winter and spring to keep the roadway clear. The level of rockfall at this site is assigned a score of 35 points.

Preliminary Design and Cost Estimates

It is important when planning highway construction projects to properly scope the desired result, which determines the project limits, the estimated construction costs, the right-of-way needs, etc. Trying to retrofit a different, more appropriate rockfall design after these items have been established is frustrating and can be completely unworkable.

Therefore, the fourth step of the RHRS process requires a preliminary design and cost estimate to be included as part of the RHRS data base. With this information, rockfall projects can be properly funded and developed. Value-engineering the level of effort and the cost associated with a particular rockfall section can help match the result to the need. A systematic method for analyzing the possible response alternatives has been described by Keaton and Eckhoff (*6*).

Covering the field of rock mechanics is beyond the scope of this paper. An excellent reference on the subject for the practitioner is an FHWA publication (*7*). Because experience is the best test of the reasonableness of a rockfall remedial design, the value of having skilled personnel in this area cannot be overly stressed. The gaps in the understanding of the mechanical properties of rock masses are still too large to rely strictly on an analytical approach. This is not to say that all of the analytical tools available will not be used, if needed. However, at this stage the goal is to provide an appropriate method to deal with the rockfall problem that can later be refined by more detailed investigation and analysis.

More than one design approach to reduce the rockfall risk should be considered for each site. A hazard reduction measure can vary from a limited-duration improvement such as slope scaling to a more positive step such as installing wire mesh to control the descent of falling rocks. Frequently, a combination of many techniques will work best.

The rockfall design cost estimate is strictly for rockfall remedial measures. A project may eventually include widening pavement, installing guardrail, adding a structural pavement overlay, etc. These actions as well as mobilization, engineering, and contingencies, etc., are not included as part of the RHRS cost estimate. Later, when different rockfall sites and the cost to deal with them are compared, these additional cost items will not interfere.

Project Identification and Development

The true benefit of implementing the RHRS—a reduction in the systemwide rockfall potential—will be realized once rockfall remedial projects are developed from the resulting data base. The following are ways to use the RHRS to identify and advance projects for construction.

1. Projects can be advanced on the basis of score. This is the most obvious use of the system. Because the most hazardous slopes are those at the top of the list, projects would be funded for construction as funds become available.
2. Projects can be advanced on the basis of their score relative to their estimated construction costs. In effect, a modification of the benefit-cost method is used. The preliminary cost estimate for the top-rated slopes is divided by the RHRS score and a list is generated with the lowest ratios of dollars to RHRS points at the top. Projects developed from this list would provide the greatest systemwide hazard reduction with a fixed investment.
3. Projects can be developed on the basis of the remedial approach. Rockfall sections containing similar construction features would be grouped into a single project. An example would be to take a length of highway and combine into one project all of the sections that include slopes screening. By doing this, a larger quantity would be contracted and could result in more straightforward, more easily managed contracts with lower unit bid prices.
4. Projects can be developed on the basis of proximity of rockfall sites along a section of roadway. A larger contract could be let because the rockfall sites have been identified and remedial measures properly determined. An example of this would be where all rated slopes along a 20-mi stretch of roadway are grouped into one project.

All these approaches rely on the data from the RHRS data base generated from implementation and periodic updates.

Annual Review and Update

The final step of the RHRS is to perform an annual review of all rated slopes. Natural conditions can change unexpectedly and these changes are often difficult to discern. Photographs taken during previous inspections will help identify changes. Any newly constructed slopes should also be evaluated and if necessary added to the RHRS database.

Eventually, all slopes in the RHRS data base should be evaluated with the detailed rating. Much of this work could be accomplished throughout the year by personnel commuting to and from other job-related responsibilities. The annual review and update would protect an agency's investment and maintain the value of the RHRS data base. Once all slopes are rated, an agency may redefine what constitutes an A or B slope using a range of scores established by the agency rather than the subjective evaluation criteria applied during the preliminary rating. The agency may elect to drop the letter designation entirely.

SYSTEM LIMITATIONS

The RHRS provides agencies with a method to address their rockfall problems by providing a relative rating among slopes. For the most part, this relative rating is subjective. The slope evaluation process is as straightforward as possible, however, there is still a range of values a slope could receive. Much depends on the abilities of the raters and how consistently they interpret and apply the rating criteria. Even though one slope receives a score of 700 and another receives a score of 600, both slopes have the potential of releasing rock onto the roadway.

Agencies will always be expected to react to rockfall accidents no matter where a particular section appears on the RHRS priority list, but the tendency to overreact should be resisted. Sites where an accident has occurred should be re-evaluated with the detailed rating to determine if the rockfall incident has increased or decreased the rockfall potential. The level of investment at the site should be consistent with the new potential relative to that on the other sites.

BENEFITS

It is not reasonable to expect an agency to have enough funds necessary to deal with all safety-related issues at once. However, it is necessary to have a system in place by which projects are identified and developed as funding is made available. ODOT experience has been that this is legally defensible. The use of the RHRS as a defense has not been tested in Oregon to date. However, Oregon has for many years had a priority list for developing rockfall construction projects. The sites listed are those identified as having an accident history or excessive maintenance costs, or both. The list generally contains only 100 sites and is not based on the rockfall potential but on the rockfall history. The sites are prioritized on the basis of a cost-benefit analysis. Even though ODOT had a definite, planned approach to deal with rockfall sites as funds became available, litigations brought against the state because of rockfall accidents either were settled out of court or were found favorably to the state. ODOT believes that having a more comprehensive, state-of-the-art process for developing the priority list will serve better.

CONCLUSION

ODOT engineering geology staff have spent many hours designing, testing, and redesigning the RHRS system. The process has been manageable, and was completed while Staff maintained a busy, normal workload. It was found beneficial to have the engineering geologists responsible for creating and maintaining the RHRS database.

ODOT's experience with the RHRS has been favorable. Management now has a uniform process that can help make practical decisions on where to allocate money for rock slope projects and they welcome having quality information to use in this area of project development. The agency believes that the issue of public safety is being properly addressed and that greater legal protection is afforded the agency by having the RHRS in place.

ACKNOWLEDGMENTS

The funding support for the study provided by the following agencies is gratefully acknowledged and sincerely appreciated: State highway departments of Arizona, California, Idaho, Massachusetts, New Hampshire, New Mexico, Ohio, Oregon, Washington, and Wyoming; the Federal Highway Administration CTIP (Direct Federal), Office of Implementation, and Office of Research.

REFERENCES

1. C. O. Brawner and D. Wyllie. Rock Slope Stability on Railway Projects. *Proceedings of the America Railway Engineering Association Regional Meeting*. Vancouver, B.C., 1975.
2. D.Wyllie. Rock Slope Inventory System. *Proceedings of the Federal Highway Administration Rockfall Mitigation Seminary*. FHWA Region 10, Portland Oregon, 1987.
3. L. A. Pierson, S. A. Davis and R. VanVickle. *The Rockfall Hazard Rating System Implementation Manual*. FHWA Report FHWA-OR-EG-90-01. FHWA, U.S. Department of Transportation, 1990.
4. *A Policy on Geometric Design of Highways and Streets*. AASHTO, Washington, D.C., 1984.
5. *Selected Climatological Publications EIS C–22*, National Oceanic and Atmospheric Administration, U.S. Department of Commerce, Asheville, N.C., 1983.
6. J. R. Keaton and D. W. Eckhoff. Value Engineering Approach to Geologic Hazard Risk Management. In *Transportation Research Record 1288*, TRB, National Research Council, Washington, D.C., 1990, pp. 168–174.
7. *Rock Slopes: Design, Excavation, and Stabilization*. FHWA Report *FHWA-TS-89-045*. FHWA, Turner-Fairbank Highway Research Center, McLean, Va., 1989.

Publication of this paper sponsored by Committee on Engineering Geology.

Rockfall Control in Washington State

THOMAS C. BADGER AND STEVE M. LOWELL

The mountainous and rugged terrain of Washington State presents major and ongoing rockfall problems along transportation corridors. Rockfall control in Washington focuses on rockfall containment, identification, and prevention or minimization. Washington State Department of Transportation (WSDOT) has developed ditch design criteria for containing rockfall, which have been in use since 1963. The criteria address ditch design and rockfall fence placement for both rock and talus slopes. Rock slope design is a critical element of rockfall control in Washington. All new and upgraded construction of rock slopes is first evaluated for kinematic feasibility of rockfall. If applicable, cut-slope orientations are also based on kinematics. Highly fractured rock masses and those with random discontinuity orientation are designed using a nonlinear failure criterion. Controlled blasting methods are required on all WSDOT projects. Slope irregularities are kept to an absolute minimum and the use of a midslope benches for rockfall catchment has been eliminated. Commonly used stabilization methods are shotcreting, rock bolting and dowelling, slope trimming and scaling, and wire mesh. A priority rating system is also in use to direct proactive mitigation work in areas of high rockfall hazard around the state. In addition, WSDOT and Washington State University are developing an expert-type computer system, the unstable slope management system (USMS), for statewide use.

The mountainous and rugged terrain of Washington State presents major and ongoing rockfall problems along transportation corridors. A significant number of accidents and nearly a half dozen fatalities have occurred because of rockfall in the last 30 years on Washington highways. A preliminary statewide inventory revealed that 45 percent of all unstable slope problems (landslides, embankment failures, rockfall, etc.) are rockfall related.

Washington has a large highway infrastructure in place, and much of the present rockfall mitigation focuses on methods for control or containment. As the state highways are improved to meet current design standards, more of the mitigation work is focusing on rockfall identification and prevention. In this paper methods of rockfall control in Washington are addressed, as well as the proactive approach of prevention. Rockfall prevention includes the use of the most current standards for rock cut-slope designs, rockfall hazard priority rating, and development of a statewide unstable slope management system (USMS).

ROCKFALL DITCH DESIGN

In early Washington highway construction, methods of rockfall control included large flat ditch sections, wire mesh, midslope benches, and so on. However, there was little basis for the application of such rockfall designs, and designers relied on educated guesses about rockfall behavior on a particular slope. As early as 1959, engineers in the state of Washington began to realize the inadequacy of some design methods to control rockfall in deep cuts (*1*). The Washington Department of Highways [now the Washington State Department of Transportation (WSDOT)] recognized that little was known about the effectiveness of standard rockfall containment measures, and that even less was known about the mechanics of rockfall.

In 1961 the Washington State Highway Commission (WSHC) and the Bureau of Public Roads (BPR) funded a research project under the direction of Arthur Ritchie, chief geologist for WSHC (*2*) to study rockfall mechanics. In the research project full-scale rockfall observations were made under varying slope conditions and additional experiments were performed with portable ditch sections and rock fences.

With the conclusions from the research, Ritchie (*2*) developed a rockfall ditch design table that took into consideration the primary variables of the rockfall—slope height and slope angle. The ditch design contained three basic elements: fallout width, ditch depth, and a steep off-shoulder slope. In the case of natural slopes flatter than 1H:1V, on-slope rock protection fences were developed.

In 1963, WSDOT adopted a standard design for rockfall control that was based exclusively on this research. The standard roadway section contained two designs: one for rock slopes (Design A) and one for talus slopes (Design B). Subsequent to the original standard plan, Design A has been modified to allow for staged development of the rockfall ditch.

Design A—Rock Slopes

The staged development concept for Design A is to provide alternatives that are based on local site conditions and an estimate of the severity of future rockfall. The use of controlled blasting in developing the rock cut is recommended in conjunction with the ditch design. The width of the ditch is controlled primarily by the slope angle and slope height (see Table 1). Stage 1 design uses a standardized ditch section

TABLE 1 WSDOT DESIGN FOR ROCKFALL AREAS—DESIGN A

Slope	Height (ft)	Width (ft)
Near Vertical	20 - 30	12
	30 - 60	15
	>60	20
0.25H:1V or flatter	20 - 30	12
	30 - 60	15
	60 - 100	20
	>100	25

Washington State Department of Transportation, P.O. Box 167, Olympia, Wash. 98504.

(see Figure 1). Stage 2 and 3 designs use rock protection fences and deeper ditch sections for more severe applications (see Figures 2 and 3). Concrete barriers may be used instead of the rock protection fence. The concrete barrier alternative in Stage 2 and 3 designs is used only after an analysis of the site in which consideration is given to factors such as potential impact velocities, ditchy capacity, and size of rockfall.

Design B—Talus Slopes

Design B is used as a treatment for rockfall generated on talus slopes. Ritchie's (*2*) research revealed that rockfall on these slopes will generally roll and stay close to the slope. Rock protection fences are specified on these slopes because of the strong horizontal component of the trajectory. The purpose of a rock protection fence is to decelerate or catch the rolling rock before it enters the roadway. The ditch treatment calls for a steep 1.25H:1V foreslope into the ditch with a minimum depth of 4 ft. Design B allows for three positions of the rock protection fence (but never more than one position at any given site). Fence positions A, B, and C are shown in Figures 4, 5, and 6, respectively. Position B is the preferred fence location for most applications.

ROCKFALL HAZARD PRIORITY RATING

In 1988, WSDOT began using a priority rating system to address rockfall problems on existing facilities around the state. The goal of the system was to assess a large number of areas where rockfall occurred and to objectively rate the slopes in terms of potential hazard. The rating provides a basis for selecting potential sites that require rock slope remediation. Ideally, rock slope remediation would first focus on sites with the highest hazard ratings and then progress to lower-rated rock slopes as funds become available.

The rating system in use by WSDOT was developed by the Oregon Department of Transportation (*3*) and uses a matrix evaluation approach. Sites are rated on 11 criteria such as rock structure, highway geometrics, slope height, and rockfall frequency. Increasing levels of severity for each criterion are given greater point values using an exponential point scale. All the points for each of the 11 criteria are totaled for each investigated site. The site with the highest point total is theoretically the most hazardous and that with the lowest point total is theoretically the least hazardous. The rating system is not meant to predict which slope will fail first, but rather to provide a logical starting point for remediation work on a large number of rock slopes.

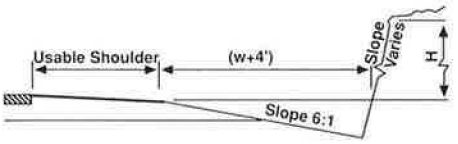

FIGURE 1 Roadway section on rock slope—Design A, Stage 1.

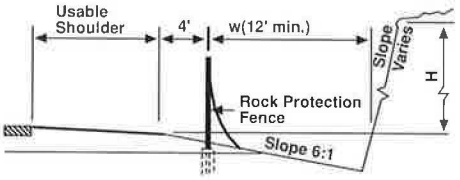

FIGURE 2 Roadway section on rock slope—Design A, Stage 2.

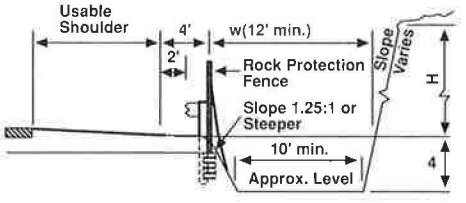

FIGURE 3 Roadway section on rock slope—Design A, Stage 3.

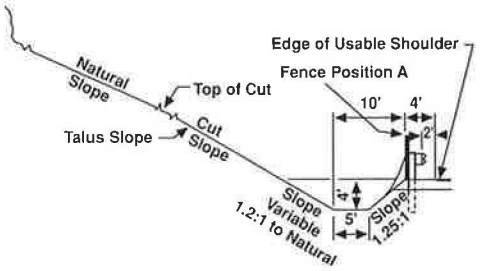

FIGURE 4 Roadway section on talus slope—Design B, fence position A.

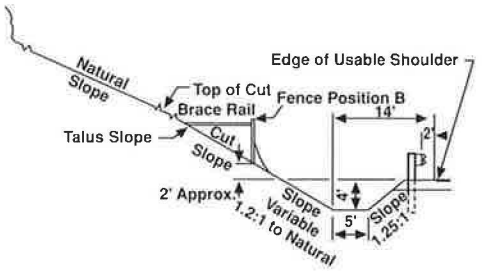

FIGURE 5 Roadway section on talus slope—Design B, fence position B.

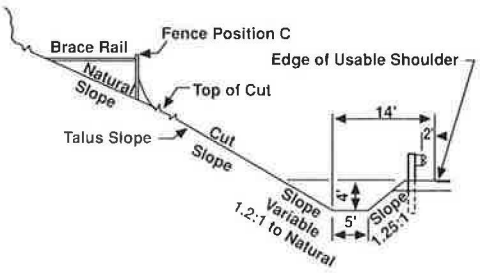

FIGURE 6 Roadway section on talus slope—Design B, fence position C.

The Geotechnical Branch of WSDOT completed a pilot project in 1989 using this rockfall hazard rating system in District 1 the northwest part of the state (*4*); 39 problem rockfall areas were identified by the four maintenance areas of the district. Phase I of the project consisted of rating and priority-ranking each of the 39 sites. The district then selected a group of high-ranking sites to address first. Phase II of the project consisted of providing final remediation design and cost estimates of the required work on the sites selected. The final remediation designs prepared in Phase II focused on long-term solutions. Final designs included work such as slope scaling and trimming, shotcreting weak zones in the rockmass, and rockbolting and dowelling. In 1990, the district appropriated $250,000 to begin work on the list. Additional funds for 1992 have been set up to continue remediation work on the list of 39 slopes.

Since this pilot project, the Geotechnical Branch has completed another rock slope priority-ranking study on a 10-mi length of Interstate in the northwestern portion of the state. Based on these pilot projects, at least three other major state highway routes representing approximately 180 mi of highway within the state are being considered for rock slope rating and ranking.

UNSTABLE SLOPE MANAGEMENT SYSTEM (USMS)

Under a research grant administered by the Washington State Transportation Commission (WSTC) and the Federal Highway Administration (FHWA), WSDOT and Washington State University (WSU) are developing the USMS (*5*). The research is being conducted by the WSU Civil Engineering Department. The USMS is a computer program consisting of a database and priority programs that prioritizes unstable slopes. Unstable slopes include not only rockfall, but also landslides, embankment failures, debris flows, etc. The priority programs are developed from the expert shell system CLIPS, a language developed by the National Aeronautics and Space Administration. The USMS identifies factors that determine the importance of a failure site such as the cause of instability, cost of repair, use of road, and safety to motorists. The data are collected and stored in the database by site. Using the priority programs, priority ratings are assigned to each site and then multiplied by a weight. The sum of the products yields the total priority, which ranges from a point value of 0 to 100, where 100 indicates the highest-priority site. The total priority of a site is independent of all other sites. The USMS develops a list of priority-ranked sites from which mitigation work can be selected.

ROCKFALL MODELLING

WSDOT has been using the Colorado Rockfall Simulation Program (CRSP) developed by the Colorado Department of Transportation to aid in rockfall mitigation design (*6*). The program allows the designer to input the geometry of the slope and define certain parameters of the slope. The program then simulates a number of rockfall events and provides output information on items such as impact force, trajectory path, and termination point. The program has provided WSDOT with design information for necessary length of a tunnel portal extension, rockfall protection fence placement, and ditch design verification.

ROCK SLOPE DESIGN

Rock slope design is a critical element of rockfall control in Washington State. The potential for rockfall can be dramatically reduced by the proper engineering of new and upgraded cut slopes. All proposed construction of rock slopes is reviewed by the Geotechnical Branch of WSDOT early in the design process.

Rock slopes are first evaluated for their potential for kinematic failure. Does the rockmass contain ordered sets of discontinuities (e.g., bedding surfaces, joints, faults) that could produce rockfall when the slope if excavated at a typically steep orientation? Rockmasses that appear to be kinematically controlled are evaluated for three failure conditions: planar failure, wedge failure, and toppling failure (see Figure 7). A nonkinematically controlled failure would more commonly fail as a circular failure. A statistically significant number of discontinuity orientations are gathered and then plotted on stereo nets. An evaluation can then be made as to whether the rockmass contains adverse discontinuity sets that could produce instability in the slope. Design slope orientation may then be adjusted to cut out many of these potentially unstable features. This design approach focuses on repeatable discontinuity sets. It does not attempt to address every possible joint set that may produce an isolated rockfall event.

Rock slopes that are not structurally controlled are also evaluated. However, the focus of rock slope engineering is on large-scale failures rather than small-scale events. Rockmasses that are not structurally controlled include ones that are highly fractured, massive slopes that contain no or few joint sets, highly weathered or hydrothermally altered rockmasses, and many Washington State sedimentary rockmasses. WSDOT uses Hoek and Brown's (*7*) nonlinear failure criteria to evaluate these rockmasses. In the evaluation, the quality of the rockmass is classified using the Council for Scientific and Industrial Research (CSIR), Geomechanics Classification of Jointed Rock Masses developed by Bieniawski (*8*), which

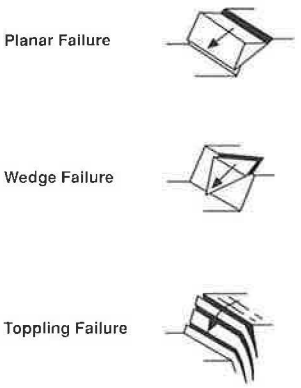

FIGURE 7 Kinematic failure conditions.

uses test hole and laboratory data from the rockmass. The Hoek-Brown (*7*) criteria then use empirically derived values for different rock types and rock quality conditions to develop a Mohr envelope. Corresponding strength parameters are then determined for a certain confining pressure and a computer-assisted stability analysis is performed using XSTABL or PCSTABL4. WSDOT has had excellent results using this method of analysis for nonkinematically controlled rockmasses.

Controlled Blasting

Many of the rockfall problems along Washington highways are a result of poor rock excavation methods used when the slopes were first constructed. Poorly designed blasting can result in excessive backbreak in the finished slope and continued rockfall problems for years after construction. Controlled blasting methods are required on all WSDOT projects for excavation in rock. These methods include the initiation of a preshear line along the finished slope before the production holes are detonated. WSDOT has had successful experience with preshearing slopes as flat as 1H:1V. Preshearing is not required by WSDOT for slopes flatter than 0.5H:1V and for burdens less than 10 ft. Before implementation, all blasting operations on state highway projects must submit a blasting plan for review by the Geotechnical Branch of WSDOT. When properties of the rockmass are sufficiently poor, mechanical excavation (e.g., ripping) is allowed, provided that finished slopes are approximately 0.5H:1V or flatter.

Midslope Benches

WSDOT designs rock slopes to be uniform, with as few slope irregularities as possible. The construction of 20-ft-wide midslope benches on steep rock slopes to catch rockfall is no longer practiced in Washington. Without continued maintenance, benches fill with rock debris. This results in a bench that is no longer flat but slopes outwards to the roadway. Rockfall striking these benches is no longer contained, and a significant horizontal component can be imparted to the trajectory path. Midslope benches are permitted only at the overburden-bedrock interface. When rockfall may originate from coarse overburden soils, a bench of 15-ft minimum width may be specified provided the soil slope is not over approximately 20 ft high. Vegetation is also stripped from the rock slope and 10-ft behind the upper catchpoint of the slope to prevent root wedging of blocks.

Rockfall Protection Fences

WSDOT uses rock protection fences for rockfall control and has developed standard plans for their construction. The fence is used in areas where rockfall would not be adequately contained by a ditch. These applications are generally used on flatter slopes such as talus slopes, where a horizontal component in the trajectory path is present. The standard plan for the fence consists of a 6-ft-high chain link fence fastened to steel posts with 2 to 3.5 in. inside diameter and 9 ft long. Upslope bracing is used for midslope anchor positions and impact attenuators are used to anchor the end of the fence.

WSDOT has had extremely good success with this rockfall protection fence. In addition to the standard plan for rock protection fences, WSDOT is considering the use of a proprietary rock protection fence developed in Europe. WSDOT would use this fence system for areas with high rockfall frequency and large rock size.

Wire Mesh Slope Protection

WSDOT uses wire mesh slope protection in areas where construction of an adequate ditch section is not feasible or where slope features would produce a large horizontal component in the rockfall. Wire mesh slope protection is used both to contain rockfall and to prevent ravelling of loose material. A typical wire mesh slope protection system consists of main vertical cable supports anchored at the top of the slope to which a wire mesh is attached, which is draped down the slope. The wire mesh is generally double twist gabion wire on galvanized chain link fence. The vertical wire mesh seams are wired or hog-ringed together to form a continuous blanket. WSDOT uses deadmans above the crest of the slope to anchor the wire mesh in overburden or weathered rock, and grouted rock anchors to attach the wire mesh in competent rock. The wire mesh typically extends downslope to within approximately 5 ft above the ditch. Wire mesh slope protection installed in mountainous areas is subject to heavy snow loads, and anchor systems are designed accordingly. WSDOT has effectively used wire mesh for near-vertical rock slopes and rock and talus slopes as flat as 1H:1V. For steep slopes it is important that rock sizes be less than 2 ft in diameter; larger rocks may have sufficient energy to break the mesh.

Gabion Barriers

WSDOT has also had extensive experience with gabion barriers for rockfall control on talus slopes. Their flexibility and relative ease of repair make them useful for areas with high rockfall frequency and very large rock size. Gabions are placed approximately 10 ft in front of the base of the slope and off the shoulder. Openings in the gabion wall are provided to allow for removal of the rock debris behind the wall. Gabions have proven to be very effective control for large rock size. In one instance, several rocks of more than 50 tons were retained by a two-tier-high gabion wall after the rocks had rolled several hundred feet down a steep talus chute.

Rock Debris Barriers

Rock debris barriers are also used in Washington State for containing rockfall. Rock debris barriers consist of 4- to 8-ft-high continuous mounds constructed of rock or soil debris near the base of the slope. These barriers provide the trapezoidal ditch section and energy attenuation required for con-

taining rock fall with high energy and frequency. Rock debris barriers are typically used on talus slopes that produce a significant amount of rockfall containing large boulders.

Scaling and Trimming

Slope scaling and trimming are used extensively for rockfall control. Scaling consists of removing loose rock debris on a slope with scaling bars, hydraulic splitters, and so on. Trimming refers to removing sizable unstable blocks and slabs from a slope, generally by use of explosives. Scaling is done on almost all new construction and remediation work in Washington State. Scaling and trimming are generally the first order of work for rock slope remediation projects. Work always progresses from the top down, moving across the length of slope and is accomplished by a crew of at least two on-slope workers and a foreman. The work can be extremely hazardous and WSDOT requires that only experienced high scalers be allowed to perform it.

Rock Bolting and Doweling

Rock bolting and doweling are commonly used on both new construction and rock slope remediation work for controlling rockfall. Rock bolts are posttensioned steel bars and tendons that are used to anchor potentially unstable masses to the slope. Rock dowels are similar except that they are not posttensioned; stresses are mobilized in the steel bar when and if the potentially unstable mass begins to move. Rock bolts and dowels are anchored into the rock with either cement grout, two-stage polyester resin, or mechanical anchors. Bolting and doweling is performed after loose rock has been scaled from the slope and is accomplished from either a crane-supported work platform or off ropes by experienced high scalers. Crane-supported work platforms generally use an air track drill for advancing the bolt and dowel holes. Platforms are typically anchored to the slope to allow for some drilling resistance. Rock bolting operations require skilled workers to perform the work safely and effectively.

Horizontal Rock Drains

Horizontal rock drains are commonly used for rockfall control in both new construction and remediation work by WSDOT. Horizontal drains dewater rockmasses and lessens the driving forces leading to slope failure. Generally the drains are uncased holes drilled into the slope by an air track drill or a portable rock drill. When horizontal drains are installed in highly fractured rockmasses, it is often necessary to case the hole with slotted polyvinylchloride (pvc) pipe to maintain the drain opening. Since most water in a rock slope is carried within discontinuities, drains are installed to intersect as many discontiuities as possible. Drains are typically installed sloping down and out of the rockmass at approximately 5 degrees. Both straight and fan-shaped drain arrays are used.

Shotcrete

Shotcrete is used in both new construction and remediation work by WSDOT. Shotcrete is used in weak, highly weathered or hydrothermally altered zones to prevent differential erosion. It has also been used for interbedded sedimentary units in which differential weathering of poorly indurated units could undermine more resistance units. The shotcrete is reinforced either with wire mesh affixed to the slope or by the use of steel or polypropylene fibers incorporated into the shotcrete mixture. Adhesion of the shotcrete to the slope is lessened under excessive moisture conditions. Weep holes through the shotcrete are installed with every application. WSDOT prefers the use of fiber-reinforced shotcrete because it conforms better to slope irregularities and is simpler and less expensive to construct. Experienced workers are an important factor in the success of shotcreting for rock slope stabilization.

Rock Sheds and Tunnel Portal Extensions

Rock sheds are in place on Washington mountain passes where the highway crosses large talus and avalanche slopes. WSDOT also utilizes portal extensions for tunnels, where necessary, to minimize risk from rockfall.

Rock Patrols

The Maintenance Division of WSDOT plays a very important role in rockfall control along state highways. Rock patrols are run on certain sections of state highways 24 hrs a day, 7 days a week because of increased rockfall frequency during late fall and winter.

Rock Slope Remediation Specifications

Until 1986, WSDOT did not have specifications for rock slope remediation. WSDOT surveyed other western states and found that none had such specifications either. WSDOT has since developed standard special provisions for scaling and trimming operations, rock bolting and doweling, horizontal rock drains, and shotcreting. The emphasis of the special provisions is quality control and amount of work experience. Rock anchors and shotcrete have performance specifications to ensure quality installation and application. All of the specifications contain language requiring a minimum level of work experience for all workers involved in remediation. WSDOT believes that only experienced workers should be allowed to perform remediation because all phases of the work are potentially so hazardous.

CONCLUSIONS

WSDOT controls rockfall containment, as well as prevention and minimization. A full spectrum of rockfall ditches, fences, and rock slope stabilization methods is employed for con-

trolling rockfall in Washington State. Increased interest in the state on maintenance issues has resulted in appropriation funds for rockfall mitigation for a proactive response to rockfall problems. WSDOT is using a rockfall priority-ranking system to identify rockfall problems on a regionwide basis and to provide a logical plan for mitigation. In addition, Washington State is developing an expert-type management system to address unstable slope problems on a statewide basis.

REFERENCES

1. S. M. Lowell. Development and Application of Ritchie's Rockfall Catch Ditch Design. Presented at Federal Highway Administration Rockfall Mitigation Seminar, Portland, Oreg., 1987.
2. A. M. Ritchie. *An Evaluation of Rockfall and Its Control*. Research Project HPS1-22. Washington State Highway Commission, 1963.
3. L. A. Pierson, S. A. Davis, and R. VanVickle. *The Rockfall Hazard Rating System Implementation Manual*. Oregon State Department of Transportation, 1990.
4. S. M. Lowell. Washington State Department of Transportation's Rockslope Remediation Pilot Study. *Proc. of the National Symposium on Highway and Railroad Slope Maintenance, 34th Annual Meeting Association of Engineering Geologists*. Chicago, Ill., 1991, pp. 65–73.
5. C. L. Ho and S. S. Norton. *Development of an Unstable Slope Management System*. Research Project GC-8720. Washington State Transportation Commission, 1991.
6. T. J. Pfeiffer and J. D. Higgins. Rockfall Hazard Analysis Using the Colorado Rockfall Simulation Program. In *Transportation Research Record 1288*, TRB, National Research Council, Washington, D.C., 1990, pp. 117–126.
7. E. Hoek and E. T. Brown. *Underground Excavations in Rock*. Institute of Mining and Metallurgy, London, U.K., 1980.
8. Z. T. Bieniawski. Geomechanics Classification of Rock Masses and Its Application in Tunnelling. *Proc. of the Third International Congress on Rock Mechanics*. Denver, Col., Vol. 11A, 1974.

Publication of this paper sponsored by Committee on Engineering Geology.

Abridgment

Selection of Rockfall Mitigation Techniques Based on Colorado Rockfall Simulation Program

RICHARD D. ANDREW

Until recently, predicting rockfall behavior has, at best, been extremely subjective. Many of the existing rockfall models had proven to be inaccurate and unrealistic in characterizing real-life rockfall occurrences with variable slope conditions. The inability to characterize a rock in motion led engineering geologists with the Colorado Department of Transportation and the Colorado Geological Survey to develop, test, and adopt the Colorado Rockfall Simulation Program (CRSP). Since its first release in late 1987, the program has been used to analyze a number of hazardous rockfall areas along the Interstate 70 project through Glenwood Canyon in Colorado. This, in turn, has led to the development of some fairly innovative mitigation techniques. Three devices have undergone extensive testing and have been applied to several locations along this scenic highway with an impressive record of performance.

For years, engineering geologists with the Colorado Department of Transportation (CDOT) and the Colorado Geological Survey (CGS) have attempted to understand the random behavior of rocks in motion and to control their effects on Colorado's highways. Many of the mountainous roadways traverse hazardous rockfall areas, which exhibit highly variable slope conditions and are difficult to analyze. During construction of the I-70 project through Glenwood Canyon, not only were these conditions encountered, but also there was the concern for minimizing the environmental impact of the mitigation procedures. The Colorado Rockfall Simulation Program (CRSP) was developed to provide an understanding of rockfall behavior along the highly irregular canyon walls. The program models varying slope conditions and provides information on the velocities, bounding heights, and energies of falling rocks at any point along the slope (*1*, *2*). This information is critical in determining the most appropriate type and location of mitigation.

Since its development in 1987, CRSP has been useful in designing several forms of mitigation, including the tire attenuator, the Colorado Flexpost fence, and, more recently, the use of geosynthetics as reinforcement in rockfall barriers. These systems have undergone extensive field testing and have proven to be effective in controlling rockfall. Several locations throughout Glenwood Canyon have received these systems for mitigation of rockfall hazards.

Colorado Geological Survey, 1313 Sherman Street, Denver, Colo. 80203.

APPLICATION

For years, the Glenwood Canyon geotechnical staff has been monitoring rockfall events on and around the 1-70 improvement project. A data base was established that reflected the areas receiving the highest incidence of rockfall. This data, in addition to extensive field review, led geologists to priority-rank the rockfall-prone areas. CRSP was used to analyze these area and assist in determining the most suitable mitigation system.

Tire Attenuator

The tire attenuator system was developed during the calibration of CRSP at the West Rifle test site near Rifle, Colorado (see Figure 1). It was designed to absorb kinetic energy and reduce bounding heights of incoming rockfall, then return to its original position without maintenance intervention. The system utilizes columns of used tires on rims supported by a series of 3-in. steel pipes, which are attached to a large-diameter wire rope suspended across a gully or draw. Rock anchors are used to secure the wire rope assembly to bedrock. For aesthetic reasons, a facade consisting of 8-in. wooden posts suspended from a separate wire rope may be placed downslope of the tire elements. Rocks that detach from the source area encounter the tire attenuator while their energy is at or near maximum. After impact, most of the energy is absorbed, thus increasing the summers of 1989 and 1990. The most durable utilized nineteen 270-ksi, 0.6-in.-diameter tendons grouted in two sections of 3½-in. inside diameter steel casing. The flexibility of the posts was provided by leaving 18 in. of the tendons uncased near the ground surface. The overall height of the posts was 11 ft. Maccaferri rock mesh strengthened with steel aircraft cables provided the net material in the fence. It was observed during the testing that when the netting was placed on the downhill side, the interaction between the fence and the rock was more prolonged, thus enabling more components of the fence to react to the impact (*4*).

The Colorado Flexpost fence has been utilized in three locations on the Glenwood Canyon Project. Construction has recently begun at 22 additional locations throughout the canyon as part of a comprehensive rockfall mitigation project for

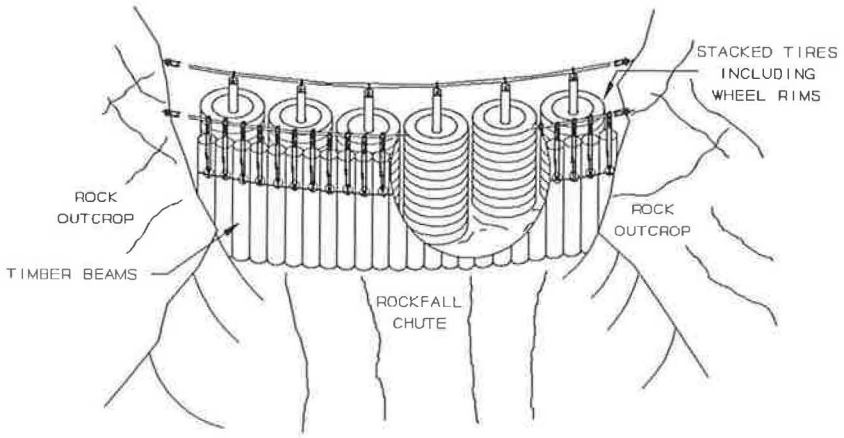

FIGURE 1 Tire attenuator.

the 15-mi-long stretch of I-70. CRSP was used to analyze all of these locations and provide the criteria for location and height.

Rockfall occurs at numerous locations throughout Glenwood Canyon; however, one location has been of special concern—an area just west of the Shoshone Dam along the Hanging Lake rest area on-ramp.

The source area is composed of quartzite interbedded with thin dolomitic layers that tend to be less resistant to weathering. The formation is jointed perpendicular to the bedding planes, which in conjunction with the highly weathered dolomite beds results in large blocks that topple away from the face. Some of the smaller rockfall occurs from a revelling cut near the base of the talus deposit, which was a result of poor grading techniques probability that the rock will be deposited on the talus and will not travel down to the roadway (*3*).

CRSP integrates with this system by providing the optimum location based on the incoming velocity and bounding height. The effects of the attenuator on the resulting rockfall may also be determined by analyzing the kinetic energy of the rock at the designated location and subtracting the energy lost to the attenuator system.

Three locations in Glenwood Canyon that have been prone to rockfall have received the tire attenuator system with promising results. Although the systems have been in place for only a few years, the early indications are that they are performing well. These areas have favorable conditions for this system including a long run-out zone for deposition of material not retained in the attenuator and narrow rockfall chutes.

Flexpost Fence

The goal of the Flexpost fence was to construct a durable and effective rockfall barrier that would utilize surplus and inexpensive elements. This was accomplished by designing a fence that would distribute the energy from a rock impact throughout the entire length of the barrier and redirect the rock to an energy-absorbing collision with the ground.

Prestressing tendons from the fenceposts in this system, and are a key component in the design concept (see Figure 2). Several configurations of the post were tested during the old Highway 6 construction.

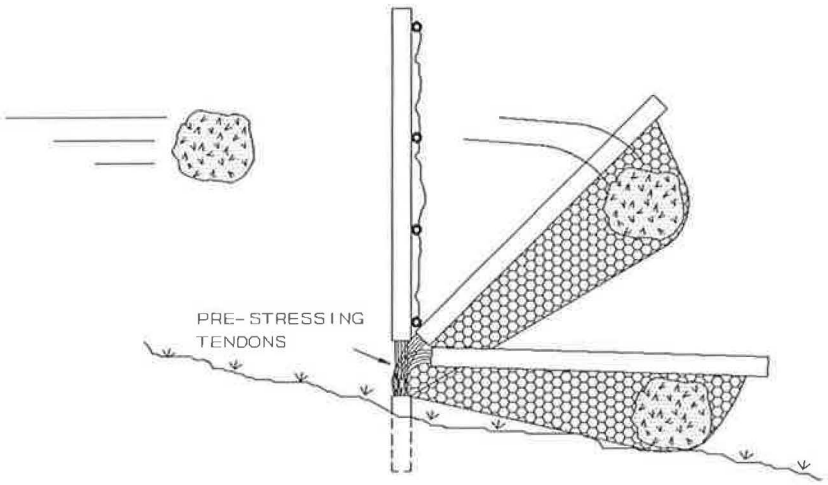

FIGURE 2 Colorado Flexpost fence (*4*).

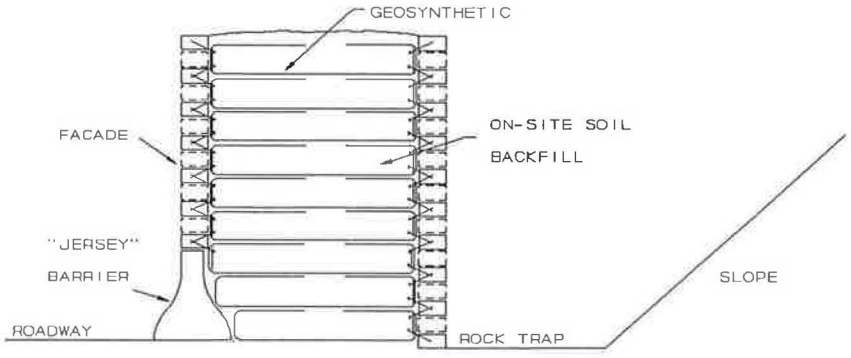

FIGURE 3 Geosynthetic rockfall barrier.

CRSP was recently used to evaluate the slope, and from this information it was determined that the Colorado Flexpost fence would be the most efficient application. The program indicated that just above the raveling cut, velocities and bounding heights were at a level such that the Flexpost fence would be most effective in controlling the maximum probable rock size of 3 ft.

Geosynthetic-Reinforced Impact Walls

Arthur Ritchie of the Washington State Department of Transportation (WSDOT) observed the implications of angular momentum on rockfall behavior and addressed its control through his ditch design criteria (*5*). However, in many mountainous regions, space and aesthetic constraints will not allow the use of a wide catchment. During the evaluation of several rockfall zones in Glenwood Canyon, it became apparent that there was a need for near-vertical foreslopes in catch basins for areas in which large ditch widths could not be constructed. The Glenwood Canyon geotechnical staff tested a double-sided geosynthetic-reinforced wall for use as a rockfall barrier at the West Rifle site. The purpose of these tests was to establish design guidelines for an impact wall to be constructed in Glenwood Canyon and to understand the limitations of geosynthetics in dynamic loading conditions (see Figure 3).

On November 15, 1990, the Glenwood Canyon geotechnical staff was contacted to investigate a rockfall that had occurred earlier that morning at a location 10 mi to the east of the Glenwood Canyon Project. Several large boulders averaging 4 to 5 ft in diameter had been detached near the crest of the hillside from a contorted zone in the Eagle Valley evaporite formation. Most of the rockfall had landed on the Interstate, closing one lane.

An investigation of the source area revealed that the majority of unstable material had not yet been detached. Two large boulders, each measuring 8 ft in diameter, had become wedged near the base of the funnel-shaped source area and were blocking an additional 20 to 30 yards of material. It was concluded that a large berm would be the most appropriate mitigation method for controlling impending and future rockfall hazards.

CRSP was used to model the slope and predict future rockfall behavior. The program indicated that a 35-ft-wide ditch would be required in front of a 15-ft-high impact wall, with the impact surface constructed to be nearly vertical. A composite wall was constructed utilizing tire-faced geosynthetically reinforced soil and L-walls. Behind the wall was a 25-ft-wide berm, which was required for the predicted high-impact energies and to blend the feature into the hillside.

The composite wall and ditch configuration were tested by blasting the large boulders loose from the funnel-shaped chute and releasing the trapped material. All the material removed by the blast was retained by the impact wall, including the two 8-ft-diameter boulders. In July 1991, the remaining unstable rock was released and the entire fall was contained by the wall.

CONCLUSION

CRSP has been instrumental in analyzing complex slope conditions in and around the Glenwood Canyon Project. This information has been necessary in determining the most appropriate and cost-effective methods for controlling hazardous rockfall. As a result of the CRSP research, three inventive and economical mitigation devices have emerged: the tire attenuator, the Flexpost fence, and geosynthetic-reinforced rockfall barriers. Through the use of these three systems, developed in conjunction with CRSP, the integrity of Colorado's transportation facilities and the safety of motorists have been greatly enhanced.

REFERENCES

1. T. J. Pfeiffer. *Rockfall Hazard Analysis Using Computer Simulation of Rockfalls*. Master's thesis. Colorado School of Mines, Golden, Colo., May 1989.
2. T. J. Pfeiffer and J. D. Higgins. Rockfall Hazard Analysis Using the Colorado Rockfall Simulation Program. In *Transportation Research Record 1288*, TRB, National Research Council, Washington, D.C., 1990, pp. 117–126.
3. R. K. Barrett, T. D. Bowen, T. J. Pfeiffer and J. D. Higgins. *Rockfall Modeling and Attenuator Testing Report*. CDOH-DTD-ED3/CSM-89-2. Colorado Department of Highways and Colorado School of Mines, 1989.
4. G. Hearn. *CDOT Flexpost Rockfall Fence*. CDOT Report CDOH-R-UCB-91-6. University of Colorado, Boulder, Colo. 1991.
5. A. M. Ritchie. An Evaluation of Rockfall and Its Control. In *Highway Research Record 17*, TRB, National Research Council, Washington, D.C., 1963, pp. 13–28.

Publication of this paper sponsored by Committee on Engineering Geology.

CDOT Flexpost Rockfall Fence Development, Testing, and Analysis

GEORGE HEARN, ROBERT K. BARRETT, AND MICHAEL L. MCMULLEN

Highways in Colorado are being protected against rockfall hazard by a new flexible fence developed in a 2-year program of prototype testing and dynamic analysis. The Flexpost rockfall fence consists of steel gabion mesh and wire rope supported on flexible posts constructed of steel pipe and 7-wire strands that are capable of elastic rotations in excess of 90 degrees out of the vertical. The rotation capacity of the posts allows the fence to respond to rockfall impact with large elastic deformation and to rebound after impact. The fence does not employ out-of-place stays, which would hamper the use of equipment to clear rockfall debris. In impacts by massive, high-velocity rocks, tensions in the steel fabric impose a centripetal acceleration on the rock and lead it to an impact with the ground, dissipating the rockfall kinetic energy. Flexpost fence prototypes were tested with rocks falling freely down a natural slope. The tests provided basic data on rockfall capacity, which were further refined by dynamic analysis using software developed specifically for the Flexpost fence. The dynamic analysis treats the fence and falling rock as separate bodies, computes contact forces, and includes modeling of a moving contact area. Analysis of prototype test cases agreed with the field observations. Flexpost fences are made of lightweight, readily available components, are inexpensive, and are already in service in Colorado.

To minimize rockfall hazard along its roads, the Colorado Department of Transportation (CDOT) maintains an active program of research into rockfall hazard prediction and mitigation. This effort has produced techniques for computer simulation of rockfall events and computation of site-specific statistics of rockfall hazard, and has led to the design and testing of innovative rockfall barriers, including earth-filled timber cribs, geofabric walls, kinetic energy attenuators, and the Flexpost rockfall fence (*1*,*2*).

Rockfall barriers are intended to prevent rocks in motion from reaching roadways and are designed for impact. The input is the kinetic energy of a falling rock, and the barrier must dissipate this energy. Impact force depends on rockfall kinetic energy and on the stiffness and mass of the barrier. Within limits, it is possible to manipulate impact force through structural design. The trade is one of greater deflection for lower force. Rigid barriers respond to rockfall impact with high force. Flexible, compliant barriers respond to the same impacts with lower force.

The Flexpost rockfall fence is compliant. The fence is a fabric of steel mesh and wire rope supported on spring-mounted posts (see Figure 1). The posts can rotate elastically through angles more than 90 degrees out of the vertical and develop only a modest resisting moment. The capacity for elastic rotation in the posts provides a large capacity for elastic deflection of the fence. Because of the low-force, elastic behavior of the posts, impact forces are reduced and the fence rebounds to be ready for other rockfalls. The fence fabric is initially slack and easily forms a pocket to trap incident rocks. In impacts by large, fast-moving rocks it is observed that the fence imposes a centripetal acceleration on the rock, leading it to an impact with the ground, which is used as a massive barrier to absorb rockfall energy. Other rockfall fence designs are comparatively rigid and may allow large permanent deflections by the use of uphill cable stays and slip mechanisms. Such fences cannot rebound, and the stays interfere with equipment for clearing. The Flexpost design avoids both of these limitations.

G. Hearn, University of Colorado, Campus Box 428, Boulder, Colo. 80309. R. K. Barrett, Colorado Department of Transportation, P.O. Box 2107, Grand Junction, Colo. 81520. M. L. McMullen, Colorado Department of Transportation, 4201 East Arkansas Avenue, Denver, Colo. 80222.

FLEXPOST ROCKFALL FENCE DESIGN

The Flexpost fence is constructed of steel gabion mesh and interwoven wire ropes supported on flexible posts. The fence is 11 ft tall with posts spaced 16 ft for interior panels and at 8 ft for end panels. The gabion mesh is suspended from a top cable along the length of the structure and wrapped around end posts. The top cable is clamped to the top of each post. Three intermediate cables are woven into the mesh as reinforcement and are attached to end posts. A bottom cable is woven into the mesh, anchored to foundations at the end posts, and connected to intermediate post foundations by 3-ft cable tethers. Cable stays run from each post foundation to the tops of adjoining posts and form X-bracing in each panel. The cable stays carry tensile loads to the post foundations during rockfall impact and constrain the posts to rotate normal to the fence run.

Each post is made of two lengths of 3-in. inside diameter steel pipe encasing a group of 7-wire prestressing strands. One length of pipe serves as a ground casing. Posts are founded by grouting this casing into the earth. The upper length is the visible post. A group of 19 prestressing strands are grouted into both pipe lengths. At the ground surface between the two pipe lengths, 18 in. of the strand group is left without casing. The unencased strands bend easily, allowing each post to behave like a bar on a spring-loaded pivot. The strands allow elastic rotations of posts in excess of 90 degrees and posts can be bent over to touch the ground and will spring back when released. In Figure 1, the total strand length is indicated in the post on the left.

Flexpost rotational stiffness was determined in 16 static tests of six posts. Flexposts were loaded at the top by a cable attached to a hydraulic ram. Cable tension was calculated from hydraulic pressure readings and ram calibration. Hori-

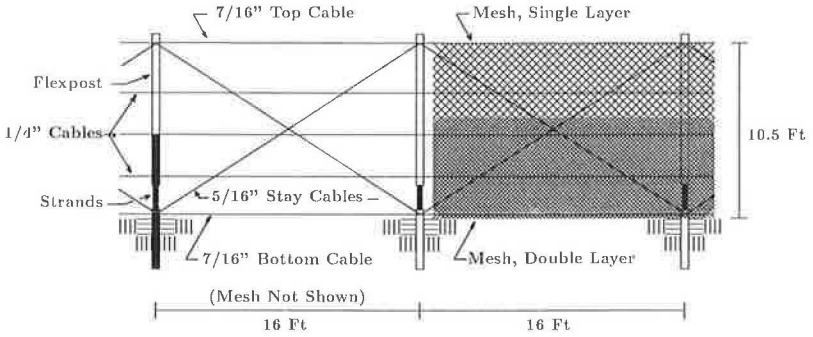

FIGURE 1 CDOT Flexpost rockfall fence elevation.

zontal and vertical deflections of the tops of the posts were recorded along with ram hydraulic pressure readings, and the data were used to compute base moment M and post rotation θ. Flexposts exhibit bilinear M versus θ behavior with an initial tangent stiffness of 90,000 ft-lb/rad for moments up to 2,300 ft-lb, and a second tangent stiffness of 1,600 ft-lb/rad for higher moments. The average M versus θ curve obtained from static tests is shown in Figure 2.

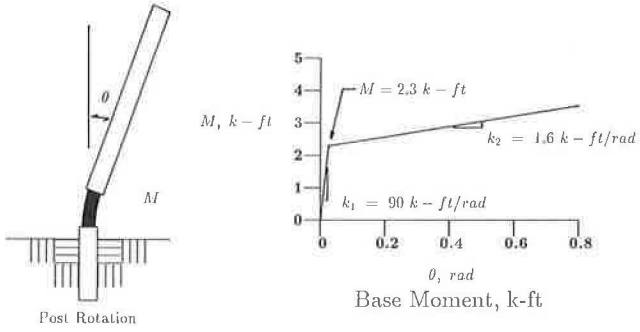

FIGURE 2 Flexpost static tests.

PROTOTYPES AND ROCKFALL TESTS

The first prototype Flexpost fence was built in 1989, and two additional prototypes, both incorporating design advances, were built and tested in 1990. Schematics of the prototypes are shown in Figure 3. The 1989 fence was 6 ft tall and had six posts spaced at 12 ft. Static load tests were conducted on individual posts, and dynamic tests of the fence were accomplished with rocks swung by a crane in the manner of a wrecking ball. Impact conditions in this dynamic test were not identical to those of rocks bounding down a slope, since attachment to the crane constrains rock trajectory. However, the test did demonstrate the resilience of strands in Flexposts and the capacity of steel gabion mesh in rockfall impacts. Analysis of data from this first test indicated that strain energy developed in the Flexpost strands was significantly less than rock kinetic energy and could not be the chief mechanism of energy dissipation. Instead, the fence arrests rockfall by developing tensions in its fabric of mesh and cables, and by altering rock trajectory. The rockfall capacity of the fence is not a function of the spring stiffness of Flexposts (Flexposts are not cantilevers resisting impacts), and therefore taller fences with similar post design could be expected to perform adequately.

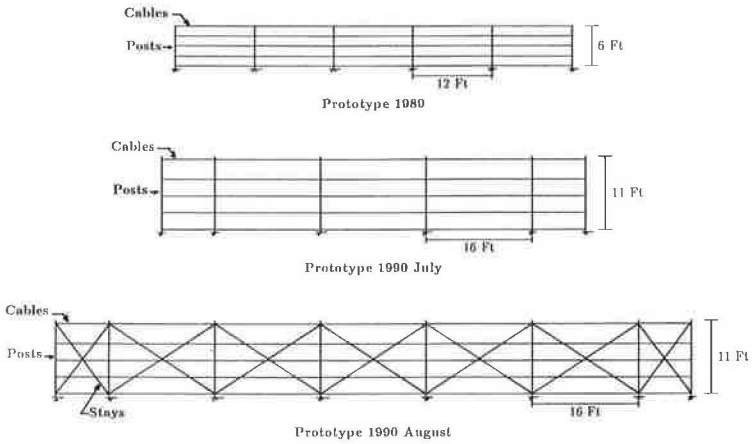

FIGURE 3 Flexpost rockfall fence prototypes: schematics for cables and posts.

In July 1990 a second prototype was built and tested. This fence was 11 ft tall with a post spacing of 16 ft. Another 11-ft fence was built and tested in August 1990. The August prototype included cable X-bracing in panels to protect post strands from tensile forces during rockfall impact. Both of the 1990 prototypes were tested with rocks rolling freely down a natural slope at a site near Rifle, Colorado. The slope is 500 ft long with an average slope of 66 percent. Rockfall velocities at impact as high as 50-ft/sec were observed in the Flexpost tests. Average rockfall velocity at impact was 32 ft/sec. Tests of other rockfall structures at this same site reported velocities as high 75 ft/sec (*1*). Rocks for prototype tests were numbered and weighed, three principal diameters were measured, and a pattern of paint dots was applied to make rock rotations more visible. The supply of test rocks ranged in weight from 145 to 9,700 lb. Rocks that hit Flexpost fence prototypes ranged from 265 to 6,040 lb. Rockfall impacts were recorded by two videocameras: one a sweep camera following the rock, and the other a fixed camera focused on the Flexpost fence.

The fence was marked with colored ribbons in the mesh to improve visibility on videotapes. The slope of the test site was also marked with ribbons at 10-ft intervals extending 60 ft uphill from the fence; these ribbons were used as reference points for estimating rock velocity from the videotapes. Time scales were added to the videotapes after testing. Data obtained from the videotapes included rock translational velocity, rock rotational velocity, vertical angle of rock trajectory, horizontal angle of rock trajectory, location of impact on fence, post rotations in response to impact, and damage to fence, if any. Rockfall weights, velocities, and energies are summarized in Table 1 and Figure 4.

During testing of the July prototype, 31 rocks were dropped resulting in 12 impacts with the fence (see Figure 5). Of these 12 impacts, 8 were stopped without damage to the fence, 1 tore the mesh fabric, and 3 overtopped the fence, which at the time was partially held down by previous rockfalls. Translational kinetic energies of rock impacts ranged from 4,700 to 166,000 ft-lbs. The July prototype was not damaged by impacts with translational kinetic energies as high as 42,600 ft-lb (a 1,490-lb rock travelling at 43 ft/sec), but was damaged by a rockfall at 44,100 ft-lb (a 1,550-lb rock travelling at 43 ft/sec). The July prototype appeared to have sufficient strength, but after repeated rockfall impacts, Flexpost strands had become permanently deformed. By the end of the testing, Flexposts would no longer rebound after rockfall impact, though the posts would remain vertical if righted. It appeared that the combination of large bending deformation and tension in the strands was the cause of damage.

TABLE 1 SUMMARY OF ROCKFALLS IN PROTOTYPE TESTS

Test Date	Rock #	Rock Weight lbs	Rock Vel ft/s	Trans. K.E. ft-lbs	Rot. K.E. ft-lbs	Total K.E. ft-lbs	Observations
July 10, 1990	22	608	31.7	9,480	4,140	13,600	No Damage
	23	1,490	42.9	42,600	11,300	53,900	No Damage
	64	597	31.3	9,090	2,510	11,600	No Damage
	70	750	28.2	9,260	4,440	13,700	No Damage
	31	597	22.5	4,710	790	5,500	No Damage
	47	1,540	42.9	44,100	17,200	61,300	Tore Mesh
	46	1,390	37.5	30,300	6,880	37,200	No Damage
	4	3,600	-	-	-	-	No Damage
	41	1,510	41.1	39,600	18,600	58,200	Held Fence Down
	1	3,820	25.1	37,400	21,200	58,600	Overtopped, Fence Held Down
	65	949	42.9	27,100	6,140	33,200	Overtopped, Fence Held Down
	38	4,700	47.6	166,000	36,200	202,000	Overtopped, Fence Held Down
August 13, 1990	5	256	26.1	2,720	1,360	4,080	No Damage
	2	-	18.8	-	-	-	Tore Stay
	40	6,040	37.5	132,000	243,000	375,000	Tore Mesh
	64	597	33.3	10,300	1,830	12,100	Through Mesh Hole
	36	1,392	13.0	4,220	959	5,180	No Damage
	48	1,700	10.9	3,160	2,050	5,210	No Damage
	37	797	35.4	15,500	6,680	22,200	No Damage
	41	1,510	50.0	58,700	15,700	74,400	Tore Mesh
	34	592	35.4	11,500	4,100	15,600	No Damage
	9	1,620	15.1	5,660	2,550	8,210	No Damage
	12	1,360	37.5	29,600	6,730	36,300	Fabric Deformed
August 21, 1990	37	797	43.8	23,700	6,680	30,400	No Damage
	13	305	33.3	5,270	468	5,740	Bent Post
	14	1,280	33.3	22,200	11,300	33,500	No Damage
	64	597	17.3	2,770	3,290	6,060	No Damage
	70	750	28.6	9,560	2,310	11,900	No Damage
	4	3,600	21.4	25,700	18,300	44,000	Tore Mesh and Top Cable

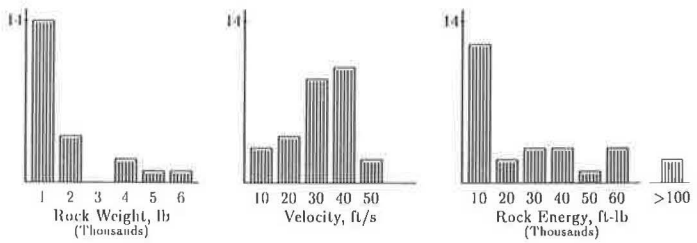

FIGURE 4 Flexpost rockfall fence: summary of field test rockfalls.

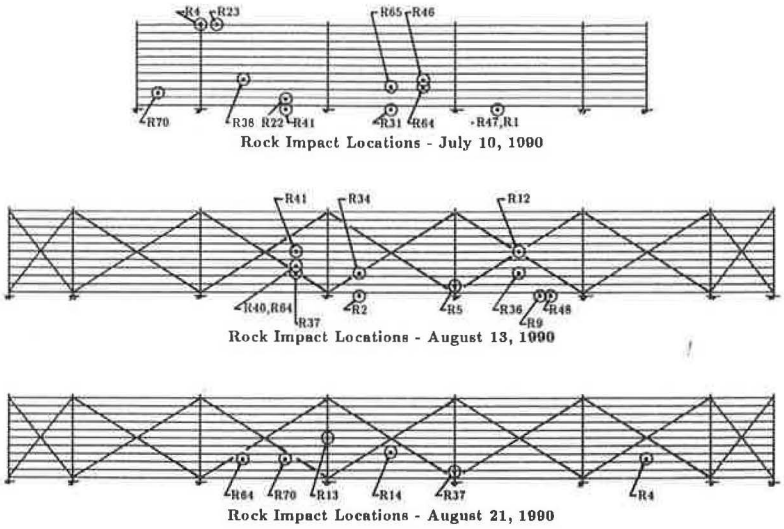

FIGURE 5 Flexpost field tests: rock impact locations.

A third prototype with a revised design was tested on August 13, and again on August 21, 1990. This August prototype had the same post height and spacing as the July prototype and in addition, had diagonal cable stays forming X-bracing in fence panels connecting post tops to post foundations. These stays take tensions during rockfall impact and protect the Flexpost strands. The August prototype was tested by 17 rockfall impacts out of 39 attempts (Figure 5). Of the impacts, 12 were stopped without damage, 2 tore the mesh, 1 bent a Flexpost (the rock was stopped), 1 tore a diagonal stay, and 1 tore the mesh and the top horizontal cable. Translational kinetic energy of the rockfalls ranged from 2,700 to 132,000 ft-lb. The August prototype withstood an impact with a translational kinetic energy of 29,600 ft-lb without damage, and was damaged by an impact of 58,700 ft-lb. The Flexposts were able to rebound throughout the 2 days of testing with no apparent loss of elasticity in strand groups. The cable stays provided adequate protection for the strands.

ROCKFALL CAPACITY OF FLEXPOST FENCE

Field Tests

The 1990 rockfall tests confirmed the mechanism of rockfall response proposed after the 1989 test. For impacts of low kinetic energy, the Flexpost fence responds through inertial resistance and through straining in mesh, cables, stays, and posts. The fence structure itself absorbs the rockfall kinetic energy. For more severe impacts, inertial and stiffness resistances remain, but a second mechanism is also observed. Large, fast-moving rocks stretch the fence fabric taut, which imposes centripetal accelerations on rocks and can lead them to impacts with the ground. For severe impacts, it is the earth, not the fence, that absorbs rockfall kinetic energy. Direct tensions in mesh and cables provide the primary means of capturing falling rocks and of altering their trajectories. Spring stiffness of Flexposts and inertial resistance of the fence masses are not significant contributors in halting large, fast-moving rocks.

The 1990 rockfall tests indicate that the rockfall capacity of the Flexpost fence is limited by the strength of the mesh. The mesh is usually the first element to fail, and its failure is associated with a specific level of rockfall energy. Other components were damaged in testing. In separate rockfalls, a diagonal stay was torn, a top cable was torn, and a Flexpost was bent. Posts and stays cannot deflect as easily as the mesh and may be damaged when hit squarely by a rock. Neither a bent post nor the loss of a stay will reduce the rockfall capacity of the fence, and indeed did not reduce the rockfall capacity of the prototypes. Loss of a stay may result in deformation of the strands in one post if there are repeated impacts after the stay is lost. The top cable failed along with the mesh in an impact directly on the top cable. Top cable failure is not a new more restrictive limit state for the fence.

Computational Analysis

A large-deformation, dynamic analysis program was developed to provide data on member forces, to compute fence response to rockfalls not observed in prototype tests, to establish the rockfall capacity of the fence, and to study design modifications. The program uses a time-step approach to compute node displacements and member forces during rockfall impact. The rock and the fence are treated as separate bodies. Information on rock position and on fence geometry is used to compute contact forces acting on fence nodes. Contact forces drive fence deformations and alter rock speed and trajectory. The analytical model of the Flexpost fence includes more than 300 lumped-mass nodes connected by a gridwork of mesh and cable members. Nodes occur at all post tops and foundations, in the mesh at post centerlines, and in the mesh at the midspan of mesh panels. Additional nodes 1 ft on center are placed in mesh panels near the location of rock impact.

This close spacing of nodes is required to model the contact of the rock with the fence fabric. Fence models with differing contact panels were prepared to handle various impact locations (see Figure 6). These models all correspond to the August prototype.

Mesh and cable members can carry tensions only (negative strains produce a computed zero-force value). Mechanical properties for cables have been taken from manufacturers' literature and developed from material tests for the gabion mesh (*2*). Flexposts are modeled as beam elements on spring mounts. Spring stiffness for post rotation is taken as the bilinear relation obtained from static tests. Rockfalls observed in the August tests were used as input rockfall cases for the dynamic analysis program (see Table 2). Fence deflections, member forces, and contact forces were computed. Analysis results were found to be in good qualitative agreement with observed performance of the prototype (for impacts that damage the fence, analysis results indicate member forces in excess of the expected breaking strength). Figure 7 shows a set of typical fence-deflected geometries during impact.

The influence of diagonal stays in the fence was investigated through a reanalysis of selected August rockfall cases using a fence model without stays. Analysis results indicate that mesh and top cable forces are lower for the fence without stays, because the fence is more flexible without them. Forces in intermediate cables are also lower, but the differences are not always great. Bottom cable force is increased. Lack of diagonal stays eliminates an important load path for transfer of fabric forces to the foundations and leaves much of this task to the bottom cable alone. Interior posts are always in compression when stays are present. Without stays, interior posts may experience net tensions.

To establish the rockfall capacity of the Flexpost fence, the dependence of member forces on rockfall energy, impact location (especially impact height), and design parameters such as post spacing was examined. It was found that member forces are proportional to the square root of rockfall kinetic energy. Plots of maximum forces in the top cable and in the interior stay cables are shown in Figure 8. Despite some scatter, a linear dependence is apparent for all components (correlation coefficients exceed 0.9). Maximum member forces only have a weak dependence on impact location. This result can be understood from an examination of deflected shapes of the fence. Most rockfalls are ultimately stopped near the top of the mesh, even when the initial impact occurs near the bottom. Rock impact near the bottom of the mesh will deflect the fence, and the fence will in turn exert forces tending to lift the rock. As a result, the pocket in the mesh that arrests the rock usually forms somewhere from the midheight to the top of the mesh. The Flexpost fence ushers rockfalls to its more compliant region, so the influence of initial impact height is minimized. It is therefore possible to state the rockfall capacity of the Flexpost fence in terms of limiting rock mass and velocity, without additional limits related to impact location within the fence. The curve of limiting rock velocity versus weight is presented in Figure 9 and indicates a limiting velocity of 41 ft/sec for a 1,000-lb rock and a limiting velocity

TABLE 2 FLEXPOST ROCKFALL FENCE: ROCKFALL INPUT CASES FOR DYNAMIC ANALYSIS

Test Date	Rock #	Rock Weight lbs	Impact Loc. X ft	Y ft	Z ft	Impact Vel. V_X ft/s	V_Y ft/s	V_Z ft/s
Aug.13	5	256	56	0	1	0.0	25.7	4.5
	40	6,040	36	0	4	-6.5	30.7	21.5
	64	597	36	0	4	-5.8	31.3	11.4
	36	1,390	64	0	3	6.5	11.3	0.0
	48	1,700	68	0	0	0.0	10.9	0.0
	37	797	36	0	3	3.1	34.9	6.1
	41	1,510	36	0	5	0.0	47.0	-17.1
	34	592	44	0	3	0.0	34.2	9.2
	9	1,620	67	0	1	-5.2	14.2	0.0
	12	1,360	64	0	5	0.0	37.5	0.0
Aug.21	37	797	56	0	1	0.0	43.1	7.6
	13	305	40	0	5	0.0	31.3	-11.4
	14	1,280	48	0	4	0.0	30.2	14.1
	64	597	29	0	3	0.0	15.7	7.3
	70	750	35	0	3	0.0	24.8	14.3
	4	3,600	80	0	3	-7.3	18.0	9.0

Coordinate origin is ground surface at the end of the fence. X is measured along the fence. Z is the gravity axis.

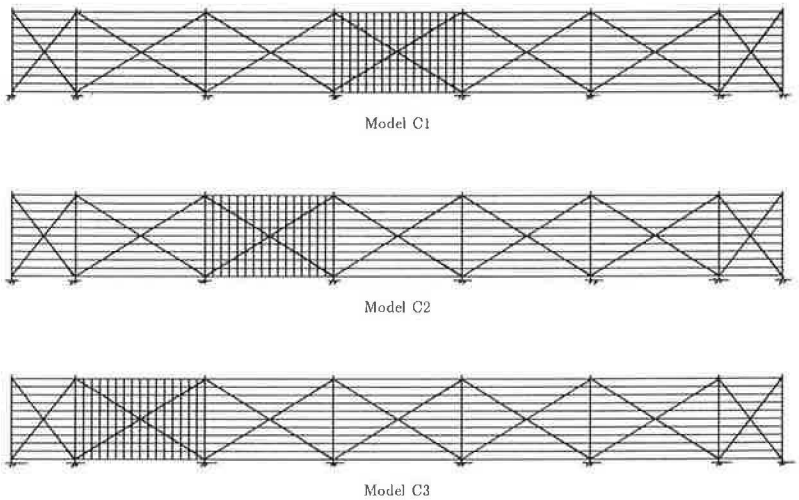

FIGURE 6 Flexpost rockfall fence: models for contact problem.

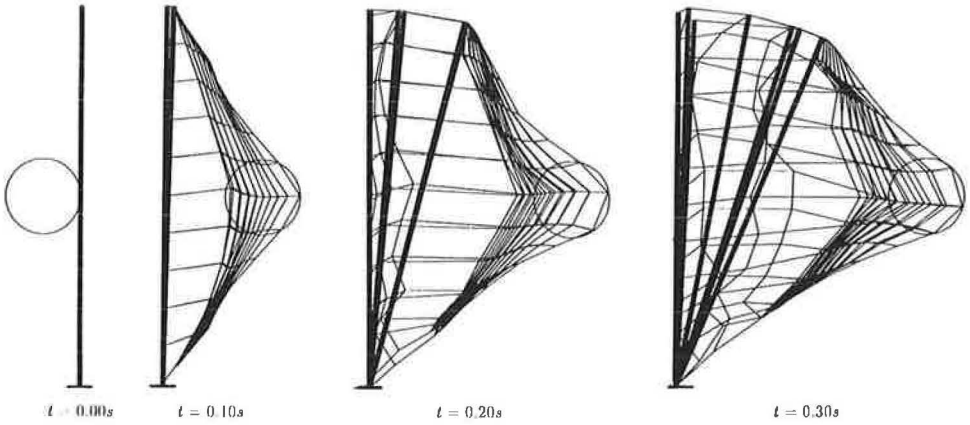

FIGURE 7 Flexpost rockfall fence: response to rock impact.

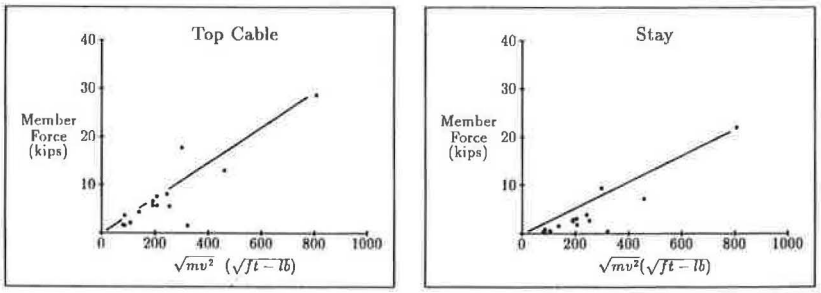

FIGURE 8 Flexpost rockfall fence: member force versus square root of rockfall kinetic energy.

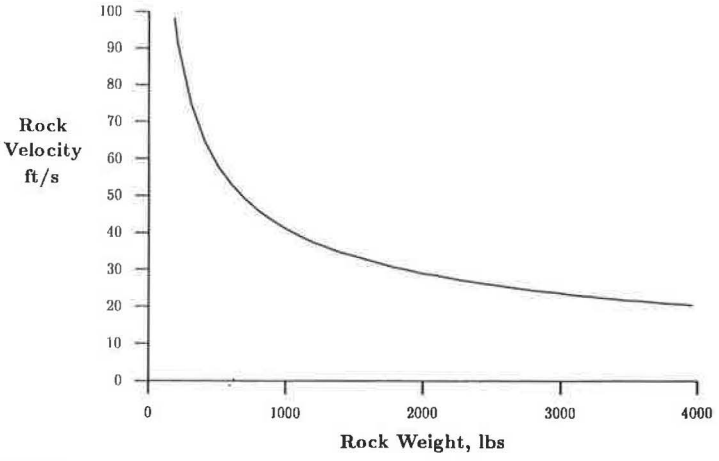

FIGURE 9 Flexpost rockfall fence: limiting rock velocity versus rock weight.

TABLE 3 FORCES IN COMPONENTS LIMIT STATE: MESH RUPTURE

Component	Force lbs
Top Cable	5,500
Rnf. Cable, Top	3,800
Rnf. Cable, Mid	6,900
Rnf. Cable, Bott	5,500
Bottom Cable	10,600
Stay, End	9,200
Stay, Interior	5,800

of 29 ft/sec for a 2,000-lb rock. Forces in other members corresponding to this limit state are given in Table 3.

For foundations at end posts, shear force at mesh limit can be expected to be about 5,000 lb and uplift about 5,700 lb. Interior post foundation will experience shear force of 3,300 lb and uplift of 800 lb. Additional information on Flexpost fence analysis may be found elsewhere (*3*).

FLEXPOST FENCE USE IN COLORADO

The first service installation of a Flexpost fence was completed in 1990 along I-70 in Glenwood Canyon. This fence has a total length of 580 ft and is similar in design to the 1989 prototype. The bid price of the installation was $65/ft. Rockfall hazard at the site is estimated to be as severe as a 700-lb rock travelling at 45 ft/sec. Rockfall hazard was estimated from data obtained in a site survey and statistical information on rock velocities and bounding heights computed by the Colorado Rockfall Simulation Program (*1*,*4*). Additional installations are planned for several miles of fence along highways in Colorado, beginning with a major rockfall remediation project in Glenwood Canyon.

In addition to its effectiveness as a protective structure, and its obvious economy, the Flexpost fence is easily maintained. There are no structural members out of the plane of the fence to hamper movement of equipment. Mesh can be easily repaired by patching, and other components may be either spliced or replaced piecewise as necessary. Compared with other rockfall protective structures, the visual impact of the Flexpost fence is minimal.

SUMMARY

Flexposts are the important source of elastic compliance in the rockfall fence. Compliance allows the fence to exercise its fabric of mesh and cables in tension as the primary load-carrying members. Since rockfall capture is achieved by direct tension in the fabric, the rockfall capacity of the fence does not depend on the spring stiffness of Flexposts. Impact height, a concern for structures that function by developing resisting base moment, is not a concern for the Flexpost fence. On the contrary, since centripetal force varies inversely with the radius of a rock's arc, high impacts mean reduced forces in the fabric. Flexpost fence height is limited only by dead weight demand on posts. Flexposts must possess sufficient stiffness to keep the fence upright. For a post spacing of 16 ft, the limiting fence height is about 15 ft for the present Flexpost construction.

The Flexpost rockfall fence minimizes impact forces by allowing large deflections. Fence deflections are elastic; the fence rebounds after impact. Two years of testing, development, and analysis have produced an efficient structure of known capacity and proven performance.

REFERENCES

1. R. K., Barrett, T. Bowen, T. Pfeiffer and J. Higgins. *Rockfall Modeling and Attenuator Testing*. Colorado Department of Highways, Denver, 1989.
2. A. P. Kabaila. *Report on Structural Study of Two Types of Gabion Mesh*. Unisearch LTD., University of South Wales, Kensington, NSW, Australia, 1979.
3. G. Hearn. *CDOT Flexpost Rockfall Fence—Review of Field Tests and Development of Dynamic Analysis Program*. Colorado Department of Transportation, Denver, 1991.
4. T. J. Pfeiffer and T. D. Bowen. Computer Simulation of Rockfalls. *Bulletin of the Association of Engineering Geologists*, Vol. 26, No. 1, 1989, pp. 135–146.

Publication of this paper sponsored by Committee on Engineering Geology.

Flexible Wire Rope Rockfall Nets

JOHN D. DUFFY

The California Department of Transportation field tested and evaluated wire rope rockfall nets designed to absorb and dissipate rockfall impact energies as high as 200 kilojoules (70 ft-tons). The nets were supplied by Brugg Cable Products of Switzerland, and L'Entreprise Industrielle of France. Over 80 tests were conducted in which rocks weighing 136 to 5900 kg (300 to 13,000 lb) were rolled down a 76-m (250-ft) long, 34-degree slope. Rockfall impact energy was calculated by adding translational kinetic energy and rotational kinetic energy. Wire rope net energy dissipation was analyzed. The nets stopped rocks delivering impact energies up to 2.5 times design load with acceptable levels of maintenance. Maintenance and cleaning of the nets was easily accomplished by personnel using normal equipment and supplies. Damaged net components were repaired in a few minutes to 4 hr by maintenance crews. Wire rope rockfall catch nets will become a part of the rockfall mitigation measures available for use along California highways.

The purpose of this research project was to construct, test, and evaluate the effectiveness of flexible wire rope rockfall nets that will be used to mitigate rockfall. All aspects of the installation and performance, including field repair and cleaning, were evaluated.

Two manufacturers participated in this research: Brugg Cable Products of Switzerland and L'Entreprise Industrielle (EI) of France. Both manufacturers had tested their systems under controlled conditions (*1,2*), but no testing had been done under actual field conditions. Therefore, the California Department of Transportation (Caltrans) conducted tests and evaluations of these systems before the installation of a state project (*3*).

Brugg's system was constructed and tested by Caltrans personnel on August 8 through August 11, and again from November 13 through November 16, 1989. The EI system was constructed and tested on December 4 through December 7, 1989.

DEFINITION OF ROCKFALL NET

A rockfall net is a flexible barrier capable of catching and containing falling rocks (see Figure 1). This capability is a result of the net's design as a flexible system rather than as a standard, fixed-wire fence system. A properly designed barrier is flexible enough to absorb the anticipated energy with minimum damage to the system. Considerable flexibility is inherent in both the net material and the support wire rope infrastructure. Additional flexibility is added by using energy-dissipating friction brakes, which are attached to the wire rope support system and dissipate energy through friction as the wire ropes are pulled in tension. The two rockfall net systems tested by Caltrans consisted of rectangular panels of woven wire rope vertically supported by steel posts and designed with frictional brake elements. Both systems utilize woven wire rope with a fiber core. This construction provides greater flexibility than conventional steel-core cable.

California Department of Transportation, 50 Higuera Street, San Luis Obispo, Calif. 93401.

ROCKFALL NET DESIGNS

Both Brugg's and EI's woven wire rope net panels were 5 m (16.4 ft) wide and 3 m (9.84 ft) high. The panels were formed by weaving a single, continuous 9.5-mm (3/16-in.) wire rope into a 200-mm × 200-mm (8- × 8-in.) diagonal pattern around a wire rope border. Brugg net grid intersections were secured with machine-crimped fasteners fabricated from mild steel that had been coated with a corrosion-resistant zinc compound, whereas EI secured intersecting points with modified stainless steel cable clips. Both nets were covered on the impact side with chain-link mesh that was connected with wire ties on 0.6-m (2-ft) spacing. Chain-link mesh was used because of its flexibility.

Brugg's panels were connected to an 18-mm (3/4-in.) perimeter wire rope (minimum tensile strength, 24 tons) with 9.5-mm (3/16-in.) wire rope lacing (see Figure 2). Adjacent net panels were also connected together with lacing. The perimeter wire rope was fitted at the top and bottom of each panel with a single friction brake (minimum tensile strength, 22 tons).

Brugg friction brakes consisted of a loop in the wire rope secured with a heavy friction clamp and four bolts. The bolts were tightened to a specified torque to provide the desired tensile strength. When forces exceed this value, the brake is activated and the loop closes when the cable slips through the friction clamp. Brugg nets were suspended by wire ropes attached to 200-mm (8-in.) wide flange steel posts secured to the ground by concrete foundations and wire rope stanchions (see Figure 3). The upslope wire ropes were fitted with a friction brake (minimum tensile strength, 13.5 tons).

EI woven wire rope panels were not hung from a perimeter wire rope, but directly attached to the support posts (see Figure 4). Adjacent panels were joined together with steel bands. EI's friction brakes are four-bolt clamps shaped to accommodate two wire ropes that are sandwiched between them and tightened to a predetermined amount by applying a torque to the bolts. Each brake is preset to a minimum tensile strength of 2.75 tons. Instead of wire rope loops as used in the Brugg system, EI's brakes have excess wire rope exiting the brake. The excess wire rope is designed to slip through the braking device under tension. The length of this wire rope is predetermined and corresponds to anticipated

FIGURE 1 Brugg flexible rockfall net in action (rock weighs 3 tons) (Courtesy of John Walkinshaw, FHWA).

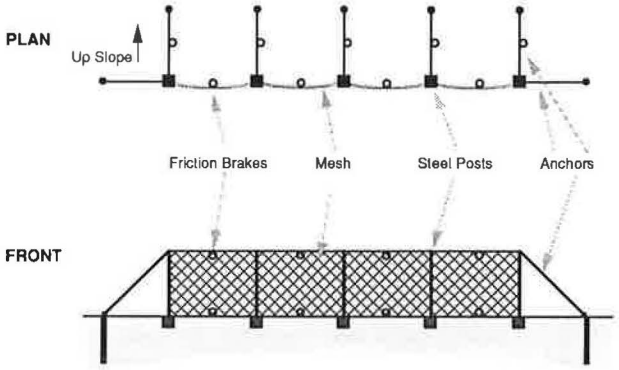

FIGURE 2 Typical plan view and front view of Brugg rockfall net.

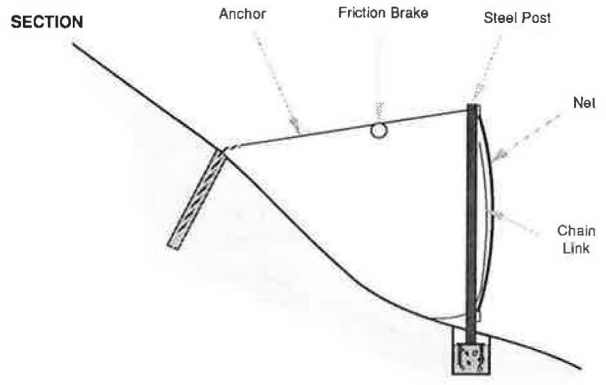

FIGURE 3 Typical side view of Brugg rockfall net.

energy dissipation. Short sections of chain, referred to as a fuse link, connect the friction brakes to fixed locations at each panel corner and ground anchor location.

EI nets were supported by four 140-mm (5½-in.), 4-mm (5/32-in.) galvanized steel box posts. A concrete foundation is not required for the EI rockfall net. Instead, the base of each steel post rests on the ground and is secured by 0.6-m (2-ft) long steel stakes driven through post baseplate holes into the ground. Each post was supported by three 12-mm (½-in.) guy wire ropes looped over the top (see Figure 5). The two end posts had a similar guy wire rope attached to lateral anchors. A single 6-mm (¼-in.) wire rope was attached to both the base of the posts and the upslope anchors to restrict the movement of the base of the post.

TEST PROCEDURE

In order to observe and analyze the flexible rockfall nets under field conditions, nets were constructed at the base of a slope and boulders of various sizes were rolled down the slope into the nets. Brugg's test section was 19.5 m (64 ft) long and 3 m (10 ft) high. EI's test section was 15 m (49 ft) long and 3 m (10 ft) high. The slope used for the tests was 40 m (130 ft) high and 65 m (215 ft) long with an overall slope angle of 34 degrees (see Figure 6). The slope measured along the ground surface was 76 m (250 ft) long. Relative to the rockfall diameters, the slope was smooth and did not greatly affect rockfall trajectories. There were, however, several gullies that affected rockfall trajectories of small, 0.3- to 0.6-m (1- to 2-ft) diameter boulders. Vegetation was sparse and had little, if any, effect on rockfall trajectories.

The slope material was composed of landslide debris consisting of 25- to 450-mm (1- to 18-in.) rock fragments in a matrix of clayey silt. This material was dry and hard during all three tests. However, in some areas, successive boulder rolls broke up the surface and created soft spots in the slope that seemed to decrease the velocity of some boulders. Test boulders were composed of hard, competent rock with a specific gravity ranging from 2.91 to 3.03. For test purposes, many of the rocks selected were round. Eighty boulders were rolled.

Before rock rolling, the three principal axes (x, y, and z) of each boulder were measured and the values were used to estimate rock weight and inertia. Fifteen boulders were accurately weighed with a load cell. Rock weights ranged from 136 kg (300 lb) to 5,900 kg (13,000 lb). Rock rolling was recorded on video and high-speed (16-mm) film from four locations along the slope. Four cameras captured two side, one oblique, and one front view.

Reference lines at 15-m (50-ft) intervals were placed on the slope perpendicular to the slope axis, which allowed detailed measurements of rockfall velocities. In addition, stadia rods 1 to 2 m (3 to 6 ft) high were randomly placed on the slope for bounce height analysis.

The nets were examined periodically during testing and net performance was recorded while repairs were made between rock rolls when necessary.

Rockfall Energy Analysis

Kinetic energy is the most common measurement used to describe rockfall for engineering design. According to Chasles' theorem, any general displacement of a rigid body (boulder) can be represented by a translation plus a rotation (*4*). On the basis of this theorem, the process of rockfall is made up of two components—translational motion and rotational motion—which can be quantified as energy in motion,

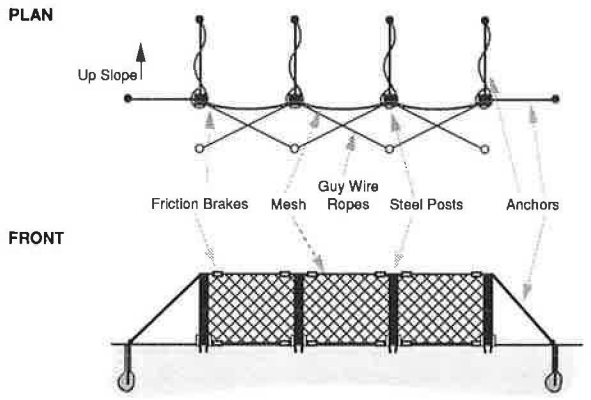

FIGURE 4 Typical plan view and front view of EI rock net.

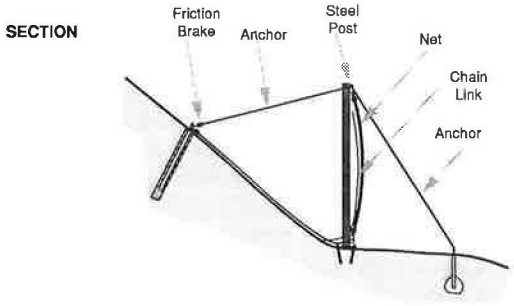

FIGURE 5 Typical side view of EI rockfall net.

or kinetic energy. Calculation of these kinetic energies (KE) is based on the assumption that the mass of the boulder is concentrated at the center of mass, and its motion revolves around the center of mass (*4*). Rockfall motion is therefore the sum of the translational kinetic energy (KE_T) and the angular kinetic energy (KE_A) (*5–7*). This sum, the total kinetic energy (KE), is expressed mathematically as

$$\text{Total } KE = KE_T + KE_A = 1/2mv^2 + 1/2I\omega^2 \quad (1)$$

where

m = mass of the boulder,
v = velocity of the boulder just before impact,
I = moment of inertia of the boulder as it spins, and
ω = angular velocity of the spinning boulder just before impact.

Rockfall kinetic energy is most commonly described in units of foot-tons, foot-pounds, or kilojoules.

Dynamic Load Path Analysis

The dynamic load path analysis was performed in an attempt to determine the forces occurring within individual net components. This information was used to study the net system and how the load is distributed. Because of the difficulties of analyzing dynamic loading, broad assumptions were made in this analysis. Therefore greater reliance should be placed on empirical field performance in the design of nets.

Rocks striking the net generate forces throughout the net system that are dissipated through the flexibility of the net. These forces emanate from the point of impact to the net system perimeter and apply loads that travel along a load path (Figures 7 and 8). The load path consists of several structural net components with various strengths and load-dissipation capabilities. When all components in the load path are in equilibrium, the net system is balanced. A balanced net system is the optimum design for load-carrying capacity.

Three rockfall impacts were analyzed dynamically to identify the load path and the loads within the load path. This was accomplished by analyzing the film footage of actual tests and using those data in the calculations.

Such events are analyzed using the vector quantities of impulse and momentum:

$$Ft = mv$$

$$\text{Impulse} = \text{momentum change} \quad (2)$$

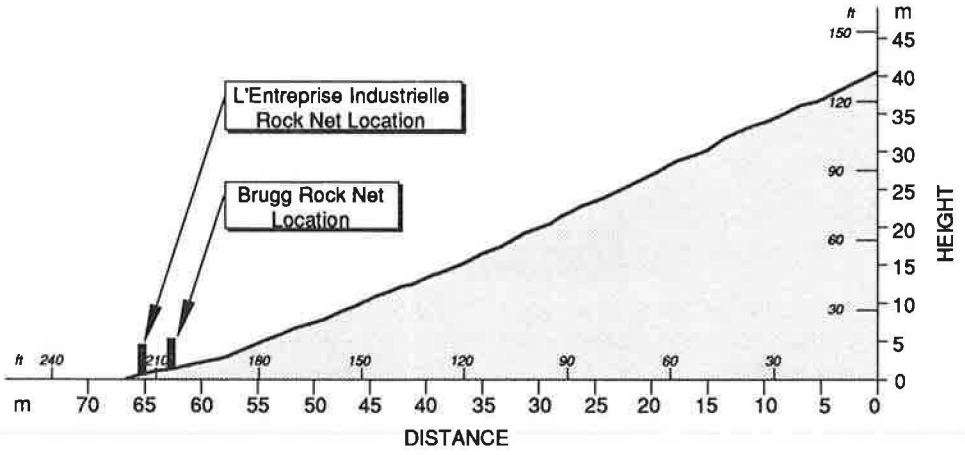

FIGURE 6 Cross section of test slope.

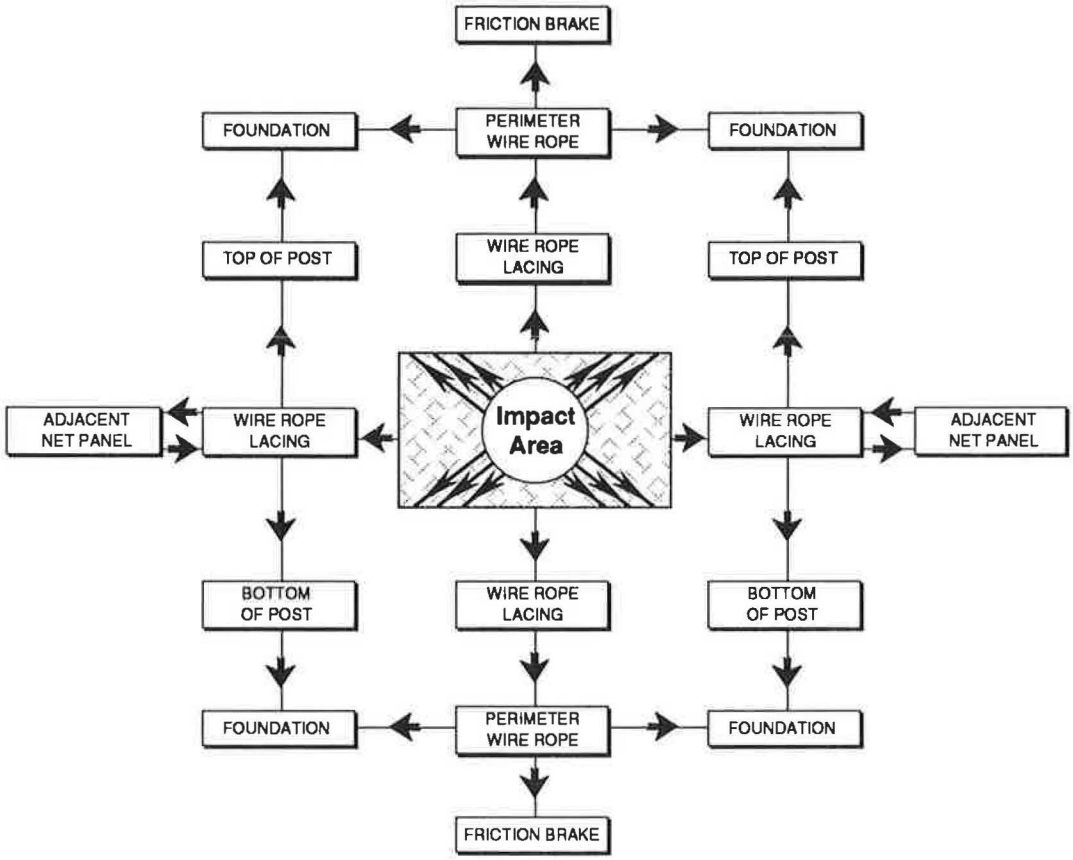

FIGURE 7 Flowchart of Brugg net system load path (arrows indicate direction of rock impact energy).

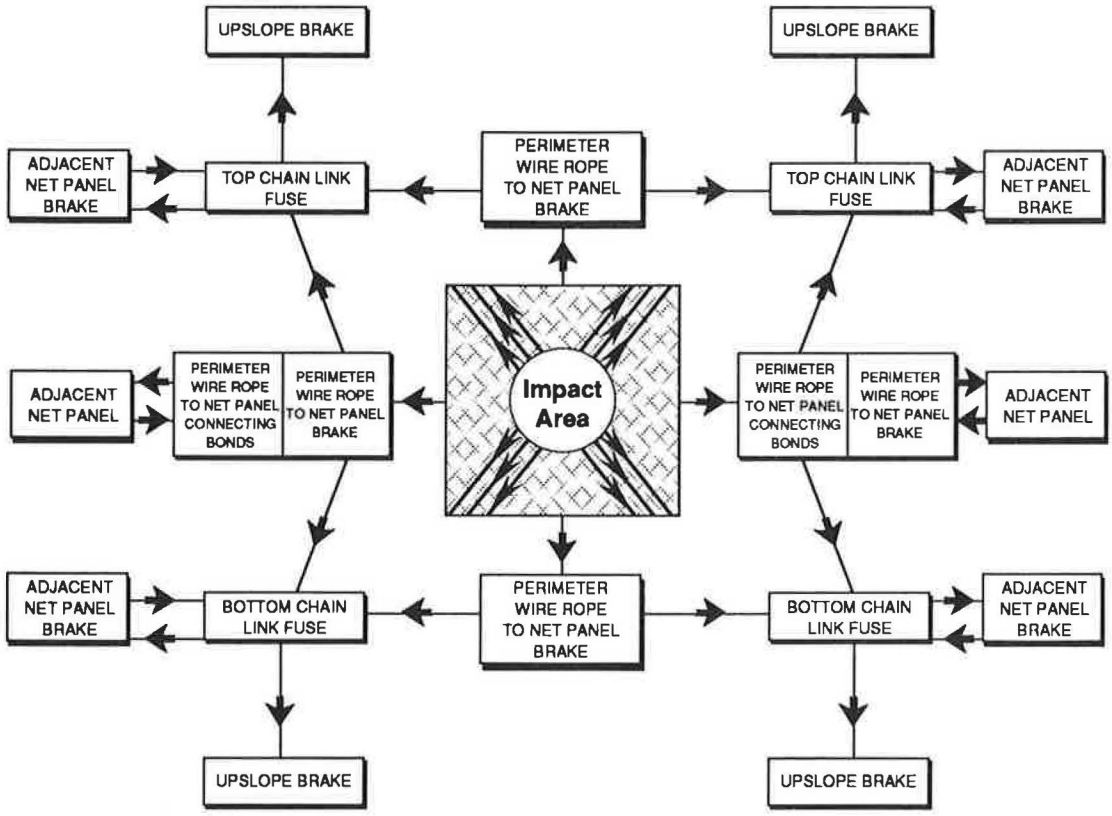

FIGURE 8 Flowchart of EI net system load path (arrows indicate direction of rock impact energy).

where

F = applied force,
t = time the boulder takes to decelerate to zero,
m = mass of the boulder, and
v = translational velocity at the initial point of impact (7).

An attempt was made to calculate the distribution of the impact loading. Because of the difficulty of mathematically predicting dynamic loading, an idealized net system was assumed. This system consisted of a 200-mm (8-in.) mesh attached to a 18-mm (¾-in.) perimeter cable. It was assumed that the rock struck the center of the net panel, although in actual testing the rocks hit all areas of the nets. This idealized analysis indicated that under the assumed conditions, the load per 100 percent loaded net strand is 2,024 kg (4,463 lb). The load in the top and bottom perimeter wire rope, where the load-dissipating friction brakes are located, was 11,984 kg (26,421 lb) in the outer third of the wire rope, 5,180 kg (11,425 lb) in the middle third of the wire rope, and 5,365 kg (11,829 lb) in the upslope anchor cable.

The values obtained in this analysis are based on broad assumptions. For detailed net design, empirical field test data should be used.

PERFORMANCE OF ROCKFALL NETS

The specified design load was 200 kJ (70 ft-tons) of impact energy. This value was intentionally exceeded to evaluate the maximum capacity of the nets. Throughout the tests, the nets were examined periodically. Typically, the nets were inspected when damage was observed. Net performance was recorded while necessary repairs or adjustments, or both, were made before the next rock-rolling sequence. Particular attention was given to maintenance of the nets.

Brugg Testing

Brugg's rockfall nets caught and contained rockfall impacts 2.5 times greater than the design load within acceptable levels of maintenance. Impacts 2 to 3.5 times greater than the design load were stopped, but maintenance was considerable. For impacts exceeding 3.5 times the design load, rock energy was attenuated but the rock passed through the net. Significant reductions in maintenance were achieved when 2.5-mm mild steel net-panel fasteners were used, when support cables were not fixed to the posts, and when chain-link mesh was used to cover the impact side of the net. Brugg's energy-absorbing friction brakes rarely activated, and weaker components in the energy path were consequently loaded to failure.

EI Testing

EI's rockfall nets caught and contained rockfall impacts 1.5 times above design load with acceptable levels of maintenance. One rock impact that was 2 times the design load was not stopped by the net. Significant reductions in maintenance could be achieved by increasing post strength to the equivalent of the posts used in the Brugg tests, and also by increasing net-panel connector strengths. EI's energy-absorbing friction brakes activated easily, even when rocks struck the net at less than the design load. As a result, net panels sagged considerably after only two rock impacts.

MAINTENANCE OF ROCKFALL NET SYSTEMS

Considerable interest has been expressed by maintenance personnel throughout California concerning the amount of repair and methods for cleaning rock-restraining nets. Because maintenance is an important consideration in the use of the nets, a significant effort was made during these tests to evaluate rock net maintenance.

Input was solicited from maintenance personnel during all phases of this study. It was concluded that rock nets could be maintained within acceptable limits using standard maintenance equipment and procedures. In most cases, repairs and cleaning were completed in 1 to 4 hr. It was determined during the study that rockfall accumulations behind a single panel could be removed easily and quickly while still providing maximum protection to workers and the traveling public. Access for clearing boulders and rockfall debris from the rock nets was gained by disconnecting the net panel along the top or bottom, and then raising or lowering the net panel.

In summary, cleaning and repair of a rock net restraining system can be accomplished by a typical maintenance crew using readily available tools such as ratchet wrenches and sockets, torque wrenches, come-alongs, pry bars, and, where possible, front-end loaders.

CONCLUSIONS

- Design load rockfalls were effectively stopped by both rock nets.
- Repair and cleaning are required and can be done quickly and safely with equipment that is readily available at all maintenance stations.
- Brugg net panels deflected downslope by as much as 2 m (6 ft) under the design load.
- EI's net panels deflected downslope by as much as 3 m (12 ft) under the design load.
- EI's net system requires more space than the Brugg system to accommodate downslope anchors and downslope deflection.
- Chain-link mesh is an integral part of the net design. The mesh prevents small rock fragments from passing through the net and reduces net damage.
- Brugg's friction brakes rarely activated. As a result, the energy that should have been dissipated by the brakes was transferred to other net components.
- EI's friction brakes were effective in dissipating energy, but activated so easily that the nets sagged considerably even after a single design load impact.
- EI's net posts were damaged by direct impacts below design load, requiring replacement or repair.
- Both foundation anchor designs provided adequate support to the net system.

- Proper selection of a rock net requires a detailed site investigation to determine rockfall trajectories and impact energies.

RECOMMENDATIONS

The following recommendations are intended to serve as a guide to reduce maintenance on rock nets designed to contain 200 kJ (70 ft-tons) of energy:

- Proper selection and design of rockfall mitigation measures should be based on a detailed site investigation. This includes, but is not limited to, determining slope geometry, rockfall size and frequency, and an analysis of rockfall trajectories and impact energies.
- The Brugg 2.5-mm mild steel net fasteners are recommended for use with their system.
- Attaching chain-link fencing to the net panels is recommended.
- All attachments of the Brugg net panels should be made exclusively to the perimeter wire rope and adjacent panels, rather than to the posts.
- When lacing is used to attach Brugg net panels, 8-mm (5/16-in.) wire rope lacing should be used to prevent net-panel failure.
- Brugg 18-m (3/4-in.) friction brake tensile strength should be reduced to balance the impact load distribution, which will reduce the need for repairs.
- EI 16-mm (5/8-in.) friction brake tensile strength should be increased to better balance the impact load distribution and reduce excessive net sag after impact.
- EI support post strength should be increased to that of a W8 × 48 steel post to eliminate the need for post replacement.

REFERENCES

1. W. Heierli. *Protection from Rock Slips and Falling Rock by Means of Steel Wire Nets.* Shultz gegen Felssturz und Steinschlag mit Drahtseilnetzen (German). Schweiz, Bauztg, 1976, pp. 611–614.
2. P. Paronozzi. Probabilistic Approach for Design Optimization of Rockfall Protective Barrier. *Quarterly Journal of Engineering Geology*, Vol. 22, 1989, pp. 175–183.
3. J. D. Duffy and D. D. Smith. *Field Tests and Evaluation of Rockfall Restraining Nets.* Research Report CA/TL-90/05. California Department of Transportation, 1989.
4. H. Goldstein. *Classical Mechanics.* Addison-Wesley Publishing Company, Philippines, 1950, pp. 9–203.
5. A. Beiser. *Applied Physics*, 2d ed., Schaum's Outline Series. McGraw-Hill, New York, 1988, pp. 37–97.
6. J. L. Meriam. *Engineering Mechanics*, Vol. 1: *Statics*. John Wiley & Sons, New York, 1978, pp. 351–391.
7. P. A. Tipler. *Physics.* Worth Publishers, Inc., New York, 1976, pp. 33–80.

Publication of this paper sponsored by Committee on Engineering Geology.

Landslide Correction Costs on U.S. State Highway Systems

JOHN WALKINSHAW

The results of a survey made to estimate the cost of landslide damage to the U.S. state highway system in the 5-year period from 1986 to 1990 are presented. The annual contract repair costs are compared with a similar survey prepared in 1976. Maintenance costs for landslide cleanup or repairs were also obtained from about half of the states. The average yearly cost of all contracts awarded by state highway departments during the 5-year period amounted to $68.5 million. Another $37.4 million per year was identified as maintenance costs. There is significant evidence that these costs are only a fraction of the total annual costs of landslides to the state highway network.

This study was prompted by members of a Transportation Research Board Task Force updating *Special Report 176, Landslides: Analysis and Control* (*1*). In 1976, Chassie and Goughnour (*2*), of the Federal Highway Administration (FHWA), reported that $50 million was spent annually to correct landslides on the Federal-aid system. At that time, the Interstate highway system was in full construction and several regions were experiencing large costs because of the lack of adequate preliminary geotechnical investigation and analysis. Some of these problems developed during construction, but others took many years to manifest themselves. The improper placement of degradable shales in large embankments (*3,4*) was one of these problems. Research to properly identify this material and to develop test procedures and implement them in several states cost around $1 million.

Since the FHWA survey was limited to Federal-aid routes under state control, Chassie and Goughnour further projected the average annual cost to be around $100 million for all state highway systems. That survey prompted reviews of the level of geotechnical engineering practiced in each state highway department. Those reviews continue to be updated periodically (*5*) and the results give direction to FHWA's geotechnical research program and the development of training courses through the National Highway Institute.

Once the Interstate Highway System was essentially complete, it was of interest to determine the magnitude of landslide correction across the country. To accomplish this, a one-page survey (see Figure 1) was sent to each state and to three Federal Lands Highway Divisions (FLHD) of FHWA asking for representative costs of landslide corrections during the past 5 years. The FLHD offices administer projects on federal lands such as national parks and forests within each state.

The 5-yr period was short and in certain parts of the country may not be representative of the long-term (20 to 30 years) problem. It was deemed important, however, to get a response from as many states as possible, as a lengthy survey that required an in-depth review of past records would have severely reduced the returns. This philosophy appears to have been successful; only two states did not respond and, significantly, only four states indicated that they had no identifiable landslide costs for the period.

Even though the response was excellent, it must be recognized that the survey was directed principally at obtaining costs on highways under state control. According to FHWA (*6*), this represents 803,400 mi (1,292,900 km) or only 20.7 percent of the 3,876,500 mi (6,238,400 km) of roadways under public agency jurisdiction in the United States.

Federal Highway Administration, 211 Main Street, Suite 1100, San Francisco, Calif. 94105.

SURVEY RESULTS

A summary of the responses to the survey is presented in Table 1. This survey attempted to get representative costs for two types of repairs:

1. Those repairs sufficiently large to require each agency to contract the work, and
2. The landslide repair costs performed by maintenance.

For the second category, only 23 of the 50 states were able to provide some data. Although these data are not as complete, they are very revealing and will be discussed later.

Contract Costs

The average annual contract value of landslide repair is shown in Column 1 of Table 1 and graphically shown on a map of the United States in Figure 2. Column 2 of Table 1 identifies the total number of contracts over the 5-year period. Thirteen of the 51 respondents (25 percent) had less than one contract project per year.

Seven states and two FLHDs reported some unusual natural disaster (storms, earthquake, etc.), which may have skewed their average as reported in Columns 4A and 4B. California's Loma Prieta earthquake in October 1989 was one of these events. On the other hand, the California Department of Transportation (Caltrans) believed that the 5-year period chosen was not representative of the annual costs because of an unusual series of dry winters. Consequently, the value shown is considered to be on the low end of the expenditures for landslide corrections in California. Having lived in California since 1975, the author can confirm this observation from personal experience. Major-storm disaster declarations have

TRB TASK FORCE A2T61. Landslides: Analysis and Control
(Revision of Special Report 176).

Using the following basic definition of a landslide. "A landslide is the movement of a mass of rock, earth or debris down a slope".

Please answer the following questions and return the form no later than March 29, 1991, to the address below. Please write in your State name here._____

1. Over the past five years, what is the average annual cost of highway contracts let to correct landslides? _____

2. How many contracts does this represent? _____(5yrs)

3.a. Are landslides a significant cost on grading projects?
NO_____ Yes_____

b. In your opinion, if the costs of landslide mitigation on grading projects were added to 1 above, the annual costs would stay the same____ Double____ Triple____ Quadruple or more____

4.a. Over the past five years, has any disastrous event occurred to skew the above answers? No_____ Yes_____

b.If yes, please give the high $_____ and low $_____ annual costs and explain the event below.

5.a. In order to maintain a safe roadway surface, are landslide related activities by maintenance an identifiable cost in your state? No_____ Yes_____

b. If not, in your opinion do you feel it would be an appreciable cost? No_____ Yes_____

c. If yes to 5.a. please report the average annual maintenance cost for your department $___ and give an estimate of what percentage of the highway maintenance cost this represents ___%.

Additional comments: _____

_____

Optional: Your name_____
Would you like to receive a copy of the national tabulation?
No____ Yes____ (include business card)

FIGURE 1 Survey questionnaire: landslide mitigation costs on state highway systems.

occurred in 1978 (Los Angeles), 1980 (Los Angeles–San Diego), and 1982–1983 (San Francisco to Reno, Nevada), none of which are covered in the survey period of 1986 to 1990. In the 1978 and 1980 events, the total damage to property (not just highways) by landslides was reported to be $120 million (*7*). In the 1983 event, the closure of U.S. Highway 50 by landslides both east and west of South Lake Tahoe caused major economic loss to this resort area. The cost of repairs to the highway was $2.2 million at the California site and $1.4 million at the Nevada site. The estimated economic loss due to 2½ months of access disruption was $70 million (*8*, p.2). This is just one illustration that repair costs greatly underestimate the public's total cost due to landslides on highways or any transportation system.

As expected, the states with the large costs are those that include the principal mountain ranges. In addition, more is spent in those states with large populations or high densities along the East and West coasts. The total annual cost of contract landslide repairs on state highways is $68.5 million (see Table 2, Column 7), which averages out to be $472,000 per contract. On federal lands, the average repair cost is $881,900 per project. The high cost of this last group is most likely due to the remoteness of the sites in the federal land and parks, severe environmental constraints, and the need to keep access open to large numbers of visitors during construction.

It is also interesting to compare the costs by FHWA Region, as presented in the previous survey and summarized in Table 2. In Column 2, the 1976 costs are reported. If one inflates the 1976 costs by the national Construction Cost Index (*9*) for common excavation from 1976 to 1990 ($1.03/yd^3 to $2.38/yd^3; the factor is 2.31), the differences in expenditures by region between the two surveys from 1976 to 1990 can be evaluated by comparing Columns 3 and 4.

In the Northeast (FHWA Regions 1 and 3), the expenditures (in constant dollars) have remained essentially the same between the two periods. In the Southeast (Region 4) the annual costs have been reduced by 50 percent, but this region still has the highest average cost per state project in the nation ($824,000).

The Central portion of the United States (Regions 5, 6, and 7) shows the greatest reduction (75 percent) in landslide costs between 1976 and 1990, and also the lowest average repair costs ($215,400). Considering that the topography in the central United States is more level, this should be expected.

In the West, the trends are mixed, with an overall reduction of 35 percent. The Rocky Mountain region shows a dramatic reduction of 65 percent, and the Northwest (Region 10), an

TABLE 1 SUMMARY OF RESPONSES TO SURVEY QUESTIONNAIRE

QUESTION	1	2	3A		3B				4A		4B		5A		5B		5C	5C	RESPONDENTS TO QUESTIONNAIRE
STATE	AVE/YR $1000's		NO	YES	SAME	2X	3X	4X	NO	YES	HIGH	LOW	NO	YES	NO	YES	$1000's	%	AND COMMENTS
MAINE	300	10																	
NEW HAMPSHIR	500	10		X		X			X					X			500	1.00	NH: F. E. PRIOR
VERMONT	200	5	X		X				X				X		X				VT: C. C. BENDA
MASSACHUSETT	1000	25	X		X				X					X			2000	2.00	MA: N. M. HOURANI
RHODE ISLAND	0		X		X				X				X		X				RI: J. A. DIFILIPPO
CONNECTICUT	100	3	X		X				X				X		X				CT: S. M. ZYSKOWSKI
NEW YORK	6000	7	X		X					X	6000	1000		X			426	0.20	NY: E. A. FERNAN (A)
DELAWARE	0	0	X		X				X				X		X				
PENNSYLVANIA	10000	105		X		X			X				X			X			PA: C. T. JANIK (B)
NEW JERSEY	0		X			X			X				X		X				
WEST VIRGINIA	1288	33		X		X			X					X			2241	1.50	WV: G. L. ROBSON
MARYLAND	200	4		X				X		X	1000	25		X			25	0.02	MD: A. D. MARTIN (C)
VIRGINIA	NR																		
KENTUCKY	2009	10		X		X	X		X					X			2770	3.00	KY: E. H. ADAMS
TENNESSEE	1000	15	X			X			X					X			(D) 762	2.00	TN: W. D. TROLINGER (D)
NORTH CAROLIN	3000	5	X		X					X	6000	500		X			1500	5.00	NC: P. A. KEANE
SOUTH CAROLIN	320	3	X			X			X				X		X				SC: F. MCRANEY
GEORGIA	100	10	X			X				X	1200	200		X			600	0.50	GA: B. R. MCWHORTER
ALABAMA	1758	7	X		X				X				X		X				AL: S. ARMSTRONG
MISSISSIPPI	5000	30	X		X				X				X		X		1000		MS: J. D. WEBB
FLORIDA	0		X						X				X						FL: J. CALIENDO
MINNESOTA	500	3	X		X				X				X		X				MN: R. A. ADOLFSON
WISCONSIN	400	4	X		X				X				X		X				WI: C. A. LAUGHTER
MICHIGAN	50	2	X				X		X				X		X				MI: D. D. DOLPH
ILLINOIS	1436	26	X		X				X					X			150	0.05	IL: J. S. DHAMZAIT
INDIANA	300	12	X		X				X					X			200	6.00	IN: W. D. DAVIS (E)
OHIO	NR																		
NEBRASKA	100	6	X		X				X					X			100	0.20	NE: K. CHENEY
IOWA	87	7	X					X					X		X				
KANSAS	600	25	X		X				X				X			X			KS: J. J. BRENNAN
MISSOURI	231	15	X		X				X					X			458	0.22	
OKLAHOMA	489	5	X		X				X				X			X	106		OK: J. B. NEVELS JR.
ARKANSAS	600	20	X			X			X				X		X				AR: J. E. CLEMENTS
NEW MEXICO	1250	5				X	X		X					X			400	0.60	NM: E. RECTOR
TEXAS	1164	22	X		X				X				X			X	(F) 2375		TX: H. ALBERS (F)
LOUISIANA	419	25		X			X		X				X			X			LA: J. B. ESNARD JR.
MONTANA	1000	10		X		X			X				X		X				MT: T. L. YARGER
NORTH DAKOTA	11	1	X						X				X		X				ND: R. HORNER
SOUTH DAKOTA	540	6		X					X				X			X			SD: W. C. SULZLE
WYOMING	1125	17	X		X					X	3500	45		X			290	1.00	WY: G. W. RIEDL
COLORADO	300	3	X				X		X				X			X	3500	3.30	CO: R. K. BARRETT
UTAH	1777	7	X			X			X(G)					X			(H) 414	1.00	UT: E. G. KEANE (G)(H)
ALASKA	800	7	X		X				X					X		X	300	0.60	AK: M. WEAVER
WASHINGTON	5846	24	X		X				X				X		X				WA: S. M. LOWELL
OREGON	3150	35	X		X	X								X		X	378	1.90	OR: G. MACHAN
IDAHO	500	8	X		X	X			X	X	4171	50	X			X			ID: T. BUU
CALIFORNIA	7333	115	X	X(I)	X					X	11933	4000	X	X			15292	4.20	CA: R. H. PRYSOCK (I)
NEVADA	432	7	X						X				X			X			NV: J. M. SALAZAR
ARIZONA	500	6	X		X				X				X	X			150	1.00	AZ: S. B. KAY
HAWAII	2000	5		X		X			X					X		X	1500	12.00	HI: D. D. SANTO
WFLHD (J)	1000	5		X	X					X	1900			X		X			WFLHD: A. PETERS (J)
CFLHD (K)	995	6		X	X				X										CFLHD: S. HOLDER (K)
EFLHD (L)	827	5	X			X				X	1690			X					EFLHD: J. J. AMENTA (L)
TOTALS	68537	726	38	12	27	16	5	2	40	9			28	23	16	13	37437		

(A) Annual costs broken down to $3 million for rock and $3 million for soil
(B) Large number of sites need permanent fixing at $300K to $2000K each. Maintenance cleans 50 to 150 sites/year but no identifiable costs.
(C) Single storm event averaged over five years
(D) Single storm event of $762K
(E) Two-year data
(F) Nine of 24 districts responded with partial data typically covering one- to three-year data.
(G) Major storms occurred in 1982–83 causing widespread damage in the West. In Utah, the Thistle slide alone cost the DOT $31,5000,000. This repair is not included in column 1.
(H) Excellent district-by-district maintenance costs.
(I) Some coastal districts reported major costs for remedial measures during construction.
(J) Western Federal Lands Highway Division
(K) Central Federal Lands Highway Division
(L) Eastern Federal Lands Highway Division

appreciable 35 percent reduction. Only Region 9 shows an increase, probably because the previous survey was limited to Federal-aid participation. Consequently, it did not include the large number of projects or contracts performed by these four states that were considered maintenance by FHWA and were not eligible for federal funds.

Further analysis of the differences by region between the two surveys is beyond the scope of this paper. Overall, the direct cost of unanticipated landslide repairs appears to have reduced by 40 percent, which is substantial.

Liability Costs

In the United States, another significant and often delayed hidden cost is that of litigation. Sometimes enormous settle-

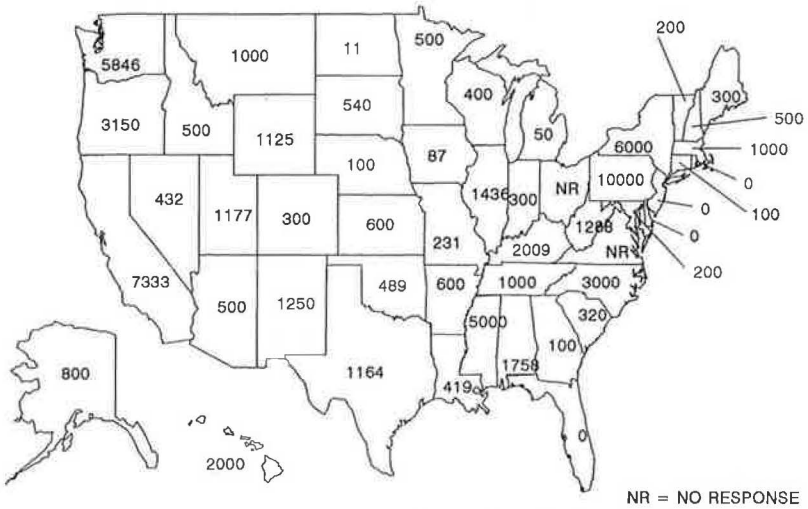

FIGURE 2 Average annual costs (in thousands of dollars) of contracted landslide repairs on state highway systems (1986–1990).

TABLE 2 COST COMPARISON OF CONTRACTED LANDSLIDE REPAIRS BY FHWA REGION

FHWA Region (States)	1976 Annual Costs Reported	1976 Costs Inflate to 1990 By Factor 2.31	1990 Annual Costs Reported	5-Year Cost 1986-1990	Number of Projects 1986-1990	Average Cost Per Project U.S. $
	Costs in columns 2, 3, 4, 5 are in million $					
1	2	3	4	5	6	7
1.ME,NH,VT, MA,RI, CT, NY	3.0	6.930	8.100	40.500	60	675,000
3.DE,PA,NJ, WV,MD,VA	6.0	13.860	11.488	57.440	142	404,500
4.KY,TN,NC,SC GA,AL,MS,FL	12.0	27.720	13.187	65.935	80	824,200
Subtotal(1,3,4)	21.0	48.510	32.775	163.875	282	581,100
5.MN,WI,MI IL,IN,OH	4.0	9.240	2.686	13.430	47	285,700
6.OK,AR,NM,TX,LA	7.0	16.170	3.922	19.610	77	254,700
7.NE,IA,KS,MD	1.0	2.310	1.018	5.090	53	96,000
Subtotal (5,6,7)	12.0	27.720	7.626	38.130	177	215,400
8.MT,ND,SD,WY, CO,UT	6.0	13.860	4.753	23.765	44	540,100
9.CA,NV,AZ,HI	3.5	8.085	10.265	51.325	133	385,900
10.AK,WA,OR,ID	7.0	16.170	10.296	51.480	74	695,700
Subtotal(8,9,10)	16.5	38.115	25.314	126.570	251	504,300
FLHD	NA	NA	2.822	14.110	16	881,900
Totals	49.5	114.345	68.537	342.685	726	472,000

ment costs are associated with these suits. For example, plaintiffs in Malibu (near Los Angeles) won settlements of $45 million for damages as the result of slides and rockfall on slopes that otherwise had minimal problems for more than 30 years. Caltrans is by no means the only highway agency that has experienced a severe blow to its budget from litigation. The New York Thruway Authority, a totally separate agency from the New York Department of Transportation (NYDOT), will spend $35 to $41 million in the next few years to stabilize some 35 rock cuts. This concentrated flurry of activity is the consequence of a lawsuit filed following a fatal accident involving fallen rock. This also is not reflected in the value of $6 million per year reported by the NYDOT respondent.

Preventive Mitigation Costs

The survey concentrated on obtaining costs for the correction of active or unanticipated landslides that had caused damage to the state highway network. It does not begin to reflect the

mitigation costs expended on new projects to maintain an acceptable safety factor against failure of problem sites identified during the design phase. These costs can range from the multi-million-dollar stabilization measures needed to cross an existing landslide area to the "extra" thousands of dollars spent on the use of retaining walls to keep an existing cut slope or embankment within the right-of-way available to the designers.

If each of these costs could be rationally identified, the real cost to society for mitigation and correction of slope stability problems could be more accurately presented.

Maintenance Costs

About half the respondents reported that they could not identify landslide repair as a specific activity of the state's maintenance program. On the survey form, the author chose the definition of the term "landslide" approved by the International Association of Engineering Geology (IAEG) Commission on Landslides and Other Mass Movements on Slopes: "A landslide is the movement of a mass of rock, earth or debris down a slope" (*10*).

The term "mass" may have been misinterpreted by many as implying a large quantity of material. Technically, it means any volume of material, such as a single rock, which requires removal from the roadway prism by maintenance personnel. In most agencies, rock or slide debris removal is not an identifiable activity; thus, it is not indicated as a separate cost item.

Another very common maintenance activity that is difficult to identify by purpose is pavement patching. This work is performed to correct many different roadway deficiencies, such as potholes or settlement due to poor compaction, but also to restore grade over slow-moving slides. There are thousands of sites like these on the highway system that rarely get proper geotechnical evaluation and are not included in cost estimates.

These previous observations are not by themselves surprising. What is surprising is the reported total maintenance costs of $37,437,000 spent annually for landslide correction by the 23 states providing data. Seven of these (Massachusetts, West Virginia, Kentucky, Missouri, Texas, Colorado, and California) spend as much as 10 times more than the contract amounts (Table 1, Column 5C). California distinguishes itself by reporting the highest annual costs for landslide maintenance of over $15 million, even during 5 years of low rainfall. However, this expenditure represents only 4.2 percent of California's total maintenance budget. Only two states, Hawaii and North Carolina, reported higher overall percentages of their total maintenance costs for landslide maintenance. However, in other states, several counties or districts may consume up to 30 percent of their individual budgets for landslide cleanup, and proper repairs are rarely made.

For most states with records, landslide maintenance represents 1 to 2 percent of the overall cost of operating existing highways. Nationally, 1 percent of state maintenance expenditures totals $76,290,000 per year (*6*). If one looks at the total public highway system, 1 percent of the maintenance costs adds up to $196,790,000. With such large sums being spent for maintenance on the national highway system, it is no wonder that more than half of the respondents could not identify an item constituting such a small percentage. However, of this half, many expressed the opinion that the costs would be quite significant. A common complaint was that maintenance personnel waited too long before requesting help from the geotechnical staff. As a consequence, small problems developed into large ones that were costly to fix.

Three states were able to provide very detailed landslide maintenance costs: Utah, California, and Texas. Other states have started programs to inventory their landslide problem areas in order to set priorities for the expenditure of capital funds for corrections. For example, in 1987 the Washington Department of Transportation (WSDOT) conducted a statewide inventory of all identifiable unstable slopes. Those in need of repair totaled 180, with an estimated repair cost of $190 million. On the basis of research performed since then, WSDOT geotechnical engineers can now provide management with decision-making tools so that they can program sites for correction. Without such an effort on the part of the geotechnical staff, it is clear that the past expenditures of $5.8 million per year would not be representative nor would they begin to solve that state's landslide problem.

CONCLUSIONS

This survey has identified that the correction of damage to the state highway system by landslides costs at least $106 million per year. There was much evidence in the responses from the highway agencies that this is only a fraction of the total cost to the public that relies on the highway system for their mobility and livelihood.

When compared with the 1976 survey, this survey gave strong evidence that less money was being spent annually to correct unanticipated failures during this period (1986 to 1990). This can be attributed to better staffing and technical expertise in geotechnical engineering by a number of state departments of transportation.

Those that have received proper support by management show the most cost-effective results. Certainly another reason is the fact that the major construction phase on new alignment of the Interstate highway system is coming to an end. On the other hand, it is quite clear that most states do not have any inventories of their landslide problems, and consequently cannot report adequately on their landslide repair-cost needs. One state that did respond reported its needs as 30 times its current annual expenditure. If this ratio held true nationally, the states' needs would be over $2 billion.

In the meantime, maintenance personnel are still faced with large expenditures to clear or patch the roadways damaged by landslide activity. From partial records, some $37 million annually was identified for landslide maintenance. This also must represent only a fraction of the real costs. This survey confirmed that landslide costs are much larger than most highway engineers believe and that better inventories of this problem are needed.

ACKNOWLEDGMENTS

This paper would not have been possible without the support and encouragement of TRB task force members; the author's supervisor, John Bates; and assistance with preparing figures

and tables by Haydee Rodrigues, Cheryl Montero, Frances Lau, and Bob Arnold—the author's thanks to all.

REFERENCES

1. R. L. Schuster, and R. J. Krizek, ed. *Special Report 176: Landslides: Analysis and Control*, TRB, National Research Council, Washington, D.C., 1978.
2. R. G. Chassie and R. D. Goughnour. 1976 National Highway Landslide Experience. *Highway Focus*, Vol. 8, No. 1, pp. 1–9.
3. J. H. Shamburger, D. M. Patrick, and R. J. Lutten. *Design and Construction of Compacted Shale Embankments*, Vol. 1: *Survey of Problem Areas and Current Practices*. Report FHWA-RD-75-61. FHWA, U.S. Department of Transportation, Aug. 1975.
4. G. H. Bragg, Jr., and T. W. Zeigler. *Design and Construction of Compacted Shale Embankments*, Vol. 2: *Evaluation and Remedial Treatment of Shale Embankments*. Report FHWA-RD-75-62. FHWA, U.S. Department of Transportation, Aug. 1975.
5. *Foundation Engineering Management Reviews—Final Report*. FHWA, U.S. Department of Transportation, July 1983.
6. *Highway Statistics 1989*. Report PL-91-001. FHWA, U.S. Department of Transportation, 1990.
7. R. B. Olshanky and J. D. Rogers. Unstable Ground: Landslide Policy in the United States. *Ecology Law Quarterly*, Vol. 13, No. 4, 1987, p. 939.
8. Highway 50 Reopens and Tahoe Rejoices, *San Francisco Chronicle*, June 24, 1983, p. 2.
9. *Price Trends for Federal-Aid Highway Construction Fourth Quarter 1990*. Report FHWA-PD-91-009. FHWA, U.S. Department of Transportation, 1991.
10. D. M. Cruden. A Simple Definition of a Landslide. *International Association of Engineering Geology Bulletin* 43, Paris, 1991.

Publication of this paper sponsored by Study Committee on Landslides: Analysis and Control.

Slope Failure Risk Mapping for Highways: Methodology and Case History

ROY E. HUNT

Roadway construction along steep slopes in mountainous terrain requires numerous sidehill cuts and fills. Design provisions for stability against slope failures require the engineer to make many difficult judgments. The competency of these judgments depends on the adequacy of geotechnical investigations to define slope conditions and the interpretation of the data available. The observational method provides an approach for evaluating the stability of slopes along transportation corridors. Slope failure risk maps are prepared to present the degree of risk or consequences of slope failures along an entire roadway alignment. The degree of risk is established by evaluation of the degree of the hazard or the potential for slope failures along the roadway. It is formulated from judgments made regarding the form (rotational slides, debris avalanches, etc.) and the magnitude of the potential slope failure to be expected. These judgments are based on assessments of geologic and surface conditions, slope geometry and activity, and weather conditions. Slope treatments for areas designated as having failure risk are determined and presented on slope stabilization maps. Governments with adequate financial resources may choose to provide stabilization treatments for all levels of risk. Alternatively, governments with limited resources can establish priorities regarding necessary treatments, beginning with areas of higher risk levels. A case history is presented in which the methodology was applied for a section of mountain roadway in Brazil.

Roadway construction along steep slopes in mountainous terrain involves numerous sidehill cuts and fills requiring many difficult judgments during design. Two options may be available, depending upon the client's desires and the amount of subsurface information available:

1. Provide complete stability of all cuts and fills. This approach may be prohibitively costly, and it may be inadequate if conditions are misjudged.
2. Accept some failure risk and minimize initial construction costs. Select cut inclinations with the anticipation that some failures may occur and that roadway cleanup and maintenance will be required in the future. Design retaining structures or other stabilization methods only for areas with the potential for failures of serious consequences.

Option 2 is often selected by governments in developing countries with limited financial resources. The objective is that, at worst, failures will be a nuisance requiring periodic cleanup of small portions of the roadway. Large failures resulting in a mass of earth completely covering a stretch of roadway or even the complete loss of the roadway because of failure of a sidehill fill are to be prevented. Even if the roadway is not completely closed, rockfalls and small slides can pose a substantial danger to the public, especially when a roadway is used heavily. At the least, public annoyance will increase as the inconvenience of slope failures continues.

For either option, success depends on the adequacy of the assessment of slope conditions. Even extensive geotechnical investigations with test borings and geophysical surveys may not sufficiently define slope conditions, and in many cases explorations are minimal because of the costs and difficulties caused by terrain. Evaluations based on mathematical analyses may not provide an adequate assessment of stability. The analytical models may not accurately depict slope conditions at failure, and forms such as progressive slides, debris avalanches, and flows are not suitable for mathematical analyses.

The observational method of assessment can efficiently obtain significant information on slope conditions. The methodology requires substantial experience in applying the principles of geology, engineering geology, and geotechnical engineering to slope problems both for existing roadways suffering failures and for the design of new roadways.

RISK MAPPING: BASIS FOR SLOPE STABILITY ASSESSMENT

Slope failure risk mapping provides the basis for predicting where failures are likely to occur and for the formulation of plans for preventive and corrective treatments along an entire roadway alignment. Risk mapping covers a wide corridor extending for some distance upslope and downslope. The methodology proceeds through several phases as follows.

Phase 1

An engineering geology map is prepared as the basis for assessing slope conditions. For new roadways, information mapped includes geologic formations, slope failure scars, erosional features, and drainage pathways. For existing roadways, conditions of cuts, fills, and roadway pavement are also mapped. When slope inclinations and vegetation are plotted, the map is used for runoff evaluations and drainage analyses for culvert designs.

The map is prepared using data obtained from landform analyses, detailed field reconnaissance, and the review of available reports, boring logs, geophysical records, and so forth. For a new roadway, a preliminary map is prepared and used for planning an efficient exploration program. A final engineering geology map is prepared using the data obtained from test borings, geophysical surveys, and other explorations.

Woodward-Clyde Consultants, 5120 Butler Pike, Plymouth Meeting, Penn. 19462.

Phase 2

A slope failure risk map is developed for the entire alignment. It depicts where slope failures have occurred or are probable, and includes a rating for each occurrence as to the degree of risk or consequences of failure along the roadway. Ratings may range through a number of levels, from no risk to very high risk. Risk levels are based on the hazard degree, which is formulated from evaluations of the potential failure form expected (fall, slump or planar slide, debris avalanche, or flow) and the failure magnitude. Potential failure forms are determined from assessments of geologic and surface conditions, slope geometry and activity, and weather history.

Phase 3

A stabilization map is prepared giving recommended slope treatments for areas designated as failure risks. Areas requiring detailed exploration and additional study are identified. The agency responsible for the roadway can then establish priorities for necessary treatments, beginning with areas of higher risk levels.

CASE STUDY: HIGHWAY BR 116, BRAZIL

Highway BR 116 connects the cities of Rio de Janeiro and Teresopolis in Brazil. In a distance of 15 km, the roadway climbs from the coastal plain at an elevation of about 100 m above sea level over steep slopes to an elevation of over 1000 m at the crest of the coastal escarpment. Since its construction in the 1950s, this stretch of roadway had suffered numerous slope failures, often resulting in closure to traffic. The failures usually occurred during the periodic heavy rainfalls common to the coastal mountains of Brazil.

During December 1978, Technosolo SA was engaged by the Departamento Nacional de Estradas and Rodagems (DNER) to perform a geotechnical overview of conditions along the 15 km where the roadway climbs the coastal escarpment. The study was performed under subcontract to Technosolo in order to

1. Determine the causes of instability of natural slopes, cuts, and fills;
2. Identify areas in which failures probably would occur in the future;
3. Recommend various treatments to improve or provide for stabilization; and
4. Establish priorities for stabilization based on the degree of the hazard and risk, thereby enabling the budgeting of treatments over time.

Physical Conditions Along BR 116

Investigation Methodology

A preliminary engineering geology map was prepared to provide the basis for field reconnaissance. Available data included national topographic maps at a scale of 1:50,000 and stereopairs of aerial photographs at a scale of 1:20,000, which were dated 1973. Enlarged to a scale of 1:10,000, the photographs provided base maps of the roadway on which cuts, fills, and retaining structures (as of 1973) were illustrated. Slide, avalanche, and erosion scars; drainage paths; and geologic data (including surface exposures of rock and soil types classified by origin) were plotted on the base maps during stereoscopic interpretation of the photographs. An aerial photograph of a portion of the higher roadway elevations is shown in Figure 1.

Field visits were made, and the significant features delineated on the preliminary map were examined, as were other pertinent conditions. Noted were new slide and erosion scars; geologic conditions exposed in cuts and slide scars, including soil and rock types; slope seepage; the inclinations of apparently stable slopes; and signs of movement, including tension cracks and tilted trees. The pavement was examined both for signs of heave along the toe areas of cut slopes and for cracks and other signs of settlement along sidehill fills. Both cases indicated probable slope movements. Final engineering geology maps were prepared incorporating the field observations. An example for part of the roadway is shown in Figure 2.

Physiography

The study began at roadway Km 104, situated in the lowlands at an elevation of approximately 100 m. After traversing hilly

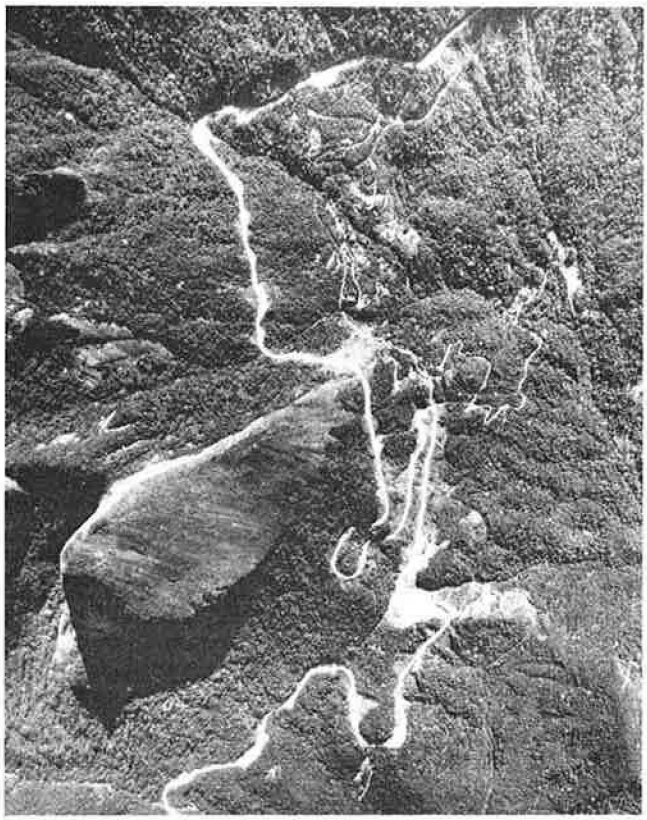

FIGURE 1 Aerial photograph, Km 91–95, BR 116 (scale: 1 cm = 200 m).

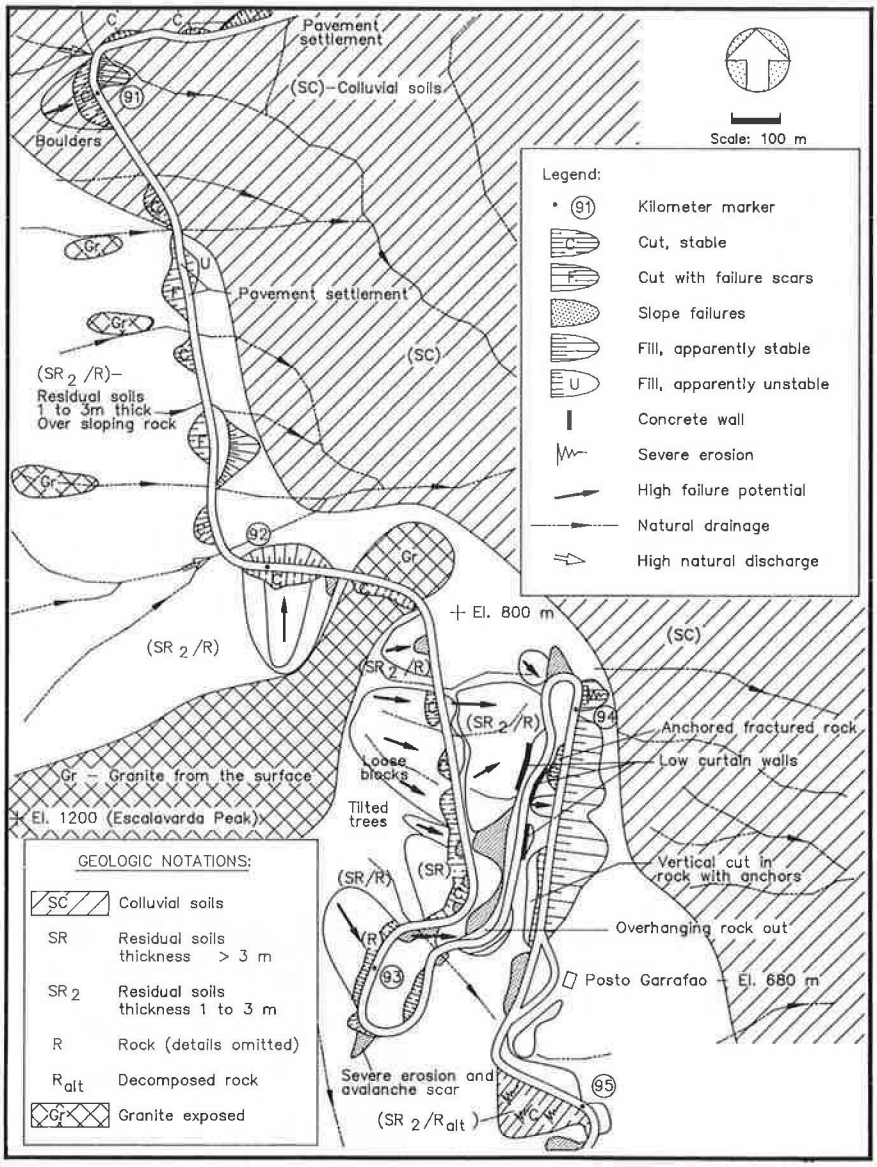

FIGURE 2 Final engineering geology map: existing conditions, cuts, fills, and geology, BR 116, January 1979.

terrain with gentle curves and shallow cuts for about 7 km, the roadway reaches the base of the escarpment formed by the Serra Dos Orgaos Mountains. From here, the land becomes steeper and more irregular, requiring the roadway to take a winding route along the side slopes of hills that rise to an elevation of 900 m or more. The roadway begins to intercept the natural drainage from the mountains and crosses a number of watercourses.

As shown in Figure 2, from Km 95, the roadway doubles back twice to climb from Elevation 680 to 800 m near the base of Escalavarda Peak. It continues on along the slopes of the escarpment to the study terminus at the summit, Elevation 1004 m (Km 89.4), where the roadway branches off to Teresopolis. Along this stretch, the side slopes of the escarpment often range from 45 to 60 degrees. Numerous cuts have been made in soil and rock, and fills were placed. Drainage from mountain runoff is intense.

Geology

For slope stability evaluations, geologic conditions were characterized by three general formations:

1. Colluvial soils (SC), the residue of slope movements, are found on the lower slopes and fill the major valleys, even at higher elevations. Consisting of boulders in a matrix of fine-grained soils, the colluvium blocks the normal slope seepage and tends to contain substantial moisture and to be unstable in cut. It can overlie residuum or bedrock, and is normally found with relatively high piezometric levels in the toe areas of the formation.
2. Residual soils (SR), formed mainly from the decomposition of metamorphic rocks, reach thicknesses of 20 m or more. The thicker deposits, usually clay-silt mixtures of stiff to very stiff consistency, are common at the lower elevations

along the roadway. The formation normally grades to saprolite, and relict joints and other discontinuities remain, representing planes of weakness. Along the higher elevations, a thin cap of residuum commonly overlies a dipping surface of fractured rock. Generally, residuum is relatively dry, with the predominant groundwater movements and seepage forces developing in the underlying fractured rock masses.

3. Bedrock consists of Precambrian igneous and metamorphic rocks. The high peaks, such as Escalavarda Peak, are composed of very resistant granite (Gr). Where exposed in cut, the granite is seen to be very hard, with tight, widely-spaced joints. The metamorphic rocks, primarily gneiss, are found with a wide range of conditions varying from highly fractured masses of intact blocks of rock to highly decomposed masses that are soft and can be dug with a geologic hammer (R_{alt}).

Recent alluvium, present in stream beds in limited deposits, is not significant in the slope stability evaluations.

Roadway Slopes

Slope failure forms usually are classified as falls, slides (rotational and planar), avalanches, and flows (*1,2*). This nomenclature was applied to the slopes along BR 116.

Planar or translational slides, involving masses of residual soils moving along a rock surface dipping downslope, are the dominant form of slope failure along the roadway. The common cause is a cut that extends into rock, exposing a face of overlying soils (see Figure 3). Failure is sudden, occurring during or immediately after heavy rains. Sufficient material is usually displaced to either partially or completely close the roadway. Additional failure will not occur if the slide reaches the crest of the hill, because it is self-corrected. The scar of a planar slide is shown in Figure 4.

Large, deep-seated rotational slides occur infrequently. The only case observed was located at Km 101, at the lower roadway elevations, involving thick colluvium overlying rock. Movement was shown by substantial pavement heave and cracking where the pavement passed over the toe of the failing mass. In most of the study area, soil cover is generally too thin for the development of deep-seated rotational slides. They are common, however, in other areas of the coastal mountains of Brazil.

FIGURE 4 Scar of planar slide that partially closed BR 116.

Debris avalanches can completely or partially close the roadway. Occurring during heavy rains, they develop along the hillsides at the higher elevations where residual soils are not thick and overlie a rock surface dipping downslope. Large quantities of runoff move masses of soil and rock fragments downslope at high velocities. Figure 5 shows the scar of a

FIGURE 5 Scar of debris avalanche that partially closed BR 116 near Km 89.

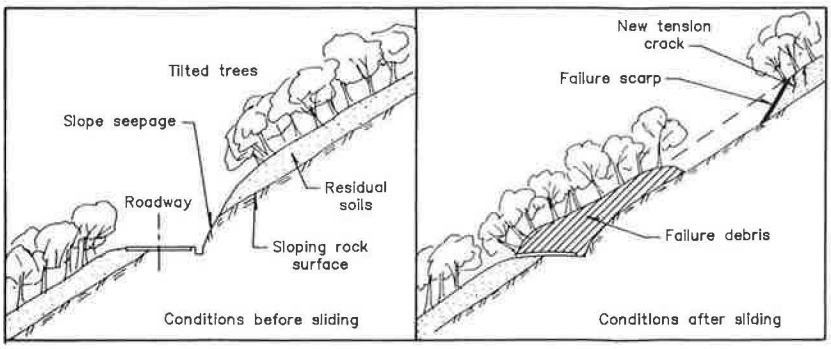

FIGURE 3 Typical planar slide occurring in residual soil cap over sloping rock surface in cuts along BR 116.

debris avalanche that occurred along the upper reaches of the roadway.

Erosion can be severe on natural slopes where the vegetation has been removed or on unprotected cut or fill surfaces. When erosion is uncontrolled, gullies form and slopes are steepened, decreasing stability.

Other forms of slope failures along BR 116 that involve smaller quantities of materials include small rotational slides in shallow colluvium, small wedge failures along relict weakness planes in residuum, and falling blocks of loose rock. In the rock masses, failure normally occurs along joints dipping downslope, and falling single blocks are common. Large failures generally occur only where a group of loose blocks in a vertical to near-vertical cut move together.

Sidehill fill stability is affected by underdrainage, surface drainage, and erosion. Apparent problems associated with sidehill fills along the roadway are the following:

1. Excessive seepage forces develop beneath fills with inadequate underdrainage. Slumping and downslope displacement occur, resulting in pavement deflection and concentric cracking. In extreme cases, complete failure occurs. Lining of drainage ditches along the roadway upslope of fills is generally inadequate to prevent runoff infiltration into embankments.
2. Poor compaction during construction results in consolidation or displacement of the fill mass and generally contributes to instability. However, where fills are constructed of relatively impervious materials, such as the local residual soils, seepage beneath the embankment is the main cause of failure.
3. Uncontrolled erosion of fills eventually removes soil from beneath the pavement, resulting in loss of support and failure along the pavement edge. Such conditions exist at several locations along the roadway.
4. Where fills are placed in stream gullies, if culverts are of inadequate capacity to provide for runoff or become clogged with debris, the fill becomes a dam. Complete roadway failure can occur as the fill slumps and fails, or if it is overtopped and washed out.

Rainfall and Runoff

Rainfall along the roadway and in the surrounding mountains is normally heavy and may reach an annual accumulation of several meters, most of which falls during the summer months of December through March (*3*). Intense storms are common, and in many areas the steep mountain slopes support little to no vegetation along the upper reaches (Figure 1). This condition permits very high quantities of runoff into the brooks that intercept the roadway at numerous locations.

Qualitative Assessment of Hazard

Failure Predictions and Slope Treatments

Slope stabilization along a roadway subjected to failures is normally approached by applying corrective treatments to stabilize existing active slides. This approach is reasonable for deep-seated rotational slides, such as that at Km 101, where movements are relatively slow and occur periodically, sidehill fills are suffering gradual displacements, or erosion is occurring. For the more common case involving the sliding of a cap of residual or colluvial soil over rock, total failure usually occurs suddenly, without much warning. Rockfalls and failure of fills over culverts during heavy rains also occur with little warning. Therefore, to avoid roadway closure in these cases, prediction and prevention of occurrence are required rather than correction.

Corrective or preventive treatment selection depends upon the degree of the failure hazard and the risk to the public should failure occur. "Hazard" refers to the potential slope failure form, magnitude, and probability of occurrence. "Risk" refers to the consequences of failure on human activities.

Rating the hazard and the risk provides the basis for establishing priorities for locations where treatment is required and for evaluating the type of treatment necessary for stabilization. The treatment selected depends on the characteristics of the hazard, that is, the form of failure that may occur and the quantity of material involved.

Qualitative assessment of slopes provides the basis for predicting the failure potential and its form at any given location and for selecting practical treatment methods.

Quantitative assessment, based on mathematical analyses, is not applicable for many forms of slope failures, particularly for most conditions existing along BR 116.

During the planning and design phases for new roadways, there are conditions of high hazard and high public risk that should be avoided, but normally, slope treatment objectives are either to reduce or eliminate the hazard by a change in slope geometry, an improvement in surface and subsurface drainage, or retention. An alternative, often selected by governments with limited financial resources, is to provide minimum treatment and permit failure. Debris is removed periodically, with the hope that, in time, the slope will reach a stable inclination. From the aspect of saving lives during intense storms, the risk can be reduced by temporary closure of the roadway.

Rating the Hazard

The hazard is rated in terms of the potential form, magnitude, and occurrence probability, and these factors influence the type of treatment feasible. Magnitude refers to the volume of material that may fail, the velocity of movement during failure, and the land area that may be affected. It depends on the failure form as related to geology, topography, and weather conditions. For example, the steeper the slope, the thinner the soil cover, and the more intense the rainfall, the greater the likelihood of a debris avalanche rather than a potentially less-destructive, small-volume planar slide. Probability is related to weather and other transient conditions such as slope inclinations (steepened by cut, erosion, or tectonic activity) and, in some areas, seismic activity. Many bases for a hazard rating system are feasible. The following is a suggested approach:

1. No hazard: A slope that is not likely to undergo failure under any foreseeable circumstances.

2. Low hazard: A slope that may undergo total failure (as compared with a partial failure involving relatively small displacements) under extremely adverse conditions that have a low probability of occurrence (such as a 500-year storm or a high-magnitude earthquake in an area of low seismicity) or whose potential failure volume and area affected are small, although the probability of occurrence is high. Potential low-hazard failure forms along BR 116 include rockfalls of single blocks and small rotational or planar slides.
3. Moderate hazard: A slope that will probably fail under severe conditions expected in the future and that involve a relatively large volume of material. Movement will be relatively slow, and the area affected will include the failure zone and a limited zone downslope (moderate displacement), which are characteristic of rotational slide forms similar to the case at Km 101.
4. High Hazard: A slope that is almost certain to undergo total failure in the near future under normal adverse weather and will involve a large to very large volume of material or a slope that may fail under severe conditions (moderate probability) but whose potential volume and area affected are very large and the movement velocity is very high. Characteristic failure forms include planar slides in layered rock masses, debris slides and avalanches, and some forms of flows. Debris slides and avalanches are characteristic of many of the failures along BR 116.

Rating the Risk

A general rating of risk levels may include the following:

1. No risk: Slope failure that will not affect human activities.
2. Low risk: An inconvenience that is easily corrected and does not directly endanger lives or property, such as a single small block of rock falling onto the roadway that is easily avoided and removed.
3. Moderate risk: A more severe inconvenience that is corrected with some effort but usually does not directly endanger lives or structures when it occurs, such as a small debris slide entering one lane of a roadway causing partial closure for a brief period until it is removed.
4. High risk: Complete loss of a roadway or important structure, or complete closure of a roadway for an extended time, that does not necessarily endanger lives by failure.
5. Very high risk: Failure that endangers lives, such as the destruction of inhabited structures or the destruction of the roadway when time is not available to warn traffic.

Assessment Factors

General

Qualitative assessment of the hazard is made from evaluations of geologic conditions, slope geometry, surface conditions, slope activity, and rainfall. The entire stretch of roadway subjected to slope failures is examined, with the objectives of formulating judgments of where failures are to be anticipated, the nature of the hazard, and the degree of the risk. Stabilization treatments that are selected are based on these judgments.

Geologic Conditions

Geologic conditions with a high failure incidence along BR 116 are summarized as follows:

1. Jointed rock masses in steep cuts can result in falls varying from a single block to many blocks of varying sizes.
2. Residual soils on moderate-to-steep slopes may fail progressively where they are relatively thick, usually involving small-to-moderate volumes in rotational slide forms. Where they overlie a downslope-dipping rock surface at shallow depths, large planar slides can occur or, under heavy rainfall, even debris avalanches or flows.
3. Colluvium is generally unstable on any slope in a wet climate, and when cut, it can fail in large volumes, usually in rotational form with progressive slumps.

Slope Geometry

The significant aspects of slope geometry are inclination, form, and height. Soil slopes often rest naturally at a safety factor near unity. When cuts are made along BR 116 where natural inclinations are greater than 30 to 40 degrees, the stability decreases substantially, especially where cuts intercept the contact between the rock surface and the underlying soils. In fractured rock masses where joint conditions are unfavorable, steeply inclined cuts are potentially unstable.

Topographic expression has a strong influence on location of slope failures, because landform provides the natural control over rainfall infiltration and seepage where other factors are constant. Failures are much more likely to occur in swales extending downslope, where runoff and seepage will be relatively high, than on promontories, or "nose-forms," where runoff is directed away from the area. Along BR 116, the highest incidence of failures is along the sides of swales. Where the slope is steep and soil cover is thin, the potential for debris avalanches is high.

Slope height above a cut influences the amount of runoff intercepted. A long slope reaching substantial heights will carry much more runoff than will a cut made a short distance from the crest of a hill. In addition, an area containing a large number of drainage paths upslope of the roadway has a greater susceptibility to failure than does an area with few if any drainage paths.

Surface Conditions

Slope seepage observations during reconnaissance are evaluated by considering the weather conditions prevailing during the weeks preceding the visit, the season of the year, and the regional climatic history. No slope seepage during a rainy period may be considered very favorable, assuming that colluvium or fills are not causing blockage, whereas seepage during a dry period signifies that a substantial increase will occur during wet periods and failures are likely. Toe seepage

in particular indicates a potentially dangerous condition, especially during dry periods.

Vegetation density is an important stability factor. Cut slopes where upslope vegetation has been cleared are much more likely to fail during severe weather conditions than if vegetation remains undisturbed. Removal of vegetation permits erosion to increase, reduction in the shallow portions of the slope from loss of root structure, increased infiltration during rainy periods, as well as an increase in evaporation during dry spells. The latter condition results in surface desiccation and cracking, and provides entrances for runoff into a potential slide area. These factors pertain also to unprotected cut and fill slopes.

Vegetation type may be an indicator of areas with a relatively high failure potential. It appears that in tropical climates, banana plants favor less stable colluvium over the stronger residuum, probably because of the higher moisture content of the colluvium.

Indicators of slope movements and existing instability include tilted or bending tree trunks and tilted poles and fenceposts, tension cracks along the slope and behind the crest, slump and hummocky topography, and failure scars. Straight but tilted tree trunks indicate recent slope movements, whereas trunks curving near the bottom and then growing vertically indicate old and progressive movement. Tension cracks are a well-known failure indicator, but for many of the forms along BR 116, such as the planar slides and debris avalanches that occur suddenly during heavy rains, tension cracks may develop only immediately preceding failure.

Slope Activity

Slopes are characterized by various levels of activity, ranging through the following stages:

- Stage 1 is a stable slope with no apparent movement.
- Stage 2 is the early failure stage, in which shallow slumping, creeping, and formation of tension cracks associated with small movements have occurred.
- Stage 3 is the intermediate failure stage. Significant movement has occurred. Progressive slumps and scarps have formed during rotational slides, blocks have separated during planar slides, and tension cracks have grown in width and depth. Movement velocities may have been in the range of about 2 to 5 cm/day, accelerating during rainy seasons and storms and decelerating during dry periods.
- Stage 4 is partial failure of the slope, with the total movement of a major block or portion of its volume to its final location.
- Stage 5 is the final failure stage. The slope has failed completely, with a final total movement having occurred characteristically during the wet season and after heavy rains.

For predicting slope failures, Stages 2 through 4 are primarily significant because they indicate that the slope is residing at a factor of safety near unity. Slopes can remain stable in these conditions for many years and then fail completely (Stage 5) as the result of either unusually heavy rains with a high level of ground saturation, the long-term decrease in material strength caused by weathering processes, or an unfavorable change in slope geometry.

Where slopes are undergoing progressive movements (such as occur in deep-seated rotational slides or large planar slides in rock masses where complete failure has not occurred), movement velocity and acceleration are important assessment factors. Such sliding masses require monitoring with instrumentation. In Brazil, experience generally shows that if velocities are relatively high—on the order of 2 to 5 cm/day and accelerating during the rainy season—complete failure can be expected in the near future.

Sidehill fill activity assessment is based on the occurrence of pavement settlements and cracking, bulging at the embankment toe, and movement velocities. Slopes where movements are judged to be excessive should be monitored.

Rainfall

Ground saturation and rainfall are major factors in slope failures and affect their incidence, form, and magnitude. Several aspects are important in slope stability assessment for a given location:

1. Climatic cycles over a period of years (whether the current cycle is one of high or low annual average precipitation);
2. Rainfall accumulation in the current year as compared with normal precipitation (i.e., higher, lower, normal);
3. The current season (wet or dry); and
4. Storm intensities (in centimeters per hour).

Evaluations of rainfall records have two important applications:

1. A basis for judging the future stability of cut slopes that have remained stable for some time interval under a particular weather history, and
2. Establishment of the criteria for early warning of impending slope failures.

An early warning system based on "danger charts" has been suggested by Guidicini and Iwasa (*4*). Such a system has been used to forecast slope failures and even to temporarily close roadways to traffic in Brazil. In the evaluation of the potential stability of an existing cut slope and the development of early warning systems, it is necessary to use records that cover as long a time interval as possible, because weather is cyclic. To judge that a particular cut slope is stable because it has remained so for a long time, its weather history and the possible weather conditions that could occur must be considered. The occurrence of the severest long-term historical conditions represents the true test of a slope's stability.

Slope Failure Risk Map

The slopes along the roadway were evaluated on the basis of the assessment factors, and judgments were made regarding the hazard degree and the failure risk. Slope failure risk maps were prepared for five levels of risk incorporating the hazard

rating; an example of one section of roadway is shown in Figure 6. The levels of risk were defined as follows:

1. Very High Risk: High slopes where relatively large failures will close the roadway are considered Level 1. Natural drainage permits substantial water to enter the area, and failures have already occurred. Conditions include steeply inclined cut or uncut slopes, generally greater than 30 degrees, with a layer of SR or SC over a rock surface inclined downslope or SC intercepted in the cut; fills subjected to severe erosion with danger of pavement undercutting causing loss of support; and culverts beneath fills in locations with potentially very high runoff.

2. High Risk: Relatively large failure probably will close the roadway. Conditions are similar to those for very high risk except that the slope is generally less steeply inclined and natural drainage is more favorable. The risk is judged to be only somewhat less than that in Level 1, and in many cases it is difficult to differentiate between these two levels. Failures have not necessarily occurred in areas assigned Level 2. Fills have consolidated or displaced, or both, causing pavement settlement and cracking.

3. Moderate Risk: Slope heights are moderate. Failures are likely to be small in volume and not likely to close the roadway or severely affect its performance. Conditions include shallow cuts in steep slopes of SR or moderate slopes with SC, very steep cuts in fractured rock with a risk of falling blocks, slopes and fills with erosion, and areas with a layer of soil overlying rock that has already been subjected to sliding, which removed most of the overburden.

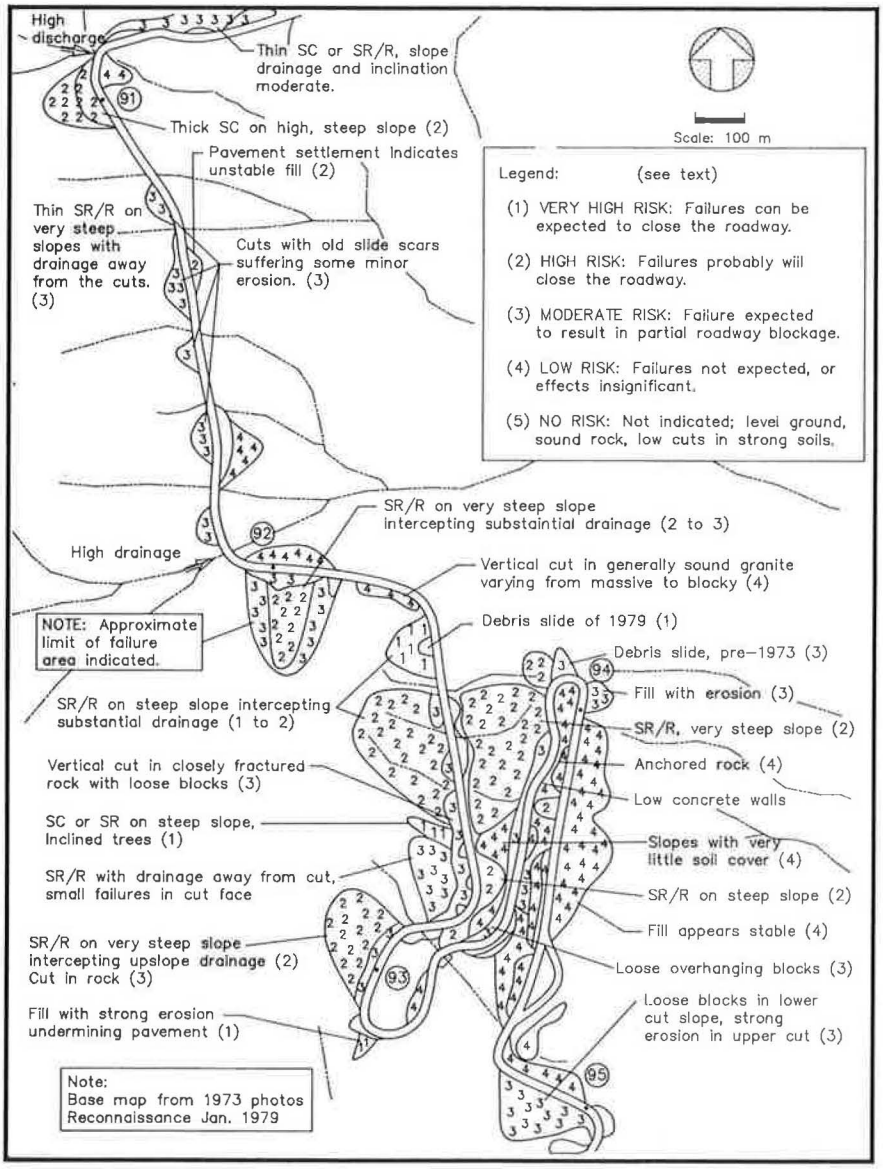

FIGURE 6 Slope failure risk map, BR 116, Km 91–95.

4. Low Risk: Slope failures are unlikely. Conditions include shallow cuts in strong soils or rock and areas in which failures have removed the overburden. Some minor erosion may occur on cut slopes. Fills appear stable and not subject to erosion or consolidation.

5. No Risk: Level ground, no cuts, or shallow cuts in very strong soils or massive hard rock present no risk.

Slope Stabilization Along BR 116

General

The risk maps provided the basis for recommending slope treatments. To establish budget priorities, immediate treatments were recommended for areas with high or very high risk, since these conditions were expected to close the roadway to traffic. High priorities were given also to unstable rock cuts and erosional features, but the large rotational slide at Km 101 was assigned a lower priority. A section of roadway with suggested treatments is shown in Figure 7. Stabilization work should be performed during the dry season, beginning in April or May.

Soil Slopes

For the dominant case of a soil cap over a rock surface, retention with an anchored curtain wall (*5*) was recommended. For other soil slopes, recommended treatments

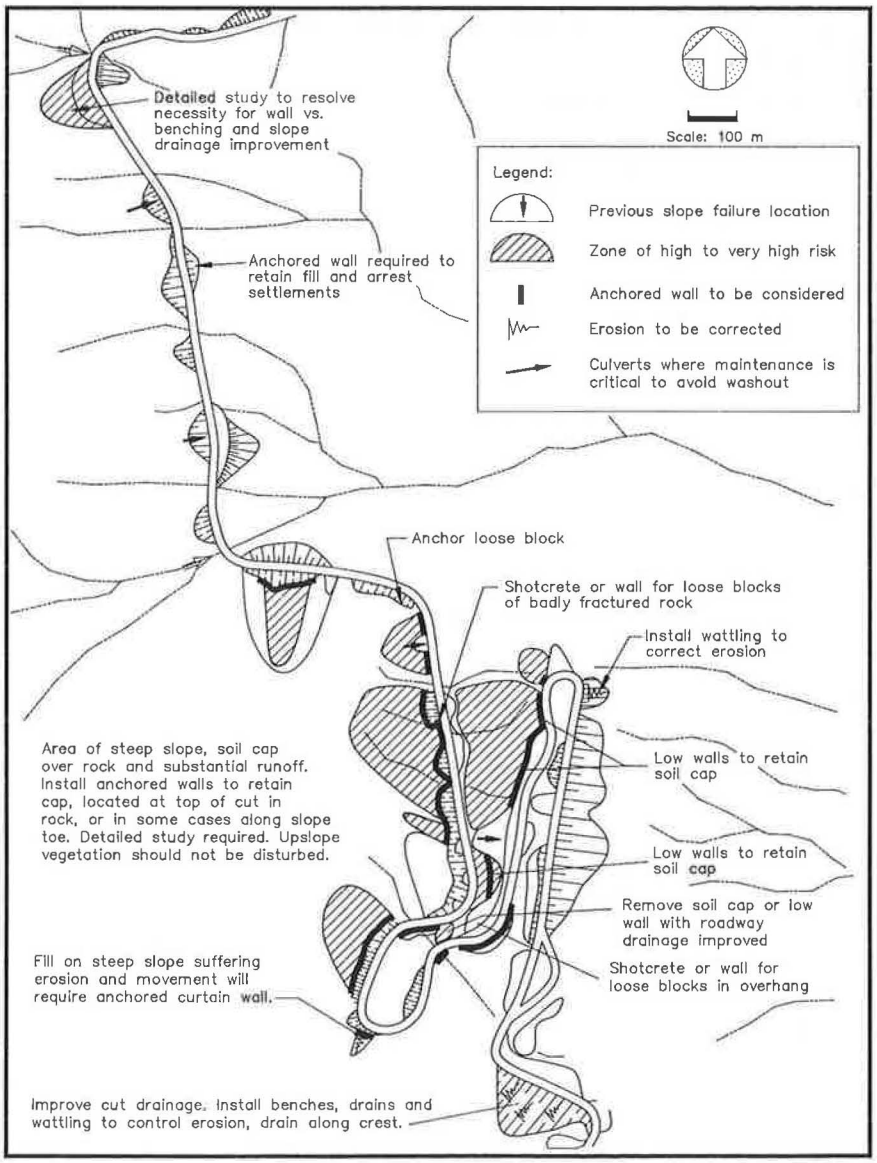

FIGURE 7 Preliminary consideration of slope stabilization schemes for high-risk areas along BR 116, Km 91–95.

included improvements of surface drainage within the cut area and erosion protection, or regrading and the installation of subhorizontal drains.

Improvements to upslope drainage were not recommended since installations would be difficult and costly on the steeply inclined and heavily vegetated slopes and the necessity of removing vegetation would decrease stability.

Rock Cuts

It was recommended that large masses of small blocks (fractured to crushed zones) in vertical cuts be reinforced by shotcreting or retained by lightly anchored walls. In either case, rock drainage must be maintained. Individual blocks judged to be free and unstable should be removed by scaling or reinforced with bolts or anchors. A group of large, unstable blocks will require anchored concrete straps or wire mesh and shotcrete. Blasting for any purpose should be strictly controlled to avoid reducing rock quality.

Sidehill Fills

Stability of sidehill fills is more critical than most cuts, since a complete failure would result in the loss of the roadway, necessitating reconstruction. Recommendations for correction of erosion included regrading the fill slope and planting heavy vegetation, and improving roadway and slope drainage. In severe cases where the sidehill fill was in danger of failing, retention with an anchored curtain wall was recommended.

Culverts

Recommendations emphasized the importance of careful maintenance of culverts and other drainage systems to prevent failures.

CONCLUSIONS

Qualitative Assessment of Slopes

By application of the techniques of landform analyses, geologic conditions along a stretch of roadway subjected to slope failures can be determined efficiently. Conditions are assessed and judgments made to identify areas with various risk levels of future instability. Recommended stabilization treatments depend on the risk level and the predicted nature of the potential failure. As an interim solution to completion of a stabilization program, early warning systems and roadway closure provide some temporary public protection, although they are an inconvenience.

Study Limitations

The evaluations of the failure risks and the determination of solutions along BR 116 were based entirely on interpretations of stereo-pairs of aerial photographs and field reconnaissance. In some areas of potentially high risk, additional detailed geotechnical studies with explorations were recommended to accurately establish geologic sections for detailed evaluations.

Postscript

In the years following the study, as budgets permitted, DNER began to install the recommended stabilization treatments. During December 1981, over 28 cm of rain fell during a 2-week period, most of it in storms of 1 or 2 days' duration. Many slope failures occurred causing loss of roadway sections, and the roadway was closed for about 2 weeks. A major failure near Km 92 resulted in a number of deaths when a bus was pushed from the roadway into a deep ravine. The location had been mapped as having a high risk. In 1982 DNER began to close mountain roadways to traffic when pluviameter measurements of rainfall reached 10 cc in 15 min (about 10 cm/hr).

REFERENCES

1. D. J. Varnes. Landslide Types and Processes. In *HRB Special Report 29: Landslides and Engineering Practice* (E. B. Eckel, ed.), TRB, National Research Council, Washington, D.C., 1958.
2. D. J. Varnes. Slope Movement Types and Processes. In *Special Report 176: Landslides: Analysis and Control*, TRB, National Research Council, Washington, D.C., 1978.
3. F. O. Jones. Landslides of Rio de Janeiro and the Serra das Araras Escarpment, Brazil. In *U.S. Geological Survey Paper 697*, U.S. Government Printing Office, Washington, D.C., 1973.
4. G. Guidicini and O. Y. Iwasa. Tentative Correlation Between Rainfall and Landslides in a Humid Tropical Environment. *International Association of Engineering Geologists Bulletin 16*, Dec. 1977, pp. 13–20.
5. R. E. Hunt and A. J. da Costa Nunes. Retaining Walls: Taking It from the Top. *Civil Engineering-ASCE*, May 1978, pp. 73–75.

Publication of this paper sponsored by Committee on Soils and Rock Instrumentation.

Seismic Response of Highway Embankments

J. David Rogers

The basic mechanisms by which natural slopes and highway embankments respond to seismic loading are explained. The response of a slope to earthquake loads depends on a number of localized conditions, such as geologic structure, topographic setting, seismologic setting, complexity of saturated zones, and the geophysical properties of soil and rock making up the mass. Observations following earthquakes suggest that slope response varies widely depending on the above-cited factors. In conclusion, how to draw the distinction between landslide and settlement-induced movement is discussed.

Through the first few generations of highway construction (1925–1955), there was scant engineering geologic input as to the routing of roads. As a consequence, much of the U.S. highway infrastructure is founded upon or adjacent to geologically unstable ground, terrain that may be particularly susceptible to reactivation through seismic loading. Figure 1 shows a schematic representation of a typical ancient landslide complex in mountainous terrain. Such complexes often lie within regions of recognized paleoseismic activity, and the potential for seismic instability is considered high. However, the accurate prediction of seismically induced reactivation of such deposits requires a thorough understanding of the various mechanisms of mass movement.

MECHANISMS OF SEISMICALLY INDUCED MOVEMENTS

Seismically induced slope movements have often been categorized as lurching, lateral spreading, liquefaction, and enhanced ground shaking. "Lurching" is a colloquial term used to describe permanent ground movements resulting from earthquakes. No distinction is made as to the mechanism of movement, which could be due to partial liquefaction, differential settlement (densification), or landslide reactivation. "Lateral spreading" is the more correct term used to describe gross lateral distortions on sloping ground, generally referring to natural as well as man-made embankments. The slope of the ground may be very slight, as little as 0.50 degree. Liquefaction is a failure mode in which pore water pressures are developed that exceed the effective strength of a porous material through buoyance (the effective confining pressure is lessened by the amount of increased pore pressure). In many instances, liquefaction may be confined to a particular stratum and thereby engender lateral spreading or lurching of higher ground.

"Enhanced ground shaking" is also a colloquial term, used to describe local enhancement of incoming seismic energy due to wave deformations induced by near-surface deposits of low modulus soil or soils. Generally, these distortions are greater in the higher vibrational frequencies (above 5 Hz), and lower in the frequencies associated with large quakes (closer to 1 Hz). Wood (*1*) originally described ground enhancement effects in reporting increased shaking intensities along the margins of San Francisco Bay during the 1906 earthquake. Naito (*2*) later made almost identical observations during the disastrous 1923 Tokyo quake. Much later, Borcherdt (*3*) did extensive experimental work in studying this phenomenon in the San Francisco Bay area, and Seed and Idriss (*4,5*) subsequently incorporated such precepts into modern geotechnical earthquake engineering theory and practice. Today, nationwide standards for performing deterministic assessments are readily available throughout the United States (*6*). Following are brief discussions of those mechanisms most pertinent to landsliding.

Rogers/Pacific, Inc., 396 Civic Drive, Pleasant Hill, Calif. 94523-1921.

Dynamically Induced Settlement

When large dynamic loads, such as earthquakes, transmit through a fill embankment, some densification invariably occurs because of the large shear stresses that are suddenly imposed on the embankment. Makdisi and Seed (*7*) were among the pioneers in providing simplified finite-element procedures for estimating embankment deformations induced by strong shaking motion. Less sophisticated pseudostatic assessments, such as those originally proposed by Seed and Martin (*8*), have generally been found lacking in predicting embankment response.

The effect of seismic wave excitation on embankments depends to a great degree on the following factors:

1. Geologic site conditions and whether subsurface embankment conditions (such as being situated along a bay margin or across an old channel or lake deposit) are favorable for producing site enhancement effects;
2. Number of equivalent load cycles in excess of about 0.10 g;
3. Ratio of horizontal to vertical acceleration;
4. Cohesive character of embankment materials (plastic embankments tend to damp and absorb more energy, whereas granular fills are more prone to densification);
5. Position of the water table within the embankment at the time of shaking (some larger embankments may have several perched levels);
6. Degree of available subdrainage built into the embankment (which helps alleviate excess pore pressures);

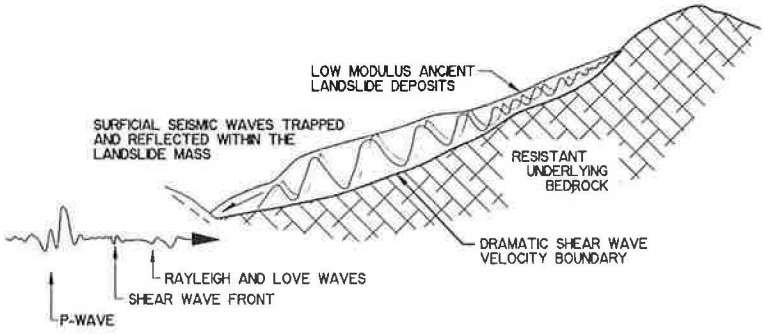

FIGURE 1 Site response of large ancient landslides in mountainous terrain, showing entrapment of surface waves in softer, yielding sediments or landslide cover.

7. Amount of previous densification induced by antecedent shaking, age of embankment, or previous cycles of groundwater rise and fall;
8. Seismologic constraints, such as near-field effects, wave entrapment, shallow bedrock escarpment reflections, Moho reflections, seismic focusing, bilateral versus uniaxial rupture scenarios at the hypocenter, and so on; and
9. Coseismic vibrations induced by adjacent ground movement, tidal waves, seiches, and so on.

Experience has shown that highway embankments are particularly susceptible to earthquake-induced settlements, especially bridge abutment approach fills (Figure 2). In the abutment area, large strains can be induced by vertical seismic acceleration and by transverse response of stiff bridge support members (the shorter supporting columns or bents will generally be of much higher stiffness).

Also particularly susceptible to quake-induced densification are older side-cast roadway fills across former gullies and ravines in steep, mountainous terrain (Figure 3). Valley fills are subject to settlement in directions transverse and parallel to the old valley trend (Figure 4). In such cases, the magnitude of observed settlement depends markedly upon strong motion duration and the water table position within the embankment. Embankments that are excited by seismic shaking in dry years tend to be most prone to dynamically induced settlement. On the other hand, earthquake loading effects on embankments are most pronounced at levels in excess of 80 percent of the static rupture strength, meaning that a large number of lower-level load cycles may have little or no effect on inducing large permanent strains (*7*).

Seismic Activation of Landslide Complexes

Most ancient slides exhibit abundant evidence of semicontinuous, long-term movement, or creep. As the slide mass is excited by either vertical or lateral earthquake accelerations, some densification inevitably occurs within units of low or moderate relative density. In addition, seismic shear waves induce excessive shear stresses, which cause the embankment to physically deform. Some portion of this physical deformation is not recoverable and results in permanent deformation, because soil and rock mixtures are elastoplastic. Dynamically induced settlements observed after earthquakes are, therefore, generally caused by a combination of mass densification and excessive shear stress. Embankments by their nature are constructed in a layered fashion, thereby engendering anisotropy of their physical properties and moduli of deformation (*9*). In addition, embankments are seldom symmetrical with respect to their foundations and as a consequence cannot be expected to show a symmetrical response. For these reasons, differential settlement of embankments or ancient landslide deposits is inevitable.

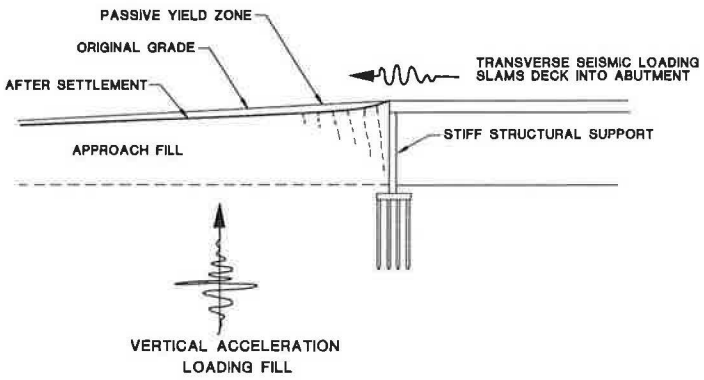

FIGURE 2 Dynamically induced settlement of viaduct approach fills.

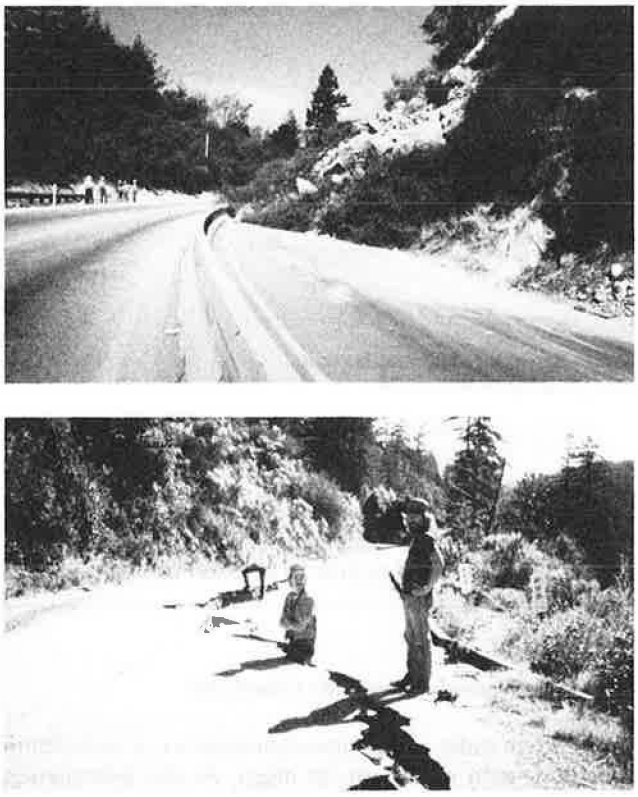

FIGURE 3 Roadway fills susceptible to quake-induced densification. *Top*: seismically induced rockfall of dry bedrock cut on California Route 17 near the epicenter of 1989 Loma Prieta earthquake (*photograph by Woodrow Higdon, Geo-Tech Imagery Int.*). *Bottom*: settlement of unkeyed fill wedge on Old Santa Cruz highway after 1989 Loma Prieta earthquake (*photograph by Dan Orange, University of California, Santa Cruz*).

Within the accepted precepts of soil mechanics consolidation theory, even dynamically induced settlement must follow lines of principal effective stress, which are not vertically inclined (although these lines are influenced by the ratio between horizontal to vertical acceleration). The lower the relative water table within a hillside compartment, the greater the potential for densification and classic settlement (because of higher effective stresses under dry conditions).

Differential densification will usually occur with a significant horizontal component of motion, causing tensile separations to form at the location of discrete but preexisting tension scarps. Often, these separations are most dramatic in old tension grabens, seen as soil-filled scarps or grabens on closer subsurface examination (Figure 5). The soil-filling of these scarps suggests that the same sort of tensile separation, settlement, and apparent downslope translation have occurred many times in the past. Downhole instruments, such as inclinometers, could be expected to register pseudo downslope motion in the event of simple densification because of the significant downslope component of movement (which would increase in accordance with slope inclination).

Graphic evidence of both consolidation and creep-induced settlement of large landslide complexes can be drawn from successive inclinometer readings. In Figure 6 a series of inclinometer readings and observations drawn over a period of 7 consecutive years is shown schematically. The uppermost cross section depicts observed groundwater levels shortly after the apparent cessation of macroslide movement. At this juncture, inclinometers were installed to record any further movement. The middle section shows observed water levels within the slide mass and indicated motion on one of the inclinometers 3 years later. Some net downslope motion appears to have occurred concurrent with an observed drop of the entrapped groundwater level. The lowest section shows the same situation some 7 years later. The inclinometer reading indicates

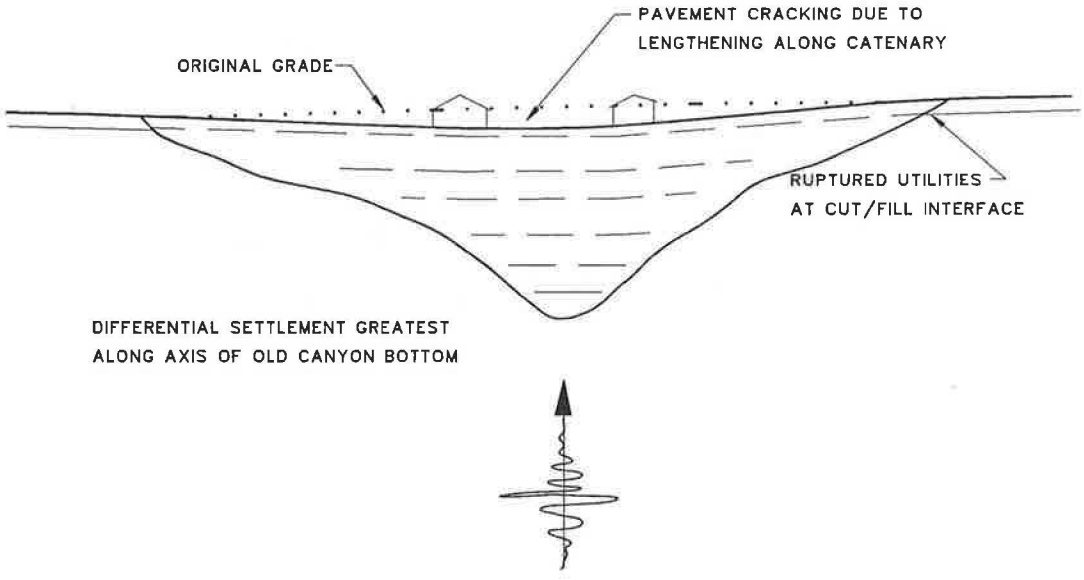

FIGURE 4 Dynamically induced settlement of valley fill.

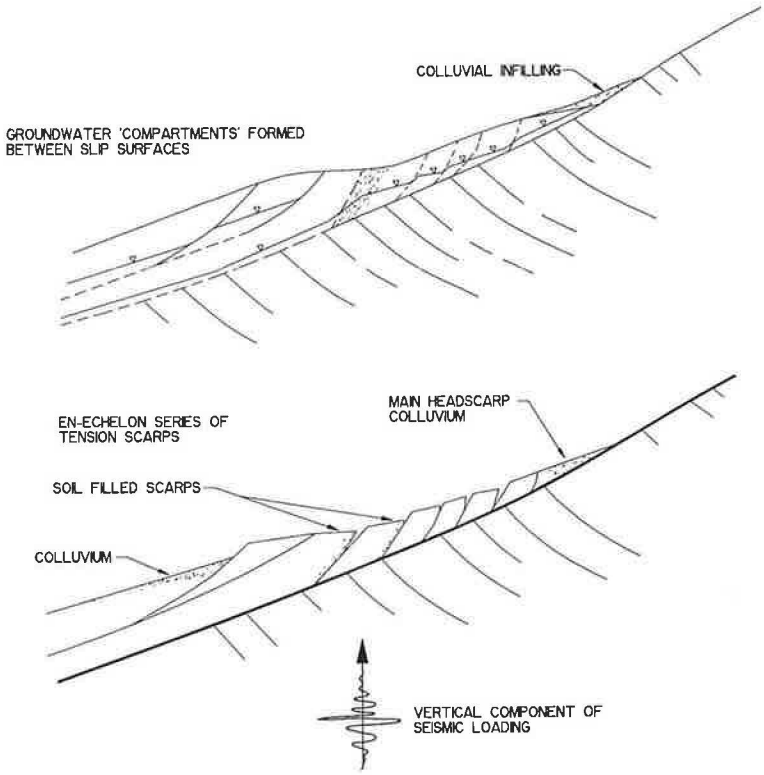

FIGURE 5 Differential densification of headscarp in ancient landslides. *Top*: coalescing ancient landslide. *Bottom*: pseudo slippage observed following earthquake.

more than twice the movement of 4 years before, and the water table has consistently continued to fall.

The curvilinear portion of the inclinometer profile appears to follow the declining water table. It is believed that the inclinometer has recorded consolidation and shrink-induced settlement of the slide mass, following dilation and swell associated with mass translation. Although significant subsurface motion is also recorded, it does not appear attributable to translation of the landslide mass on its own slip surfaces. Nevertheless, such movement, or macro creep, could be expected to shift any structure extending across the mass onto more stable adjacent ground. This would therefore be an example of pseudo landslide motion, induced by a combination of shrink, creep, and settlement as the slide mass slowly dries out and consolidates.

In general terms, the response of large ancient slides to seismic loading would appear to be heavily influenced by the following factors:

1. The relative static safety factor (SF) at the time of seismic shaking; no slide mass with a static SF of 1.70 or greater has failed in an earthquake, no matter of what intensity (*10,11*);
2. The relative amount of groundwater entrapped within the slide mass at the time of shaking; earthquakes during years of high precipitation tend to reactivate many more slides than those occurring in dry years;
3. The geographic position of the slide mass with respect to the earthquake focal area; and
4. The geophysical properties of the landslide mass and the duration of strong shaking (number of equivalent load cycles).

The latter two factors were discussed previously. The relative position of entrapped groundwater tables is critical to static slope stability assessments and probably even more critical to seismic stability evaluations. In general, higher levels of moisture, or saturation, tend to occur in zones subjected to downslope accretion (as shown in Figure 1) or adjacent to structural aquacludes, such as faults.

A schematic cross section of a hypothetical headscarp is shown in the upper part of Figure 5. Individual groundwater compartments are typically formed between both lithologic and old slip surface boundaries. Old tension scarp grabens, typically exposed as areas of gentle slope or closed depressions, usually funnel large amounts of surface run-off into the slide mass.

RESPONSE OF EMBANKMENTS

In order to study the deformational potential of highway embankments, some basic understanding of static effective stress distributions within such slopes is necessary. Prediction of the dynamic performance of an embankment is intrinsically related to the static stress history of the embankment.

Figure 7 is a schematic section through a nonkeyed embankment composed of clayey fill subjected to varying groundwater levels. Shallow groundwater commonly accumulates in fills because of perching along less-permeable strata or older native soils buried beneath the embankment. In Figure 7 the relative change in effective stress (defined as the total stress minus the pore pressure) at two different positions in the

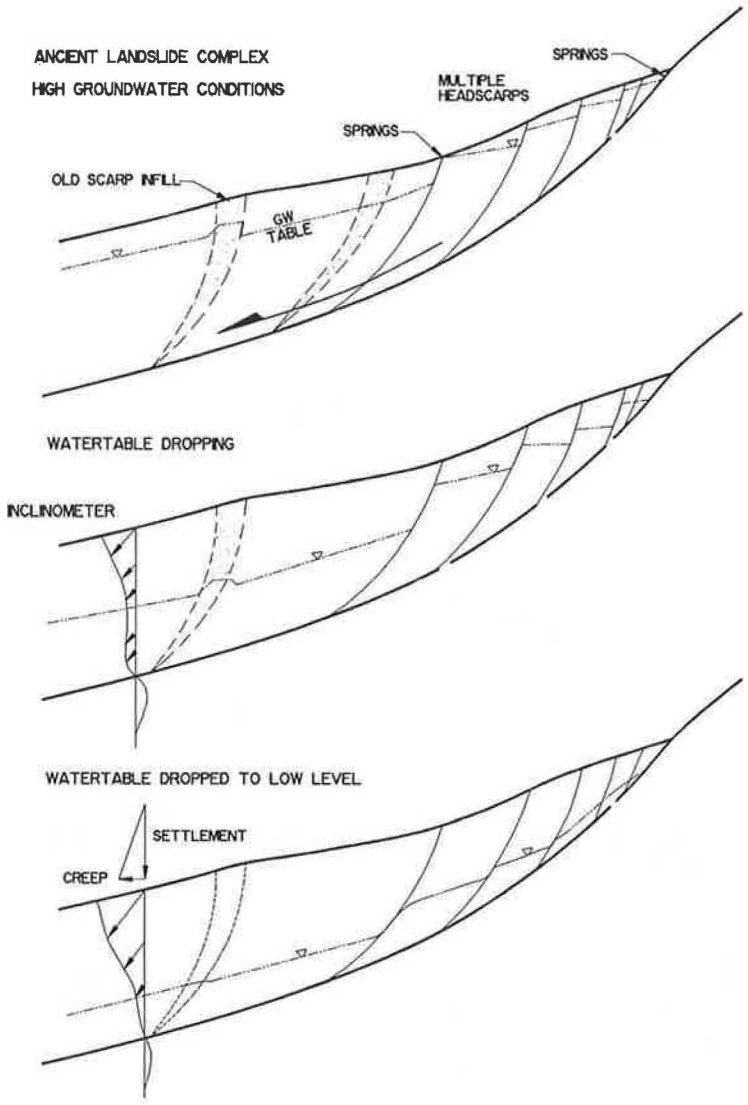

FIGURE 6 Consolidated shrink-induced settlement.

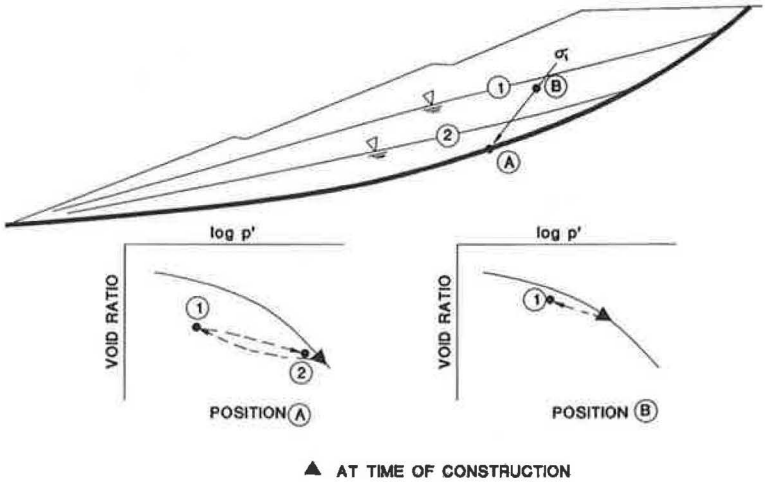

FIGURE 7 Effective stresses in valley-side fill during periods of high and low groundwater accumulation.

embankment is represented on conventional pressure-void ratio consolidation plots. Position *A* represents the approximate position of maximum effective stress at the time of construction. Note that this location lies on the virgin compression curve. If groundwater accumulates to a Level 1 (approximately five-eighths saturation of the embankment), the soil at Position *A*, through buoyance, swells along the rebound curve to Point 1, a reduction of two-thirds of the effective stress it originally felt. The amount of shear strength that could be mobilized at Position *A* is thereby greatly diminished through buoyance.

Soil situated somewhat higher in the embankment, at Position *B*, does not experience as dramatic a change, because of its less-confined position. At the time of compaction, it is just beginning to plot on the virgin consolidation curve, because of its overconsolidated nature (assuming a clay with moderate plasticity). When the water table rises to Level 1, the soil swells along its respective rebound curve. Through the process of cyclic swelling and shrinkage, the stress history of a clayey material (imprinted by mechanical compaction at the time of construction) is slowly erased (*12*). In addition, through such load cycling, intrinsic cohesion may be greatly diminished. Simple long-term saturation can also cause a loss of cohesion, as described by Morganstern and Eigerbrod (*13*) and demonstrated by Rogers and Pyles (*14*) (Figure 8).

As in the example of an ancient landslide, the prediction of settlement or lurching of embankments is strongly influenced by the in situ effective stress field. Figure 9 (*top*) shows the trajectories of maximum principal stress in valley-side sliver fill (unkeyed) embankments. A similar distribution of maximum-stress trajectories for keyed embankments is shown in the lower part of Figure 9. Note the influence of the slope face on the principal stresses, causing them to be inclined downslope.

Figure 10 shows expected settlement vectors in the same embankment as that in the upper half of Figure 9. Settlement

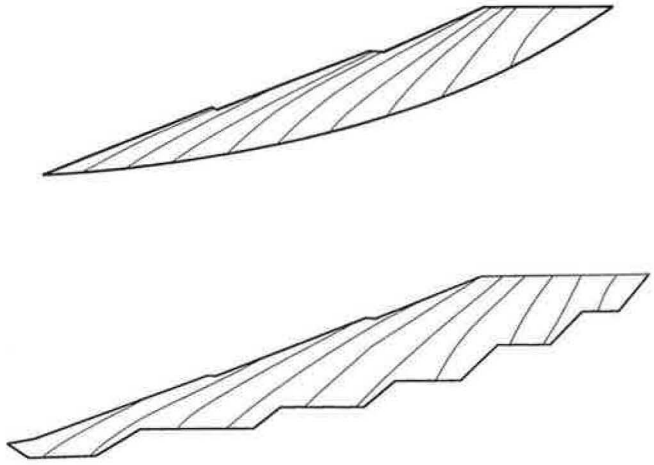

FIGURE 9 Principal effective stress distribution. *Top*: valley-side sliver fill. *Bottom*: keyed valley-side fill embankment.

vectors will tend to mimic the principal stress trajectories, engendering a significant horizontal component of movement much like a landslide. Outward surface manifestations of such movements—typically a down-dropped roadway shoulder, tension cracks aligned in an accurate manner around the deepest portions of the fill wedge, and asymmetric settlement of midslope drainage terraces—are very similar to incipient land slippage. Note how the horizontal component of motion can be fairly severe. Such slopes may continue to creep because of any number of environmental factors, such as a declining water table or groundwater feeding into discrete zones of the fill (through increased subsurface percolation generally caused by periods of excessive percolation).

If shrink-swell cycles continue unabated, embankment settlement due to creep will continue to manifest itself. Examination of inclinometer time-deformation histories suggests

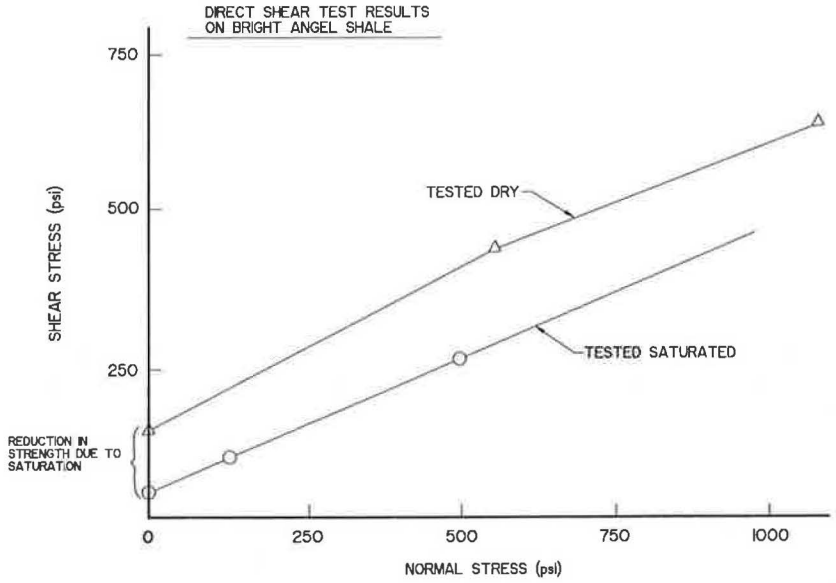

FIGURE 8 Reduction in effective cohesion of dense Cambrian-age shale subjected to shear testing parallel to bedding (*19*).

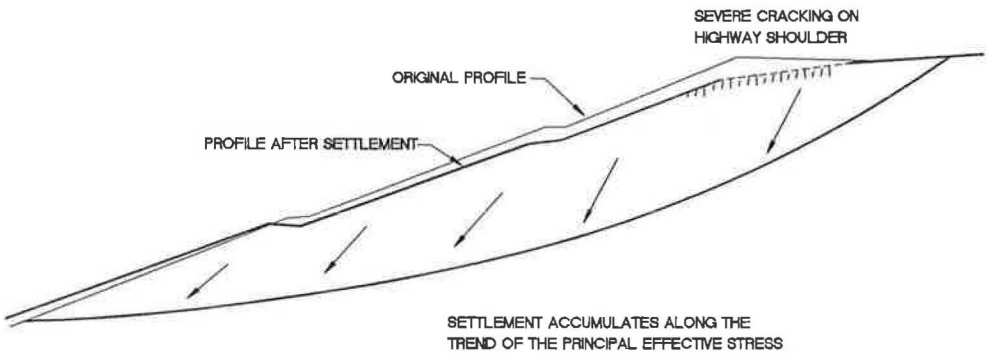

FIGURE 10 Expected settlement vectors in valley-side wedge fill.

that creep and settlement-induced strain is accumulated upslope, close to basal boundaries of the embankment, as shown in Figure 10. When the strain accumulates sufficiently to supersede the limiting strain of the soil, rupture will begin, generally along some of the shoulder tension cracks. In most embankments, this rupture is progressive from top to bottom of the slope. As accumulated strain levels approach 0.5 to 1.5 percent of the basal fill-contact length (L) as shown in Figure 11, rupture will progress at successively higher rates of strain until macrorupture occurs somewhere near the position indicated as MR. After shearing through the soil progresses to the vicinity of MR, sufficient driving forces are generally mobilized to rapidly overcome the remaining unsheared portion of the embankment toe. At this juncture, true landslide motion begins, where a semicoherent mass freely translates downslope. As macromotion of the entire slide mass continues, residual shear strength levels develop along the newly formed slide surface, thereby causing the resisting forces to degrade below prefailure peak strength levels. If the mobilized shear strength drops to residual values, landslide motion may continue for some period of time with less apparent connection to environmental conditions such as rainfall.

The progressive failure sequence described in Figure 11 has long been recognized by both highway and railroad engineers, who casually refer to such a sequence as a landslide that "creeped itself to failure" (*15*). Indeed, examples exist of large continuous slide motions without any apparent relation to weather extremes, for example, the Palolo Valley slide, first described by Peck (*16*), which has continued to move even through a significant drought from 1973 to 1988. In other instances, such as the celebrated slides along the Culebra Cut in the Panama Canal, an equal number of major bedrock slides reach their rupture points in dry years as in wet years (*17*).

With the above observations in mind, it would appear that virtually every slope or embankment possesses unique geologic, hydrologic, and construction history characteristics. These characteristics and the load history due to plasticity, creep, and cycling of entrained pore pressures likely serve to imbue each slope with a unique threshold with respect to future movement. In more colloquial terms, some slopes have "creeped" enough (through any number or combination of the above-cited factors) to be close to failure at any particular time. The concept of the continuously degrading slope safety factor was first proposed by Terzaghi (*18*) and has been cited by many others in explaining why some extremely large slides survive large storms and then are seemingly triggered by smaller ones (*16,19*).

DISCRIMINATING BETWEEN SETTLEMENT AND LANDSLIDING

Much confusion has arisen from recent postearthquake reconnaissances in which scores of ground cracks have been observed within and adjacent to large embankments and known ancient landslide complexes. The author believes that much of what has previously been described as seismically induced "landslippage" is actually seismically induced "settlement," the surface manifestations of which are strikingly similar but the analytical procedures for which are dramatically different.

Appreciating the similarities and variance between settlement and landslide-induced embankment deformations would appear particularly relevant to highway engineering maintenance, modification, and mitigation assessments. Illustrative case histories of embankments subject to both settlement (Figure 12) and landslide (Figure 13) are given.

Figure 12 shows a set of circumstances typical of a modern-day keyed highway embankment. The highway fill was keyed into underlying bouldery colluvium (Step 1). With time and seasonal precipitation, shallow groundwater can build up within the embankment (Step 2). At high water levels, the embankment may begin to exhibit outward manifestations of apparent downslope movement. At this juncture, most highway departments simply overlay the subsiding area with asphalt, but prudent engineers may opt for installing inclinometers to monitor long-term movement. In Step 3, inclinometers have been installed and the readings taken indicate a falling water table with apparent settlement and downslope motion. However, the apparent horizontal offsets measured in the inclinometers should mimic the fall of the water level (as shown in Figure 6) and will tend to decrease toward the brow of the embankment slope. This would be the classic subsurface pattern associated with simple consolidation and settlement of the embankment.

Figure 13 shows incipient landslide motion in a nearly identical geologic setting. As in the previous study, a keyed

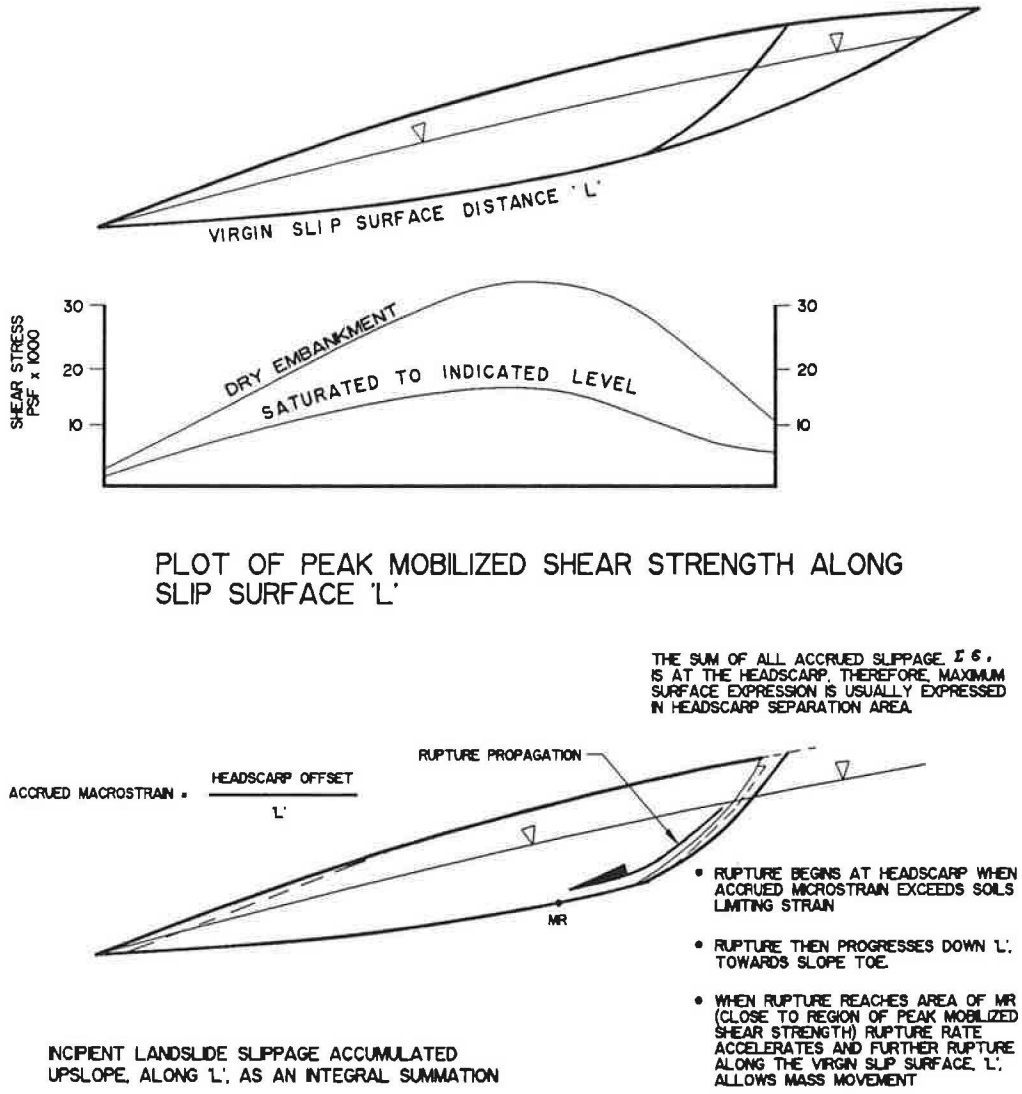

FIGURE 11 Plot of peak mobilized shear strength along slip surface *L*.

embankment was founded upon a bouldery colluvium with an overconsolidated clay matrix (Step 1). Once again, the roadway shoulder exhibited evidence of movement, so inclinometers were installed. In this instance, the ground surface settlement distribution was observed to be similar to that shown in Figure 12. The exception was that a sharp offset was noted in vicinity of the headscarp. Measured settlements to the roadway side of the headscarp were minimal when compared with those on the slope side. The headscarp separation appeared to mimic the approximate location of the embankment's upper key backslope. Inclinometer readings indicated a consistent increase in measured motion toward the brow of the embankment slope. This would be the classic subsurface deformational pattern associated with landsliding.

After macrotranslation of a landslide begins and the mass starts to translate downslope as a semicoherent mass, inclinometer casings are usually sheared off and little controversy remains as to what is occurring. Less often, large, translatory slide masses can creep along with similar movement levels manifest throughout the mass (although inclinometer readings still tend to be smaller at the toe and larger toward the headscarp). If an ancient translational slide is reactivated, less obvious precursory motion in terms of strain levels ascending upslope is measured.

CONCLUSIONS

Although engineering geologists are capable of identifying ancient landslide areas and highway embankments on a broad scale, the assessment of seismic instability potential is, at the present time, exceedingly difficult to predict. Permanent slope deformation under earthquake loading appears to be dependent on a large number of site-specific variables relating to geology, hydrology, seismology, and construction practices. However, certain slopes, through their geologic and topo-

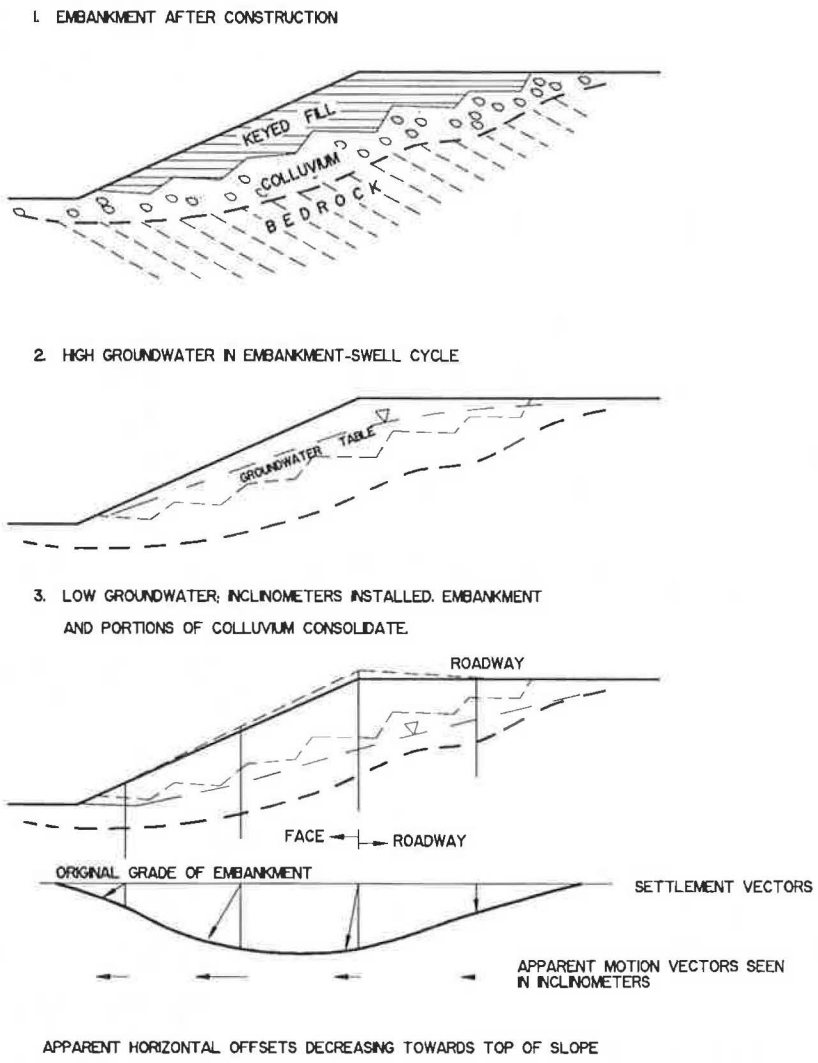

FIGURE 12 Slope strain by settlement.

graphic setting and previous site history, are likely more prone to failure because their static factors of safety have degraded to a point of marginal stability.

No simple limit equilibrium or pseudostatic loading relationship presently exists that can coprocess all of the geologic and seismologic variables. At this time, judicious engineering, geologic mapping and analyses, in situ instrumentation, and surface alignment surveys are the most proven approaches for defining potential problem areas. Ancient landslide reactivation can be analyzed using gross empirical estimates such as those posed by Wilson and Keefer (*20*) of the U.S. Geological Survey. Analysis of gross permanent embankment deformations can still be effected using simplified procedures developed by Makdisi and Seed (*7*) for earth dams, but these procedures should not necessarily be applied to more foreign situations, such as sanitary landfills. It is likely that an expansion of analytical techniques can be expected in the coming decade if federal funding for research in this area continues through the Federal Highway Administration, state transportation departments, or the National Earthquake Hazard Reduction Program.

ACKNOWLEDGMENTS

The author is grateful to the many individuals with whom he has associated who are astute observers of seismically induced slope movements, including David K. Keefer, Edwin Harp, and Ray Wilson of the U.S. Geological Survey; William C. Cotton; the late H. Bolton Seed; J. Michael Duncan; Ralph B. Peck; and Richard E. Goodman. John Walkinshaw solicited and kindly reviewed the article, which is a synopsis of a considerable body of information that the author is currently researching.

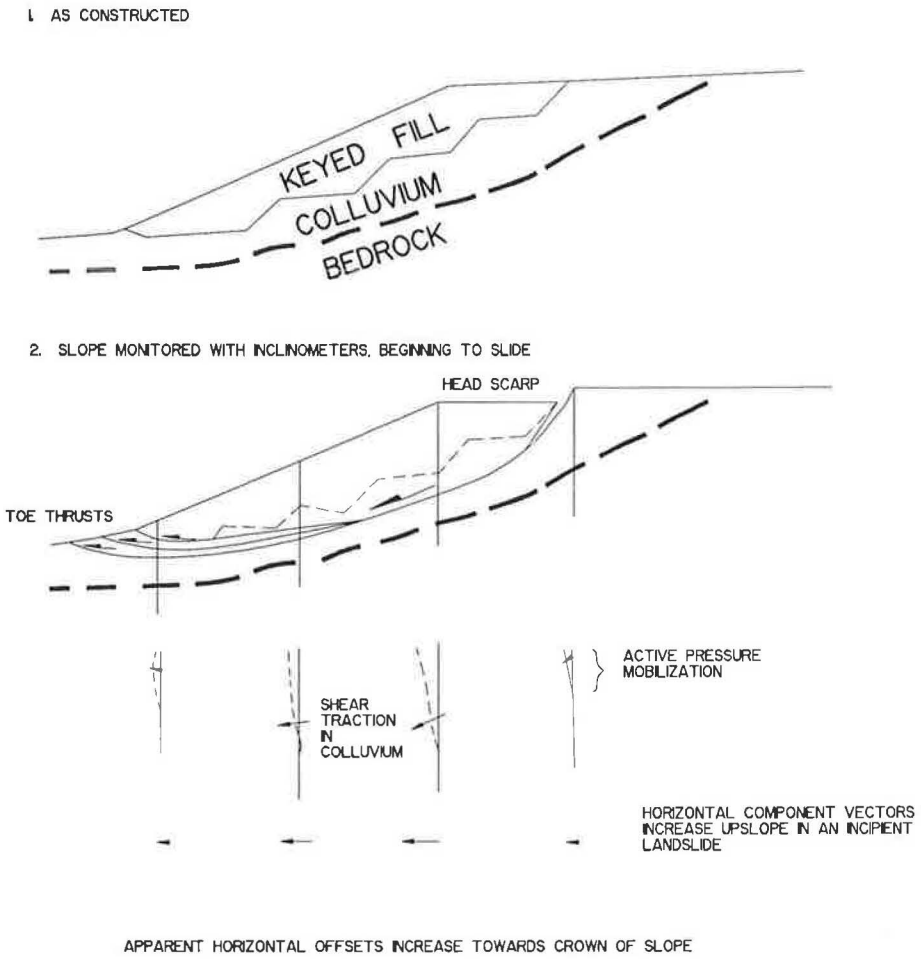

FIGURE 13 Embankment subject to landsliding.

REFERENCES

1. H. O. Wood. Distribution of Apparent Intensity in San Francisco. In *California Earthquake of April 18, 1906*, Carnegie Institution of Washington, D.C., Publication 87, Vol. 1, Part 1, 1908, pp. 220–254.
2. T. Naito. Earthquake-Proff Construction. *Bulletin of the Seismological Society of America*, Vol. 17, No. 2, 1927, pp. 57–94.
3. R. D. Borcherdt. Effects of Local Geology on Ground Motion Near San Francisco Bay. *Bulletin of the Seismological Society of America*, Vol. 60, 1970, pp. 29–61. R. D. Borcherdt and J. F. Gibbs. Effects of Local Geological Conditions in the San Francisco Bay Region on Ground Motions and the Intensities of the 1906 Earthquake. *Bulletin of the Seismological Society of America*, Vol. 66, 1976, pp. 467–500.
4. H. B. Seed and I. M. Idriss. Influence of Soil Conditions on Ground Motions During Earthquakes. *Journal of the Soil Mechanics and Foundation Engineering Division*, ASCE, Vol. 95, No. SM1, 1969, pp. 99–137.
5. H. B. Seed and I. M. Idriss. Influence of Soil Conditions on Building Damage Potential During Earthquakes. *Journal of the Structural Division*, ASCE, Vol. 97, No. SM9, Proc. Pap. 8371, Sept. 1971, pp. 1249–1273.
6. E. L. Krinitzsky and F. K. Chang. *State-of-the-Art for Assessing Earthquake Hazards in the United States: Report 25 Parameters for Specifying Intensity-Related Earthquake Ground Motions*. Misc. Paper S-73-1. U.S. Corps of Engineers, Waterways Experiment Station, Vicksburg, Miss., 1987, 83 pp.
7. F. I. Makdisi and H. B. Seed. *A Simplified Procedure for Estimating Earthquake-Induced Deformation in Dams and Embankments*. Earthquake Engineering Research Center Report UCB/EERC-77-19. University of California, Berkeley, 1977.
8. H. B. Seed and G. R. Martin. The Seismic Coefficient in Earth Dam Design. *Journal of the Soil Mechanics and Foundation Engineering Division*, ASCE, Vol. 92, No. SM3, May 1966.
9. R. E. Goodman. *Introduction to Rock Mechanics*. John Wiley & Sons, New York, 1980, 478 pp.
10. H. B. Seed. Earthquake Resistant Design of Earth Dams. In *Seismic Design of Embankments and Caverns: Proceedings of a Symposium*, Geotechnical Engineering Division, ASCE National Meeting, Philadelphia, 1983, pp. 41–64.
11. M. E. Hynes-Griffin and A. G. Franklin. *Rationalizing the Seismic Coefficient Method*. Misc. Paper GL-84-13. U.S. Army Corps of Engineers, Waterways Experiment Station, Vicksburg, Miss., 1984, 37 pp.
12. T. D. Stark and J. M. Duncan. Mechanisms of Strength Loss in Stiff Clays. *Journal of the Geotechnical Engineering Division*, ASCE, Vol. 177, No. 1, Jan. 1991, pp. 139–154.
13. N. R. Morganstern and K. Eigenbrod. Classification of Argillaceous Soils and Rocks. *Journal of the Geotechnical Engineering Division*, ASCE, Vol. 100, No. GT10, 1974, pp. 1137–1159.
14. J. D. Rogers and M. R. Pyles. Evidence of Cataclysmic Erosional Events in the Grand Canyon of the Colorado River, Arizona. In

Proceedings of the Second Conference on Research in the National Parks, San Francisco, National Park Service, Washington, D.C., Physical Sciences, Vol. 5, 1979, pp. 392–454.
15. G. E. Ladd. Landslides, Subsidence and Rockfalls. In *Proc., 36th Annual Convention*, American Railway Engineers Association, Chicago, Vol. 36, 1935, pp. 1091–1163.
16. R. B. Peck. Stability of Natural Slopes. *Journal of the Soil Mechanics and Foundation Engineering Division*, ASCE, Vol. 93, No. SM4, 1967, pp. 403–417.
17. D. F. McDonald. Panama Canal Slides. In *The Panama Canal Third Locks Project*: Department of Operations and Maintenance, Panama Canal Commission, Balboa Heights, Canal Zone, 1947, 73 pp.
18. K. Terzaghi. *Mechanisms of Landslides: Applications of Geology to Engineering Practice* (Berkey Volume), Geological Society of America, 1950, pp. 83–123.
19. J. M. Duncan. Prevention and Correction of Landslides. Presented at Sixth Annual Nevada Street and Highway Conference, Section II, April 7, 1971.
20. R. C. Wilson and D. K. Keefer. Prediction Areal Limits of Earthquake-Induced Landsliding. In *Evaluating Earthquake Hazards in the Los Angeles Region—An Earth Science Perspective*, U.S. Geological Survey Professional Paper 1360, 1985, pp. 317–346.

Publication of this paper sponsored by Committee on Soils and Rock Instrumentation.

Accelerated Movement of Large Coastal Landslide Following October 17, 1989, Loma Prieta Earthquake in California

JOAN E. VAN VELSOR AND JOHN L. WALKINSHAW

The January storms of 1982 mobilized an ancient landslide in the coastal bluffs of Marin County, California. Slow, intermittent movement of portions of the large slide mass required periodic maintenance by the local highway district through 1989. A significant increase in the rate of movement occurred following the October 17, 1989, Loma Prieta earthquake. Because the new rate of movement made it impossible to keep the highway open, the highway was closed for 13 weeks following the earthquake. The roadway was ultimately relocated behind the failure plane and the approximately 765 000 m^3 (1,000,000 yd^3) of excavation material placed in the ocean (as an erodible fill) against the lower slope of the landslide. Before the earthquake, approximately 5.5 m (18 ft) of intermittent downslope movement occurred between 1982 and October 1989. During the 17-month monitoring period between the earthquake and landslide repair some 28 m (92 ft) of downslope movement was recorded. The rate of slide movement increased to more than 50 mm/day between October 1989 and the spring of 1990, decreased, and then accelerated to 284 mm/day just before construction began in the spring of 1991.

In 1991, the California Department of Transportation (Caltrans) repaired a large landslide, called the Lone Tree landslide, in the coastal bluffs of Marin County (see Figure 1). Historic landsliding at this site began when the January storms of 1982 mobilized a portion of an ancient landslide. In the years following 1982, the remobilized landslide experienced relatively slow, intermittent, downslope movement.

The steep ocean-fronting cliffs of Marin County have long been associated with landslide processes. The combination of a young, geologically recent, uplifted terrain; active coastal erosion by wind and waves; and an inherently weak geologic foundation material (the Franciscan formation) has resulted in landslides' being the dominant erosional process in the region. The scalloped coastline is formed of overlapping active and dormant landslides and resistant narrow ridges (see Figure 2).

Before the October 17, 1989, Loma Prieta earthquake, movement on the Lone Tree landslide varied from 60 mm to 300 mm/month (2.4 to 12 in./month). After the earthquake, movement increased from 910 mm to 1220 mm/month (3 to 4 ft/month). The rate of slide movement following the earthquake made it impossible to maintain a traversable roadbed and the highway was closed on January 15, 1990.

J. E. Van Velsor, California Department of Transportation, District 4, P.O. Box 7310, San Francisco, Calif. 94120. J. L. Walkinshaw, Federal Highway Administration, Region 9, 211 Main Street, Suite 1100, San Francisco, Calif. 94105.

LONE TREE LANDSLIDE

The Lone Tree landslide extended from just above sea level to approximately Elevation 120 m (400 ft) mean sea level (MSL) and was about 140 m (600 ft) wide and 30 m (100 ft) deep under the roadway. State Route 1 traverses the landslide at Elevation 65 to 70 m (210 to 230 ft) MSL.

Portions of the larger landslide were active during the 1980s (see Figure 3). Between 1982 and 1989, the northern and southern parts of the slide were active. Landslide movement had occurred both above and below the road. The maximum amount of movement occurred in the northern portion, known as the Lone Tree landslide.

A foundation investigation and landslide analysis resulted in a repair strategy of unloading the upper portion of the slide approximately 765 000 m^3 (1,000,000 yd^3) and relocating the highway 70 m (230 ft) inland, behind the slide plane.

Because the project area is surrounded by overlapping and adjacent park land and public agency jurisdictions, selecting a geotechnically suitable and environmentally acceptable disposal site for the excavation material became a major part of the environmental processing of the project. In all, 13 public agencies had jurisdiction or permit authority over the project. Vigorous public debate and the concerns of permitting agencies resulted in about 15 months of environmental evaluation and alternative disposal selections while the highway remained closed.

Hauling the excavation material up to 26 km (19 mi) to existing disposal sites was opposed by the small communities both north and south of the landslide because of the anticipated lengthy community disruption from passing haul trucks. Hauling would also have caused substantial damage to the two-lane state highway. Exclusive of actual hauling costs, it was estimated that the 160-day continuous haul would cause pavement damage equal to 3 years of normal traffic usage, at an equivalent cost of $210,000 to $270,000.

On-land disposal of the material in upland areas was opposed by the adjacent state and federal public park jurisdictions and was geotechnically unacceptable because of the high probability of initiating other slope failures by overloading the already marginally stable slopes.

Ocean disposal was opposed by marine protection agencies because of the anticipated damage to marine organisms from direct burial and from future sedimentation from the eroding fill. A federal marine sanctuary is located approximately 460 m

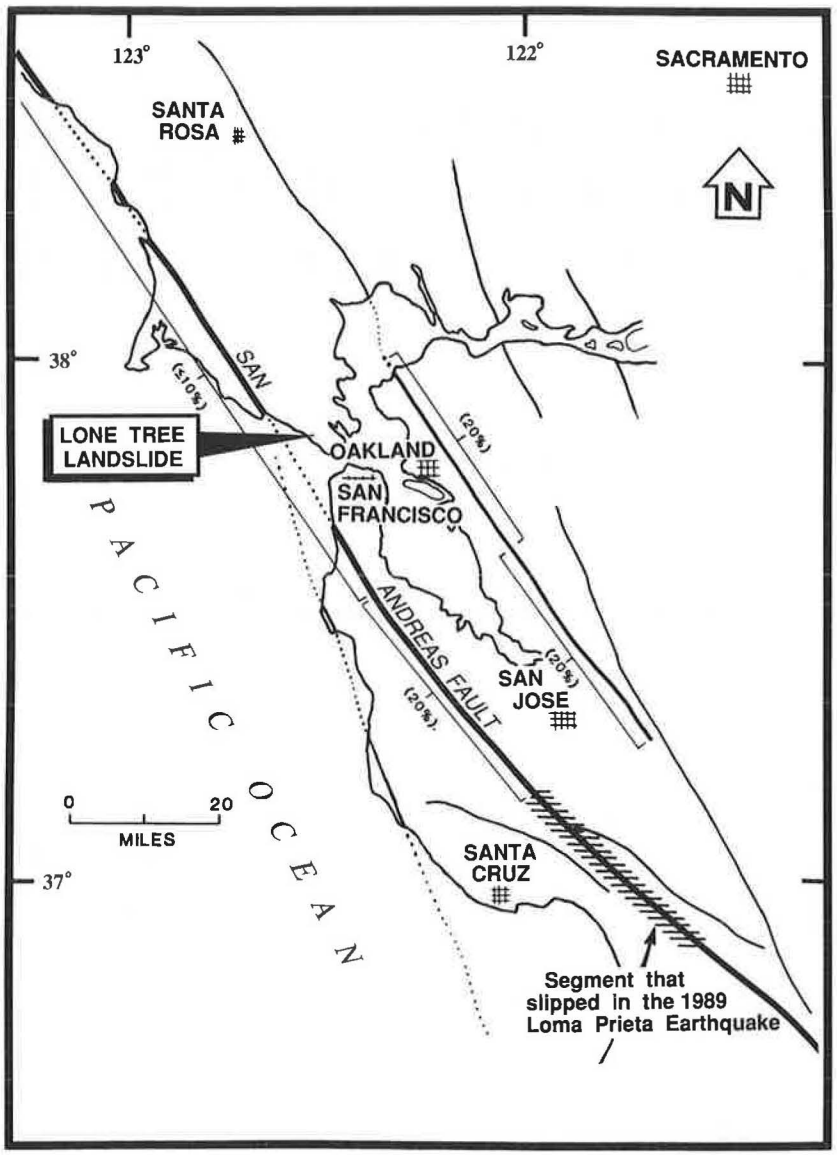

FIGURE 1 Location map; diagram shows conditional probabilities of major earthquakes in Bay Area (*12*).

(1,500 ft) offshore and was a major concern. Before landslide repair, 1525 to 1990 m^3 (2,000 to 2,600 yds^3) of soil and rock were already entering the marine environment each month because of slide movement. It was estimated that 2038 to 2650 m^3 (2,670 to 3,470 yds^3) would be eroded from the proposed fill each month, a 30 percent increase over the expected 25- to 30-year lifetime of the fill.

Lengthy discussions and negotiations with permitting agencies were required. Proposals to remove the excavation material by barges (estimated cost $1.8 million), installation of offshore cofferdams or Longard geotubes, and engineered construction of the proposed fill with a permanent rock revetment (estimated cost $550,000) were evaluated. All these alternatives were rejected on the basis of feasibility or likelihood of causing more environmental damage than was prevented.

Ultimately, approval was obtained to dispose of the 765 000 m^3 of excavation material by placing it on the rocky beach and near-shore area as a lightly compacted fill against the lower slope of the landslide below the highway (see Figure 4). The involvement of elected local, state and federal senators and representatives and the state or national heads of the jurisdictional agencies was required to obtain the needed permits.

The fill extends some 55 m (180 ft) into the ocean and is anticipated to erode gradually over a period of years. Aggressive erosion control on the erodible fill and new cut slope; removal of fill infringing on a coastal stream approximately 2 mi to the south, which had been placed in the past by non–highway agencies to create a parking lot for beach access; and a 5-year offshore sedimentation and biologic community monitoring program in the slide area were conditions required

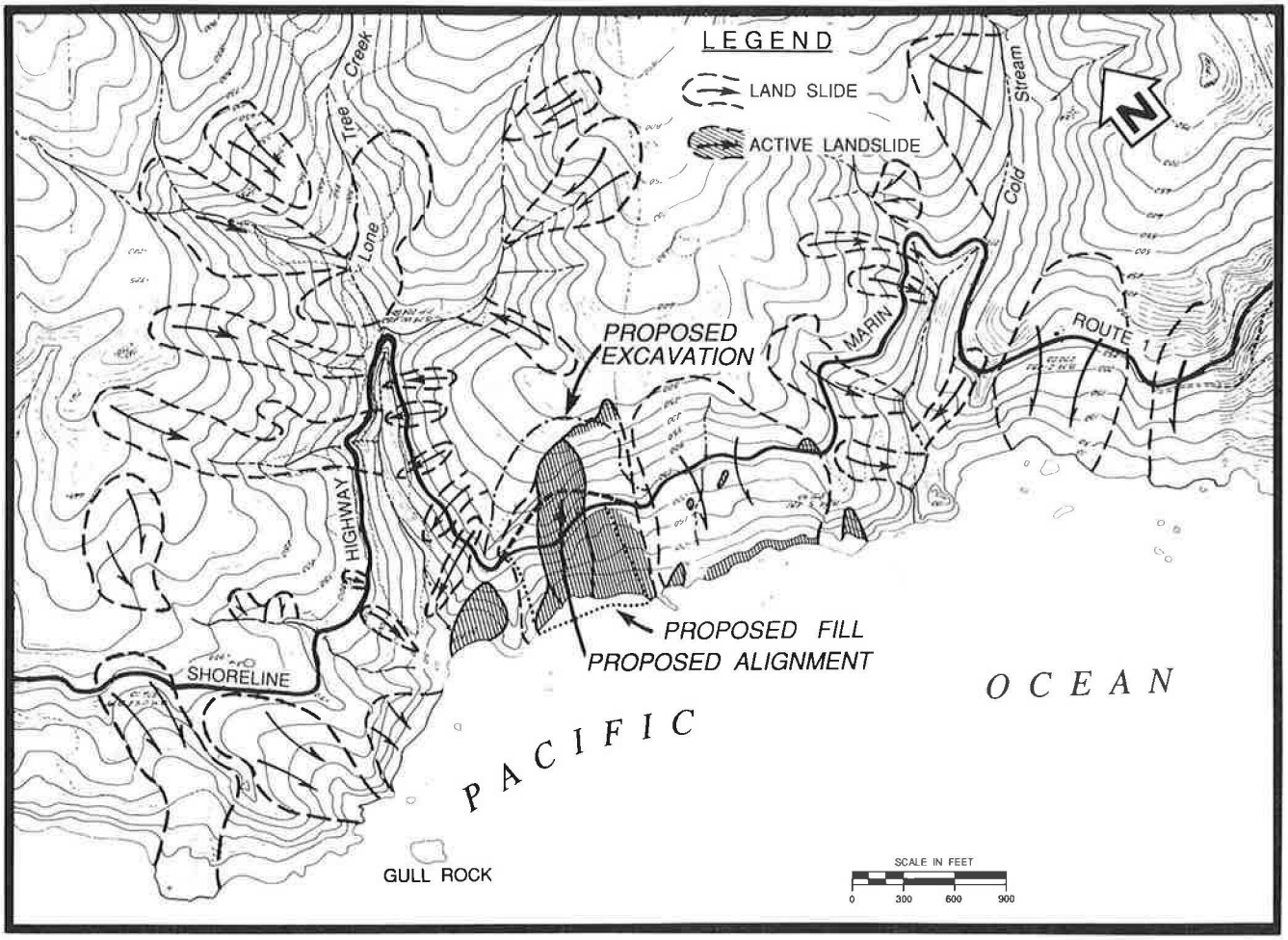

FIGURE 2 Regional landslide map.

by the permitting agencies as mitigation for the landslide repair. Mitigation costs are anticipated to reach at least 50 percent of the $2.1 million expended for actual construction to relocate the roadway to stable ground.

FOUNDATION CONDITIONS

The landslide is within the Jurassic-Cretaceous Franciscan formation. Eugeosynclinal deposits of greywacke, greenstone, chert, limestone, and exotic metamorphic rocks have been profoundly deformed and sheared by regional tectonics (*1*) in this region. The Franciscan formation is widely exposed over much of the California coast ranges and is often associated with large, deep-seated landslides. Landslides of all dimensions are present within the region.

The Franciscan formation is a complex assemblage of sedimentary, volcanic, and metamorphic rocks characterized as a melange—a heterogeneous mixture of disrupted rock masses in a pervasively sheared and crushed matrix material (*2*). Melange is believed to form at shallow depths in subduction zones where compressive forces between moving crustal plates crush and mix rocks of different origins.

Typically, repair of landslides in this type of formation is difficult. The heterogeneous and sheared nature of the Franciscan formation results in disrupted, unpredictable drainage paths, large boulders, and widely varying strengths of material.

Thirteen borings were placed for the investigation of this landslide. Borings SI-1 through SI-6, were placed for groundwater and inclinometer monitoring and were not sampled. Borings P-7 through P-13 were core borings placed to evaluate foundation conditions in the excavation back slope.

The rock recovered in the core borings was primarily highly friable and sheared black shale with sparse clasts [up to 7 m (23 ft) in diameter] of hard gray sandstone and lesser amounts of chert and metamorphic rock. Sieve analyses of core and bulk samples found 24 to 42 percent passing the 0.074-mm (#200) sieve. Dry unit weights averaged 2240 kg/m^3 (140 lb/ft^3) with moisture contents of 4 to 12 percent. Core recovery ranged from 76.5 to 100 percent and averaged 90.4 percent. The high core recovery rate in this difficult-to-sample material is due to the highly skilled state drill crew on staff with the District 4 Geotechnical Section.

The average rock quality designation (RQD), a measure of the degree of fracturing and therefore strength of a rock mass, was recorded for each core sample. RQD is defined as

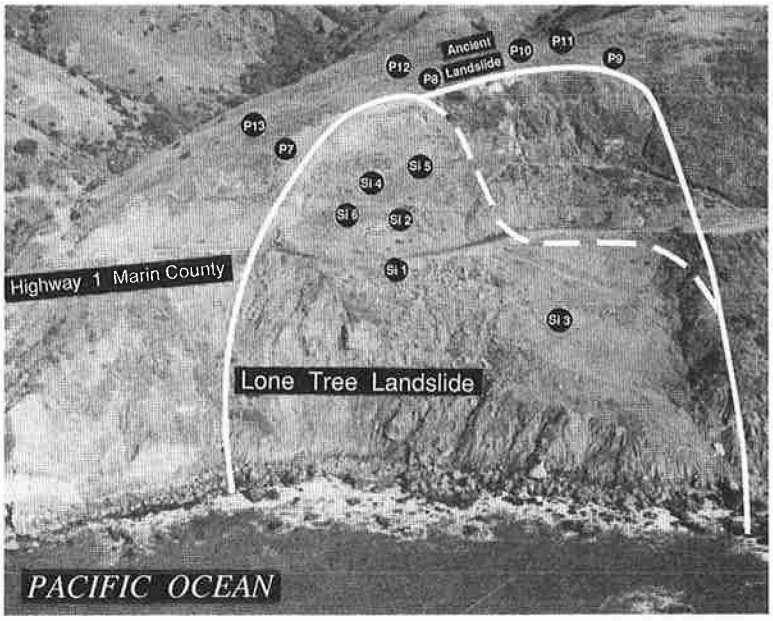

FIGURE 3 Aerial photograph of Lone Tree landslide.

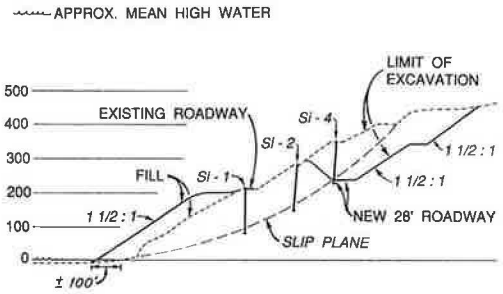

FIGURE 4 Cross section of Lone Tree landslide (Section A-A').

the total length of recovered core pieces greater than 100 mm (4.0 in.) in length expressed as percent of 1.5 m (5 ft) or more of core drilled (*3*). The average RQD was 16 percent but ranged from 0 to 100 percent.

The sheared and fractured state of the rock was also expressed in the frequent severe water loss zones encountered during drilling. For 70 to 80 percent of the coring operation, drilling fluids were not returned to the surface but flowed into the fractured rock.

Samples recovered from the core borings were subjected to soil strength tests. The unconfined tests found cohesion ranging from 29 to 86 kPa (600 to 1,800 psf). Triaxial testing [confining pressures 27 to 90 kPa (4 to 13 psi)] indicated an average ϕ of 24 degrees and cohesion of 50 kPa (1,000 psf).

PRE-EARTHQUAKE SLIDE CONDITIONS

Because of the landslide-prone terrain and the chronic but intermittent and slow rate of slide movement, little documentation of slide movement before the earthquake exists. Available data consists primarily of personal recollection, aerial photographs, snapshots, records of maintenance expenditures, and sparse pavement profiles.

The movement history of this site is typical of many state routes with chronic maintenance problems. For a long time, landslide movement was not documented in any kind of consistent, scientific manner.

The winter of 1981–1982 brought unusually high rainfall to the San Francisco Bay Area (see Figure 5). Unusually high antecedent moisture conditions were aggravated by the storm of January 3–5, 1982, which caused substantial damage throughout the Bay Area and closed State Route 1 at the Lone Tree slide for several months. During the January storm some 300 to 400 mm (12 to 16 in.) of rain fell in the 30-hr storm, which is about equal to the total annual rainfall for the area.

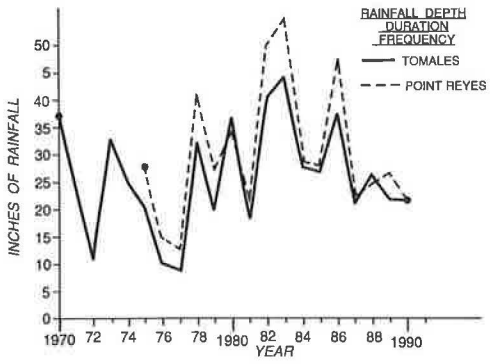

FIGURE 5 Rainfall data, Marin County, California, 1970–1990.

In 1982 it was recognized that the storm had reactivated a portion of an ancient landslide. In addition to landsliding above the road, which had occurred both above the subsiding roadway and to the north, subsidence below the roadway had occurred in the southern portion of the ancient landslide.

An inclinometer was installed at highway level in the southern portion of the landslide in May 1982 at a depth of 47 m (155 ft). The inclinometer was sheared off 8 to 12 months later, at a depth of 12 m (39 ft).

The $500,000 repair implemented in 1982 consisted of high, steep but relatively thin sliver cuts 3 to 4 m (10 to 15 ft) thick; a deep underdrain at highway level; improved surface drainage; and horizontal drains. To buttress the roadway, the excavated material was placed below the road at about Elevation 30 m (100 ft) MSL upward. Because of the steepness of the terrain and the need to minimize impacts to adjacent Mount Tamalpias State Park, the cut slopes were set at 1¼:1 (horizontal:vertical).

During the 1982 construction it was evident that the buttress itself was marginally stable because cracks quickly reappeared in the pavement and movement continued in the slope below the roadway. The 1982 repair was only temporarily effective because the landslide was deeper and laterally more extensive than originally believed. The roadway was reopened to traffic after a 4-month closure.

The northern slide area (the future Lone Tree landslide) began to develop between 1982 and 1983. By 1985 the landslide was clearly defined by cracks in the upper slope and pavement patches where the side scarps crossed the highway.

Unusually heavy rainfall occurred in 1982–1983 and landslide movement continued after the 1982 repair. Movement was generally slow (on the order of several centimeters per month) with brief localized episodes of movement of up to 300 mm/month (12 in./month). Highway maintenance staff repaved the highway periodically to maintain the road surface and highway maintenance expenditures were typically $20,000 to $40,000/year during this time.

During 1985–1986, cumulative subsidence of the roadway in the southern area became so pronounced that a lightweight fill (sawdust) was placed on the roadway in order to restore the highway grade and additional horizontal drains were installed.

The annual maintenance expenditures for this section of highway are graphically shown in Figure 6. About every fourth year there was a major reconstruction, reflecting the accumulation of slow displacement, which required periodic regrading.

In 1989 another increase in the rate of landslide movement was noticed, with almost a foot of vertical drop in August. Cumulative movement had once again lowered the highway profile, which resulted in an unacceptable vertical curve. The highway was once again leveled in August 1989 at a cost of $90,000.

Field reviews were conducted by Caltrans District 4 Geotechnical Section in August and September 1989. An attempt was made to install an inclinometer at roadway grade with a contract drill rig on October 10–11, 1989 because the District 4 state drill crew and rig were already committed to other projects. The contract rig supplied proved to be inadequate. After several equipment failures it was dismissed from the job and plans were made for installation of the inclinometer

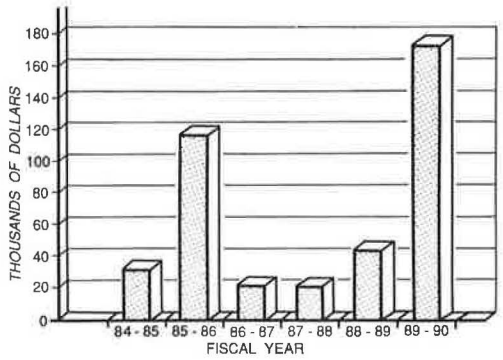

FIGURE 6 Maintenance expenditures at Lone Tree landslide, 1984–1990.

with a different drill rig. In view of the earthquake that followed on October 17, this delay was unfortunate.

The inclinometer was successfully installed on October 23–24, 1989, 7 days after the Loma Prieta earthquake. Inclinometer depth was 33 m (108 ft), and it was initialized on October 26. By November 6, the inclinometer had sheared off at a depth of 31 m (102 ft). Even though the bottom of the hole was no longer accessible, groundwater levels continued to be recorded in the inclinometer on a regular basis. This inclinometer also became the reference point for surface movement recorded by surveys taken from October 30, 1989, until April 9, 1991, when reconstruction of the highway began (see Figures 3 and 4).

On the basis of various highway profiles, topographic maps, aerial photography, and maintenance records we have estimated that 5.5 m (18 ft) of vertical settlement occurred during the 90 months between the January 3–5, 1982, storm and the October 17, 1989, earthquake. The amount of settlement averages to 61 mm (2.4 in.)/month, or 2 mm (0.08 in.)/day. Actual rates varied seasonally and (by some estimates) approached 300 mm/month (12 in./month) during some winter months. In all cases over the 7-year period the intervals of faster movement were brief, lasting 1 to 2 months, and followed by lengthy periods of slower movement.

POSTEARTHQUAKE SLIDE MOVEMENT

In the extraordinarily difficult and busy period that followed the Loma Prieta earthquake, the magnitude of the accelerated movement at the Lone Tree landslide was not immediately reported, nor was it anticipated that the accelerated movement would continue. It took several months to determine that the accelerated movement was not a temporary anomaly (such as had been experienced at brief intervals in the prior 7 years) but instead a permanent change in the slide regime. In the meantime, the roadway was maintained as serviceable through the weekly paving efforts of the local maintenance staff.

On January 15, 1990, after more than 3 months of accelerated movement and a drop of the highway of more than 2.4 m (8 ft), it was recognized that it was no longer possible to keep the road open, and the highway was closed.

On January 17, 1990, a survey monitor line was established across the landslide and periodically monitored until April 9, 1991. In addition, the surface location of the inclinometer placed in October 1989 was monitored. Figure 7 is a plot of total movement from 1982 through 1990; the period from 1982 to 1989 depicts the reconstructed data. The period 1989 to 1991 is from survey data. The total resultant movement (vertical and horizontal) of the top of the inclinometer casing recorded by surveys between October 30, 1989, and April 9, 1991 is shown in Figure 8.

From January 19–21, 1990, five more slope indicators were installed in the landslide: one below the highway, and four in the slope above the highway. Groundwater was found at depths of 7.4 m (24 ft) in Boring SI-3 and 29.6 m (97 ft) in Boring SI-6. In 2 to 6 days, these slope indicators sheared at depths ranging from 14.5 to 23 m (48 to 76 ft).

STABILITY ANALYSIS

Three stability analyses were conducted for this landslide using the computer model PC-STABL4M (Purdue University). The initial analysis used the back-calculated soil strength parameters along the slide plane defined by inclinometer data. The second analysis was conducted to evaluate the stability of the original slide plane after 765 000 m³ of material were removed from the head of the slide and placed as a temporary buttress against the lower slope. This analysis also used the back-calculated soil strength parameters. The third analysis was conducted to design the back slope for the proposed excavation and used the soil strength parameters obtained by triaxial testing of core samples from the new back-slope material.

Back calculation of safety factors along the failure plane defined by the inclinometers resulted in soil strength values of ϕ = 11 degrees, C = 19 kPa (400 psf), and factor of safety = 0.99. Using these same shear-strength parameters, and adding pseudostatic earthquake forces derived from those measured at the Point Bonita seismograph for the Loma Prieta earthquake (0.11 *g* horizontal, 0.06 vertical), the factor of safety drops to 0.826—a 17 percent drop.

Analysis of the proposed repair strategy yielded an initial factor of safety of 1.6 with the buttress in place. Removal of the buttress, as is anticipated to occur eventually through erosion, yielded a factor of safety of 1.24; therefore, the highway has been relocated behind the slide plane.

The excavation backslope was 60 m (200 ft) high. Stability analysis slope, using soil strength parameters of ϕ = 24 degrees and C = 50 kPa (1,000 psf), resulted in the recommendation of a 1½:1 slope, a midslope bench 15 m (50 ft) wide, and extensive subdrainage (horizontal drains) to achieve a minimum factor of safety of 1.3 to 1.9.

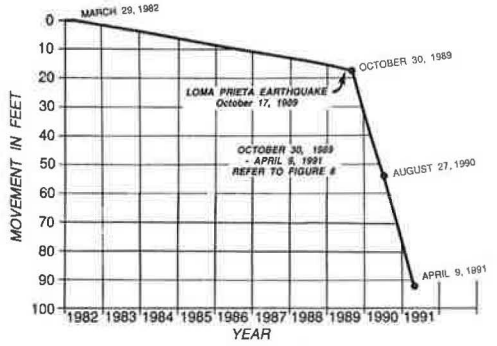

FIGURE 7 Resultant slide movement, 1982–1991, Lone Tree landslide.

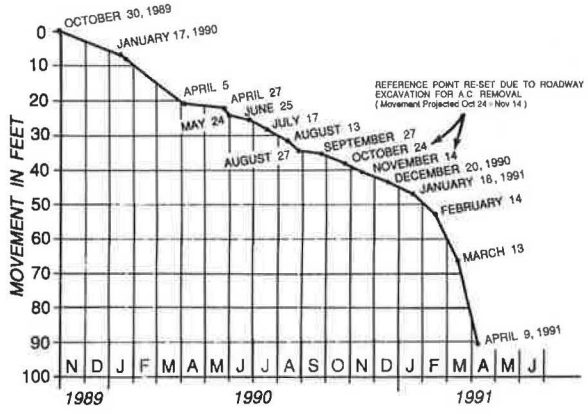

FIGURE 8 Resultant slide movement, October 30, 1989–April 9, 1991, Lone Tree landslide (resultant movement is vectorial summation of horizontal and vertical displacements).

EARTHQUAKE PARAMETERS

The Loma Prieta earthquake, which was 7.1 M_s (surface wave magnitude), occurred along a recently seismically quiescent portion of the San Andreas fault (see Figure 1). The fault segment had been identified as having a relatively high probability for an earthquake of this magnitude because of low microseismicity and the absence of historic earthquakes along this segment. A previous earthquake of a similar magnitude is believed to have occurred in the region in 1865, and the 1906 earthquake rupture zone included this segment.

Primary surface rupture was not found along the San Andreas fault following the Loma Prieta earthquake. The earthquake occurred at a depth of 19 km (11.5 mi), and fault rupture dissipated before it reached the surface. The duration of shaking was 10 to 15 sec; the strongest ground shaking recorded near the epicenter reached 0.64 *g* horizontal and 0.60 *g* vertical (*4,5*).

The Loma Prieta earthquake triggered 131 seismograph stations in the region; 77 recorded ground motion and the remainder were located on buildings. At the Lone Tree landslide, modified Mercalli intensities were estimated at IV. The recording station closest to the Lone Tree slide is the Point Bonita seismograph, located approximately 10 km (6 mi) to the east. The Loma Prieta earthquake recorded 0.11 *g* horizontal and 0.06 *g* vertical at this station. The Point Bonita seismograph is located on a fractured sandstone bedrock.

The epicenter of the Loma Prieta earthquake was located some 113 km (70 mi) southeast of the Lone Tree landslide. The primary wave motion at the site from the 7.1 M_s main shock and the subsequent aftershock swarm would have had

a strong southeasterly component. In addition to the primary southeasterly wave, recorded ground motion also showed a strong transverse wave (Love wave). The direction of the transverse wave (Point Bonita) rotated clockwise from east to west and southwest to northeast, as frequencies increased from 0.4 to 0.8 Hz and 3.2 to 6.4 Hz (*6*).

The Lone Tree landslide is within a southeast to northwest trending ridge, and landslide movement is therefore to the southwest (S15°W). The higher frequency ground motion, (3.2 to 6.4 Hz) was therefore parallel to the direction of slide movement. The earthquake induced ground motion (normal to the free face of the slope) is seen as a factor in the change in the rate of landslide movement observed after the Loma Prieta earthquake.

ANALYSIS OF MOVEMENT AT LONE TREE SLIDE

Before the earthquake, the landslide moved at an average rate of 2 mm/day with brief episodes of 10 mm/day. Immediately after the earthquake, the landslide was moving at 22.8 mm/day (0.9 in.). During the period between October 30, 1989, and January 17, 1990, the landslide averaged 27 mm/day (1.0 in./day).

Varnes (*7*), Hungr (*8*), Morgenstern (*9*), and Cruden (*10*) have presented velocity classifications for landslides and separated them into six or seven classes. Each class covers a range of velocities within two orders of magnitude (see Table 1).

The Lone Tree landslide rate following the earthquake of 27 mm/day, or 3.1×10^{-4} mm/sec in SI units (ASTM E380-89), places this slide in Cruden's (*10*) slow category (Class 3). This rate is close to the middle of Class 3, with a lower limit of 50×10^{-6} mm/sec, or 1.6 m/year (5.25 ft/year), and a high limit of 5×10^{-3} mm/sec, or 13 m/month (42.6 ft/month). In our opinion, the SI units suffer from a lack of logical perception by the public and even the engineering community because of their small scale.

TABLE 1 CLASSIFICATION OF LANDSLIDE MOVEMENT RATES (*10*)

OLD		NEW			
m	mm/sec	CLASS	DESCRIPTION	m	mm/sec (SI Units)
		7	Extremely rapid		
3 m/sec	3×10^{3}			5 m/sec	5×10^{3}
600 **		6	Very Rapid	*100* *	
0.3 m/min	5			3 m/min	50
288		5	Rapid	*100*	
1.5 m/ day	17×10^{-3}			1.8 m/hour	0.5
30		4	Moderate	*100*	
1.5 m/month	0.6×10^{-3}			13 m/month	5×10^{-3}
12		3	Slow	*100*	
1.5 m/year	48×10^{-6}			1.6 m/year	50×10^{-6}
25		2	Very Slow	*100*	
0.06 m/year	1.9×10^{-6}			16 mm/year	0.5×10^{-5}
		1	Extremely slow	*100*	

** Velocity increment between classes*

Fukuzono (*11*) presented the results of the work of a number of authors who have studied the problem of developing predictive models for catastrophic failures. In discussing Salt's work (unpublished paper, Disaster Prevention Research Institute, 1988), Fukuzono reports that Salt's critical limit for the model velocity of a slide that has strained to its residual strength is 50 mm/day (5.8×10^{-4} mm/sec). At this velocity, Salt proposes that a landslide poses a substantial risk for imminent catastrophic failure. This rate is in the middle of the slow class (Class 3). Salt also suggests that the critical limit in terms of acceleration is 5 mm/day/day.

Salt suggests that had his limits been used, several days of forewarning would have been available on several catastrophic slides. The use of these values for real-time hazard prediction requires frequent reading of instrumentation and the immediate interpretation of the results. This is difficult to achieve with conventional instrumentation systems and geotechnical staffing levels in state highway agencies. This monitoring would perhaps lend itself well to some of the automated systems being marketed today.

After closing the roadway on January 15, 1990, a survey monitor line was established across the landslide at approximately roadway level. Between January 17 and April 5, the movement increased to an average of 54.7 mm/day (2.15 in./day), a critical rate by Salt's criteria, indicating possibly imminent failure. From April 5 to August 13 and August 13 to December 20, the average rates slowed down to 34.5 mm/day (1.4 in./day) and 23.8 mm/day (0.94 in./day), respectively. The slowing down gave a false indication of what was to happen over the winter of 1990–1991 (see Figure 7).

Monthly readings over the winter of 1990–1991 show successive rates of 38.9 mm/day (1.5 in./day), 67.7 mm/day (2.7 in./day), 145.6 mm/day (5.7 in./day), and 284.4 mm/day (11.20 in./day) or 3.3×10^{-3} mm/sec [still in the slow class defined by Cruden (*10*)] between December 20, 1990, and April 9, 1991. April 9 is the date of the last reading before any construction activity was started.

Salt's critical acceleration rate was exceeded sometime between February 14 and March 13 approximately a month after exceeding the 50 mm/day rate. The average acceleration for this period was 5.6 mm/day/day, 0.6 mm above Salt's critical acceleration rate. Some additional monitoring was performed during construction and the movement peaked at 800 mm/day (30 in./day) without catastrophic failure.

RAINFALL

Before the earthquake, slide movement responded to winter rains and the subsurface exploration program found zones of high permeability within the slide material. At the time of the earthquake in October 1989, however, it was the end of the summer and this region was experiencing the consequences of its third lower-than-average rainfall season. In October 1989, there were 31 mm (1.25 in.) of rainfall, the first of that rainfall season. Rainfall remained low, 53 mm (2.1 in.) in November and no rain occurred in December 1989, yet the rate of landslide movement did not diminish. The spring of 1990 received 440 mm (17.37 in.) of rainfall, and movement of the landslide continued. There were slight increases or decreases in the rate of landslide movement that

appear to correlate with the seasonal rains; however, there was no change in the overall trend. The landslide continued to move over the summer of 1990, with very little reduction in the rate of movement. The winter of 1990–1991 also experienced below normal rainfall (see Figure 5). Acceleration in the rate of landslide movement occurred in December, when antecedent rainfall was still low [60 mm (2.34 in.)] and continued to accelerate over the spring of 1991. Substantial rainfall in February [105 mm (4.14 in.)] and March [312 mm (12.29 in.)] coincided with continued acceleration.

Because the acceleration of landslide movement began in 1989 and 1990 before substantial antecedent rainfall, and the rate of landslide movement failed to diminish significantly over the summer of 1990, the author believes the more than tenfold increase in rate (2 mm/day to 22.8 mm/day) immediately following the earthquake is not tied to a change in the groundwater regime.

POSTCONSTRUCTION MONITORING

Six inclinometers were placed in the new back slope after construction. Potential slope movement and groundwater are being monitored in the inclinometers. A grid of survey points has been established across the erodible buttress to record its gradual removal by erosion and ocean waves.

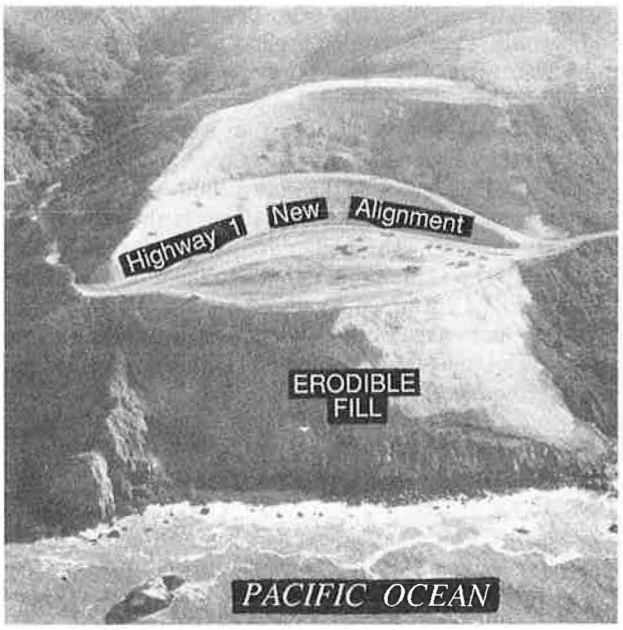

FIGURE 9 Aerial photograph of completed landslide repair, Lone Tree landslide.

CONCLUSIONS

The authors have presented the monitoring and analysis performed to correct a large, slow-moving landslide on State Route 1 in the northern coast of California. Also presented is a comparison of recorded rates of movement with critical velocities and accelerations proposed by others as warnings of imminent catastrophic failure.

Before the Loma Prieta earthquake, the slide was moving at a rate generally manageable by maintenance forces, although road closures were necessary from time to time. After the earthquake, the rate of movement increased to an intolerable, although still subcritical, level, according to published values. After continued movements over a long period, the slide accelerated to the critical values proposed by Salt, although sudden and rapid movements were never reached. Salt's critical velocity was reached in early 1990. Subsequently, there was a decrease in velocity, and the critical velocity threshold was again reached in early 1991, a month or so before reaching his critical acceleration threshold. During the earthwork for landslide repair (Figure 9), the rate of slide movement increased to 16 times the critical velocity and catastrophic failure did not occur.

Continued studies to provide a reliable method for predicting the time of rapid failure of a landslide is necessary. This landslide did not fit existing models.

The authors believe that the accelerated rate of movement at Lone Tree landslide is due to a combination of factors; large movements over the years lowered the shear strength of the material in the failure plane, and earthquake shaking accelerated the process. Other factors include seasonal rainfall and the continued erosion of the toe of the landslide by the ocean, which prevented natural buttressing. The linkage of increased landslide movement with earthquake acceleration is supported by statements in Salt's work, which shows that frictional materials in the fine fraction range are more sensitive to earthquake accelerations than cohesive soils. The lowering of the factor of safety by just a small percentage in these materials can lead to accelerated movement rates.

This case history documents a unique failure by deterioration of the shear zone because of long-term shearing and earthquake shaking. The monitoring program and analysis show that the increase in rate of slide movement coincides with the earthquake event and suggest that it was a major contributory factor.

REFERENCES

1. M. C. Blake, Jr., et al. *Preliminary Geologic Map of Marin and San Francisco Counties, and Parts of Alameda, Contra Costa and Sonoma Counties*. Map MF-484. U.S. Geological Survey, 1974.
2. S. Ellen, D. M. Peterson, and G. O. Reid. *Map Showing Areas Susceptible to Different Hazards from Shallow Landsliding, Marin County and Adjacent Parts of Sonoma County, California*. Map MF-1406. U.S. Geological Survey, 1983.
3. *Manual on Subsurface Investigations 1988*. AASHTO, Washington, D.C., 1988.
4. T. E. Spittler, E. L. Harp, D. K. Keffer, R. C. Wilson, and R. H. Sydnor. *Landslide Features and Other Coseismic Fissures Triggered by the Loma Prieta Earthquake, Central Santa Cruz Mountains California*. California Division of Mines and Geology, Special Publication 104, 1990.
5. S. R. McNutt and T. R. Toppozada. *Seismological Aspects of the 17, October 1989 Earthquake*. California Division of Mines and Geology, Special Publication 104, 1990.
6. J. E. Vidale and O. Bonamassa. Strong Shaking Directions from the 18 October 1989 Loma Prieta Earthquake and Aftershocks in San Francisco and Oakland. *Proc., Seminar on Seismological and Engineering Implications of Recent Strong-Motion Data*, Sacramento, Calif., May 30, 1990.

7. D. J. Varnes. *Special Report 29: Landslide Types and Processes in Landslides and Engineering Practice*. HRB, National Research Council, Washington, D.C., 1958, pp. 20–47.
8. O. Hungr. *Dynamics of Rock Avalanches and Other Types of Slope Movements*. Ph.D. thesis. University of Alberta, Edmonton, Alberta, Canada, 1981.
9. N. R. Morgenstern. Geotechnical Aspects of Environmental Control. *Proc., 11th International Conference on Soil Mechanics and Foundation Engineering*, Vol. 1, San Francisco, Calif., 1985, pp. 155–186.
10. D. M. Cruden. A Simple Definition of a Landslide. *Bulletin of the International Association for Engineering Geology*, 1991.
11. T. Fukuzono. Recent Studies on Time Prediction of Slope Failure. *Landslide News*, No. 4, July 1990, pp. 9–12.
12. *Lessons Learned from the Loma Prieta, California, Earthquake of October 17, 1989* (G. Plafker and J. P. Galloway, eds.). Circular 1045. U.S. Geological Survey.

Publication of this paper sponsored by Study Committee on Landslides: Analysis and Control.

Back Analysis of Olmsted Landslide Using Anisotropic Strengths

GEORGE M. FILZ, THOMAS L. BRANDON, AND J. MICHAEL DUNCAN

An analytic model of existing landslides on the Illinois shore of the Ohio River at the proposed Olmsted Locks and Dam site has been developed. This model is based on field and laboratory investigations that characterize the geometry, material distribution, and groundwater levels at the existing slides. Back analyses of landslide stability were used to determine the soil strengths, which were necessary to complete the model. Trial residual friction angles for the back analyses were based on the results of laboratory shear tests and on a correlation with the plasticity index. However, because of difficulties in performing the laboratory shear tests, greater reliance was placed on the correlation with the plasticity index. One of the most important materials involved in the landslides is the McNairy I formation, which consists of interbedded layers of clay, silt, and sand. The McNairy I is inherently anisotropic, and strength variations with inclination of the failure surface were incorporated in the back analyses.

Locks and Dams 52 and 53 are located on the Ohio River, near its confluence with the Mississippi River. These structures, built in the 1920s, are in poor condition. Additional temporary locks were added in 1969 and 1980 to help handle the increasing volume of river traffic, but these locks are also deteriorating. Because the capacity of the facilities is limited, river traffic is impeded at Locks and Dams 52 and 53. To provide sufficient and reliable navigation capacity through this portion of the Ohio River, the U.S. Army Corps of Engineers is replacing Locks and Dams 52 and 53 with a single facility that will include two new locks positioned side by side. The new locks and dam will be built near Olmsted, Illinois, at the location shown on the vicinity map (see Figure 1).

The Olmsted Locks and Dam are being designed by the U.S. Army Corps of Engineers. The project will include two locks, each 110 ft wide and 1,200 ft long, adjacent to the Illinois shore; a 2,200-ft-wide navigable pass controlled by 220 wicket gates, each 10 ft wide; and a 426-ft-long fixed weir composed of a series of gravel-filled sheet-pile cells extending to the Kentucky shore (*1*).

The location of the new locks and dam is fixed by navigation requirements upstream and an environmentally sensitive area downstream. Unfortunately, the bank on the Illinois side of the river at the dam site is a massive active landslide more than 3,000 ft long, with the head scarp located some 600 ft from the shoreline. Remedial stabilization measures will be incorporated in the project design. To assess the impact of construction on stability, back analyses were performed to evaluate the strengths of the materials involved in the landslide. A special feature of the back analyses is the incorporation of anisotropic strength parameters for one of the materials involved in the landslide.

Department of Civil Engineering, Virginia Polytechnic Institute and State University, 200 Patton Hall, Blacksburg, Va. 24061.

BACK-ANALYSIS PROCEDURE

Back analysis is a useful procedure for developing an analytic model of a failing slope. The resulting model can be used to help design remedial stabilization measures and to assess the impact of various construction operations. An analytic model of a slope consists of the following five components:

1. The landslide geometry. This includes the location of the ground surface, the location of the sliding surface, and the locations of the boundaries between different material types.
2. Pore water pressures at the sliding surface. These are necessary for effective stress analyses.
3. External loads acting on the slope. In the case of static back analysis of the Olmsted landslide, the only external load is the water pressure from the Ohio River at the toe of the slope.
4. The unit weights of the materials involved in landslide.
5. The strengths of the materials along the failure surface.

For the Olmsted landslide, the first four components of the model could be evaluated with reasonable accuracy on the basis of field and laboratory investigations. Back analysis was used to establish the fifth component of the model, the soil strengths. In back analysis, the known conditions in the slope and the fact that the factor of safety (FS) was equal to 1.0 (at the time of the failure) are used to evaluate the soil strength, which must have been mobilized during the slope movement.

Based on observations of scarp development and survey monument movement at the Olmsted landslide, the displacements have been in the range of several ft. Because of the large displacements, residual strengths are in effect along the existing failure surfaces, and the material strengths can be characterized by values of effective stress residual friction angles (ϕ_r') greater than zero, with effective cohesion intercepts (c_r') equal to zero (*2,3*).

If only a single material were to exist along the sliding surface, and if the material had $c_r' = 0$, back analysis would result in a unique value of residual friction angle for the material. On the other hand, if there are two or more materials along the sliding surface, as there are for the Olmsted landslide, back analysis does not result in unique residual friction angles for the materials. Consequently, other means, such as laboratory tests and correlations, must be used to guide the

FIGURE 1 Location of Olmsted Lock and Dam site.

analyses. A reasonable back analysis procedure for a slope with more than one material along the failure surface includes the following steps:

1. Laboratory test results and correlations with index properties are used to establish trial values of shear strength parameters for the materials along the failure surface. For the Olmsted landslide, only the values of the residual friction angles, ϕ_r', are needed because the displacements are large enough to reduce the shear strengths to their residual values and can be closely approximated by values of ϕ_r', with $c_r' = 0$.
2. A stability analysis is performed using the known slope geometry, groundwater levels, and external loading conditions at the time of the failure. The analysis yields a FS corresponding to the trial strengths from Step 1.
3. The trial strengths from Step 1 are adjusted using the FS computed in Step 2 according to the following formula:

$$\phi'_{r\text{adjusted}} = \tan^{-1}\left[\frac{\tan\left(\phi'_{r\text{trial}}\right)}{\text{FS}}\right] \quad (1)$$

If extensive local experience with a particular material is available, this experience along with Equation 1, could be used to adjust the strength of some of the materials more than others.

4. The results of Step 3 can be verified by reanalyzing the slide using the strengths from Step 3. The value of FS calculated using these strengths should be 1.00. The final back-calculated strengths, which produce a FS equal to unity, are appropriate for the existing sliding surface where the shear strength has been reduced to residual.

This procedure takes full advantage of the information provided by the large-scale shear test, which an existing landslide represents. Whereas laboratory tests use relatively small specimens whose properties must be extrapolated to entire formations, a landslide involves all of the material along the failure surface and the shearing resistance of all this material is reflected in the back analysis. As long as the location of the failure surface, groundwater conditions, external loads, and material unit weights can be estimated with reasonable accuracy, a useful analytical model can be developed. Minor inaccuracies in the location of the failure surface or the phreatic surface will result in compensating changes in the back-calculated strengths in order to produce an internally consistent model that can be used to evaluate the effectiveness of remedial stabilization measures.

Confidence in the analytic model, obtained from back analysis is increased when the same set of strengths results in an FS value close to 1.0 for several cross sections throughout the landslide and when the back-calculated strengths are in reasonable agreement with laboratory tests and correlations with index properties.

For the Olmsted landslide, a complicating factor is the presence of the layered McNairy I formation along significant portions of the failure surfaces. The McNairy I consists of interbedded layers of clay, silt, and sand. As a result of the layering, the strength properties of the formation are highly anisotropic, with the lowest strengths on horizontal and near-horizontal surfaces that pass primarily along the clay layers, and with the higher strengths on inclined surfaces that cut across the clay, silt, and sand layers. Here, the term "anisotropic" is used to refer to the inherent strength anisotropy of an entire formation, as described by Ladd and Foott (*4*) for varved clays.

The following sections describe how the back-analysis procedure was applied to the Olmsted landslide and how strength anisotropy of the McNairy I formation was incorporated into the analyses.

DESCRIPTION OF EXISTING LANDSLIDES

Evidence of instability on the Illinois shore at the Olmsted site was first discovered in 1987 during the foundation investigation for the proposed locks and dam. On the basis of observations of geomorphic features such as scarps, cracks, leaning trees, and hummocky terrain, the approximate extent of unstable ground was mapped. The boundary of the unstable area is shown by the line labeled Upper-Bank Slide Scarp in the site plan, as shown in Figure 2. The upper-bank slide is about 3,300 ft long and the head scarp of the slide is about 600 ft from the shoreline. Because of the observed instability, slope inclinometers and additional piezometers were installed in the slide area.

In late May and early June of 1988, a rapid drop in the river level from Elevation 290 ft to Elevation 283 ft took place over a 10-day period. In the lower portion of the river bank, near-vertical scarps up to 3 ft high developed 150 to 200 ft from the shoreline. Over the next month, the scarps and cracks propagated laterally along the river and eventually reached a total length of 3,100 ft. The location of the summer 1988 scarp is shown in Figure 2 by the line labeled Lower-Bank Slide Scarp.

Geology

Cross-section 1, which is located on the dam centerline, cuts through both the lower- and upper-bank landslides. The lower-bank portion and the upper-bank portion of Cross-section 1 are shown in Figures 3 and 4, respectively. The most important stratigraphic units in the lower-bank area are presented in Table 1, and their distributions at Cross-section 1 are shown on Figure 3.

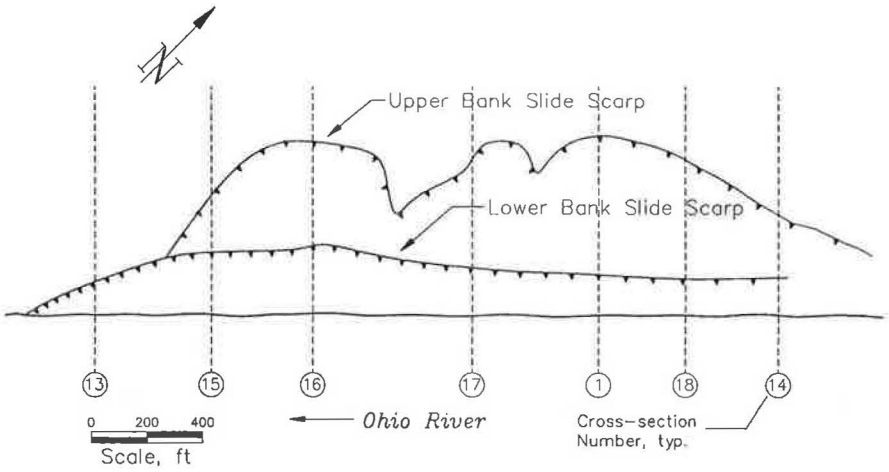

FIGURE 2 Plan view of Olmsted Lock and Dam site showing the scarp for the lower- and upper-bank slides.

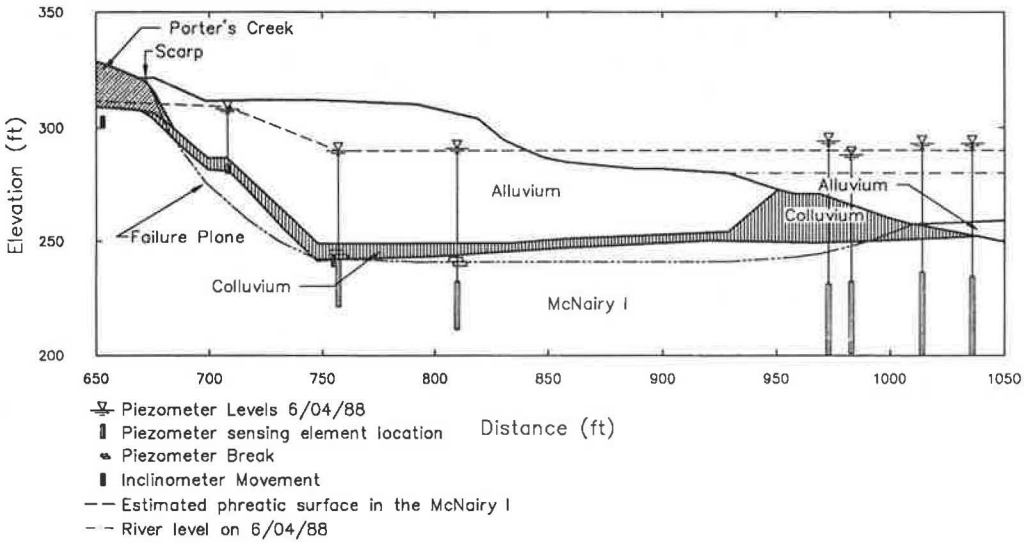

FIGURE 3 Cross section of lower-bank slide at Section 1.

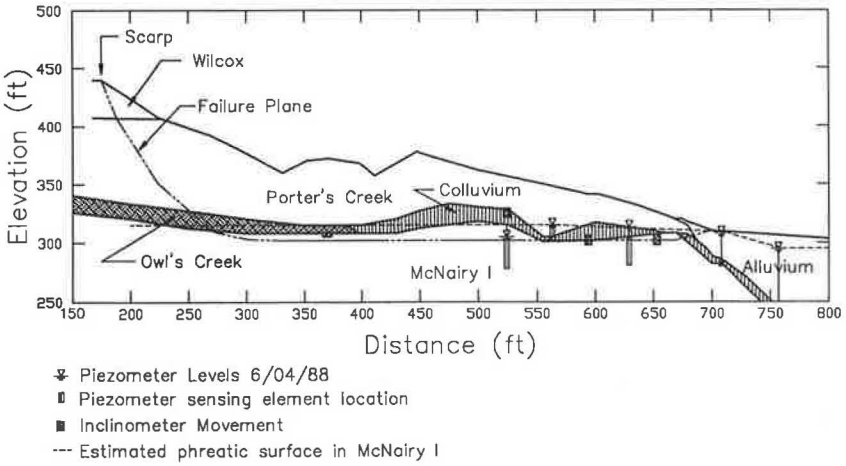

FIGURE 4 Cross section of upper-bank slide at Section 1.

TABLE 1 STRATIGRAPHIC UNITS IN LOWER-BANK SLIDE AREA

Unit Name	Description
Alluvium	Very soft to stiff silty clay with interbedded colluvial layers and occasional fine sand lenses.
Colluvium	A heterogeneous mixture of clay, silt, and gravel.
McNairy I	Medium stiff to stiff interbedded clay, silt, and very fine to fine sand. Based on SPT N-values, laboratory tests, and shear wave velocity measurements, the upper few feet of the McNairy I are softer than the deeper portions.

The most important stratigraphic units in the upper-bank area are presented in Table 2 and their distributions at Cross-section 1 are shown in Figure 4. In comparing Figures 3 and 4, it should be noted that the head scarp of the lower-bank slide in Figure 3 is at approximately the same location as the toe of the upper-bank slide in Figure 4.

Topography

The Ohio River flows southwest at the Olmsted site. The normal pool level is at Elevation 290 ft; however, the level seasonally fluctuates between low water at about Elevation 280 ft in the summer to high water at about Elevation 315 ft in the winter. The lowest elevation of the river bottom is 250 ft. Typical ground surface slopes on the Illinois shore in the area of the existing landslides range from 8 to 14 degrees. A gently rounded ridge line is located about 700 ft from the Illinois shoreline. The ridge elevation is about 390 ft at the downstream end of the locks and about 445 ft at the upstream end of the locks.

TABLE 2 STRATIGRAPHIC UNITS IN UPPER-BANK SLIDE AREA

Unit Name	Description
Wilcox Gravel	Iron oxide cemented sandy gravel with fine sand and sandy clay.
Porter's Creek	Stiff to hard, fat clay. Montmorillonite is the predominant clay mineral in this unit.
Owl's Creek	This unit is mineralogically similar to the underlying McNairy I. Its consistency is stiff to hard.
McNairy I	Medium stiff to stiff interbedded clay, silt, and very fine to fine sand. As in the lower bank area, SPT N-values, laboratory tests, and shear wave velocity measurements indicate that the upper few feet of the McNairy I are softer than the deeper portions.

Groundwater

Piezometric levels in the McNairy I formation slope down toward the river but at a shallower rate than the ground surface slopes. Artesian conditions exist near and beneath the river. Because the McNairy I formation consists of near-horizontal layers of clay, silt, and sand, the formation undoubtedly has higher horizontal than vertical permeability. This high horizontal permeability is believed to be a factor in the development of artesian pressures. Elevated pressures near and beneath the river are probably driven by the higher groundwater levels upslope to the north and possibly upstream to the east.

Piezometer readings taken during summer 1988 landslide indicate that piezometric levels in the slope only dropped 1 to 3 ft in response to the 7-ft drop in the river level of late May and early June.

Location of Failure Surfaces

Twelve slope inclinometers installed in the landslide areas helped define the location of the failure surface. In addition, five standpipe piezometers were obstructed or broken during the lower-bank slide in 1988. The elevations of the piezometer disturbances were determined. The information from the inclinometer casings and piezometer disturbances, with the location of the surface scarps, was used to estimate the location of the failure surface at several cross sections through the landslides. The estimated failure surface locations at Cross-section 1 are shown in Figures 3 and 4.

Slide Mechanism

The instrumentation data, surface feature observations, and information from the foundation exploration present a consistent picture of the slope movements at this site. The data indicate that sliding is primarily translational and that separate upper- and lower-bank slides exist. The base of the upper slide is at Elevation 298 to 322 ft and the base of the lower-bank slide is at Elevation 238 to 256 ft. These locations put the central portions of both the upper- and lower-bank slides within the top several feet of the McNairy I formation.

This position for the failure plane indicates that weak layers exist in the top of the McNairy I formation. In fact, as presented in Tables 1 and 2, the foundation exploration disclosed that the top of the McNairy I is softer than the rest of the formation. In addition, the McNairy I contains interbedded horizontal layers of clay, silt, and sand. Horizontal, or near-horizontal, sliding of the central portion of the landslides is probably taking place along the weaker clay layers in the upper part of the McNairy I.

Away from the central portion of the landslides, the failure surface cuts across the bedding planes of the McNairy I formation. The strength along an inclined surface that cuts through clay, silt, and sand layers would be expected to be much higher than the strength along a horizontal surface in a clay layer. Thus, layering is the source of inherent strength anisotropy in the McNairy I formation.

The lower-bank slide in 1988 occurred during an abrupt drop in river level from 290 ft to 283 ft. The decrease in

stabilizing force due to this drop in the river level was sufficient enough to cause movement of the lower-bank slide mass toward the river.

Data from inclinometer readings taken after the 1988 slide, show that there is continuing movement of both the lower and the upper bank slides. This indicates that the FS for the existing slope has been close to unity since the slide. Relatively small changes in river level or small changes in piezometric levels within the slope appear to be sufficient to cause additional increments of downslope movement.

The slope movements have been large enough that there is little doubt that the shear strengths along the failure surfaces have been reduced to their residual values. A survey monument in the lower-bank area moved down 1.3 ft and 2.0 ft toward the river over a 2.5-year period encompassing the 1988 slide. As mentioned previously, near-vertical head scarps of the lower-bank slide range up to 3 ft high. These facts indicate that relatively large movements have taken place in this area. Consequently, residual friction angles appear to be appropriate for the analysis of sliding on existing failure surfaces.

TRIAL STRENGTH VALUES FOR BACK ANALYSIS

Trial strength values are necessary to begin the back-analysis procedure. Both laboratory shear tests and correlations with index properties were used to select the trial strength values for the Olmsted slide.

Laboratory Shear Tests

Repeated direct shear tests were performed on small samples of alluvium, colluvium, McNairy I, and Porter's Creek soils to determine values of the drained residual friction angles, ϕ'_r. Table 3 presents the results of all the tests that were carried to sufficient displacement in order to develop residual strength conditions. There is considerable scatter in the results. The test data are believed to be erratic because of the difficulties involved in sampling, trimming, and testing representative samples of these materials. The alluvium tended to be soft and difficult to sample, the Porter's Creek material tended to be brittle and difficult to trim, and the alluvium and colluvium were highly variable. Variability in the materials probably contributed to scatter in the data because of the small size of the laboratory test specimens. In addition, the laminated character of the McNairy I made trimming difficult. During testing, it was sometimes difficult to determine which components of the McNairy I were involved in shearing.

TABLE 3 SUMMARY OF RESIDUAL DIRECT SHEAR TESTS

Soil	Boring	Sample	c'_r (tsf)	ϕ'_r (degrees)	LL	PL	PI
Alluvium	AS-105	5A	0.00	22.5	46	24	22
	UD-21A	1	0.00	33.0	31	23	8
Colluvium	AS-105	7A	0.00	19.5	52	25	27
	UD-21	1	0.00	29.0	46	25	21
	UD-21A	2	0.00	9.0	101	37	64
McNairy I	UD-214	1A	0.05	10.0	85	34	51
	UD-214	3C	0.10	15.2	64	23	41
	UD-214	2C	0.20	18.0	47	20	27
	UD-214	2C	0.03	13.0	47	20	27
	UD-214	1C	0.20	6.7	70	29	41
	UD-214	3E	0.00	21.0	47	26	21
Porter's Creek	TP-7	1	0.20	5.0	111	45	66
	TP-7	2	0.20	10.0	112	38	74
	TP-7	3	0.20	12.0	114	43	71
	TP-7	4	0.20	10.0	117	43	74

Correlations with Index Properties

There have been successful efforts to correlate ϕ'_r with the index properties of soils (*2,5–7*). Typically, these correlations employ the PI, and the percentage of the clay fraction (less than 0.002 mm) composing the soil. One of these correlations could have been used to estimate reasonable ϕ'_r values for the Olmsted project. However, because numerous additional data were available from more recent literature, it was considered desirable to update the previous correlations. A total of 154 different pairs of ϕ'_r – PI values were collected (*8*). The data include values of residual friction angles determined from the back analysis of existing slides, from repeated direct shear tests, and from ring shear tests. For estimating trial values of ϕ'_r for the Olmsted project, the subset of these data consisting of natural soils having no cohesion ($c'_r = 0$) was used. Figure 5 shows the data and the estimated ϕ'_r – PI trend. For comparison, the relationship proposed by Voight (*5*) is also shown. It can be seen that the two trend lines are quite similar. The trend line by Brandon et al. (*8*) shows a sharper curvature, and lower ϕ'_r values in the PI range from 20 to 50.

Trial Shear Strengths

Trial residual friction angles for the important soils involved in the landslides were based on the results of the laboratory shear tests and on the correlation with PI. However, more reliance was placed on the correlation with PI because of (a) difficulties in performing the laboratory shear tests cast some doubt on the accuracy of the test results, and (b) more Atterbert limits tests than repeated direct shear tests were performed on the site soils. For each soil type, Table 4 presents the range of values of PI, residual friction angle measured by laboratory tests, residual friction angle obtained from the correlation in Figure 5, and the trial residual friction angle adopted for beginning the back analyses.

Because of the interbedded nature of the McNairy I, the shear-strength parameters for this formation are undoubtedly anisotropic. The residual friction angle from the correlation with PI listed in Table 4 for the McNairy I soil ranges from 10 to 30 degrees. The lower friction angles in this range correspond to the higher PIs, which are representative of the clay layers that would be involved in horizontal shearing. The higher friction angles correspond to the lower PIs, which are

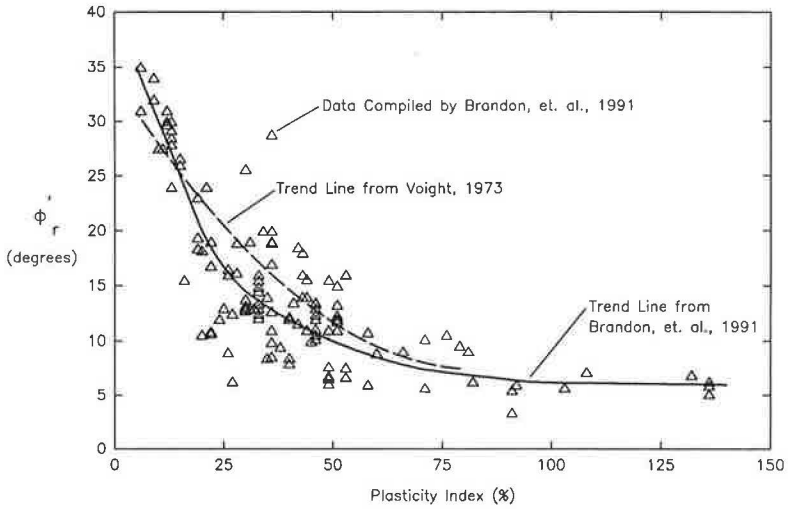

FIGURE 5 PI–residual friction angle relationship (*5,8*).

TABLE 4 MEASURED, CORRELATED, AND TRIAL VALUES OF ϕ'_r FOR OLMSTED SOILS

Soil	Representative PI range[a]	$\phi'_{r\ measured}$ (degrees)	$\phi'_{r\ cor}$ (degrees)	$\phi'_{r\ trial}$ (degrees)
Alluvium	20 to 30	22.5 to 33	14.5 to 20	18
Colluvium	20 to 35	9 to 29	12.5 to 20	15
McNairy I	10 to 50	7 to 21	10 to 30	see text
Porter's Creek	50 to 80	5 to 12	6.5 to 10	8

[a]The representative ranges of plasticity index values listed in Table 4 exclude atypical Atterberg limits tests results (*8*).

representative of mixtures of the coarse and fine material that would be involved in inclined shearing. On this basis, these trial friction angles for the McNairy I soil were selected for beginning the back analysis: $\phi'_{r\ (hor)}$ = 10 to 11 degrees and $\phi'_{r\ (non-hor)}$ = 25 degrees. Arbitrarily, $\phi'_{r\ (hor)}$ was applied for sections of the failure surface to within ±5 degrees of horizontal and $\phi'_{r\ (non-hor)}$ was applied for steeper sections of the failure surface.

As shown in Figures 3 and 4, the Owl's Creek and Wilcox deposits play relatively minor roles in the sliding at this site. Their trial residual friction angles were estimated on the basis of visual classifications. A summary of the trial residual friction angles used for the back analyses is presented in Table 5, which also includes the unit weights of the materials.

STABILITY ANALYSES

Slope stability analyses were performed using the computer program SPENCER. SPENCER is a modern version of the program SLOPE8R (*9*) for analysis of noncircular slip surfaces using Spencer's method (*10*).

Stability analyses were performed at four sections throughout the landslide. In addition to the upper- and lower-bank slides at Cross-section 1, which are shown in Figures 3 and 4, the lower-bank slides at Cross-sections 14, 16, and 18 were also analyzed. At these sections, sufficient data were available regarding the location of the failure surface and groundwater levels at the time of the 1988 landslide to define the conditions required for analysis. The location of Cross-sections 14, 16, and 18 are also shown on Figure 2.

Two analyses were performed for each section: one with $\phi'_{r\ (hor)}$ = 11 degrees in the McNairy I and another with $\phi'_{r\ (hor)}$ = 10 degrees in the McNairy I. In every case, a $\phi'_{r\ (non-hor)}$ value of 25 degrees in the McNairy I was used. Table 6 presents the results of the analyses.

TABLE 5 MATERIAL PROPERTIES FOR BACK ANALYSES

Soil	Trial ϕ'_r (degrees)	Total Unit Weights (lbs. per cu. ft.)
Alluvium	18	117
Colluvium	15	112
McNairy I	10 to 11 (horizontal) 25 (non-horizontal)	118
Owl's Creek	18	117
Porter's Creek	8	105
Wilcox	24	122

TABLE 6 FACTORS OF SAFETY DETERMINED FROM SLOPE STABILITY ANALYSES

Section	Factor of Safety	
	McNairy I $\phi'_{r(hor)}$ = 11°	McNairy I $\phi'_{r(hor)}$ = 10°
1 Lower	1.05	0.99
1 Upper	1.08	1.00
14	1.03	0.99
16	1.07	0.99
18	1.00	0.96

As indicated in the table, the calculated values of FS are generally slightly greater than 1.0 for $\phi'_{r\ (hor)} = 11$ degrees and are close to 1.0 for $\phi'_{r\ (hor)} = 10$ degrees. Because the calculated values of FS are so close to 1.0 for the analyses performed with $\phi'_r = 10$ degrees, it was judged unnecessary to adjust the trial strengths. It was therefore concluded that the residual friction angles listed in Table 5, with $\phi'_{r(hor)} = 10$ degrees in the McNairy I, provide results in good agreement with all available information. These values of residual friction angle complete the analytic model of the Olmsted landslide.

Confidence in the analytic model is relatively high but not solely because of the use of the back-calculation procedure to establish the residual friction angles. The number of unknowns (seven values of ϕ'_r) is greater than the number of analyses that could be performed (five cross sections). For this reason, and because of the inherent uncertainty in all of the measurements and interpretations made to characterize the landslide, it cannot be concluded that the set of ϕ'_r values obtained from the back analyses are the true values in an absolute sense. In fact, infinitely many other sets of ϕ'_r values could be found, which would also give factors of safety close to 1.0. However, most of these sets of ϕ'_r values would not be consistent with the other information known about the site soils.

Confidence in the model obtained from these back analyses is relatively high because

1. The analyses incorporate what is known about the stratigraphy and geologic characteristics of the site soils, including anisotropy in the McNairy I formation.
2. The strengths corresponding to a value of FS equal to 1.0 are in reasonable agreement with the laboratory test results and the estimated strengths from the PI correlation.
3. The same strengths yield FSs close to 1.0 for all of the sections throughout the landslide for which there is sufficient data for analysis. Because there are variations from section to section in the distribution of materials, the position of the piezometric surface, and the position of the failure plane, the confidence increased in the model in comparison to a back analysis performed at only one section.

SUMMARY AND CONCLUSIONS

An analytic model of existing landslides on the Illinois shore of the Ohio river at the proposed Olmsted Locks and Dam site was developed. The model was based on field and laboratory investigations to characterize the geometry, material distribution, and groundwater levels at the existing slides. Back analyses of landslide stability were used to determine the soil strengths necessary to complete the model. The model will be useful for assessing the effects of proposed construction operations on the slope and for evaluating the effectiveness of remedial stabilization measures.

Trial residual friction angles for the back analyses were based on the results of laboratory shear tests and on a correlation with the PI. However, because of difficulties in performing the laboratory shear tests, more reliance was placed on the correlation with the PI.

One of the most important materials involved in the landslides is the McNairy I formation, which consists of interbedded layers of clay, silt, and sand. The McNairy I formation is inherently anisotropic, and strength variation with inclination of the failure surface was incorporated in the back analyses.

Confidence in the analytic model obtained from the back analyses is relatively high because the same strength values yield FSs very close to 1.0 for all of the five cross sections for which there are sufficient data for analysis, and because the strengths agree reasonably well with the laboratory test results and the index property correlation.

ACKNOWLEDGMENTS

The writers wish to express their appreciation to the U.S. Army Corps of Engineers, which performed the field investigations and laboratory tests. Jane Ruhl, John Jent, Jeff Schaefer, David Kiefer, Don Tupman, and Bruce Murry, all of the Louisville District of the Corps of Engineers, made many valuable suggestions and provided much helpful information for the studies and analyses described in this paper.

REFERENCES

1. U.S. Army Corps of Engineers. *Design Memorandum No. 1: General Design Memorandum*. Main Report, Vol. 1, Olmsted Locks and Dam, Dec. 1988.
2. L. Bjerrum. Progressive Failure in Slopes of Overconsolidated Plastic Clay and Clay-Shales. Third Terzaghi Lecture, *Journal of the Soil Mechanics and Foundations Division*, ASCE, Vol. 93, No. 5, Sept. 1967, pp. 1–49.
3. A. W. Skempton. Residual Strength of Clays in Landslides, Folded Strata, and the Laboratory. *Geotechnique*, Vol. 35, No. 1, 1985, pp. 3–18.
4. C. C. Ladd and R. Foott. New Design Procedure for Stability of Soft Clay. *Journal of the Geotechnical Engineering Division*, ASCE, Vol. 100, No. 7, July 1974, pp. 763–786.
5. B. Voight. Correlation Between Atterberg Plasticity Limits and Residual Shear Strength of Natural Soils. *Geotechnique*, Vol. 23, No. 2, June 1973, pp. 265–267.
6. R. J. Chandler. The Effect of Weathering on the Shear Strength Properties of Keuper Marl. *Geotechnique*, Vol. 19, No. 3, 1967, pp. 321–334.
7. J. F. Lupini, A. E. Skinner, and P. R. Vaughan. The Drained Residual Strength of Cohesive Soils. *Geotechnique*, Vol. 31, No. 2, 1981, pp. 181–213.
8. T. L. Brandon, G. M. Filz, and J. M. Duncan. *Review of Landslide Investigation, Phase I—Part B, Olmsted Locks and Dam*. U.S. Army Corps of Engineers, Louisville, Ky., June 1991.
9. J. M. Duncan and K. W. Wong. *SLOPE8R: A Computer Program for Slope Stability Analysis with Non-Circular Slip Surfaces*. Department of Civil Engineering, Virginia Polytechnic Institute and State University, Blacksburg, Va., April 1984.
10. E. Spencer. A Method of Analysis of the Stability of Embankments Assuming Parallel Inter-slice Forces. *Geotechnique*, Vol. 17, No. 1, 1967, pp. 11–26.

Publication of this paper sponsored by Committee on Soils and Rock Instrumentation.

Instrumentation Systems for Selborne Cutting Stability Experiment

E. N. BROMHEAD, M. R. COOPER, AND D. J. PETLEY

A full-scale cutting slope failure experiment has been carried out at Selborne, Hampshire, England. The experiment used an extensive instrumentation system comprising inclinometer tubes, string inclinometers, piezometers, and surface wire extensometers. A high proportion of the instruments were connected to an electronic data gathering system that incorporated alarm-level outputs. Slope failure was successfully induced by pore-pressure recharge. The rationale of instrument selection and the performance of all the instrumentation systems in capturing comprehensive data are described.

The Selborne slope study is a collaborative investigation that draws together particular expertise from Southampton University, Warwick University, and Kingston Polytechnic. One face of a brickworks' clay pit was steepened to an overall slope of 1:2. An intensive instrumentation system was installed to monitor the behavior of the 9-m-high slope as it was brought to failure using pore-pressure recharge.

The general nature of the project is described, and a detailed account of the instrument systems adopted and their performance is given. The wider aspects of the experiment and a full presentation of the instrument results and observations on the nature and development of the failure are in the preparation stage. Following publication of the comprehensive paper, the research team intends to make all appropriate site data and instrument results available in a standard spreadsheet format. Construction details of individual instruments have not been included because they are not significantly different from standard systems. The measures adopted to provide multiple options for instrument-reading methods along with the measures to establish automatic alarm systems that warn of approaching failure are emphasized.

It should be noted that the instrumentation in this study was designed to record a single failure event and was not intended for routine performance monitoring. Therefore, it was essential that, whatever conditions prevailed at failure, the required readings could still be obtained. Several aspects of the system's design were influenced by this requirement.

STUDY SITE AND GROUND CONDITIONS

The Selborne slope study site is 4 km east of Selborne, near Alton in Hampshire, England, as shown in Figure 1. Its National Grid reference is SU-768342. The actual study area occupies about a quarter of the west face of the clay pit at the Honey Lane Brickworks of the Selborne Brick and Tile Company.

A feasibility study conducted in 1984-1985 showed the ground profile of the slope to be composed of about 1.5 m of soliflucted slightly gravelly clay over 6 m of slightly weathered gault clay. Unweathered gault clay made up the lowest 1 to 2 m and extended at least another 5 m below the pit-base level, where a 1- to 2-m thick basal layer separated it from a thin transition layer to the lower greensand. This ground profile sequence has been confirmed by further exploratory borings, which were conducted as part of the present study.

E. N. Bromhead, School of Engineering, Kingston Polytechnic, Canbury Park Road, Kingston-on-Thames, Surrey, England. M. R. Cooper, Department of Civil Engineering, University of Southampton, Southampton, Hants, England SO9 5NH. D. J. Petley, Department of Engineering, University of Warwick, Coventry, England.

GEOTECHNICAL DATA

Laboratory tests on 75-mm-dia. triaxial and 60-mm shearbox specimens gave the effective stress shear strength parameters samples obtained by HWF rotary coring, as shown in Table 1 (*1*).

The preexisting groundwater regime, established from prolonged standpipe observations during the feasibility study, can be characterized as being underdrained to the lower greensand with a downward hydraulic gradient of about 0.75 and a pore pressure of 0 at ground level.

GENERAL DESCRIPTION AND RATIONALE

The instrumentation design evolved in response to the three main objectives of the experiment:

1. It should provide a very detailed record of the condition of the slope at all stages of the experiment.
2. It should give useful information on prefailure strains and displacements as part of a study of progressive failure.
3. The system should contain sufficient redundancy and duplication to produce results up to, and if possible beyond, the final failure event, even with a high level of component failure.

The instrument layout plan shown in Figure 2 was developed in response to these requirements.

The study area is 25 m wide and the cut slope is 9 m high. The instrumented area extends for 18 m back from the crest of the slope and 6 m beyond the toe. The resulting 1,050 m^2 of plan area contains:

- 30 pneumatic piezometers,
- 30 vibrating wire piezometers,

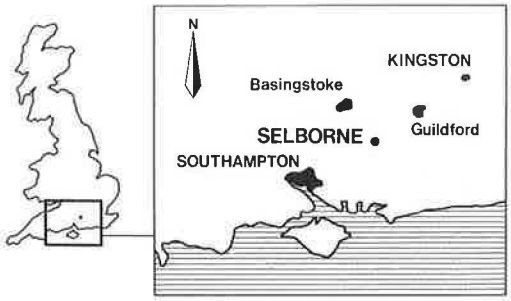

FIGURE 1 Site location.

TABLE 1 EFFECTIVE STRESS SHEAR STRENGTH PARAMETERS

Soil type	c'_{peak} kN/m²	ϕ'_{peak}	$\phi'_{residual}$ ($c'_r=0$)
Soliflucted Layer	5	20°	13°
Upper Weathered Gault	10	22-24°	13°
Lower Weathered Gault	15	22-25°	14°
Unweathered Gault	20-25	23-26°	15°

- 12 inclinometer access tubes,
- 2 in-place inclinometer strings (total 20 monitoring elements),
- 10 wire extensometers (on 2 cradles), and
- 20 recharge wells.

On the average, the system provides one monitoring instrument for each 8.6 m² of plan area.

This level of instrumentation is not common. The size of most natural slides subjected to detailed study generally leads to sparse coverage. Devin et al. (*2*) present a table of inclinometer usage at 13 landslide sites. The highest intensity of coverage noted was equivalent to 8 access tubes/hectare, or about 1/30 the intensity at Selborne (without considering the string inclinometers). Previous investigations have used special study sites to undertake prolonged monitoring but have rarely been able to instrument so intensively. The excellent study at Saxon Pit (*3*) used five piezometers, three magnet extensometers, five manually read extensometers, and three deep leveling points. Surface movement points and photogrammetry completed the coverage on a 200-m-long study face.

Perhaps the most intensive instrumentation use in Geotechnical Engineering is associated with earthfill dams. The instrumentation used to monitor displacement of the Kielder Dam is described by Millmore and McNicol (*4*). The 1140-m-long, 52-m-high embankment contained 11 inclinometers, 29 extensometers, 62 settlement devices, and used 185 piezometers of various types. On a surface area basis this represents about 1/100 the Selborne intensity.

The decision to install the large number of piezometers was a direct consequence of the proposed recharge method of inducing failure and would produce an entirely new pore-pressure regime requiring precise definition.

The inclinometer coverage was designed to give detailed displacement readings throughout the body of the slope and

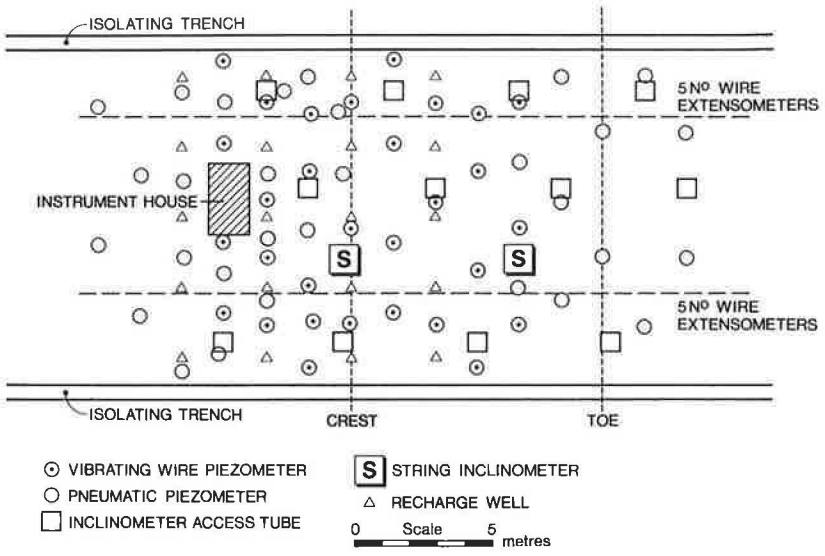

FIGURE 2 Instrument layout plan.

through the entire prefailure period. A standard manually read inclinometer probe was used to monitor displacements in 12 access tubes, which gave good spatial coverage. The string inclinometers were intended to give continuously logged movement-depth profiles at two key locations.

Rates of movement and strains within the slip mass were also of interest, and it was decided that useful information could be obtained using continuously logged surface-mounted wire extensometers.

The vibrating wire piezometers, string inclinometers, and wire extensometers were all continuously logged. Great care was taken in designing a system that had considerable flexibility in reading procedures. It was essential that readings could be taken even if some component of the data logging system were to fail during a critical period. Alarm systems were required to warn on- and off-site researchers of the possibility of impending failure.

The whole instrumentation system was designed with strict cost constraints. The overall study had a maximum possible funding limit of £200,000, and after all other costs were determined the amount available for instrumentation was less than £80,000. Both the total number of instruments and the balance of the complete installation were primarily determined by the stringent requirement that this overall figure (in 1987 prices) could not be exceeded.

PIEZOMETERS

Two types of piezometer were used to give the maximum coverage of pore-pressure measurement and recharge control within the established cost limits. A cross section showing the arrangement of the piezometer installations is shown in Figure 3*a*.

The 30 vibrating wire piezometers were concentrated in the zone below the slope face and the front part of the crest. This distribution was designed to cover the range of expected positions of the eventual failure surface. Vibrating wire piezometers can be continuously monitored electronically. In this case they were intended to provide frequent pore-pressure readings in the critical zone up to and during the failure event. It was also hoped that the piezometers above the eventual failure surface would continue to monitor postfailure pore-pressures.

The 30 pneumatic piezometers were installed in the areas at the toe. They were farther back from the crest and at depth,

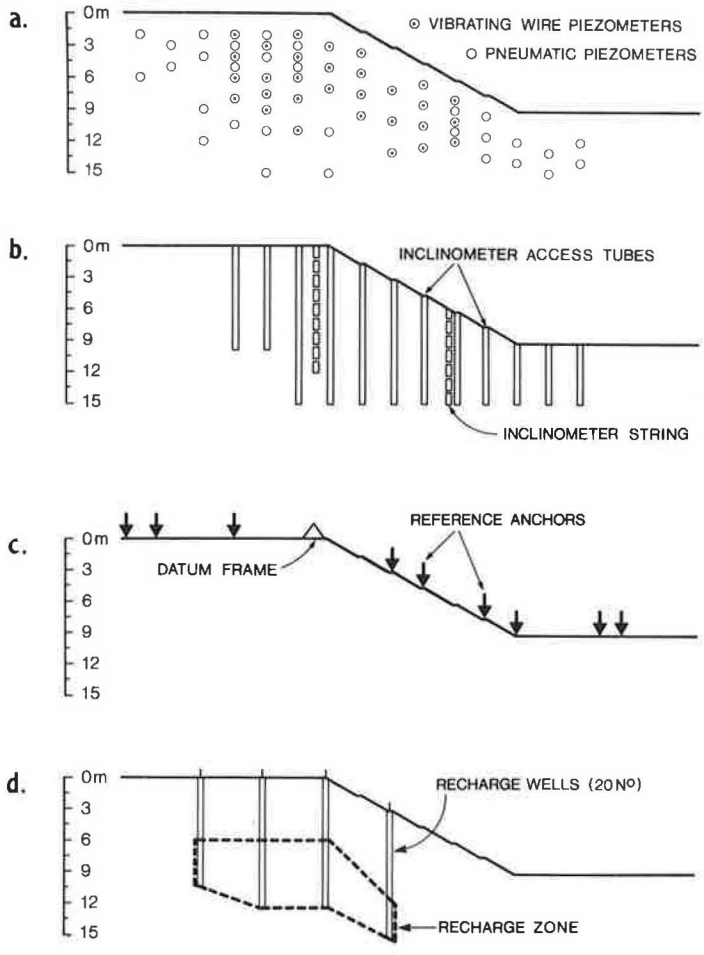

FIGURE 3 Instrument layout sections: *a*, piezometers; *b*, inclinometers; *c*, extensometers; *d*, recharge system.

areas where it was thought the failure would be less critical. Their main purposes were to extend the area over which pore pressure information would be available and to set the detail from the vibrating wire instruments in a wider framework. Although this type of piezometer cannot be read electronically, it does have a considerable cost advantage over the vibrating wire type (in this case approximately a fifth the cost). By using this cheaper system in areas thought to be less important, a considerable cost saving was produced, and money could then be diverted to ensure that critical areas were well served with continuously logged instruments.

The two systems were overlapped at the toe and at the crest to enable their outputs to be cross-checked and if necessary cross-calibrated. The filter dimensions and grouting up arrangements were the same for both systems. In all cases a 200-mm filter length was formed at the base of the installation borehole. The filter was sealed above with bentonite pellets and the hole filled to ground level with bentonite-cement grout. The short filter length was chosen to give a precise location for the measured pore pressure.

The pneumatic piezometer layout in the toe area was also intended to model a typical low-cost monitoring arrangement. It was suggested in preplanning discussions that the onset of instability in this passive zone might be preceded by noticeable changes in pore pressure. Pneumatic piezometers represented a low-cost means of monitoring these changes.

INCLINOMETERS

As with the piezometers, two different types of instruments were chosen to give a balance between detail and cost. The positions of the inclinometer installations are shown in cross section in Figure 3*b*. Twelve standard plastic inclinometer access tubes were installed to give broad, manually obtained coverage of lateral displacements. The main functions of this part of the system were to give an indication of the way in which the early stages of the failure developed and, by virtue of their greater sensitivity, to give an early indication of possible failure.

Continuous electronic monitoring of displacements within the slope was achieved by means of two in-place inclinometer string installations, one at the crest of the slope and the other at the lower-third position. Both installations were on the same near-central cross section of the slope. The string at the crest was made up of 12 independent inclinometer sensors on 1-m gauge lengths between 1 and 13 m deep, with each sensor being separately and continuously monitored. The lower string comprised 8 similarly arranged sensors between ground level and 8-m deep. The string inclinometers were the most expensive single items in the system but fulfilled three important functions:

1. Continuous monitoring of displacements within the slope. The shortest possible reading cycle for the manually read inclinometers could yield only two or three complete sets of readings per week, if other systems were not to be neglected. This would be insufficient to yield useful information on actual variations in rates of movement.
2. Taking of continued readings through the failure event. Manually read inclinometers require access at ground level and it was not intended to allow personnel on the slope if rapid failure was indicated. Conventional access tubes, at quite modest distortions, do not allow free passage of the reading torpedo. The string inclinometers overcome both of these shortcomings because they are remotely monitored and because they continue to function at much greater distortions.
3. Automatic alarm triggering. By providing continuous monitoring of displacements the string inclinometers allowed the provision of an automatic alarm system, which warned of any sudden increase in the rate of displacement on the slope.

WIRE EXTENSOMETERS

Surface strains on the slipping mass and larger relative movements between the slip mass and the adjacent ground were monitored by 10 wire extensometers, arranged in two groups of 5. Each group was based on a datum frame, anchored at the crest of the slope with four minipiles. Each datum frame carried five gearboxes, and each gearbox was driven by a sprocket carrying a chain connected to the free end of the invar extensometer wire. The positions of the datum frames and wire anchorage points are shown in Figure 3*c*. Relative movements of the anchor points and the datum frame are thus converted into rotations that are detected and measured within the gearboxes, which also contain the signal conditioning circuitry. By selecting the gearing at the datum frame, it was possible to fix the required range and sensitivity of each extensometer. In the event all the extensometers, irrespective of range, were found to give output to a precision of 1 mm, which was thought to be the maximum achievable stability of the cradle/wire/anchor system.

The wire extensometers were continuously monitored electronically and were incorporated into the automatic alarm system. It was intended that they would provide a continuous record of the amounts and rates of slip-mass movement throughout the final failure event and yield peak velocity components of the slip mass.

RECHARGE WELLS

The recharge wells comprise simple standpipes in long filter zones. The extent of the zones for each row of wells is shown in Figure 3*d*.

The recharge-well tubes were also to serve a secondary function as simple slip surface position indicators. However, as it became necessary to provide a closed, surcharged recharge system the slip indicator function had to be abandoned.

INSTALLATION

The instruments were installed in August–September 1987. Each subsurface instrument was placed in its own 150-mm-diameter hole, which was drilled by means of a continuous-flight auger technique that gave precise control over drilling depth. Instruments under the slope face were installed from temporary benches cut as part of the formation of the eventual slope. Drilling was therefore synchronous with the major earthworks.

READING SYSTEM

The reading system used at Selborne was of particular interest in two respects. First, a comparatively high proportion of instruments were connected to the continuous monitoring system and the inclusion of inclinometer and wire extensometer output in the data logging system is unusual. Second, the failsafes incorporated into the system are considered to be unusually thorough. It must be appreciated that in this application the function of the instrumentation was not just to warn of possible failure, nor simply to monitor the compliance of an as-built structure with design assumptions. The system had to record all of the details of a major one-off event, which could not be predicted in time or position to an accuracy that would permit reliable preprogramming.

The electronic reading system comprised two parallel subsystems. Each subsystem carried half of the vibrating wire output and half of the analog output from the string inclinometers and wire extensometers. Each subsystem was made up of the following:

- All the instruments were connected to a switch card–multiplexor, which handled all of the electronic switching during scanning and also incorporated EEPROMs to refine input signals and to give fully reduced and corrected output in engineering units directly.
- The switch cards–multiplexors were controlled by programmable data loggers, with each containing approximately 170 kb of internal memory (enough for about 86,000 readings). In normal operation either the data loggers could output continuously to printers and personal computers, or the readings could be extracted and transferred using independent interrogators. The latter was the preferred mode of operation onsite.

The data loggers could be programmed to a variety of logging strategies. Scan rates and intervals, for instance, could be varied according to the rate of change being recorded in any reading. More routinely, a threshold mode could be used where readings are taken at a scan rate of 1 set/min. but only recorded if different from the previously stored value by a preset threshold amount. The program also allowed the use of alarm levels as described in the next section.

Considerable attention was given to designing in alternative reading paths to cover any component failure. The first safeguard was the cross division between the two data loggers. The failure of one data logger would still leave half of the instruments of each type on-line. The following reading hierarchy was established:

1. Normal operation with automatic output to printers and automatic or interrogator transfer to floppy disk storage.
2. In the event of a computer failure, output would still be recorded on the printers and held in the internal memory to be accessed later.
3. In the event of failure of the data logger, the switch cards–multiplexors could still be accessed directly by manual readout units, each with internal memory sufficient to store 500 readings. This system required that a plug-in connection be made in the instrument house. As circumstances might have led to this house being positioned within the failure zone, special long fly leads were ordered to enable the manual readout units to be operated at a safe distance. They did not prove to be necessary.
4. In the extremely unlikely event of a switch card–multiplexor failing at a critical moment, the manual readout units could be connected directly to signal cable ends, but this would depend on the rate and position of failure and the degree of risk involved. Fortunately this option did not have to be attempted.

ALARM SYSTEMS

Special facilities incorporated within the programmable data loggers allowed different levels of alarm event to be recognized and acted on. Alarm levels were to be set at absolute values, fixed and modified for each instrument.

Approximately half of the instruments were programmed to trigger a first-level alarm in the instrument house and the remainder were set at a much higher level (selected as a possible indicator of incipient failure). If this level were reached, a set of contacts would close to activate an auto-dialer, which in turn would send a prerecorded message to key telephone numbers. On-site audible alarms and floodlighting were also to be triggered at this higher level.

PERFORMANCE

The performance of the complete instrumentation system was most satisfactory in that the failure event was recorded in the full level of detail hoped for and expected. In some respects, such as durability and displacement compliance, the performance was generally well above expectations. Many points of interest concerning the performance are still coming to light as the data produced are analysed. Among the observations to date, the following are highlighted:

1. Of the 89 independent instruments employed, 86 were still operative at the onset of failure, a reliability for the 2–year on-site period of 98.9 percent a year. One of the three lost instruments was damaged by site operations and the other two were either transducer or connection failures. Although still operative, the pneumatic piezometers recording negative pressures had become very difficult to keep on-line and were disrupted very early in the development of the failure. This very high retention rate was mainly due to two factors. First, this dedicated research site could be carefully managed and suffered none of the damaging interference often experienced when instrumenting working construction sites. The nature of the site, with fewer commercial pressures, also permitted very careful and high-quality initial installation. Second, the site itself was on remote private land and well protected from vandalism by the reputation of the site owner.
2. Three piezometers recovered during postfailure excavations were returned to the manufacturers (Geotechnical Instruments, Ltd.) for recalibration. The calibration results are presented in Table 2; they show remarkable stability over a 22-month period of burial. The units of pressure reported by the manufacturers are also retained for clarity.

TABLE 2 POSTFAILURE PIEZOMETER CALIBRATIONS AFTER 22 MONTHS OF BURIAL

Instrument Type, Number	Applied Pressure psi	Readout psi
Pneumatic, PP1.3	0.0	0.0
	0.3	0.3
	1.0	1.0
	15.1	15.2
	35.0	35.3
	50.0	50.0
Vibrating Wire, S/N 034	0.0	0.0
	10.0	10.0
	20.0	20.02
	30.0	30.10
	40.0	40.26
	50.0	50.34
Vibrating Wire, S/N 010	0.0	0.0
	10.0	10.01
	20.0	20.06
	30.0	30.14
	40.0	40.19
	50.0	50.25

3. Initial piezometer equalization times were between 1 and 3 months. This order of magnitude is longer than would be predicted by using the simple theory for pore-pressure equalization following stress disturbance around a driven pile (*5*). Soderberg's analysis, admitted to becoming inaccurate at high degrees of equalization, would predict 95 percent pore-pressure equalization of between $30.r^2/C_h$ and $60.r^2/C_h$. Falling-head permeability tests carried out in standpipes during the feasibility study had given (horizontal?) permeabilities near 10^{-9} m/sec, suggesting a C_h value of about 0.04 m²/day. The predicted 95 percent equalization time would therefore be 8 days. The true equalization rates are clearly shown in Figure 4, where the stabilization of a newly installed piezometer is compared with readings of an adjacent instrument that had been in place for 1 year. The slow equalization, though of wider interest, was not of significance for the project because all the piezometers were in place well before the final critical phase.

4. System response times were not considered to be a problem. Both types of piezometer contained a small-volume closed cavity that gave very low system compressibility, typically less than 10^{-3} cm³/F.S.D. for the vibrating wire instruments. It has long been accepted that such installations will have response times on the order of a few seconds (*6,7*). The response behavior, related to known driving events, is shown in Figure 5.

5. Groups of piezometers were consistent within themselves in the pattern of their response. Figure 6 shows the response records of three piezometers at the same level, but at different distances from the recharge wells.

6. Negative pore pressures were recorded at the toe of the slope. These were probably the result of the stress reduction caused by substantial excavations in this area. This effect

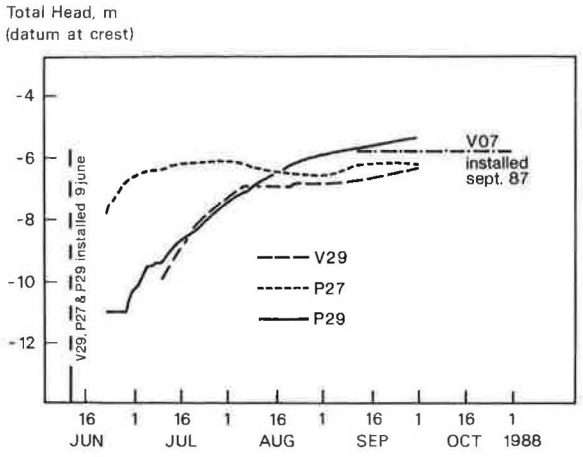

FIGURE 4 Typical piezometer equalization curves.

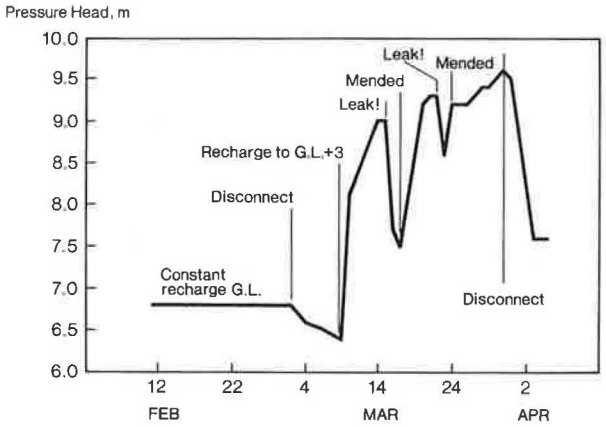

FIGURE 5 Typical piezometer responses to driving events (Piezometer P24, GL = 8 m).

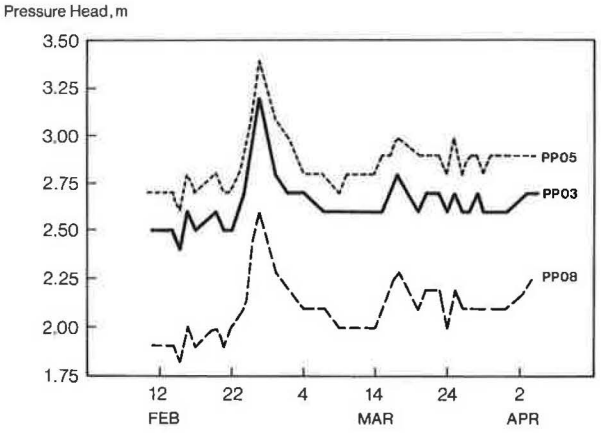

FIGURE 6 Adjacent piezometer responses (GL = 5 m).

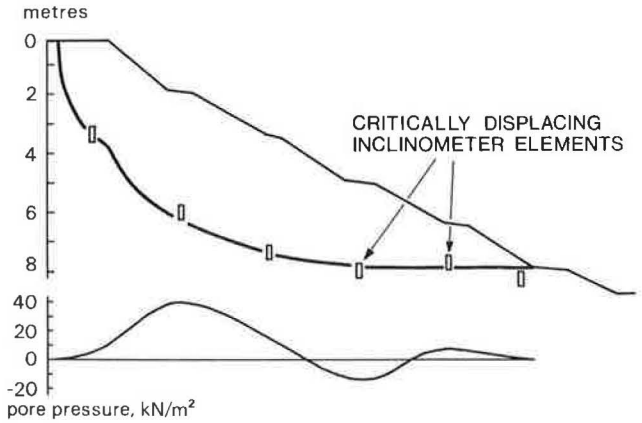

FIGURE 7 Interpolated slip-surface section on centerline.

is described by Bishop and Bjerrum, (*8*) and has subsequently been confirmed by a number of field studies (*9*). The pneumatic piezometers are not well suited to measuring negative pore pressures in low-permeability soils, and special procedures were devised that will be described in detail elsewhere.

7. The inclinometer records faithfully recorded the position of the slip surface as it was eventually exposed during the postfailure excavations. The interpolated shape of this surface at the center of the study area is shown on Figure 7.

8. The inclinometer torpedo calibration remained constant, although some maintenance of wheel bearings was necessary. Had a longer monitoring period been required, replacement of the running wheels would have been essential. By the end of the project, the torpedo had been used for readings equivalent to 17 km of travel.

The stability of the calibration was confirmed by observations of deflections over the very long fixed lengths below the movement zone, as well as the usual wall-mounted calibration frame. In all access tube inclinometers, the recorded cumulative deflection over the fixed length (up to 8-m long) was less than 2 mm over a period of more than 500 days, as shown in Figure 8.

9. Three inclinometer access tubes were carefully exposed during postfailure excavations. In each case, the deformed profile of the tube was aligned very closely along the exposed failure surface and had been pulled down out of its grout surround within the moving mass and laid flat along the failure surface. Figure 9 shows the relative positions of the distorted tube, slip plane, and empty grout column for an access tube that underwent about 4 m of relative displacement.

10. The string inclinometers and wire extensometers performed their special functions very well. Both types of instrument provided continuous displacement-time plots of a type that could not have been obtained with manually read instruments, and both continued to function at very large displacements. Wire extensometers continuously recorded relative movements up to 150 mm at 1-min intervals over 3 hr, and the string inclinometers were still functioning with angular distortions between successive 1-m gauge lengths of up to 42 degrees. A 0.5-m torpedo passed through a maximum angular distortion of 35 degrees, but it did so at great risk to the instrument. At greater distortion, the lower part of the access tube became inaccessible, whereas the lower parts of the inclinometer strings remained operative even after large distortions had developed higher up.

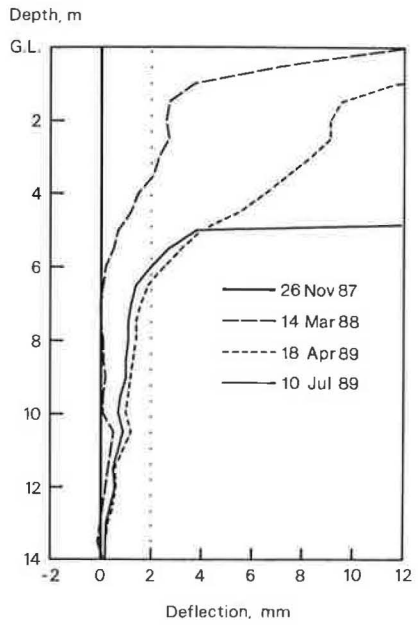

FIGURE 8 Typical inclinometer fixed-length behavior (Inclinometer 06).

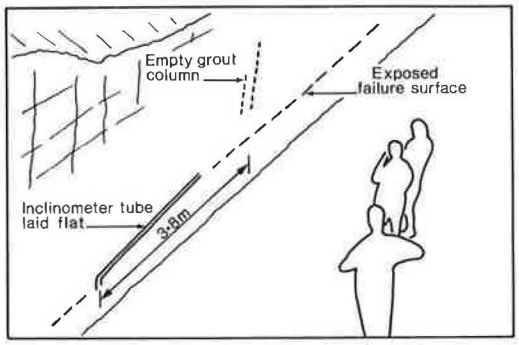

FIGURE 9 Inclinometer tubing compliance.

11. During the slope failure, the behavior of the connections to the pneumatic piezometers was very different from that of the vibrating wire connections. The very extensible tubing of the pneumatic instruments deformed and easily stretched to accommodate some very large movements. The vibrating wire signal leads were much less compliant, and many snapped very early in the failure event.

12. The full hierarchy of reading options was not required, although it was proved in practice routines.

13. The reading strategy adopted was the threshold change approach, which scans at 1-min intervals; values are only recorded if one of the readings is significantly altered. Instrument flutter frequently exceeded the very tight threshold limits that were set and about 60 percent of the scans resulted in recorded readings. By excluding the less-stable instruments or setting wider threshold tolerances, this percentage could have been greatly reduced.

14. The first alarm level triggered very quickly as the failure developed, and the majority of failure data was obtained from the simple 1-min interval reading strategy on all channels. The enormous quantity of data generated has caused some problems in subsequent data processing. This is acceptable in a research application for which detail and duplication are paramount in the design philosophy, but it would cause problems in the more usual monitoring applications for which delay in accessing data cannot be countenanced.

CONCLUSION

The instrumentation systems used for the Selborne cutting stability experiment performed well and have provided a detailed record of a unique experiment. The few shortcomings identified during the data processing are associated more with site pressures and manpower shortages (giving less than planned for reading frequencies on some instruments at some times) and financial constraints (a third string inclinometer would have been extremely useful) than with inadequate instrument performance. There is little doubt that instrument systems exist to cover all site-monitoring requirements for an exercise such as the Selborne experiment. The main difficulties to be overcome are in planning a successful layout for the instruments, in planning an efficient and workable reading schedule in which manual reading is employed, and in planning a data access system that allows rapid, user-friendly access to electronically logged data.

ACKNOWLEDGMENTS

The collaborative study was sponsored by the Science and Engineering Research Council by means of three separate grants to the participating institutions. The collaborators (E. N. Bromhead of Kingston Polytechnic, D. J. Petley of Warwick University, and M. R. Cooper of Southampton University) wish to express their appreciation of the generosity of J. A. de Benham Crosswell and the Selborne Brick and Tile Company in making such a large part of their active clay pit available for such a long period.

The authors would also like to acknowledge the extensive and invaluable assistant in the form of time, advice, expertise, and material support given by R. C. Weekes and R. G. Gillard of Geotechnical Instruments, Ltd.

The installation of the instrumentation described here were carried out under the direction of E. N. Bromhead, with the assistance of I. R. Sandman and Southampton University's D. I. Grant.

REFERENCES

1. D. J. Petley, E. N. Bromhead, M. R. Cooper, and D. I. Grant. Full Scale Slope Failure at Selborne, *U.K. Proc., Conference on Developments in Laboratory and Field Tests in Geotechnical Engineering Practice*, Bangkok, Thailand, 1991.
2. P. E. Devin, G. Pezzetti, C. Ricciardi, and P. Tommasi. Assessing the Precision of Inclinometric Measures by Means of an Experimental Apparatus. *Proc., 5th International Conference on Landslides*, Vol. 1., Lausanne, Switzerland, pp. 393–398.
3. J. B. Burland, T. I. Longworth, and J. F. A. Moore. A study of Ground Movement and Progressive Failure Caused by a Deep Excavation in Oxford Clay. *Geotechnique* Vol. 27, 1977, pp. 557–591.
4. J. P. Millmore and R. McNicol. Geotechnical Aspects of the Kielder Dam. *Proc., Institution of Civil Engineers*, Part 1, 1983, pp. 805–836.
5. L. O. Soderberg. Consolidation Theory Applied to Foundation Pile Time Effects. *Geotechnique*, Vol. 12, 1962, pp. 217–225.
6. G. Margason, M. J. Irwin, and M. A. Huxley. The Effect of Tides on Subsoil Pore-Water Pressures at a Site on the Proposed Shoreham By-pass. Report LR 195. U. K. Transport and Road Research Laboratory, Crowthorne, Berkshire, England, 1968.
7. P. R. Vaughan. The Measurement of Pore Pressures with Piezometers. *Proc., Symposium Field Instrumentation in Geotechnical Engineering*, 1973, pp. 411–422.
8. A. W. Bishop and L. Bjerrum. The Relevance of the Triaxial Test to the Solution of Stability Problems. *Proc., ASCE Research Conference on Shear Strength of Cohesive Soils*, Boulder, Colo., 1960, pp. 427–501.
9. P. R. Vaughan and H. J. Walbancke. Pore Pressure Changes and the Delayed Failure of Cutting Slopes in Overconsolidated Clay. *Geotechnique*, Vol. 23, 1973, pp. 531–539.

Publication of this paper sponsored by Committee on Soils and Rock Instrumentation.

Landslide Cases in the Great Lakes: Issues and Approaches

TUNCER B. EDIL

A review of the experience gained over a decade of studying the mechanics of coastal bluff erosion and stability along the Great Lakes shorelines and the approaches to dealing with this problem are presented. Shore recession affects planning, design, and maintenance of transportation facilities in coastal areas in a significant way. The erosional processes resulting in significant mass wasting include wave erosion, solifluction, rain impact and rill-sheet erosion, wind erosion, sapping, and ice erosion. Another important process is mass sliding and slumping of bluff materials in response to and in conjunction with the erosional processes. The methods of approach to this problem are grouped as structural (stabilization) and nonstructural (planning and management) solutions. These approaches and the required information to implement either of them are discussed. Because of the length of the slopes and the variable nature of geology and soil properties, a probabilistic approach to stability analysis has been adopted for planning and managing the stabilization efforts. Two specific cases, one in an undeveloped segment and another in an urban segment of the shoreline, are presented to demonstrate the stabilization approach.

This paper presents a review of the experience the author has gained over a decade of studying the mechanics of coastal bluff erosion and stability along the Great Lakes shorelines. Nearly 65 percent (10 444 km) of the 16 047-km-long Great Lakes shoreline is designated as having significant erosion; about 5.4 percent (860 km) of it is critical. The total damage to the U.S. shoreline of the Great Lakes due to wave action during the high-lake-level period, May 1951 through April 1952, is placed at about $50,000,000 (1952 price level). Nearly 32 percent of the U.S. shoreline of the Great Lakes, not including the islands, consists of erodible bluffs. Extensiveness of the shoreline formed in erodible bluffs and dunes (an often complex response of this type of shoreline) to wave erosion makes slope processes an important part of the shore recession problem. The shore recession, in turn, affects the planning, design, and maintenance of transportation facilities in coastal areas in a significant way. The coastal bluff processes are briefly described, and the methods of approach to this problem are presented along with two specific cases.

SLOPE PROCESSES

The interaction of driving forces (gravity and climate) and soil shear resistance results in a number of processes that lead to debris production and removal. The commonly encountered processes in the Great Lakes coastal bluffs can be separated into two broad groups, mass and particle movements. In the mass group, debris begins to move as a coherent unit (rigid body movement or viscous flow). Movements in which particles move individually, with little or no relation to their neighbors, are particle movements. The erosional processes caused by waves, currents, rain, groundwater, and winds seem to be mainly particle movements. These concepts are presented in Figure 1.

CERMES, Ecole Nationale des Ponts et Chausées, 93167 Noisy-le-Grand Cédex, France. Current affiliation: Department of Civil Engineering, University of Wisconsin, Madison, Wis. 53708.

Wave Erosion

Probably the most significant geomorphic process along the Great Lakes shoreline is the erosion and removal of shoreline materials by waves. Wave action is important, both in itself and in initiating and perpetuating other geomorphic processes in segments of the shoreline where bluffs are encountered. The most notable factor that affects the wave erosion in the Great Lakes is water-level fluctuation. For the long-term water level changes, the intervals vary from 10 to 30 years and the magnitudes are up to 2 m.

Sliding and Slumping

Slides (both rotational and translational) and flows (including solifluction) are the two types of movements most commonly encountered in the Great Lakes region. Coastal bluffs are in constant evolution because of the combined effects of toe erosion, slides, and face degradation.

Edil and Vallejo (*1*) described bluff stability at two sites on the shore of Lake Michigan. Where unexpected stability occurred, it could be explained in a rational manner by the process of delayed failure that results from the unloading of clays by erosion. Barring the presence of gross inhomogeneities, rotational slides involving approximately circular rupture surfaces have been observed and analyzed in the Great Lakes bluffs formed in cohesive soils (*1–3*). Deep-seated rotational slips occur in clay soils but are not observed in sands. One method of analysis of rotational slides that is accurate for most purposes is that advanced by Bishop (*4*). The failure arc predicted by the Bishop method has been found to compare very well with the actual failure surfaces in bluffs in the Great Lakes and other places. Using the effective stress approach and the Bishop method, Vallejo and Edil (*5*) developed stability charts for rapid evaluation of the state of stability of actively evolving Great Lakes coastal slopes. These charts indicate the stability status as well as the type of potential failure, whether deep or shallow, to which the bluffs may

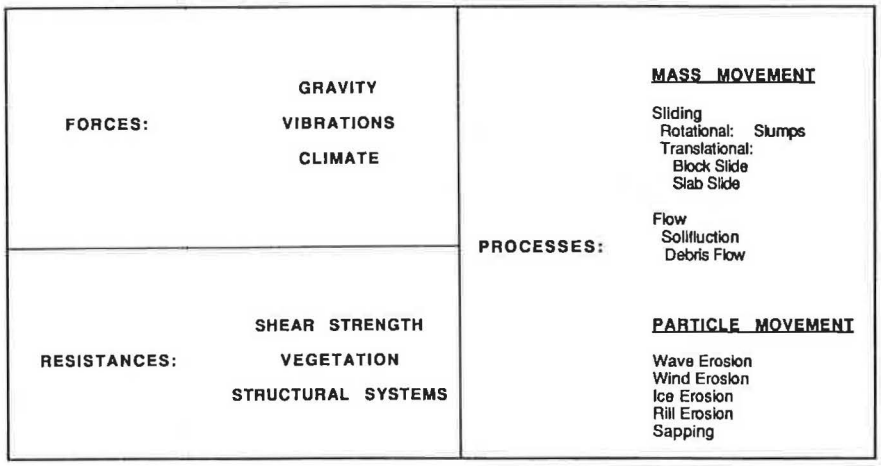

FIGURE 1 Forces, resistances, and slope processes in Great Lakes.

be subjected. The geometric changes can be discerned from the stability charts.

A translational slide in which the moving mass consists of a single unit that is not greatly deformed, or a few closely related units, may be called a block slide. An example of such a failure involving a block of fractured till in the upper part of a coastal bluff in Milwaukee County, Wisconsin, was reported by Sterrett and Edil (*6*). Translational slips can also occur in a homogeneous soil mass. In particular, granular materials such as sand and gravel fail in surface raveling and shallow slides with the failure surface parallel to the slope surface. Similar failures occur in a mantle of weathered or colluvial (granulated) material from clay slopes and are referred to as slab slides. An infinite slope analysis is often representative of such failures. Sterrett (*7*) reported slab slides with a depth of about 6.0 m from Milwaukee County. This depth coincided closely with the depth of desiccation cracking and soil structure change from fine to prismatic beds to massive intact blocks. Sterrett (*7*) also observed that frozen slabs of soil measuring 0.6 m × 10 m × 13 m failed in early spring, and attributed this failure to differential melting of the bluff face.

Flows and Solifluction

Flows commonly result from unusually heavy precipitation, thaw of snow, or frozen soil. The flows observed in the Great Lakes bluffs take place mostly in spring and result primarily from ground thawing and snow and ice melting. Therefore, they can be classified largely as solifluction. Solifluction is the downslope movement of water-saturated materials that follows thawing in previously frozen slopes. Vegetation appears to be the most restraining factor for solifluction. The size of the flows along the western Lake Michigan shoreline varies from 0.3 to 0.6 m wide up to 15 to 20 m wide and 21 m long. A number of approaches for the analysis of solifluction failures have been suggested. Vallejo (*8*) introduced a new approach to the analysis of solifluction that reflects the particulate structure of the flowing mass. Vallejo and Edil (*9*) applied this analysis, with successful field verification, to a coastal bluff in Kewaukee, Wisconsin. The critical depth of thaw normal to the slop face at which failure occurred was measured to be 0.25 m.

Rain Impact, Rill and Sheet Erosion, Sapping, Wind, and Ice Erosion

These processes are also important in general mass wasting that occurs in the exposed coastal slopes of the Great Lakes. In slopes formed in granular material, these processes are dominant. A description of these processes given by Sterrett (*7*) determined on the basis of field observations that most of the material removed from the slopes during summer is by way of sheet-wash and rill erosion. Sterrett (*7*) found that the universal soil-loss equation, in its modified form as suggested by Foster and Wischmeier (*10*), is useful in predicting soil loss from steep slopes.

STRATEGIES FOR DEALING WITH ACTIVELY EVOLVING SLOPES

The most significant characteristic of the coastal slopes in many areas of the Great Lakes shoreline is the fact that they are actively evolving natural slopes—the slope geometry continually changes. This characteristic sets these slopes apart from other natural slopes in terms of stabilization approaches. There are basically two approaches to the problem of actively evolving coastal slopes. The first approach involves structural or stabilization solutions on a site-specific basis. The structural approach, with some additional considerations, is similar to other natural slope stabilization efforts. A proper stabilization program should include (a) protection against wave action in all cases, (b) slope stabilization against deep slips if needed (important in the delayed instability often observed in bluffs formed in stiff clay soils), and (c) stabilization against face degradation and shallow slips. Shore protection is a major component and may be more costly than the slope stabilization. The problems associated with the execution of this category of solutions are of two types: (a) many attempts are not engineered and fail to cope with the problems, and (b)

those engineered solutions often neglect to consider all aspects of the problem as described. For stabilization works, site-specific studies are undertaken at numerous locations. In these studies, an attempt is made to identify and understand slope-stability problems at a single site over a relatively short period of time.

The second approach, the nonstructural planning and management approach, is particularly suitable in undeveloped tablelands where hazard mitigation to transportation facilities can be planned and managed over an extensive part of the shoreline (the size of a county or at least several kilometers are usually considered). These studies are usually aimed at minimizing future losses. In this case the need for understanding bluff processes is critical because predictions of future recession over a long period of time with changing water-level and climate conditions are necessary. This approach necessitates models of bluff evolution (*1,11*). The main problem concerning prediction of slope evolution is understanding the response times to environmental changes and the time necessary for bluffs to pass through an evolutionary sequence. Evidence from other areas with evolving slopes such as riverbanks and marine coasts as well as from the Great Lakes suggests that there are possibly three time scales over which the natural cycles of evolution take place: 2 to 3 years, 50 to 100 years, and thousands of years.

The main tool used in the nonstructural or management approach is the establishment of a setback requirement for new transportation facility development. This requires a knowledge of coastal recession over a long time—say, 30 to 50 years—and the determination of stable slope angles. Typically, historical aerial photographs are used to establish the recession rates and geological and geotechnical analyses are used to determine the stable slope angles. Research conducted primarily during the last decade or two has identified the operating processes and their possible magnitudes (*12*). A nonstructural setback distance can be estimated as shown in Figure 2 (*13*). Setback distance consists of two components. Erosion risk distance is the distance from the existing bluff edge that could be affected by recession of the bluff over time and by the regrading of the bluff to a stable slope angle. Minimum facility setback distance is considered to be an additional safety zone intended to prevent facilities from being placed too close to the bluff edge. The solution strategies for active coastal slopes are given in Table 1.

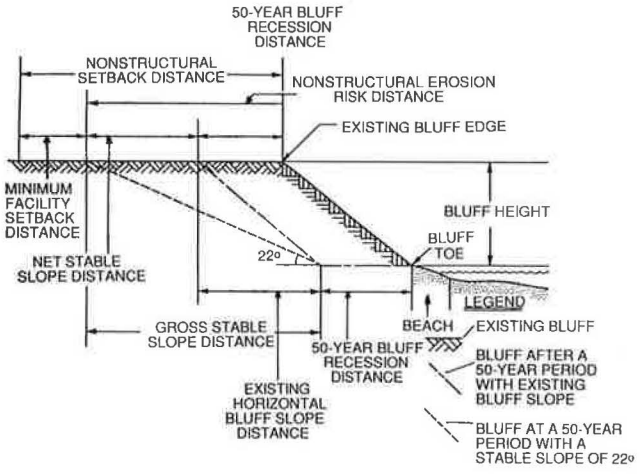

FIGURE 2 Procedure for estimating nonstructural setback distances (*13*).

TWO CASE HISTORIES

In this section slope conditions and stabilization strategies at two specific sites along the southwestern Lake Superior and the western Lake Michigan shorelines are presented, respectively.

Madigan Beach—Lake Superior

The bluffs of this site are reached by a 4-km secondary road that is directed northeastward of U.S. State Highway 2, approximately 25 km east of Ashland, Wisconsin. The site is located 610 m west of the mouth of Morrison Creek in the Bad River Indian Reservation. This site provides an example of a situation in which the main highway is quite far from the shore for immediate threat and the upland is undeveloped. The shoreline profile at the Madigan Beach site consists of bluffs rising 18 m above the beach and maintaining temporary steep inclinations in excess of 40 degrees with the horizontal. The processes of undercutting and slumping are evident and the bluff faces are mostly exposed because there are no vegetation and trees, which are dominant in the upland. Geologically, northwestern Wisconsin, where Madigan Beach slopes are, is a glaciated area.

The borings and observations of the materials exposed on the bluff face indicated the presence of a 4.5- to 6-m-thick reddish-brown stiff, silty, clay layer of low plasticity on the top, underlain by a thick (more than 12 m), very dense, brown sandy silt or silty sand. The geotechnical properties of the bluff materials are presented in Table 2. This highly erodible (cohesionless) sandy silt makes up most of the bluff material and is underlain by a reddish brown, rather stiff clay layer of high plasticity, mostly below the lake level. A mineralogical analysis of this lower clay layer revealed the presence of quartz, illite, kaolinite, and a small quantity of montmorillonite. The difference in the plasticities of the upper and lower clay layers appears to stem primarily from the difference in their clay fractions (26 and 63 percent, respectively) rather than from a mineralogical difference.

Madigan Beach appears to be subject to severe climatological forces and this, coupled with the erodible (cohesionless) materials forming the bulk of the bluffs, results in a highly active environment for slope evolution. Photoreconnaissance surveys conducted periodically since 1974 have revealed the action of bluff face degradational processes such as sheet wash, solifluction, seepage effects, and also the dominant action of waves. The sandy silt material of the bluffs, while highly erodible under surface processes, is strong below the surface when it is confined (the effective angle of internal friction is 37 degrees). This makes the bluffs highly stable against immediate rotational slips, and they sustain fairly steep inclinations, in excess of 40 degrees, in many parts of the shoreline. This situation is helped by the presence of clay layers some 6 m thick that cap the top of the bluffs.

TABLE 1 SUMMARY OF STRATEGIES FOR COASTAL BLUFF RECESSION

PROCESSES	SOLUTIONS	
	STRUCTURAL (STABILIZATION): DESIGN	NONSTRUCTURAL (MANAGEMENT): PREDICTION
TOE EROSION	SHORE PROTECTION (groins, seawalls, etc.)	SHORE RECESSION RATE (long-term, cyclic)
DEEP ROTATIONAL SLIPS	SLOPE STABILIZATION (regrading, dewatering, etc.)	STABLE SLOPE ANGLE AGAINST DEEP SLIPS
FACE DEGRADATION AND SHALLOW SLIPS	SURFACE PROTECTION (vegetation, drainage)	ULTIMATE ANGLE OF STABILITY

TABLE 2 GEOTECHNICAL PROPERTIES OF SOIL SAMPLES FROM MADIGAN BEACH BOREHOLES

Soil Description and Depth	Group Symbol*	Texture** %Sand	%Silt	%Clay	Liquid Limit %	Plasticity Index	Water Content %	Unit Weight (kN/m^3)	Average+ N	Angle ++ of Internal friction ϕ	Cohesion++ Intercept C (kPa)
Reddish brown, stiff silty clay of low plasticity (Upper clay, 0-6m)	CL	10	64	26	31	14	18	21.4	18	19°	80
Brown, very dense sandy silt or silty sand (6-16m)	ML or SM	7-18	78-90	3-4	---	---	18	19.9	>100	37°	0
Reddish brown, rather stiff clay of high plasticity (Lower clay 16m)	CH	11	26	63	51	31	31	19.2	14	21°	0

* According to the Unified Soil Classification (ASTM Designation: D 2487-69 and D 2488-69).

**4.76 mm > Sand > 0.074 mm; 0.074 mm > Silt > 0.002 mm; 0.002 mm > Clay

\+ Standard Penetration Resistance, N(ASTM Designation: D 1586-67).

++Drained Shear Strength Parameters.

To monitor the changes in slope morphology, a number of cross sections (perpendicular to the shoreline) have been periodically surveyed. The changes in most of the cross sections were indicative of face degradational processes without any deep rotational slips. The bluff top recession, measured using 1976 and 1978 aerial photographs, indicated a variation of recession on the order of 3 to 11 m during this period. In 1977, a shore protection demonstration project was initiated, which involved the placement of longard tubes filled with sand in different configurations (*14*) along the beach, as shown in Figure 3. Longard tubes are constructed of a geotextile, and they come in various sizes. Those used at Madigan Beach were 1.75 m in dia and weighed about 4500 kg/m once they were hydraulically filled with sand. Four of the tubes were placed at the toe of the bluff parallel to the shoreline acting as a seawall and six 33-m-long tubes were placed perpendicular to the shoreline to act as groins. The recession rates measured in the field, as well as discerned from aerial photographs, indicated a significant reduction in the recession from the 1976–1977 values. It should be noted, however, that one of the sections experienced a large recession of 2.9 m during this period because of a deep slip.

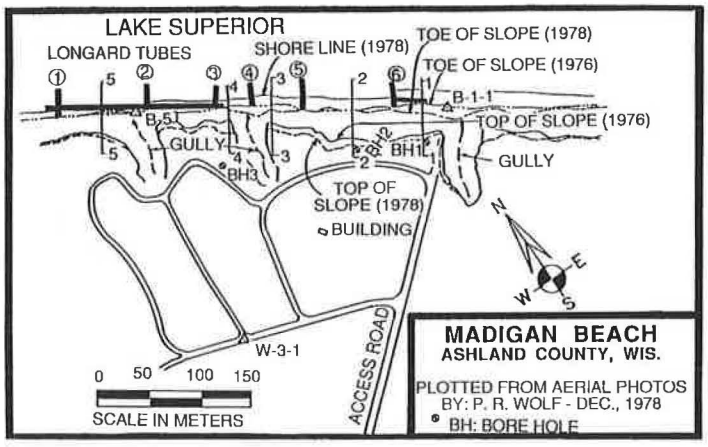

FIGURE 3 Longard tube layout and bluff conditions at Madigan Beach (number circled indicates tube location).

The stability of the bluffs was analyzed using the Bishop method in a conventional manner. The method used the effective stress analysis of slope stability, the drained strength parameters of the bluff materials, and the measured porewater pressures as estimated from the piezometer readings. The stability analyses performed on the initially measured profiles of Cross-sections 1, 2, and 3 (Figure 3) resulted in safety factors of 1.36, 1.16, and 1.30, respectively, which indicated the general stability this segment of the site had against sliding. When surveyed in 1976, Cross-section 2 had already gone through a deep-seated major slide involving a 3.4-m drop of an 8.8m-wide section at the top. The initially surveyed profile of Cross-section 4 resulted in safety factors less than unity and were therefore unstable. A safety factor of less than unity implies potential instability (long-term) for a currently standing slope because the analysis performed is an effective stress (long-term stability) analysis, and it may also imply that some of the assumptions, such as zero pore pressure above the groundwater table, are too conservative. This bluff maintained its stability until the latter part of the summer of 1978, when slumping occurred, which resulted in the recession of the bluff top as marked by the approximate intersection of the predicted failure surface.

Another cross section, Cross-section 5, was also analyzed; it was found to have potential for slumping as shown by the failure surface in Figure 4. The bluff segment in this area was chosen for a slope stabilization demonstration. After considering several alternatives—including terracing, berms, and various combinations of these—it was decided to regrade the bluff to a uniform slope of about 25 degrees. On the basis of a similar analysis, this inclination was determined to be safe. The bluff stabilization demonstration included surface water diversion in the upland and seeding of the bluff face to prevent surface erosion. The project was completed in the fall of 1977. The toe of the bluff was protected with a longard tube that was placed parallel to the toe and another longard tube placed perpendicular to the shoreline (see Figure 3), which effectively built up the beach in front of the longard tube acting as a seawall. The six longard tubes that were placed as groins perpendicular to the shoreline were all destroyed by spring 1980. The other tubes that were put as seawalls, for the most part, lasted for a while and did provide some degree of protection. In 1984, these tubes were mostly deflated and buried in the beach sand, exposing the stabilized bluff section to renewed wave attack.

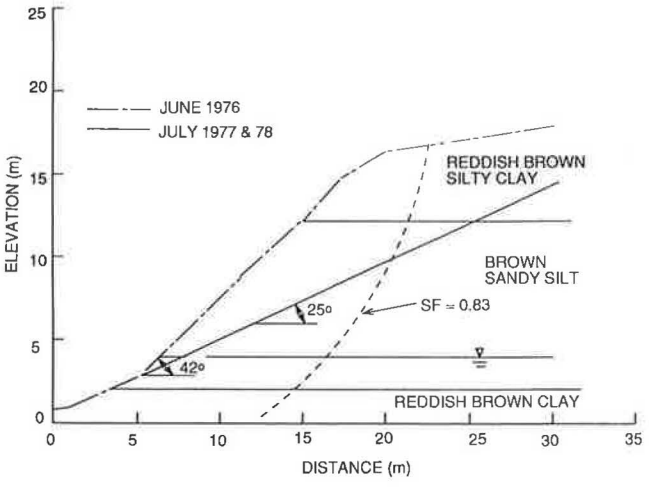

FIGURE 4 Bluff profiles in Cross-section 5.

Whitefish Bay—Lake Michigan

The topland in the case of these slopes is in a highly developed urban setting in a northern suburb of Milwaukee, Wisconsin. Within 50 m from the edge of the bluffs are expensive homes, behind which a major urban road passes. A 1983 landslide threatened six to eight homes when their front yards dropped nearly a meter. This coastal area is formed in glacial deposits ranging up to 40 m in thickness. The layer nearest to the surface is known as the Ozaukee Till, which consists of a silty clay with reddish color. The Oak Creek Till lies beneath the Ozaukee Till; it is composed of a pebbly silty clay. Lake sediments of various textural characteristics are often found between these two tills. Directly beneath the Oak Creek Till lies another very stiff till known as the New Berlin Till, which was deep below the lake level at this location. This till is coarse-grained, sandy in texture, and dominated by pebbles and cobbles. These formations are often exposed in the active slopes along the western shore of Lake Michigan. The stratigraphy was identified on the basis of field surveys, historic geological records of soil boring data, and new soil borings performed at selected sections of the shoreline.

The geotechnical properties of the glacial materials forming the bluffs were obtained from historic data and laboratory analysis of the samples collected from the exposed slope surface and soil borings. In terms of the known values and standard deviations based on the samples collected from different parts of the shoreline, the strength parameters and the unit weights of the bluff material are presented in Table 3.

Along the northern Milwaukee County shoreline, groundwater generally flows toward the lake and is discharged into the lake either at or below the base of the bluff. The lake sediments consisting of coarse-grained soils may act as water-bearing units. Additionally, a perched water table is usually found within the fractured Ozaukee Till at the top of the bluffs, which produces seeps on the bluff face. The groundwater elevations used in the slope stability analysis of each profile site were based on observed groundwater seepage, soil boring data, groundwater observation wells, and electrical resistivity analysis.

The area shoreline studied extending nearly 3.7 km, was considered to be a single section with similar physical and erosion-related characteristics. Field surveys were conducted to delineate the section boundaries and to identify the causes and types of beach erosion and slope failure occurring in the section. Unlike the earlier case, both conventional deterministic slope stability analyses and probabilistic soil stability analyses were conducted to establish the state of stability of this entire section.

Conventional Analyses

The worst-case groundwater conditions are assumed in the conventional deterministic analyses. Late winter and early

TABLE 3 GEOTECHNICAL PROPERTIES OF SOILS ENCOUNTERED IN SLOPES ALONG LAKE MICHIGAN'S MILWAUKEE COUNTY SHORELINE

Soil Unit	Unit Weight (kN/m^3)	Friction * Angle (Degrees)	Cohesion* Intercept (kPa)
Tills			
New Berlin	21.7	34 ± 3	0.5 ± 0.25
Oak Creek	21.2	30.5 ± 2	5.0 ± 3.75
Ozaukee	21.1	30 ± 3	7.5 ± 5.0
Fractured Ozaukee	21.1	30 ± 3	0 + 3
Lake Sediments			
Medium Fine Sand	18.9	33 ± 2	0 + 0.25
Sand and Gravel	18.9	33 ± 2	0 + 0.25
Silt	20.4	31 ± 2	200 ± 50
Silt and Fine Sand	17.3	31 ± 2	0.5 + 0.5
Clay and Silt	20.4	27 ± 2	22.5 ± 17.5
Fine Sand and Silt	19.7	33 ± 2	5.0 ± 3.75
Gen'l Lake Sediment	19.7	27 ± 3	5.0 ± 3.75
Fill			
Concrete Rubble/Soil	20.4	35	0

spring have been found to be the most critical periods for the stability of Lake Michigan coastal slopes for both deep-seated and shallow slides (*5*). The slope stability program named STABL (*15*) was used to calculate the safety factor for a slope profile measured in an adjacent segment of unfailed bluff within the study area. The lowest safety factor calculated was 0.95, and the corresponding failure surface was located in the middle portion of the bluff slope. However, a bluff segment in the study area had already failed in a rotational slide. The safety factor for this failed bluff was calculated to be 1.56 (*16*).

In the deterministic approach, mean values of soil properties based on the available test results in Table 2 were used in computing a safety factor against failure, along with the geometrical and geological measurements of the slope at the specific site. An assessment of the general stability of slopes of a shoreline section, based on the deterministic safety factors of a number of slope profiles located within the section, could conceivably be in error if the slope parameters chosen as input for the stability program are not reliable. For example, adequate information may be available at certain sections because of the excellent exposure of slope soil stratigraphy and the rather uniform characteristics of the slopes and soils within the section. At such locations, adequate information is available for what may be called a reliable analysis. However, for many other sections, between borehole locations and poorly exposed slope faces because of vegetative cover, soil properties, position of stratigraphic unit interfaces, and groundwater table in the slope have to be interpolated or estimated based on an examination of the general slope conditions. In view of the variability of soil properties and other slope parameters that have to be estimated, the computed safety factors would not be as reliable for these profiles as they would be for the profiles at the borehole locations and those with good exposure.

Probabilistic Analyses

The objective of the probabilistic analysis was to verify the results obtained from the deterministic slope stability analyses and to provide an assessment of overall slope stability within the entire section, rather than just specific profile sites. The probabilistic model used is based on the Monte Carlo method (*17–19*). As much as possible, the uncertainty and variability of the basic controlling geological, geotechnical, and environmental factors involved must be incorporated into the model. The significant variable parameters for this model included soil strength parameters, watertable elevation, and soil interface lines. Slope geometry for the slope profiles was measured in the field, representative of the general morphology of the slopes in the section; therefore, it was not considered to be a significant source of variability. The β-distribution was used to generate the variable parameter distributions. Mean values and standard deviations of the variable parameters and the limits of their variation were required to generate β-distributions of these parameters. The spread of these distributions was established on the basis of the measured or expected standard deviations of these randomly varying properties. By setting limits on the variation of the parameter, unreasonable possibilities such as negative cohesion are avoided.

The original STABL program was modified to permit the input of random variables (*19*). A random number generator randomly generates the values of the variables based on the given β-distribution of the variables. For each combination of these variables, a slope stability analysis is performed, based on the consideration of approximately 100 random failure surfaces. At least 20 such analyses are needed to provide an assessment of the risk of instability. Running more than 1,000 analyses does not seem to provide any additional information (*19*). The probabilistic stability analysis performed on the unfailed slope segment in the study area indicated that of the 200 analyses, 159, or 80 percent, gave minimum safety factors of less than 1.0. For the same slope profile, the deterministic safety factor was calculated to be 0.95, as indicated earlier.

Hazard Classification

A set of general guidelines was developed to classify the slope sections for rotational slides on the basis of their stability. The cumulative probability of safety factors being less than or equal to unity can be used as a way of assessing the overall

landslide hazard potential. Southeastern Wisconsin Regional Planning Commission (*13*) adopted a hazard classification system in which a probability of more than 75 percent (75 percent of the safety factors less than 1) indicated unstable or high-hazard condition and less than 25 percent stable or low-hazard condition. On the basis of this classification, this section of Whitefish Bay was classified as unstable.

Stabilization Effort

A structural solution was pursued because of the immediate threat presented to the homes and the urban highway directly behind these slopes. This solution involved construction of a terraced berm using concrete demolishing debris. Use of a waste material reduced the cost significantly. The berm was constructed from the beach level up. Dumping materials from the slope top was avoided to prevent further movements of existing slump blocks and an access road was cut to the beach. The configuration of the berm is shown on Figure 5. The toe of the berm was protected against wave action by limestone riprap. A 0.3m-thick soil cover was placed on the berm surface to provide vegetation. A deterministic slope stability analysis was also performed using the profile after restoration as shown in Figure 5. This analysis indicates a stable bluff slope with respect to rotational sliding. The lowest safety factor calculated was 1.75, with a corresponding failure circle beneath the top portion of the fill layer.

SUMMARY

The processes that operate on coastal slopes often lead to significant mass wasting, instability, and recession of the slopes. Transportation facilities existing on the upland are threatened by the slope failures and shoreline recession. Stabilization strategies for long stretches of coastal slopes are described in terms of management or stabilization approaches. Because of the length of the slopes and the variable nature of geology and soil properties, a probabilistic approach to stability analysis has been adopted for planning and managing the stabilization efforts. Two case histories from the Great Lakes region were presented to demonstrate the low-cost stabilization approach. Once a hazard classification is established, a variety of methods can be used to stabilize unsafe or marginally unsafe coastal slopes. Potential slope stabilization measures commonly used include regrading the slope to a stable angle, installing groundwater drainage systems to lower the elevation of the groundwater and prevent groundwater seepage from the face of the bluff, constructing surface water control measures, and revegetating the slope.

The stable long-term inclination used in the cutbacks of the oversteepened bluffs of the western Lake Michigan shoreline is 22 degrees (1V:2.5H). The typical material used in slope stabilization and restoration fills is concrete rubble. Depending on the type of material used for filling, a steeper angle than the usual stable angle of 22 degrees (often approximating 35 degrees) may be used for portions of the filled bluff slopes. The restored slopes are normally terraced or contain compound slopes. Filling should begin at the slope bottom, and some bluffs may need to be filled only along the lower portions of the slope. Soil cover a minimum of 0.3 m thick is placed over the rubble fill, and seeding and mulching is required to develop a vegetable cover. Adequate toe protection is required for long-term stability. Usually a riprap revetment of rock or quarry stones is used for this purpose. Before the placement of the fill materials, trench drains are usually required to intercept and divert the groundwater of the water-bearing lacustrine deposits usually found at the mid-height of the bluffs.

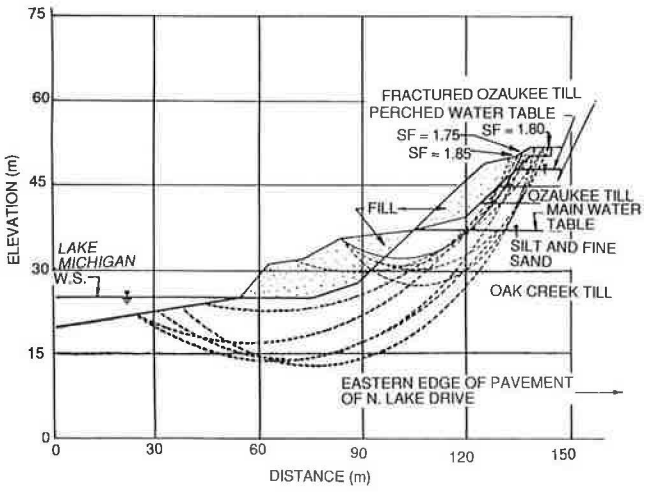

FIGURE 5 Bluff profile from Whitefish Bay (*13*).

ACKNOWLEDGMENTS

The author wishes to acknowledge the contributions of his colleagues, David M. Mickelson and Peter J. Bosscher, and many former students to his understanding of the coastal bluff slumping problem over the years. The financial support provided by the National Oceanic and Atmospheric Administration, U.S. Department of Commerce through the Wisconsin Sea Grant Program and the Wisconsin Coastal Management Program over the years supported the author's research. Southeastern Wisconsin Regional Planning Commission supported the latter developments in probabilistic method and provided the data base for the Whitefish Bay case. Financial support was received from the U.S. Environmental Protection Agency for the Madigan Beach bluff stabilization project.

REFERENCES

1. T. B. Edil and L. E. Vallejo. Shoreline Erosion and Landslides in the Great Lakes. *Proc., 9th International Conference on Soil Mechanics and Foundation Engineering*, Vol. 2, Tokyo, Japan, 1977, pp. 51–57.
2. R. M. Quigley and D. B. Tutt. Stability—Lake Erie North Shore Bluffs. *Proc., 11th Conference on Great Lakes* Res, 1968, pp. 230–238.
3. T. B. Edil and B. J. Haas. Proposed Criteria for Interpreting Stability of Lakeshore Bluffs. *Engineering Geology*, No. 16, 1980, pp. 97–110.
4. A. W. Bishop. The Use of the Slip Circle in the Stability Analysis of Slopes. *Geotechnique*, Vol. 5, No. 1, 1955, pp. 7–17.

5. L. E. Vallejo and T. B. Edil. Design Charts for Development and Stability of Evolving Slopes. *Journal of Civil Engineering Design*, Vol. 1, No. 3, 1979, pp. 231–252.
6. R. J. Sterrett and T. B. Edil. Ground-Water Flow Systems and Stability of a Slope. *Ground Water*, Vol. 20, No. 1, 1982, pp. 5–11.
7. R. J. Sterrett. *Factors and Mechanics of Bluff Erosion of Wisconsin's Great Lakes Shorelines*. Ph.D. thesis. Department of Geology and Geophysics, University of Wisconsin, Madison, 1980.
8. L. E. Vallejo. A New Approach to the Stability Analysis of Thawing Slopes. *Journal of Civil Engineering Design*, Vol. 1, No. 3, 1979, pp. 231–252.
9. L. E. Vallejo and T. B. Edil. Stability of Thawing Slopes: Field and Theoretical Investigations. *Proc., 10th International Conference Soil Mechanical and Foundation Engineering*, Vol. 3, Stockholm, Sweden, 1981, pp. 545–548.
10. G. R. Foster and W. H. Wischmeier. Evaluating Irregular Slopes for Soil Loss Prediction. *Transactions, American Society of Agricultural Engineers*, Vol. 17, 1974, pp. 305–309.
11. C. Peters. *Models of Short- and Long-Term Geomorphic Evolution of Bluffs in the Great Lakes*. M. S. thesis. Department of Geology and Geophysics, University of Wisconsin, Madison, 1982.
12. T. B. Edil. Causes and Mechanics of Coastal Bluff Recession. *Proc., Workshop on Bluff Slumping*, Ann Arbor, Mich., 1982, pp. 1–48.
13. *A Lake Michigan Shoreline Erosion Management Plan for Milwaukee County, Wisconsin*. Report 163. Southeastern Wisconsin Regional Planning Commission, Waukesha, 1989.
14. T. B. Edil and P. L. Monkmeyer. Demonstration of Shoreline Protection on Lake Superior. *Proc., Conference on Voluntary and Regulatory Approaches for Nonpoint Source Pollution Control*, Chicago, Ill., 1978, pp. 134–157.
15. R. A. Siegel. *STABL Users Manual*. Joint Highway Research Project C-36-36K. Purdue University, West Lafayette, Ind., 1975.
16. W. T. Painter. *Contract Report North Shore Drive Shoreline Landfill*, Phase I. Foundation Engineering, Inc., Milwaukee, Wis., 1983.
17. J. R. Benjamin and C. A. Cornell. *Probability, Statistics and Decision for Civil Engineers*. McGraw-Hill, New York, N.Y., 1970.
18. T. B. Edil and M. N. Schultz. Landslide Hazard Potential Determination Along a Shoreline Segment. *Engineering Geology*, No. 19, 1983, pp. 159–177.
19. P. J. Bosscher, T. B. Edil, and D. M. Michelson. Evaluation of Risks of Slope Instability Along a Coastal Reach. *Proc., 5th International Symposium on Landslides*, Vol. 2, 1988, Lausanne, Switzerland, pp. 1119–1125.

Publication of this paper sponsored by Committee on Soils and Rock Instrumentation.

Proposed Correction of Landslide for Relocation of Kentucky Highway 9 Using Deep Drainage Gallery

DARYL J. GREER AND HENRY A. MATHIS

The proposed relocation of Kentucky Highway 9 places the new alignment in a known landslide area. The geotechnical investigation for the proposed alignment required correction of the landslide problems. Deep drainage galleries were proposed to lower the groundwater tables in the landslide area. The deep drainage gallery consists of a series of interconnected vertical wells with intersecting horizontal drains. A 100-ft-long test section was built to confirm the practicability of constructing such a system, to test the effectiveness of the system in lowering groundwater levels, to see the effects of lowering groundwater on landslide movement, and to evaluate the costs of constructing such a system. Extensive monitoring of the test section was performed using observation wells and slope inclinometers. Groundwater tables were effectively lowered, and landslide movements were significantly reduced. The cost to construct the deep drainage gallery is expected to be 40 percent less than its alternative, a tied-back retaining wall. Results of the test section monitoring were implemented in the final roadway plans.

Recent industrial development in the Cincinnati area is prompting reconstruction of major and secondary roads in adjacent Northern Kentucky. The reason for relocating Kentucky Highway 9 (KY-9) in Campbell County, Kentucky, is to provide access to the Riverport Industrial Area. Existing KY-9 is a winding, two-lane road leading from Interstate 275 (I-275) north to Wilder, Kentucky, approximately 2.3 mi. Reconstruction of this section of highway will tie into the existing four-lane section of KY-9 north of Wilder and the new AA Highway (formerly KY-9), which is south of the I-275 interchange. Landslides along the existing alignment of KY-9 result in continual maintenance problems and expenses for the Kentucky Department of Highways (KYDOH). About 2,800 linear-ft of the new alignment will pass through a known landslide area.

Planning for this section of relocated KY-9 began in August 1984, and several alternative alignments were proposed. Factors considered in selecting the final alignment were (a) providing access to the Licking River, (b) resolving landslide problems that plague the area, and (c) avoiding relocating or disrupting facilities that currently exist in the area. The alternatives proposed were as follows:

- Place the alignment to the east of existing KY-9. The location would be on top of the hill in a more stable area and would not be in the influence of the Licking River.
- Follow existing KY-9 but lower the grade 9 to 10 ft.
- Place the alignment west of existing KY-9 closer to the Licking River. This alternative would provide the best access to the Riverport Industrial Area but place the roadway in known unstable areas.

Kentucky Transportation Cabinet, Division of Materials, Geotechnical Branch, Wilkerson Boulevard, Frankfort, Ky. 40622.

Because the expressed intention of the project was to serve the industrial base of the area, the chosen alignment was west of existing KY-9. Therefore, the geotechnical investigation for this project required developing a solution to the existing landslide problems that occurred along the proposed alignment. Figure 1 shows a site map of the area showing the proposed alignment.

This paper describes the correction method proposed to facilitate construction of the new alignment, the construction of a test section to study the proposed correction method, the results obtained from instrumentation for the test section, and the incorporation of the instrumentation results into the design of relocated KY-9. The scheduled contract date for this project was March 1992.

GEOLOGY AND TOPOGRAPHY

Subsurface investigation along the proposed alignment reveals alluvium, colluvium, and terrace deposits as well as bedrock from the Ordovician Age formations. The alluvium, colluvium, and terrace deposits consist of silty clays with minor sands and gravels. The Ordovician Age bedrock consists of the Kope formation with minor outcrops of the Point Pleasant formation. Figure 2 shows a cross section of a typical natural landslide on the Kope formation.

The Kope formation consists of shale (75 to 80 percent) and limestone. It ranges from medium gray to light bluish gray, and when weathered it becomes greenish gray to dark yellowish orange. The shale of this formation slumps readily when wet, and extreme care must be taken to provide adequate drainage for structures placed on the Kope formation (*1*). A weathered rock zone typically occurs between the shales of the Kope and the overburdened soils.

The shale of the Kope formation shows a very low permeability (*2*). Small fractures in the interbedded limestone can transmit additional water into the slopes in addition to the natural groundwater that is already seeping downhill in the weathered rock zone. The weathered rock zone is typically more permeable than either the underlying shale or the overlying soils, and landslides in the Kope typically occur in this zone.

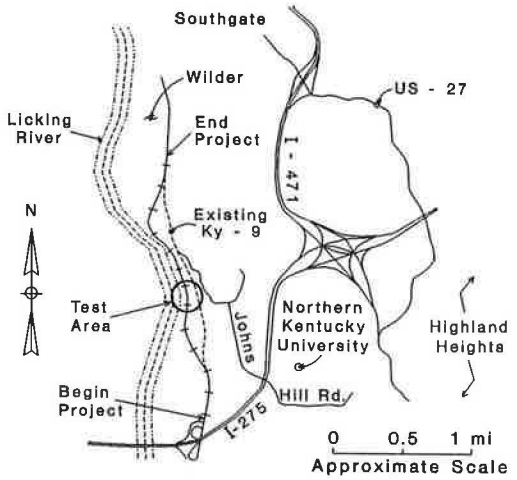

FIGURE 1 Project location map.

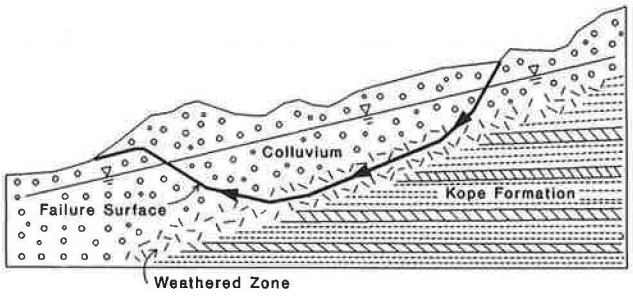

FIGURE 2 Sketch of typical landslide on Kope Formation—modified from Fleming (*2*).

Groundwater is usually not encountered in drilling until the weathered rock zone is reached. However, water levels measured by observation wells some time after drilling are typically much higher than those encountered during drilling. Therefore, a reasonable explanation for the slope failures is excess water pressures in the weathered rock zone. In addition, increased rainfall and its effect on the water table can drastically accelerate movement.

The Point Pleasant formation lies beneath the Kope and consists of limestone (45 to 65 percent) and shale. This unit is resistant but poorly exposed because of weathering and slumping of the upper-lying, shale-rich Kope formation (*1*).

Topography of the area is of a hilly nature. However, the existing ground surface in the test section area slopes downward to the west from the existing alignment of KY-9 on approximately a 1-vertical to 4- or 5-horizontal ratio (1V:4H or 1V:5H) toward the Licking River.

SITE HISTORY

Landslide deposits extend along existing KY-9 from I-275 north to the C&O railroad bridge in Newport, Kentucky. This is evident by the distress of the road and the many pavement overlays required to maintain traffic on existing KY-9. Some of the winding nature of existing KY-9 is due to landslide movement displacing the alignment of the highway.

Several homes and other structures in the area have been abandoned or condemned because of structural damage resulting from landslide movement. Typically, the slopes both above and below the existing alignment are unstable. Movement appears to be of a creep type; however, in some areas the movement is more rapid than in others.

Many landslide investigations have been conducted in this area. In general, the sliding planes of the landslides were located along the weathered shale interface. In addition, excess pore pressures were present in the weathered rock zone. Sliding planes were generally determined by slope inclinometers, whereas observation wells were used to determine water table levels and pore pressures. In many cases, the landslides were not repaired because they did not extensively affect the roadway or because the expense of repair outweighed the costs to maintain the road in its current state.

Correction of a slide on KY-9 immediately south of the I-275 interchange involved construction of a shear key (*3*). Instrumentation installed at this site indicated that the failure surface was located in the weathered rock zone. Although large movements occurred during excavation for the shear key, this correction method has performed well since its installation in 1974. A perforated pipe placed in the bottom of the shear key collects groundwater and maintains a steady flow even during the typically dry periods of the year.

Slope inclinometers were installed along existing KY-9 alignment in the fall of 1979. These inclinometers were installed as part of a cooperative agreement between KYDOH and the Northern Kentucky Port Authority to provide subsurface information concerning industrial development along the Licking River and for possible relocation of KY-9. Readings were obtained from eight inclinometers from November 1979 to June 1980. As with other slides in the area, excess pore pressures as measured by observation wells were present in the weathered rock zone and failure surfaces were at the weathered shale interface. The slope inclinometers indicated the average rate of movement of the landslide at about 4 to 15 in. of movement per year with a mean rate of 8 in./year. Four of the eight inclinometer casings closed off in 90 days or less; these casings closed off during winter when movement is typically slow.

At the time of this writing a slide in a cut section on the new AA Highway south of the I-275 interchange was being investigated. Observation wells installed in the slide area indicated that excess pore pressures were present in the weathered rock zone. The proposed method of correction for this slide was dewatering using horizontal drains.

PROPOSED STABILIZATION METHODS FOR NEW ALIGNMENT

The potential landslide-prone area affects about 2,800 linear-ft of the proposed alignment (stations 112+00 to 140+00). Construction in this area is further complicated by its proximity to the Licking River. Static water tables are high because of the proximity to the river, and excess pore pressures in the weathered rock zone are relatively large because of the large hillside recharge area above the area.

Consolidated-undrained triaxial tests were performed on the foundation soils to determine their peak shear strengths.

These tests indicated that the mean cohesion and friction angle were about 450 psf and 27 degrees, respectively. If the foundation soils were to actually exhibit these strengths, the proposed embankments would be stable even with the high pore pressures. However, KYDOH's experience indicates that the residual shear strengths of the foundation soils in this area are much less than the strengths obtained from triaxial tests. Using the slope inclinometer movement data, a failure plane for the test area was determined and backed-in soil parameters were calculated for a factor of safety of 1.0. The backed-in friction angle was calculated to be about 16 degrees (cohesion was arbitrarily set to zero). This value was consistent with the backed-in parameters for other landslide corrections in this area and in the Kope formation in general.

Excavation and replacement of the foundation soils (shear key) is not feasible. The depth of the foundation soils in this area is about 40 ft, and excavation of this material could create further landslides. These landslides would most likely close existing KY-9, which must remain open during construction. In addition, the proximity to the Licking River would make it difficult to keep the excavation dewatered during construction. Stone columns are an effective method of foundation soil replacement, but it would be difficult at this location to penetrate the failure surface (weathered rock zone) adequately in order to prevent sliding. In addition, some method of dewatering would be required for the stone columns to be reasonably effective.

KYDOH narrowed the alternatives to two methods: a tied-back retaining wall and a deep drainage gallery consisting of interconnected vertical and horizontal drains. A tied-back wall at this area would consist of either a soldier pile and lagging wall or a drilled caisson wall. Either type of wall would have been an effective method of correcting the landslide problems, but the cost of constructing such a wall was prohibitive. Some provision for lowering the groundwater table would still have been necessary to provide an adequate factor of safety. The estimated cost in 1989 for a tied-back wall with some provisions for subsurface drainage at this location was $5,900,000.

The deep drainage gallery system is similar to that used by the California Division of Transportation on a landslide on I-80 near Pinhole, California (*4*). The proposed deep drainage gallery system is shown in Figure 3. The system proposed for this project consists of a line of drilled vertical wells placed on the uphill side of the new embankment. Each vertical well would have a diameter of 3 ft, be placed on 6-ft centers, and be drilled at least 10 ft into the formation. The vertical wells would be interconnected either by overlapping belled bases or by interconnecting tunnels. Every third vertical well would then be fitted with horizontal drains that would intersect near the base of the vertical well. The wells would then be filled with free-draining material and capped. This interconnected system would serve as a net to catch and drain groundwater that is seeping downhill.

Because this method of correction had never been used in Kentucky, the KYDOH Division of Materials was reluctant to recommend its use without knowledge of its operations and effects. Without the benefit of this information, the Division of Materials would recommend retaining walls. As a result, approval was granted to construct a 100-ft-long test section, which was to provide the following information:

- The ability to construct the proposed deep drainage gallery system.
- The effectiveness of the deep drainage gallery in lowering the groundwater table.
- The effects of groundwater lowering in the area on landslide movement, and
- The costs of constructing a deep drainage gallery system.

TEST SECTION INSTRUMENTATION AND CONSTRUCTION

The area chosen for the test section construction was located near the center of the landslide area between Stations 124 + 50 and 125 + 50. Before construction, extensive drilling was performed in the test section area between Stations 124 + 00 and 126 + 00. A total of 30 borings were performed in this area, and either observation wells or slope inclinometers were installed in all but three of the boreholes. Monitoring of the instrumentation at the site began in October 1985. Figure 4 shows a plan view of the instrumentation locations.

Construction of the test section drainage gallery began April 1, 1986, and was completed April 30, 1986. Additional observation wells and slope inclinometers were placed in selected vertical wells. Construction of the embankment was delayed until May 29, 1986, because of utility relocation. The embankment was completed on June 28, 1986, with an additional 1 ft of fill being added on July 18, 1986.

Sixteen of the 38 observation wells installed either closed off or were destroyed during construction. However, the obser-

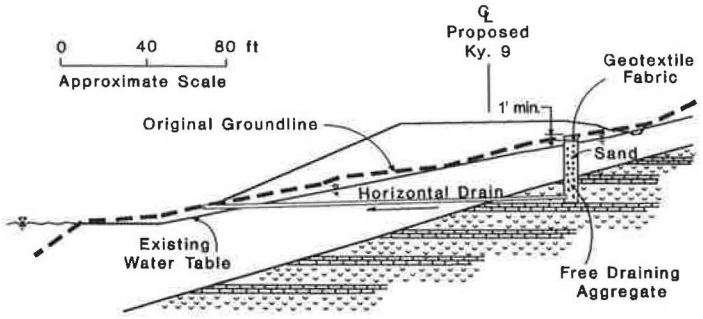

FIGURE 3 Deep drainage gallery system—Cross-section view.

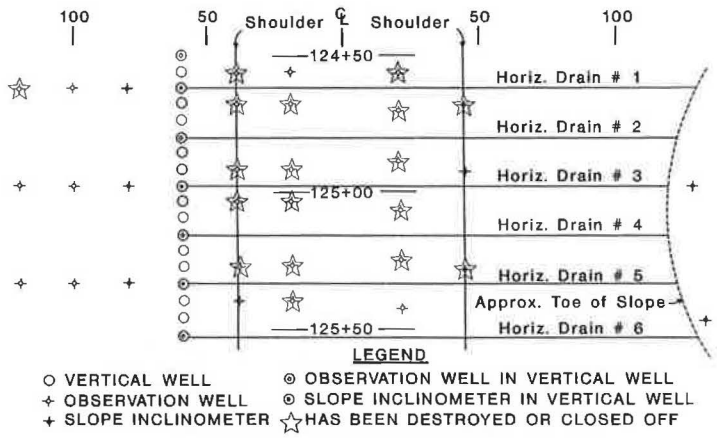

FIGURE 4 Instrumentation plan view.

vation wells that remained open showed an approximate drop in the water table in the drainage gallery area of 10 to 20 ft after construction. This drop corresponded with the water table being at or near the elevation of the horizontal drains. Figure 5 shows a typical cross section of the drainage gallery with anticipated water tables both before and after construction.

Drought conditions were common from the end of construction of the test section until spring 1989. From spring 1989 to present, rainfall amounts have been at or above normal levels. However, only minor fluctuations in the water table have been observed since the test section was completed. A typical plot showing the water table elevation versus days is shown in Figure 6; this plot shows Observation Well 24, Station 125+40 at ground surface elevation of 532.0 ft mean sea level (MSL). The initial reading was taken November 15, 1985.

Monitoring of the slope inclinometers in the test section area indicated a rate of movement of about 1 in./year before construction. Movement during construction was relatively large and was mainly due to dewatering, lateral squeeze from embankment construction, and consolidation of the foundation soils. From the end of construction to April 1991, the average rate of movement was about 0.35 in./year. No significant fluctuations in the rate of movement were noted as a result of precipitation amounts or pool elevations of the Licking River. Figure 7 shows a typical movement versus days plot for the test section area; it shows Inclinometer 4 in Campbell County. Depth was 6 ft, and initial reading date was December 3, 1985.

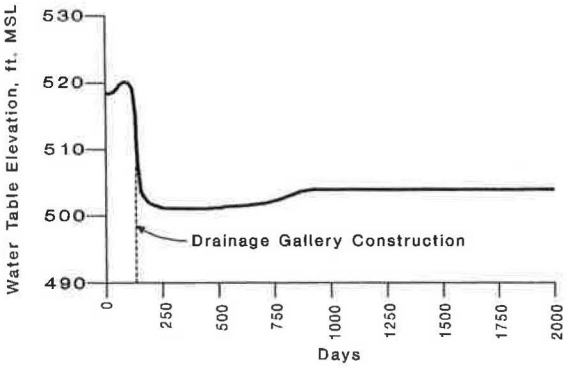

FIGURE 6 Typical water table elevation-versus-days plot.

IMPLEMENTATION OF TEST SECTION DATA INTO FINAL ROADWAY DESIGN

Monitoring of the test section indicated that the deep drainage gallery was effective in lowering the groundwater level under

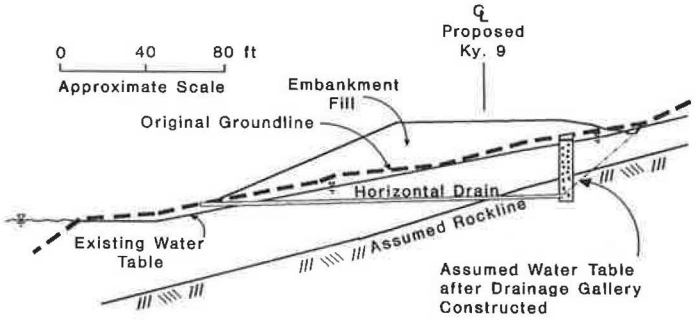

FIGURE 5 Anticipated water tables before and after drainage gallery construction.

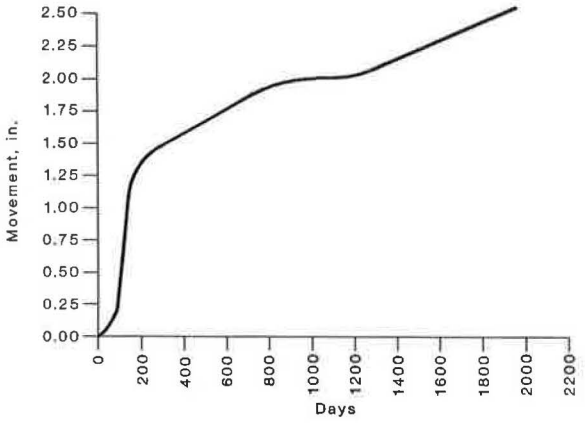

FIGURE 7 Typical movement-versus-days plot for drainage gallery test section.

the test embankment by 10 to 20 ft. The lowering of the groundwater table did not completely stop the deep creep movement of the hillside, but it apparently slowed the rate of movement and prevented some of the large rates of movement from occurring.

Additional drilling was performed along the proposed alignment of the vertical wells to define the depth of rock. Drilling was also performed at selected critical stations for the purpose of performing slope stability analyses. Embankment heights through the deep drainage gallery area averaged about 45 ft.

Stability analyses were performed on the assumption that the groundwater table would drop to the elevation of the horizontal drains. These analyses were conducted using the backed-in parameters and the failure planes determined from slope inclinometer movements (wedge analysis). These analyses indicated that marginal factors of safety (FS = 1.2 to 1.3) exist for constructed embankments in the drainage gallery area. KYDOH's typical target factors of safety for roadway embankments are 1.4 to 1.8. Figure 8 shows a typical embankment stability analysis for the test section area. Stability analyses (rotational) using the strength data obtained from triaxial tests were also run to further check the stability of the embankments.

Some minor landslide and embankment stability problems are expected to occur during and after construction even though the analyses indicate factors of safety greater than 1.0. These problems are expected because of variations in construction practices, spatial variation in subsurface conditions, and so on. In addition, KYDOH's experience with embankments on the Kope formation with factors of safety less than 1.5 is that settlement, embankment squatting, and creep movements occur.

On the basis of the unit bid items from construction of the test area, the estimated cost for the drainage gallery is about $2,250,000. Therefore, the expense of constructing a deep drainage gallery was estimated to be 40 percent of that of constructing a tied-back retaining wall. After considering the engineering and economic data, KYDOH decided to proceed with the deep drainage gallery.

Project specifications call for the installation of 441 vertical wells and 147 horizontal drains in addition to those already installed for the test section. Other embankments, cuts, and a reinforced concrete box culvert outside the landslide area were also a part of the scope of the project. Dewatering of selected cut sections will be performed by using horizontal drains. Provisions were included in the specifications for the department to install additional slope inclinometers throughout the proposed deep drainage gallery area so that long-term monitoring can be performed.

CONCLUSION

KYDOH found that the deep drainage gallery system was effective in lowering the groundwater table at this location. Even with the lowering of the groundwater table, it is expected that long-term creep of the landslide will continue, and it is believed that the rate of movement will be such that typical maintenance practices can maintain the roadway. The average rate of movement for the test section area was 0.35 in./year compared with the average rate of 8 in./year as measured in 1979. Construction of the deep drainage gallery will be cost-effective compared with tied-back retaining walls.

Several questions remain unanswered. Most important is the effect that long-term creep movements will have on the deep drainage gallery. Damage to the drainage gallery could

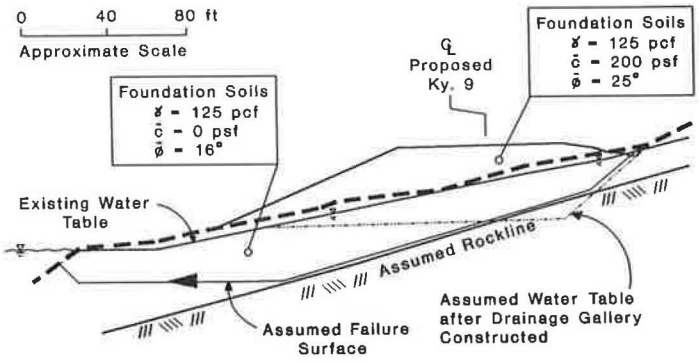

FIGURE 8 Typical embankment stability section (effective stress analysis: using existing water table, FS = 1.0; using lowered water table, FS = 1.2).

render it useless and result in massive movements. In addition, the test section is relatively short in comparison with the proposed area that is to be treated. It is expected that the edge effects of groundwater flowing around the drainage gallery will be less critical with a longer drainage gallery, and movements are expected to be less with a longer drainage gallery. Instrumentation will be installed to monitor construction of the drainage gallery and to observe its long-term effects.

REFERENCES

1. A. B. Gibbons. *Geologic Map of Parts of Newport and Withamsville Quadrangles, Campbell and Kenton Counties, Kentucky*. Geologic Quadrangle Map GQ-1072. U.S. Geological Survey, 1973.
2. R. W. Fleming. Geologic Perspectives—The Cincinnati Example. *Proc., 6th Ohio Valley Soils Seminar*, Ft. Mitchell, Ky., Oct. 17, 1975.
3. H. A. Mathis. Regrading Failed Slopes. *Proc., 6th Ohio Valley Soils Seminar*, Ft. Mitchell, Ky., Oct. 17, 1975.
4. T. W. Smith, R. H. Prysock, and J. Campbell. Pinhole Slide, I-80, California. *Highway Focus*, Vol. 2, No. 5, Dec. 1970, pp. 51–61.

Publication of this paper sponsored by Committee on Soils and Rock Instrumentation.

Stabilization of Debris Flow Scar Using Soil Bioengineering

MICHAEL R. THOMAS AND ALAN L. KROPP

On January 4, 1982, a large debris flow occurred in an undeveloped hillside and flowed into an area of residential housing in Pacifica, California. This debris flow (which originated in a previously unrecognized colluvium-filled swale) destroyed two houses approximately 300 vertical-ft below the source area and killed three children. Emergency grading and erosion control measures were soon implemented but these measures did not stop the continuing erosion. Deterioration of the temporary erosion control facilities was rapid. The magnitude of erosion from the slope also prevented vegetation from being reestablished in the scar area. In March 1988, plans were developed to regrade the source area of the debris flow (to remove additional colluvium) and install long-term soil bioengineering erosion control measures. These measures were designed to immediately reduce surficial erosion. A reduction in the surface water flow rate would allow increased infiltration into the ground and help rapid root growth of the bioengineering materials to allow root reinforcement of the upper soils. Over several years, this system would reduce the surficial erosion and allow indigenous plants in the area to become reestablished in the debris flow track. Design concepts and methods of construction are related. A long-term monitoring program is being performed by the consultants originally involved in the project to determine the success of the stabilization effort. This program consists of periodic visits to the site to walk the slopes and develop a photographic log of the vegetation development.

During an intense rainstorm on the evening of January 4, 1982, a large debris flow occurred in an undeveloped hillside and flowed into an area of residential housing in Pacifica, California (Figure 1). The debris flow happened with little or no warning to the residents some 300 vertical-ft below the source area. Approximately 3000 yd^3 of colluvium were mobilized in the flow. The colluvium mobilized by the failure moved rapidly down the slope at an estimated speed in excess of 20 mph. Three children were killed, two homes completely destroyed, and two other homes severely damaged when the mobilized soils hit them. The source area was approximately 150 ft long and 80 ft wide, and the track was about 460 ft long and 40 ft wide.

Immediately after the debris flow event, emergency remedial measures were taken to minimize the potential (in the short term) of another debris flow in the same area. After temporary emergency remedial measures were taken, numerous investigations were carried out. These investigations generally concluded that the debris flow occurred along the centerline of a colluvium-filled bedrock hollow. Depth-to-bedrock contours within the flow developed by Shlemon (*1*) indicated the presence of two deep depressions in the bedrock aligned in the downslope direction (see Figure 2). Theories stated that these depressions were caused by past episodes of fluvial downcutting, the high point between the two depressions being a more resistant bedrock material.

Generally, it was concluded that the upper depression in the bedrock was the source area for the flow. The high bedrock ridge that separated the two bedrock depressions acted to concentrate groundwater in the upper basin until the overlying colluvium became saturated and mobilized in the form of a debris flow. The flow material crossed the lower depression en route to the level, developed areas at the base of the slope.

The land where the debris flow originated was open space owned by an adjacent condominium homeowners' association. This group wanted to institute remedial work of the flow area, but its budget was limited. Engineering analyses of the slope led to the development of two alternative remedial plans. One plan involved the complete reconstruction of the slope to the pre–debris flow configuration. To achieve this, up to 5000 yd^3 of fill would have to be brought in and placed in the source area. In addition, to reestablish the original inclination of the slope, geogrid reinforcement of the soil would have to be added as the fill was placed. The alternative plan was to accept the existing conditions and install protective measures to minimize the likelihood of future debris flows and surficial erosion. To minimize the risk of future debris flows emanating from the existing source area, it would be necessary to remove most of the colluvial soil from both the center and the denuded flanks. Once this removal had taken place, stabilization measures could be installed to minimize future erosion, shallow sloughing, or small debris flow initiation. It was decided that an appropriate form of stabilization would involve the installation of soil bioengineering measures. Soil bioengineering slope stabilization involves the use of both quasivegetative and vegetative elements to arrest and protect against shallow slope failures and erosion.

Ultimately, the second alternative was selected and detailed plans were developed. The selection was based on both the cost of design and the feasibility of construction. A situation in which soil bioengineering slope stabilization was used to minimize soil loss from a large debris flow scar and a report on the performance of soil bioengineering to date are presented.

PREVIOUS TEMPORARY REMEDIAL OPERATIONS

After the debris flow occurred, emergency grading operations started to remove a portion of the remaining colluvium around

M. R. Thomas, SEC Donohue, Inc., 2800 East Parham Road, Richmond, Va. 23228. A. L. Kropp, Alan Kropp and Associates, Inc., 2140 Shattuk Avenue, Berkeley, Calif. 94704.

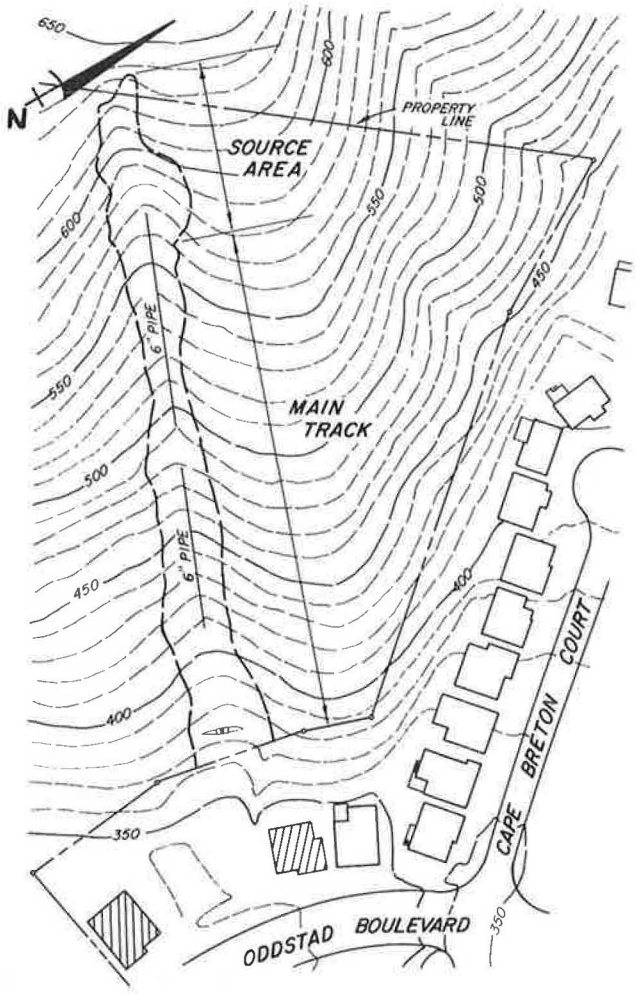

FIGURE 1 Oddstad Boulevard debris flow; two destroyed homes have been removed, and shading indicates severely damaged homes.

the perimeter of the source area. The limits of the grading extended beyond the limits of the source area to help reduce the inclination of the flanks of the slide while minimum earth movement was being done in the track area where the disturbance was small during the debris flow event. During these grading operations several thousand cubic yards of colluvium were removed from the source area. On completion of the grading, the source area had the configuration of a broad bowl, and the track area was essentially unchanged. V-ditches, debris baffles, and silt fences were constructed in the flowtrack. A siltation basin designed to contain erosion and small debris flows was also constructed at the bottom of the hill where the two residences had once stood.

By the fall of 1983 the temporary remedial operations had been completed, and the slope was seeded and left alone in hopes that vegetation would become reestablished in the giant scar that was left behind by the debris flow and the earthmoving operations. However, little vegetation was established on the slope that year because the inorganic soils that had been left behind did not promote plant growth and the steep inclination of the slope encouraged erosion of the surficial soils. The homeowners' association made many attempts to minimize erosion of the surficial soils exposed on the slope and increase the plant population by planting various types of grass seed. These additional plantings did not do much to increase the number of plants on the slope and reduce erosion.

By late 1985 erosion in the debris flow scar had become severe. A gully approximately 5 ft deep had been incised into the centerline of the flowtrack and more uniform, shallow, surface erosion over the remainder of the graded area led to large quantities of soil being deposited in the v-ditches and behind the silt fences. This accumulation of eroding soils required constant maintenance by the homeowners' association in order to keep the features operating. However, even with constant maintenance, deterioration of the temporary erosion control facilities was rapid. The silt fences had almost completely overloaded and broken down, and the siltation basin at the base of the slope had been substantially filled.

LONG-TERM REMEDIAL PLAN DEVELOPMENT

In 1986 a long-term solution to the slope stability and erosion problems was being sought. Investigations of the initial debris flow event led to the belief that accumulation of groundwater in a bedrock hollow near the top of the hillside during prolonged or intense rainstorms would saturate the colluvial soils in the hollow. During an intense rainstorm on January 4, 1982, the colluvium became saturated and ultimately liquefied and flowed down the slope in the form of a debris flow. An investigation by Shlemon (*1*) established depth-to-bedrock contours in the debris flow area. These contours outlined two bedrock hollows on the hillside that were aligned in the downslope direction. Consultants spot-checked these estimated depths to bedrock by drilling exploratory test borings. Many of the borings were extended to the bedrock surface and terminated, several others were advanced into the bedrock by coring. The deeper borings were drilled in an effort to examined the type and quality of the underlying materials. The borings generally confirmed the depth-to-bedrock contours developed by Shlemon (*1*).

Once the contours were verified, it became apparent that the emergency grading measures had not removed the entire build-up of colluvial soils from the upper bedrock hollow. This kindled fears that additional debris flow activity might occur during similar rainstorm events. A decision was made to remove the colluvium in the central portion of the bedrock hollow to within 3 to 5 ft of the bedrock surface. The remaining thickness of colluvium could then be adequately stabilized in-place through the use of soil bioengineering methods. Draining of groundwater from the source area was also considered a prime objective of the remedial measures. Ultimately, it was demonstrated that the removal of colluvium from the central portion of the bedrock hollow in combination with the installation of subsurface drainage and construction of soil bioengineering stabilization measures would provide adequate protection against future flow events.

The depth-to-bedrock contours developed by Shlemon indicated that the horizontal extent of the bedrock hollow was significantly larger than that of the debris flow source area. Therefore, the extent of additional colluvium removal had to

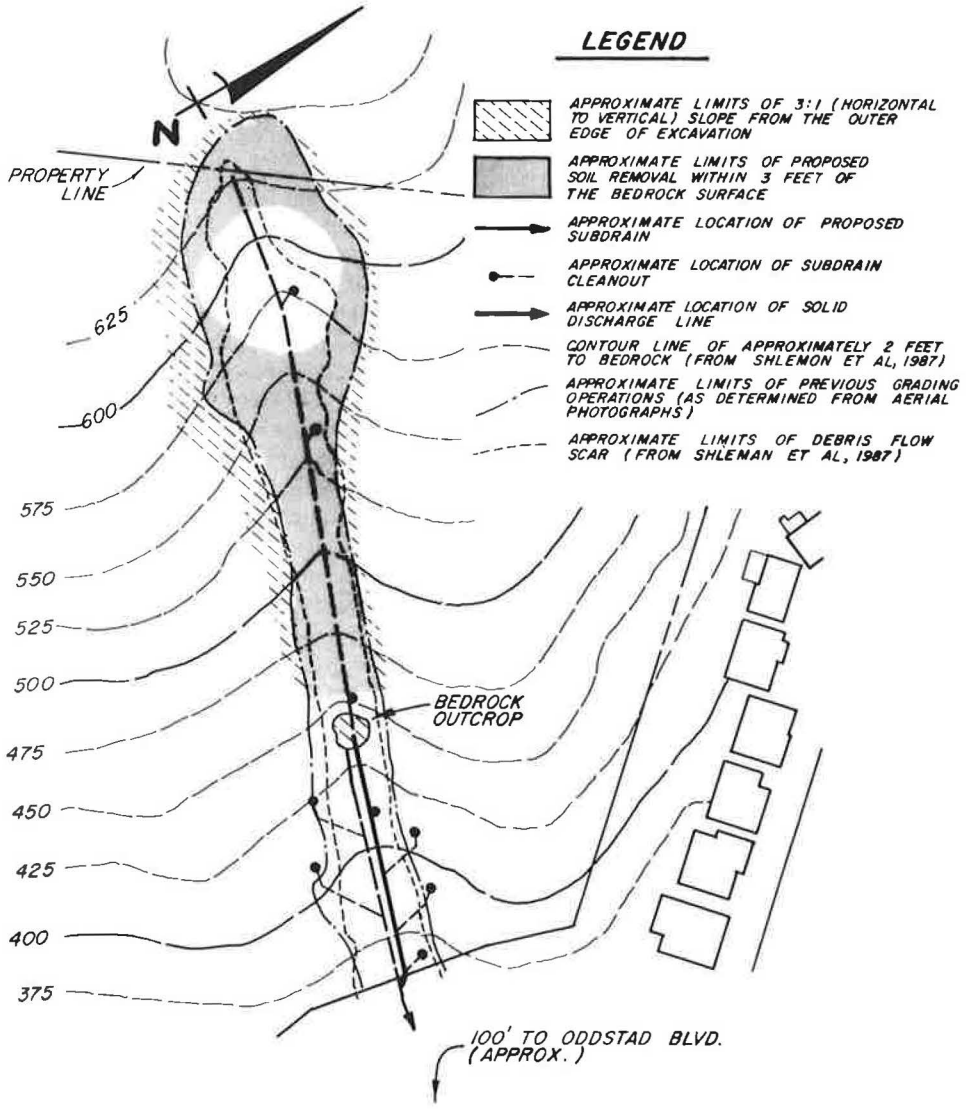

FIGURE 2 Depth-to-bedrock contours in relation to debris flow.

be determined. The central portion of the source area appeared to be immediately above the deepest portion of the bedrock hollow and a substantial thickness of colluvium still appeared to be present under the flanks of the debris flow. It was decided colluvium would be removed within the central portion of the bedrock hollow down to within 3 to 5 ft of the bedrock surface. This removal would generate approximately 5000 yd^3 of colluvium to be removed during the grading operations in the source area.

A subdrain, designed to relieve build-up of hydrostatic pressures, was to be constructed down the centerline of the source area (Figure 3). Because previous investigators had theorized that a perched groundwater table may exist during heavy or extended periods of rain on the bedrock surface, the subdrain was to be excavated through the remaining colluvium and approximately 1 ft into the underlying bedrock. The subdrain was to consist of a 6-in. rigid, perforated, plastic pipe embedded in washed gravel. The gravel was to be extended to within 1 ft of the ground surface and the entire gravel-pipe unit was to be wrapped in a nonwoven geotextile. Natural soils were to be placed above the gravel and geotextile.

In order to excavate down to within 3 to 5 ft of the bedrock surface along the flanks of the source area, it would be necessary to remove a significant amount of existing, well-established vegetation and to disturb vast areas of previously undisturbed ground. Because a subdrain was to be constructed through the central portion of the bedrock hollow, it would be unlikely that the colluvium in the flanks could become saturated and mobilize into a debris flow. Therefore, the two primary concerns for the flanks of the graded area were local slope stability and surficial erosion. The grading operations proposed for the central portion of the source area would oversteepen the flanks and make them susceptible to localized sloughing and slope failures.

To minimize the likelihood of such failures, it was recommended that the flanks of the source area be cut back to a maximum inclination of 3:1 (horizontal to vertical). This cutting-back operation would minimally affect the existing

dense vegetative cover outside the source area (see Figure 3). Therefore, the area susceptible to surficial erosion would only be slightly increased by the recommendations for the grading scheme. Once the flanks were cut back, soil bioengineering slope stabilization measures would be installed to minimize erosion from the slopes and provide root reinforcement of the surficial soils.

SOIL BIOENGINEERING SLOPE STABILIZATION

Soil bioengineering slope stabilization entails the use of vegetative elements to arrest and minimize the potential for slope failures and erosion (*2*). These vegetative elements include seeding, live transplants, and quasivegetative methods such as brush layers and contour facines (wattling).

Bioengineering is different from biotechnical engineering in that biotechnical engineering includes the use of mechanical elements such as small walls and earth reinforcing. The mechanical elements of biotechnical engineering provide relatively deep soil stabilization; bioengineering measures provide stabilization of surficial soils. Soil bioengineering also acts to reduce the erosive power of surface water by directly intercepting rainfall, binding soil particles, filtering soil from runoff, dissipating the energy of runoff, and maintaining good infiltration. In addition, woody plants, trees and shrubs provide root reinforcement to depths of 3 to 5 ft, which adds to the general stability against sliding and mass movement. Once stabilization and erosion control are achieved, indigenous vegetation may then reestablish itself. The ultimate goals of soil bioengineering stabilization are to provide relatively shallow slope stabilization and to inhibit the erosive action of surficial water long enough to allow the imported and indigenous plant materials to establish a vegetated mat over the ground surface.

It should be noted that soil bioengineering methods of slope stabilization are only slowly gaining popularity in North America. Generally, these methods are used in areas of relatively constant soil moisture such as along stream banks or where groundwater is at a constant, shallow depth. The subject debris flow is located along the flank of a small mountain in the California coast range in an area where the depth to groundwater is typically greater than 20 ft. In addition, even though the area typically receives more than 22 in. of rainfall each year, it is seasonal in nature. The rainy season usually lasts from mid-October to April, and rainfall during the remainder of the year is rare. Nevertheless, it was concluded that with proper timing and plant selection, soil bioengineering methods would be effective in terms of both cost and results in controlling erosion from the debris flow scar.

To minimize the likelihood of future mass failures in the debris flow source area, it was decided that additional grading that involved the removal of existing colluvial soils from both the flanks and bottom of the basin would be performed. The proposed grading operations would remove all but 3 to 5 ft of soil from the debris flow scar, so the engineering consultants, in conjunction with the landscape architect, decided that the primary function of the soil bioengineering stabilization effort were to minimize erosion of the surficial soils so that plant life could become reestablished on the slope and to provide mechanical stabilization of the surficial soils during the interim when vegetation was becoming established. The three soil bioengineering stabilization processes chosen to

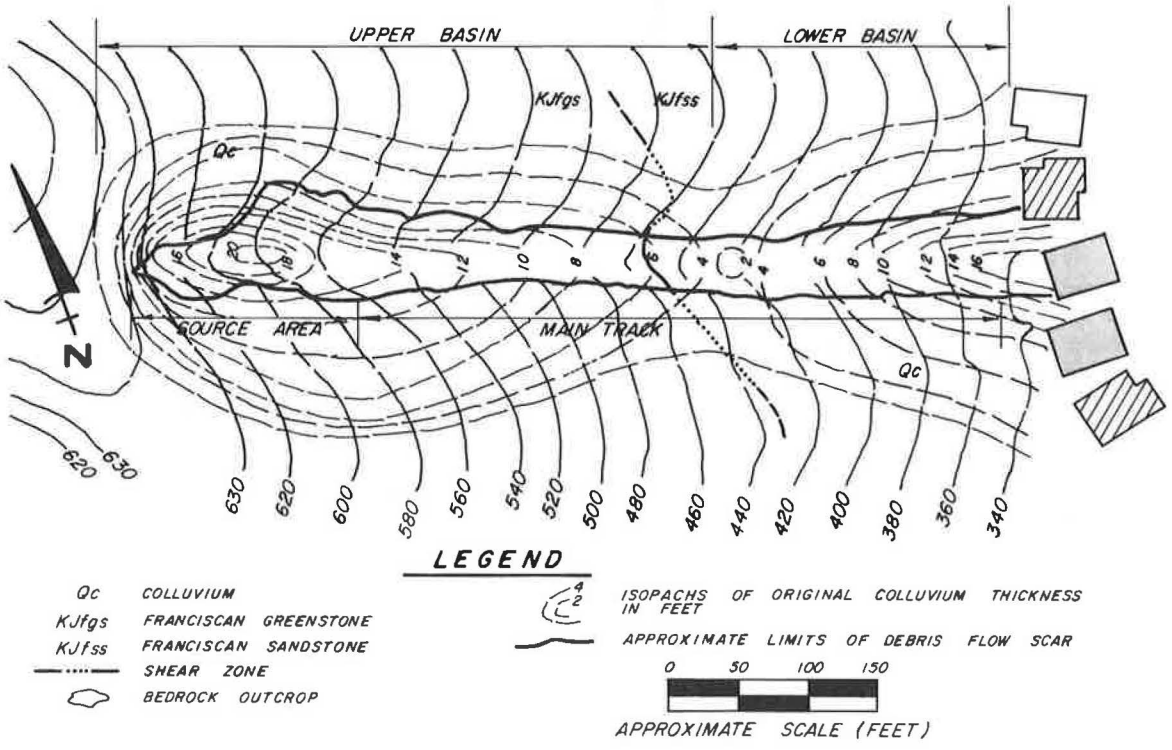

FIGURE 3 Remedial work area.

accomplish this goal were contour facines, live transplants, and seeding. The contour facines were to provide mechanical stabilization that would allow the transplants and seeds to become established on the slope.

Because soil bioengineering slope stabilization is not commonly used throughout North America, brief descriptions of the methods used for the subject stabilization are presented. For additional information about these and other soil bioengineering stabilization methods, refer to the text by Gray and Leiser (*2*).

Facines (Contour Wattling)

Facine construction consists of placing bundles, approximately 12 in. in diameter, of suitable plant materials (generally quick rooting woody vegetation that is in abundant supply) in shallow trenches, on contour, and on either cut or fill slopes (*2*). The function of the facine is to stabilize the surficial soil layers, dissipate the erosive power of surficial water, entrap sediments, and increase infiltration of surficial water. The proper construction and installation of facines is critical. Freshly cut stems should not be allowed to dry out or they will die and no rooting will occur. Death of the vegetation will not destroy the mechanical properties of the facine, but no new growth of vegetation will be supplied by the facine. Improper installation of the facine may also lead to unacceptable results. Failure to adequately cover the facine with soil may prevent the fresh stems from sprouting. In addition, failure to tightly pack soil around the facine may lead to ponding of surficial water in the trench around the facine, which often leads to shallow sloughing failures that extend beneath the facine.

In general, it was considered that within the debris flow scar, contour facines would provide immediate stabilization of the surficial soils so that additional vegetation could become established in the area. The ability of the facine to act as a check dam would increase infiltration of surface water while reducing erosion. It was considered that the facines would provide this type of protection for up to 3 years, and this would allow both imported and indigenous vegetation to become established in the scar and take over those functions.

Live Transplants

Use of transplants is one of the best methods of establishing woody vegetation on difficult sites. The advantage of transplants is that the plants do not have to undergo germination in the typically harse site conditions, therefore giving them a distinct advantage over seeding of woody vegetation. In addition, the survival rate of transplanted woody vegetation is significantly higher than that of seeded woody vegetation. However, the cost of transplants is greater than seed because they have to be grown and then planted at the site by hand. Transplanting should be restricted to seasons in which adequate moisture is available in the soil; otherwise, irrigation may be necessary. As live transplants become established, they reduce erosion of surficial soils by intercepting rainfall in their vegetative canopy, increasing infiltration of surficial water into the soil, and increasing the quantity of organic debris on the ground surface, which retains moisture. In addition, the roots of woody plants reinforce the surficial soils, which increases slope stability.

Of the three types of soil bioengineering stabilization selected for this site, live transplants have the longest potential life span. The woody vegetation that makes up the majority of live transplants has the potential to survive on the slope anywhere between 10 and 80 years or more, at which time natural succession would take over.

Seeding

Seeding for herbaceous plants provides the most immediate form of ground cover. Once the seeds have germinated, plants rapidly develop and act to minimize surficial erosion, provided that rill and gully erosion is minimized during this time through other methods such as contour facining. The ideal species should have strong root development and minimal green growth (*2*). The green growth that does occur will help minimize the impact of raindrops on the slope, and the root development will reinforce the surficial soils. Ground cover established through seeding minimizes surficial erosion while the live transplants become established. Once transplants have become established on a slope, their roots provide deeper soil reinforcement. Providing an adequate mix of grass and herbaceous plant types is of particular concern when specifying seeding. Some grasses are quick to develop but are only short-lived, and therefore only provide immediate protection; other grasses take much longer to develop and spread but provide more long-term erosion protection. Another concern is selecting a mix of both annual and perennial vegetation so that more than one season of protection may be obtained. However, even with a good selection of species, seeded plants generally provide 2 to 5 years of slope protection.

SOIL BIOENGINEERING PLAN DEVELOPMENT

Factors Affecting Plant Selection

Exploratory borings that were drilled as part of the geotechnical engineering investigation generally encountered stiff, inorganic, sandy, and gravelly clays immediately above the bedrock surface. This soil was expected to support and sustain the plant materials used in the soil bioengineering stabilization program. In general, stiff clayey soils that are exposed at the surface retain moisture and nutrients well. However, these soils had been buried for an extended period of time, so it was unlikely that they contained many nutrients. In addition, it was likely that the denseness of these soils would cause them to lack oxygen, which is vital to plant development. During initial site inspections, sparse vegetation, apparently introduced to the area during the temporary remedial measures, was noted within the debris flow source and track areas. This vegetation consisted of the hardy *Rhamnus* and *Baccharis* species. Growth was observed to be nonuniform and the plants appeared to be small for their age. This was reflective of the severe environmental conditions and the nutrient deficient soils.

Climatic conditions at the site also played a major role in the development of the soil bioengineering stabilization plan.

These conditions presented both positive and negative factors that could affect plant selections and expected growth rates. In relation to the rest of the San Francisco Bay Area, the site is located in an area that receives relatively generous rainfall. On the average, the Pacifica area receives about 22 in. of rainfall per year. However, most of it occurs between mid–October and mid–April. The rest of the year is dry except for an occasional rainshower in May or September. Because the site is located within 2.5 mi of the Pacific Ocean, seasonal temperature variations are not extreme. Typically, during the winter months, temperatures at night drop as low as 40 degrees; summer daytime temperatures rarely exceed 75 degrees. Often during the summer, coastal fog blankets the hillsides, which creates a cool, humid environment for plants but does little to replenish soil moisture.

The lack of summer moisture in this area dictates that the plants growing here be tolerant of drought conditions. Typically, such plants do not grow throughout the season. The rainfall and temperature characteristics also dictate that in nonirrigated areas, plantings be scheduled during the wet winter months and not in the dry spring or summer months.

Plant Selection

Budgetary constraints imposed by the homeowners' association did not allow extensive testing of the soils in the debris flow track. Such testing would have aided in plant selection by determining nutrient levels, soil pH, salinity, and the presence of potentially toxic ions such as those produced by serpentine bedrock. To compensate for this lack of laboratory data, an extensive plant survey was conducted on the adjacent slopes. The purpose of this was to determine the plant types and populations on the adjacent slopes in order that similar species could be selected for the soil bioengineering stabilization plan. A list of the plant types noted during this survey is presented in Table 1.

TABLE 1 SURVEY OF EXISTING PLANT MATERIALS

Debris Flow Source and Track Areas*	Undisturbed Adjacent Slopes***
**Baccharis species (Coyote Brush)	Salvia species (Sage)
**Rhamnus californica (Coffeeberry)	Mentha species (Mint)
	Ceanothus species (Wild Lilac)
	Ribes species (Gooseberry)
	Sambucus (Elderberry)
	Rhamnus species (Coffeeberry)
	Baccharis species (Coyote Brush)
	Rhus diversiloba (Poison Oak)
	Heteromeles arbutifolia (Toyon)
	Pinus radiata (Monterey Pine)
	Cornus species (Dogwood)
	Salix species (Willow)

* The slide path contained a scant mixture of grasses

** These plants were sparse and small for their age

*** Undisturbed areas contained dense growth of grasses as well as the indicated plants

Often, texts describing soil bioengineering stabilization strongly recommend that only indigenous plants be used for stabilization efforts. They suggest that local seed be collected and used in reestablishing vegetation to ensure compatibility of the remedial work area with the surrounding areas. It is also thought that, in general, species that thrive in an area do so because they are best suited for the soil and climatic conditions. However, it was decided that additional plant types may also thrive on the slope. The genera of the plants noted during the plant survey were used as to indicate the types of plant materials that would thrive in this type of environment. The criteria used in selection of the plant materials for transplants and seeding of the debris flow area were that the plants be well adapted for the expected soils and moisture conditions, deep rooting, tenacious and hardy, commercially available, and highly adaptable to varying climatic conditions. On the basis of these criteria, a list of acceptable plants from which contractors could select was prepared (Figure 4).

Contour facines were selected to provide immediate vegetative and mechanical stabilization of the surficial soils. The plant material selected to create the facine would have to be strong, resilient, quick rooting, and in abundant supply. Because the primary function of the facine is to provide immediate surficial soil stabilization and erosion control while indigenous and transplanted vegetation becomes established on the slope, its required life span is only 1 to 3 years. Therefore, selection of a plant type with the proper mechanical properties is more important than selecting a plant that will have a long-term survival rate on the slope. Willow is abundant along the stream banks and possesses the required mechanical properties, so

Transplant list	Seed Mixture
Artemisia california (Sagebrush)	Berber orchardgrass (20 lbs./acre)
A. suksdorfii (Sagebrush)	Crimson Clover (3 lbs./acre)
Baccharis pilularis subs. pilularis	Wilton Rose Clover (10 lbs./acre)
Ceanothus cuneatus (Wild Lilac)	California Poppy (1 lb./acre)
C. incanus (Wild Lilac)	Blando Brome (10 lbs./acre)
C. intergerrimus (Wild Lilac)	Annual Rye (5 lbs./acre)
C. papillosus (Wild Lilac)	
C. parryi (Wild Lilac)	
C. ramulosis (Wild Lilac)	
C. thyrsiflorus (Wild Lilac)	
Cornus glabrata (Dogwood)	
Cupressus macrocarpa (Monterey Cypress)	
Fremontodendron california (Flannel Bush)	
Heteromeles arbutifolia (Toyon)	
Pinus radiata (Monterey Pine)	
Rhamnus california (California Coffeeberry)	
R. crocea (Redberry)	
Rhus integrifolia (Lemonade Berry)	
R. laurina (Laurel Sumac)	
Salvia apiana (White Sage)	
S. columbariae (Chia)	
S. leucophylla (purple Sage)	
S. mellifera (Black Sage)	
S. sonomensis (Creeping Sage)	
Sambucus callicarpa (Elderberry)	

FIGURE 4 Recommended transplant list and seed mixture.

it was selected for use as facine material. However, because willow adapts to wet environments and summers at the site are typically drought periods, its expected survival time on the slope is not much greater than 1 to 2 years.

GRADING AND INSTALLATION OF BIOENGINEERING MEASURES

In August 1989 grading operations began in the debris flow scar. During these operations approximately 5000 yd^3 of colluvial soils were removed from the center and flanks of the source area. Upon completion of the excavation operations, the grading contractor was instructed to rip the remaining soil to a depth of 18 in. to provide a more suitable medium in which the plants could become established. A subdrain was then installed from the center of the source area down the slope to the lowest v-ditch in the track area. During excavation of the subdrain, pockets of water were encountered and drained within several days of their exposure. The grading and subdrain installation operations were generally completed by the end of October.

Installation of the soil bioengineering measures commenced in mid-November. Several light rains had occurred during the period between the completion of grading and the commencement of installating the bioengineering measures. These rains dampened the ripped soils but were not intense enough to cause substantial erosion.

The landscaping contractor charged with the installation of the bioengineering measures obtained willow for the facines from a natural source in the southern part of California. The willow stems were cut in the morning, trucked to the site (a drive of about 5 hr) in late afternoon, bundled into facines, and placed the following day. The assembly of the facines was performed at the top of the hillside and the completed facines were conveyed down the slope to the installation area by a wireline assembly rigged by the contractor. The live transplants were obtained from a local nursery and arrived at the site within several days of planting.

The contractor's first objective was to install the facines in the debris flow area. The facines were placed on contour at a vertical spacing of about 6 ft. This spacing was determined by the inclination of the slope and the type of soil to be stabilized. In practice, this is a common facine spacing. Installation of the facines progressed from the top of the debris flow scar toward the bottom. By the Thanksgiving weekend, approximately the top quarter of the source area had been covered with the facines, which were placed on contour. A storm which produced approximately 2 in. of rain in a 12-hr period occurred over the weekend, causing substantial erosion from the untreated portion of the slope. Very little erosion was noted on the upper portion of the slope where the facines had been installed the previous week. During the following days approximately 20 yd^3 of eroded soils were removed from the v-ditches on the slope and the siltation basin at the base of the track area. In the lower portion of the source area runoff from the rains had created a gully approximately 2 ft deep. This gully was repaired by backfilling with lightly compacted soil and with the placement of a brush mattress, which was intended to reduce the erosive action of surface runoff. By mid-December the remainder of the facines and approximately 3,000 live transplants were installed and the area hydroseeded without further severe rainfall incidents.

After completion of the bioengineering planting there was a period of approximately 6 weeks where little or no rain fell. During this critical time for all of the plantings the slope was irrigated with a spray from a hydroseed machine. Although this method of irrigation was expensive, it appeared that most of the plantings survived the period of drought. The remainder of the winter was drier than usual; however, there was sufficient rainfall to allow the transplants to survive and the seeds to sprout. Little of the willow in the facines sprouted and grew; however, the mechanical properties of the facines did not appear to be compromised. During the few heavy rainfalls that occurred that winter, some erosion was observed in the source area. However, the facines acted to intercept the eroded material much as a silt fence would; therefore, little soil washed off the slope and gullies did not have an opportunity to form.

By the spring of 1990 the seeds had sprouted and a thick mat of grass and weeds covered the slope. Many of the live transplants were also thriving; however, deer in the area were aware of this recently transplanted vegetation and feasted on the young plants. This browsing by the deer population reduced the number of surviving transplants by at least 50 percent. During summers in this area very little vegetation grows. The plants that survived the first winter and the browsing of the deer also survived the first summer on the slope. The grasses and weeds went to seed, and the following winter a new crop sprouted. During a visit to the site in the spring of 1991, it was noted that native vegetation species from the area were beginning to encroach into the debris flow area. These species included sagebrush, toyon, and poison oak. None of the willow facines had survived, but they were still intact and functioning as vegetative silt fences. In addition, some of the live transplants had survived. These species included Monterey cypress, Monterey pine, coffeeberry, lemonade berry, and elderberry. It appeared that the Monterey pines had the greatest survival rate, and many of these trees ranged in height from 24 to 48 in.

The original specifications for the bioengineering recommended a 20 percent second planting of the live transplants 1 year after the initial planting. The condominium homeowners' association did not want to incur this additional expense and therefore did not authorize the second planting. Despite this, it appears the debris flow scar has stabilized and native vegetation from the surrounding hillsides is invading the area. Therefore, this project to date is considered a success.

REFERENCES

1. R. J. Shlemon, R. H. Wright, and D. R. Montgomery. Anatomy of a Debris Flow, Pacifica, California. In *Debris Flows/Avalanches: Process, Recognition, and Mitigation* (J. E. Costa and G. F. Wieczorek, eds.), 1987, pp. 181–199.
2. D. H. Gray and A. T. Leiser. *Biotechnical Slope Protection and Erosion Control, Van Nostrand Reinhold Company*, New York, N.Y., 1982.

Publication of this paper sponsored by Committee on Soils and Rock Instrumentation.

Partial Landslide Repair by Buttress Fill

ALAN L. KROPP AND MICHAEL R. THOMAS

Two residences in Orinda, California, were threatened by the enlargement of an existing landslide area. Published geologic literature described the characteristics of landsliding in the geologic materials present in the Orinda formation. Site specific studies were performed using aerial photographs, small and large diameter exploratory borings, and laboratory testing. The studies indicated that the previous landslide was massive in character and that complete repair was probably economically impossible. However, buttress-fill grading could be performed at the rear of the two properties to stabilize those areas and leave the remaining portions of the landslide unchanged.

Two residences in Orinda, California, are immediately adjacent to an area that experienced significant landsliding more than 20 years ago. The rear of one residence was within 10 ft of the lateral scarp of the landslide, and the improvements behind the second home were about 30 ft from the lateral scarp. A slow retreat of this scarp threatened both properties. The owners of the homes had access to a significant amount of soil that could be used for grading to help stabilize the rear of the properties. Therefore, geotechnical studies were performed on the portion of the landslide in the rear yards of the two properties. These studies were intended to characterize the landslide materials and identify a reasonable engineering solution to protect the homes and their associated improvements. The general location of the Orinda area is shown in Figure 1.

INTRODUCTION

In the years following World War II, significant development pressures to provide housing opportunities occurred in the suburbs of the San Francisco Bay Area. Access to the suburban Orinda area had recently been improved by constructing a tunnel (completed shortly before the war began) through the hills that bound the immediate Bay Area. The state highway serving the Orinda area had significantly easier access using the Broadway tunnel than with the previous winding alignment across the top of the hills or through the earlier narrow tunnel. However, the geologic environment in the Orinda area posed many problems regarding landsliding. For example, a major landslide occurred in December 1950 that buried the highway just east of the Broadway tunnel. This landslide was more than 300 ft wide and extended up the hill adjacent to the highway for approximately 800 ft. Because previous instabilities had been observed on the hillside an extensive network of horizontal drains was installed to help stabilize the area (*1*).

The Federal Housing Authority (FHA) sponsored a significant portion of the subdivision construction in the Orinda area during the 1950s. Because of the geologic instabilities that were observed, the FHA contracted with the U.S. Geological Survey (USGS) to perform an engineering geology investigation of the area in Orinda where the Warford Mesa subdivision was proposed. The results of this evaluation were published as a USGS open-file report (*2*). The results concluded that the area was generally underlain by interbedded conglomerates, sands, and clays of the Orinda formation. These materials were described as chiefly continental, lacustrine, and fluviatile deposits, formed during the Pliocene epoch. X-ray diffraction evaluations of the clay materials indicated that they contained 35 to 95 percent montmorillonite, averaging 45 to 50 percent. Free-swell tests performed on this montmorillonite material indicated that the clays expanded from 20 to 100 percent, with a typical value of 30 percent expansion. The study indicated that there were widespread landslides in the proposed subdivision area and that the landsliding was not restricted to dip-slope environments. It also concluded that significant subsurface water could be carried by conglomerate or sand beds to the less pervious and weaker clay beds where slippage occurred. Furthermore, it concluded that joint planes in the bedrock appeared to be planes of greater weakness than the bedding planes. The report then provided some conclusions regarding the engineering criteria to be used in the grading and development of the proposed subdivision.

Continued landsliding in the general area led to more-detailed studies of the landslide problems by USGS. These further studies were published in an open-file report which studied an area of approximately 6 m^2 around Orinda (*3*). To evaluate the general characteristics of the study area, the authors collected data on approximately 195 landslides. They noted that many more landslides were present, but picked these landslides as representative of the largest and most clearly defined landslides in the area. All of the landslides were then tabulated and described with regard to their form, type of material present, geologic setting, vegetation present, and any observed damage to man-made structures. The authors concluded that rainfall was the most common triggering mechanism in the landslide areas. They further concluded that landslides often occurred because of combinations of geologic setting and site exposure. One of the most interesting findings was that landslides appeared to be more prevalent on slopes on which the bedding dipped in a direction opposite to the hillslope rather than on a dip-slope environment. They also pointed out the common relationship between the grading activities used to develop the subdivisions and the subsequent landslide movements.

A. L. Kropp, Alan Kropp and Associates, Inc., 2140 Shattuk Avenue, Berkeley, Calif. 94704. M. R. Thomas, SEC Donohue, Inc., 2800 East Parham Road, Richmond, Va. 23228.

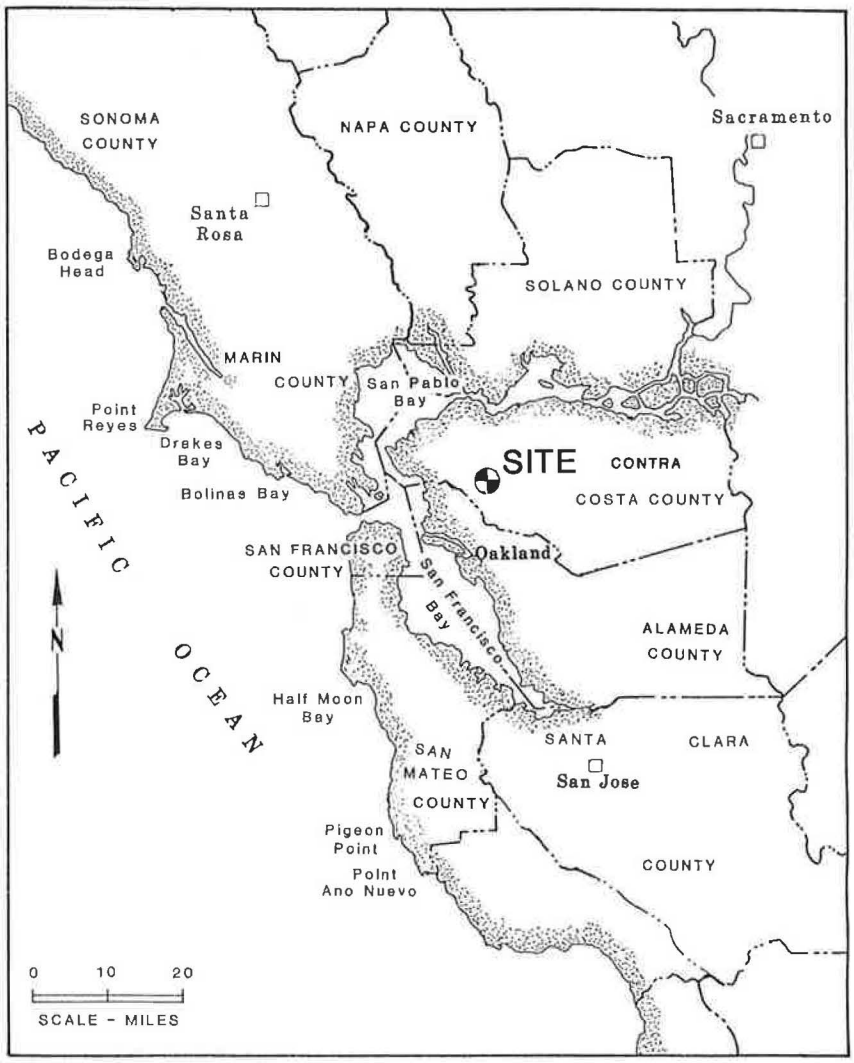

FIGURE 1 Vicinity map.

SITE HISTORY

The two Orinda lots that contained the homes threatened by the landslide evaluated in this study were located at the end of Silverwood Court (see Figure 2 for the configuration of the lots in the vicinity). Silverwood Court is a short cul-de-sac road that extends westerly off the main thoroughfare of the area, Tahos Road. An evaluation of a series of historic aerial photographs and records from the Contra Costa County Grading Department were reviewed to develop the historic site conditions. Aerial photographs taken through the mid-1950s indicated that this area was generally vacant except for a narrow unpaved road, which extended along the top of a major ridge line where Tahos Road was later constructed. At this time, the area where Silverwood Court was later built was a secondary ridge extending off of the main ridge line. The rear of the two lots studied extended into a swale area that extended downhill from Tahos Road in a westerly direction and ended in a canyon about 1,000 ft from the road. The general conditions around the secondary ridge where Silverwood Court was built appeared to be relatively stable, but the swale feature contained sparse vegetation and hummocky typography.

Aerial photographs taken in 1957 indicated that improvements had been made to Tahos Road. The road had been widened, and a number of areas of sloughing were observed along the shoulders of the widened road. These failures were most likely due to heavy rainfalls that occurred in the area during the winter of 1957 (shortly before the photographs were taken). Photographs and county records indicate that a major fill embankment was placed into the swale area along the west side of Tahos Road to develop two level building pads along Tahos Road for home construction. Homes were subsequently built on these two lots and soon after Silverwood Court and the building pads along this roadway were graded. A home was built on Lot A; Lot B remained vacant.

A major landslide occurred in the former swale area during the heavy winter rains of 1967 as shown in Figure 2. The homes previously on the two lots next to Tahos Road were either destroyed or removed from the property. The lateral scarp along

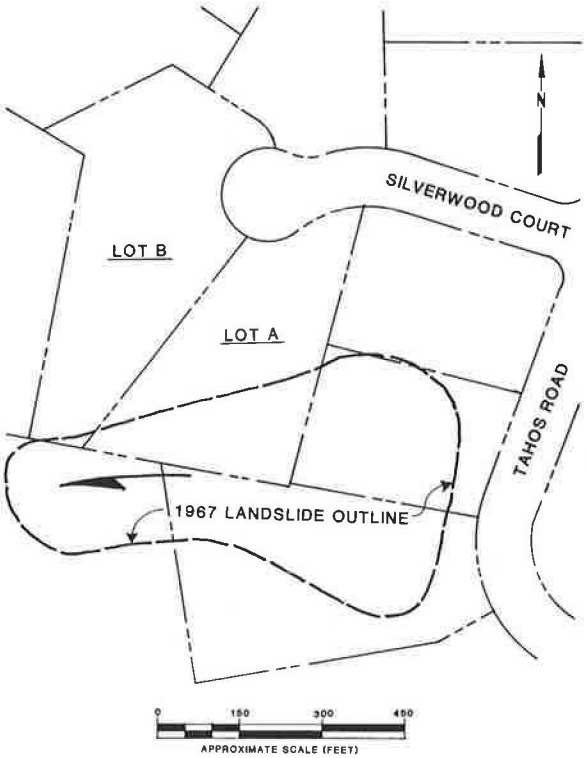

FIGURE 2 Lot plan.

the northern edge of the slide extended very close to the rear of the home on Lot A. This lateral scarp was about 10 ft in height, and the main head scarp adjacent to Tahos Road was approximately 20 to 25 ft in height. The overall dimensions of the landslide were approximately 250 by 400 ft.

The home on Lot B was built in the late 1970s. From 1967 to the late 1980s, there was a slow sloughing and lateral migration of the head and lateral scarps of the landslide, which led to the concern of the two homeowners on Silverwood Court that their houses or improvements might ultimately be threatened by future landslide movement or continued sloughing of the landslide margins.

SUBSURFACE EVALUATION

The mapping by Kachadoorian (*2*) indicated that the area of Silverwood Court and Tahos Road was clearly underlain by Orinda formation materials. It indicated that bedding in the area generally trended in an east-west direction and that a number of conglomerate beds crossed through the area. These beds seem to form the secondary ridge feature where Silverwood Court was constructed and another secondary ridge feature along the southern limits of the swale. There was an absence of conglomerate beds shown within the swale, so the conglomerate beds seemed to form a structural control along the northern and southern boundaries of the swale feature.

For the current investigation, both small- and large-diameter subsurface borings were extended into the landslide area within the two subject properties. Twelve small-diameter borings ranging from about 3 to 8 in. across were drilled using various types of drilling equipment, depending on access requirements. Selected samples from these borings were taken to the laboratory for testing. These borings were generally extended to depths of 10 to 60 ft. To further define the subsurface geologic environment, five 24-in. borings were drilled and downhole-logged by the engineering geologist. These borings generally extended to depths of approximately 15 to 30 ft. The locations of both the small- and large-diameter borings are shown on the site plan in Figure 3.

The upper materials encountered in the borings generally consisted of silty and sandy clays, which included fill materials, natural residual soils, and old landslide debris. The clays contained abundant angular rock fragments, and often thin layers of soft, saturated clays were encountered in the thicker layers of stiff to very stiff clays. Various slickenside planes were noted in the softer clay materials. At the base of the fill embankment placed in the swale to create the building pads on Tahos Road, a layer of top soil was encountered at a depth of approximately 25 ft. Generally, the clayey soils were underlain by 5 to 10 ft of highly weathered, soft-hardness claystone, siltstone, and sandstone bedrock. Some slide planes or slickensided surfaces were observed in these bedrock materials. These materials were underlain by moderately weathered bedrock and contained no obvious evidence of past shearing.

Groundwater was encountered in several of the borings and caving of the large-diameter holes limited the logging by the engineering geologist. In several cases, groundwater rose to within 10 to 15 ft of the ground surface. Soil inclinometer casings were installed in five of the small-diameter borings, so longer-term groundwater monitoring was not possible in these holes. These casings were installed to provide future slope movement monitoring during the anticipated grading operations and subsequent heavy winter rainfall events.

LABORATORY TESTING

As noted above, three general categories of materials were encountered in the borings. These included clay soils (both native materials in-place and native materials placed as fill—most of which became landslide debris), highly weathered bedrock materials, and moderately weathered underlying bedrock. Typical properties obtained from laboratory testing and standard penetration resistance values, which were obtained during the sampling process, are presented in Table 1.

In addition to the laboratory test data presented in Table 1, one direct shear test and one multistage, U-U triaxial test were performed on clay soils at field moisture content levels. The results of these additional strength tests are presented in the following table:

	Apparent Cohesion (kips/ft²)	*Apparent Friction Angle (degrees)*
Direct shear	0.27	16
Triaxial (U-U)	1.06	10

ANALYSIS

The landslide that occurred in 1967 appeared to conform to the pattern of landslides in the area described by previous

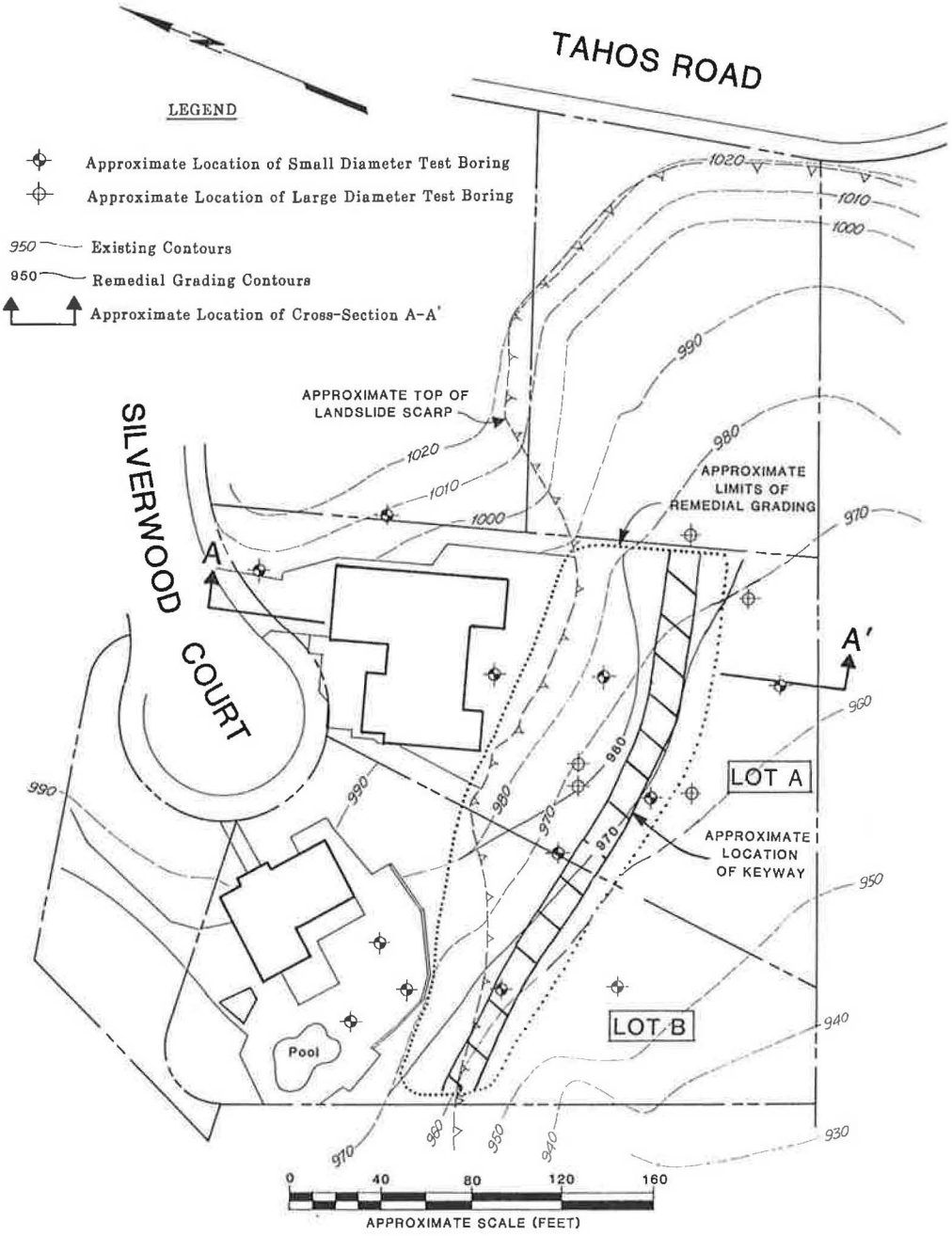

FIGURE 3 Site plan.

investigators. This landslide was apparently structurally controlled by the geologic framework present in the area. The published geologic maps indicated that conglomerate beds were present along the north and south borders of the swale area. No conglomerate material was encountered in any of the subsurface studies within the landslide. Therefore, it appeared that the lateral limits of the landslide were controlled by stronger secondary ridges that were underlain by conglomerate. Not only did the geologic structure limit the extent of the landsliding, but the presence of the conglomerate beds (and, to a lesser extent, the presence of the sandstone beds) provided a source for significant infiltration of subsurface water into the swale area during heavy winter rains. The water weakened the natural soils, the highly weathered bedrock underlying the fill embankment, and the clay soils in the embankment itself. The presence of slickensides within the natural clay soils and the highly weathered bedrock materials indicated that multiple slippage planes were present and the landslide may have been slowly developing over geologic time as the slippage surfaces became more defined and interconnected. With the added weight of the fill embankment, mass failure occurred.

Laboratory strength measurements of the clay materials probably gave strength properties higher than the strength of the materials present at the time of the failure. This is a result of significant weakening because of increased water content

TABLE 1 MATERIAL PROPERTIES

	SOIL		HIGHLY WEATHERED BEDROCK		MODERATELY WEATHERED BEDROCK	
	Range	Average	Range	Average	Range	Average
Standard Penetration Resistance (Blows/Foot)	4-30	14	27-88	49	70- >100	>100
Water Content (%)	12-25	18	12-20	17	10-18	15
Plasticity Index (%)	25-41	30	-	-	-	-
Liquid Limit (%)	42-59	49	-	-	-	-
Unconfined Compressive Strength (Kips/Square foot)	1.3-4.5	3.0	-	-	-	-

during heavy rainy winters and the slow decline toward residual strength on the slide planes. Previous analyses of the soil and bedrock failures in the Orinda formation were performed by Duncan (*4*). Using back analysis with charts by Taylor (*5*), he assumed a friction angle of 20 degrees and found that a fairly consistent cohesion intercept of 20 and 55 psf would be obtained for soil and bedrock at failure, respectively, in the Orinda formation. Using an assumed friction angle of 10 degrees in soil, he also found that the back-analyzed cohesion necessary for stability varied from about 75 psf for a slope 8 ft high to about 200 psf for a slope 25 ft high. It should be noted that these values are not the fundamental properties of the soil but simply empirical coefficients whose values reflect the behavior of the soil and bedrock under the particular climatic conditions of the area. A comparison of our laboratory test data to the back-analyzed strength values indicated that the laboratory test values provided a significant overestimation of the strength of the soil along the shear plane at the time of failure for the reasons mentioned earlier.

The focus of the investigation was to provide increased stability to the area immediately behind the two homes on Silverwood Court. It was clear that the stabilization of the entire landslide was not economically possible for the two landowners and that a complete repair would also involve the coordination and cooperation of multiple homeowners in the area. Therefore, the repair analysis concentrated solely on the portion of the landsliding within the two subject lots and recognized that the remainder of the landslide might reactivate. Using the back-analyzed strength values from Duncan (*4*), analyses indicated that the lateral margin of the landslide would continue to fail even if the main slide mass did not displace significantly. The scheme chosen involved installing a buttress fill along the rear of the two properties. Because of the relatively high strength of the moderately weathered bedrock materials, it was decided that adequate stability could be achieved by notching or keying and benching into these materials and installing subsurface drainage blankets to collect subsurface water flow. Analyses of the mass stability of a failure plane immediately behind and below the buttress fill and the stability of a potential failure plane through the buttress fill were conducted, and both yielded satisfactory factors of safety. An idealized cross section taken through Lot A is shown in Figure 4 and illustrates this buttress-fill concept.

PROJECT CONSTRUCTION

Grading to create the buttress fill begin in summer 1988. The initial excavation extending into moderately weathered bedrock was performed first. It was found that significant vari-

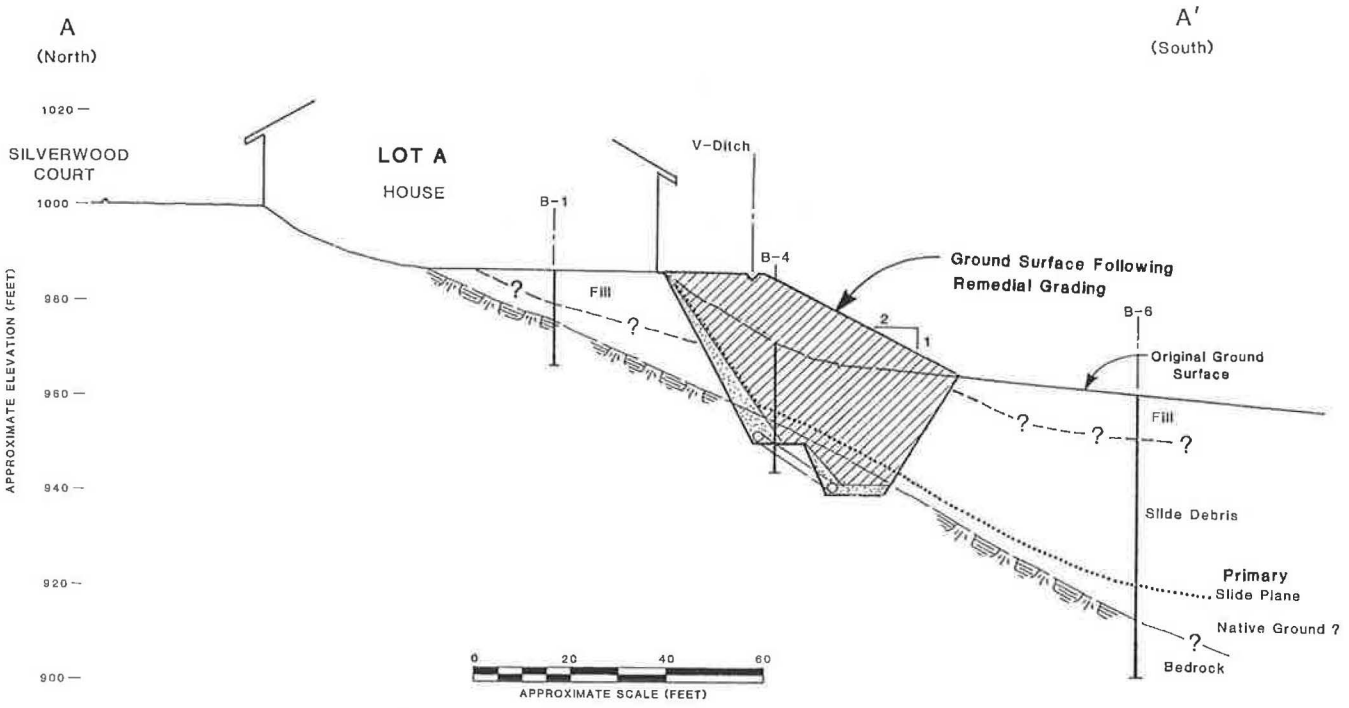

FIGURE 4 Idealized cross section.

ation in the depth of the bedrock occurred between boring locations. Whereas the moderately weathered bedrock was encountered in the keyway (lowest notch) at a depth of about 30 ft at the boring locations as predicted, the bedrock dipped to as deep as 50 ft below the existing ground surface between the borings. The excavation work was performed with bulldozers and front-end loaders that continued to shave the side slopes of the excavation back as it became progressively deeper. A drainage blanket was installed in the bottom of the keyway. This blanket consisted of a 4-in.-diameter ABS pipe surrounded by a 12-in. layer of ½- to ¼-in. clean gravel, which was encircled by a nonwoven, polyester geotextile. To provide gravity-flow discharge for water collected in the drainage blanket that was placed in the bottom of the keyway, hydrauger pipes were drilled from downslope to connect to these drainage blankets. Two additional notches or benches were made upslope of the keyway. The native soils and bedrock that were excavated at the site were stockpiled and moisture-conditioned for reuse as fill. These materials were placed in thin layers and compacted to at least 90 percent relative compaction (in accordance with ASTM 1557-78). The majority of the work was completed within 2 months. Surface drainage measures were also provided on top of the buttress fill, and erosion-resistant vegetation was planted.

The owners of the project did not notify the grading contractor of the presence of slope inclinometer pipes before commencement of grading. Therefore, the final monitoring of most of these inclinometer pipes occurred before they were destroyed by the major excavations, and no movement was recorded during that period. Subsequent financial concerns by the owners have eliminated any readings of the slope inclinometer following the completion of the grading work. Although the area has endured drought-type conditions since the grading work was completed, no obvious indications of movement have been observed in the buttress fill.

SUMMARY AND CONCLUSIONS

Stabilization of the rear slopes behind two residences became necessary when ongoing sloughing of the lateral scarp of a large landslide occurred. Literature about the geologic characteristics of landslides in the area provided general insights into the landsliding. Site-specific studies indicated that a buttress fill would stabilize the rear yards, even if new movements occurred in the rest of the landslide. The remedial grading work to install the buttress fill was completed in 1988 and has performed satisfactorily to date.

REFERENCES

1. E. P. W. Herlinger and G. Stafford. *Orinda Slide*. California Department of Highways and Public Works, Vol. 31, No. 1–2, 1952.
2. R. Kachadoorian. *Engineering Geology of the Warford Mesa Subdivision, Orinda, California*. Open File Report, U.S. Geological Survey, 1956.
3. D. H. Radbruch and L. M. Weiler. *Preliminary Report on Landslides in a Part of the Orinda Formation, Contra Costa County, California*. Open File Report, U.S. Geological Survey, 1963, pp. 63–12.
4. J. M. Duncan. Prevention and Correction of Landslides. Presented at the 6th Annual Nevada Street and Highway Conference, 1971.
5. D. Taylor. *Fundamentals of Soil Mechanics*. John Wiley & Sons, New York, N.Y., 1948.

Publication of this paper sponsored by Committee on Soils and Rock Instrumentation.

Case Histories of Landslide Stabilization Using Drilled-Shaft Walls

KYLE M. ROLLINS AND RALPH L. ROLLINS

The Manning Canyon shale formation underlies many of the slopes adjacent to the Wasatch mountain range near Provo, Utah. The climate in Utah is relatively dry, so the strength of the shale is normally sufficient to prevent slope instability. During wet periods, however, the shale exhibits a significant decrease in strength that has led to a number of landslides. One method that has been employed to stabilize some of the slopes is the installation of closely spaced drilled shafts. Successful application of this stabilization procedure requires (a) accurate evaluations of the geometry and strength of the materials composing the slope, (b) reasonable evaluations of the location of potential failure surfaces, (c) estimations of the horizontal force required to increase the factor of safety against sliding to a suitable value, and (d) design and construction of drilled shafts capable of resisting the required horizontal force. The application of the method is illustrated with the use of several case histories for slopes on which slides have developed. Continued sliding threatened homes upslope and closed roadways to traffic. The success of the stabilization technique was recently proved in one of the cases in which the slope behind the drilled-shaft wall became wet. Although a slide developed in the slope immediately adjacent to the wall, the slope behind the wall has remained stable. Damage to the homes and roadways because of the movement of the slides has been arrested since the walls were constructed.

During the past 15 years, considerable development has taken place on the western slopes of the Wasatch mountain range in northern Utah. Unfortunately, many of these slopes east of Provo, Utah, are underlain by the Manning Canyon shale formation. This formation is known to exhibit significant decreases in strength following wetting, and it is frequently associated with landslides. Because the climate in Utah is relatively dry (annual precipitation is typically less than 20 in./year) the strength of the shale is normally high enough to prevent slope instability. During wet periods, however, the decrease in strength has frequently led to landslides. For example, during the period from 1981 to 1984, precipitation ranged from about 150 to 200 percent of the normal (*1*) and many landslides developed in the foothills east of Provo. In most cases, the Manning Canyon shale or residual soils derived from the shale were found to be responsible for the sliding.

One method that has been used to stabilize some of the slopes is the installation of closely spaced drilled shafts. The successful application of this procedure has been described by several investigators (*2,3*). In contrast to conventional concrete cantilever and counterfort walls, drilled shafts are capable of more economically resisting large lateral forces. Drilled shafts can easily be passed through the failure surface, and they can be constructed without excavating the toe of the slope and exacerbating the sliding problems. Recent cost comparisons between drilled-shaft walls and conventional walls at sites in Utah indicate that a savings between 40 and 50 percent can be expected.

In order for the drilled-shaft stabilization procedure to be successfully employed, it is necessary to (a) make accurate evaluations of the geometry and strength of the materials comprising the slope, (b) make reasonable evaluations of the location of potential failure surfaces, (c) make estimations of the horizontal force required to increase the factor of safety against sliding to a suitable value, and (d) design and construct drilled shafts capable of resisting the required horizontal force.

The principles and methods used in the analysis will be discussed in general terms, and then the application of the procedure will be illustrated with several case histories. Two of the case histories involve slopes on which shallow failure surfaces developed. The sliding caused significant damage to homes upslope from the slides; continued sliding threatened to destroy the homes. The slides also moved into adjacent roadways and caused disruption of traffic. Drilled-shaft walls were installed along with drainage systems and the homes and roadways were repaired. Two additional case histories involve much larger landslides, which damaged roadways but did not directly affect houses. Drilled-shaft walls have been designed, along with other measures, to stabilize these slopes.

GENERAL PROCEDURE

Evaluation of Geometry and Strength of Materials Composing Slope

The profile of the slope before failure was initially approximated on the basis of available topographical maps. However, in some cases cutting and filling operations associated with construction of the houses had changed the geometry significantly. In these cases it was necessary to use old photographs, construction plans, and eye-witness accounts to reconstruct the slope profile. Profiles of the failed slopes were determined using conventional surveying techniques.

The subsurface profile along the length of the slide was determined by drilling a number of boreholes that extended through the failure surface and into the more intact shale formation at depth. The shale boundary was generally found to be rather irregular, and this irregularity may be a result of previous landslides or normal faulting on the Wasatch fault in the immediate vicinity. Undisturbed samples of the cohesive overburden material were obtained using 2.5-in. diameter

Civil Engineering Department, Brigham Young University, 368 Clyde Building, Provo, Utah 84602.

thin-walled shelby tubes. Miniature vane shear tests were performed on each sample in the field and unconfined compression tests were conducted in the laboratory.

Disturbed samples were obtained in cohesionless overburden using a standard split-spoon sampler. In addition to standard penetration testing, testing in these materials was limited to grain-size analysis. The boreholes were generally extended 10 to 20 ft into the intact shale, and core samples of the shale were obtained for compression testing. The range of undrained strengths typically involved for the various material types encountered are shown in Figure 1. Companion tests on wet and dry samples of the residual clays indicate that the undrained shear strength at saturation is only about 30 percent of the strength at its normal moisture content.

Evaluation of Location of Potential Failure Surfaces

Because all cases involved active landslides, the locations of the head and toe of the slide were known. During drilling operations an engineering geologist was present to log the hole and estimate, if possible, when the failure surface was located. Based on field observations, the subsurface profile, and the shear strength test data, it was normally possible to make a reasonable estimate of the location of the failure plane. For the larger landslides, the failure plane appeared to follow the boundary of the shale layer; for the smaller slides the failure was located within the residual clays above the shale boundary.

The average strength on the failure surface was evaluated by back-calculating the strength necessary to produce a factor of safety of 1.0 using Spencer's method of stability analysis, which satisfies both force and moment equilibrium. The computer program SSTAB1 was used to perform the analyses (*4*). Both circular and noncircular failure surfaces were used in the analyses. The critical failure surface was generally in good agreement with field observations, and the back-calculated strength compared favorably with the low end of the range of laboratory test data.

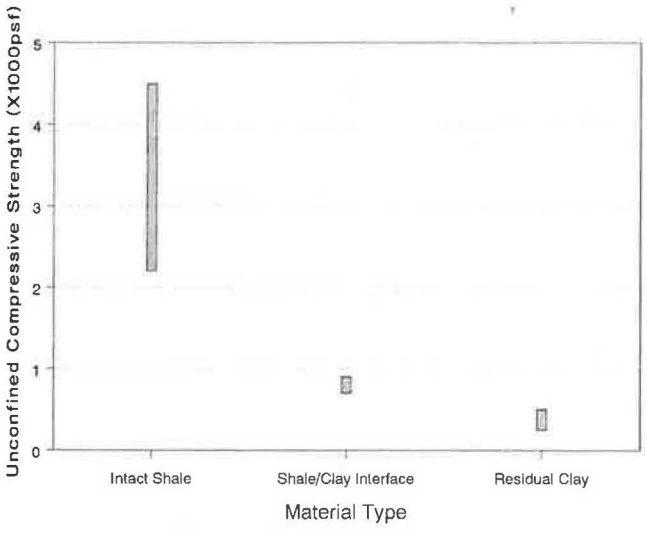

FIGURE 1 Comparison of undrained strength of various materials under saturated conditions.

Determination of Horizontal Force Required To Increase Factor of Safety Against Sliding

Once the soil profile and strength properties had been defined, the force required to increase the factor of safety against sliding to acceptable levels was determined. Horizontal forces were applied to the slope at locations where the drilled-shaft walls were to be located and slope stability analyses were performed. The analyses were performed again for potential circular and noncircular failure surfaces. Variations in the reconstructed slope angle and horizontal force were made until the computed minimum factor of safety for static conditions was between 1.4 and 1.5.

Although the sites are near the Wasatch fault, a formal evaluation of the wall under seismic loading was not considered necessary for several reasons. First, the probability of an earthquake on the Wasatch fault is less than 10 percent for a 50-year period, and—considering the dry climate of Utah—the likelihood is very small that the soil would be at a critical degree of saturation at the same time an earthquake occurred. Second, none of the soils involved were susceptible to strength loss because of earthquake shaking and therefore, a flow slide was not possible. Finally, the horizontal force on the wall already included a safety factor of 1.5, and this force was subsequently multiplied by a load factor in designing the shaft as will be described. Thus, a significant seismic force could be tolerated before any sizable deformations would be expected.

Design and Construction of Drilled Shafts Capable of Resisting Required Horizontal Force

The required horizontal force per foot of length was multiplied by the center-to-center spacing to provide the horizontal force acting on each shaft. On the basis of the required force, the necessary embedment below the failure surface and the maximum moment in the shaft were computed using Broms' method for free-headed piles (*5,6*). The shaft was then designed to resist the computed maximum shear force and bending moment multiplied by a load factor of 1.6. This load factor was necessary because the concrete design used was based on the ultimate strength method, which follows American Concrete Institute (ACI) code requirements. Computations for the required reinforcement were simplified by treating the shafts as if they were square beams that fit entirely within the diameter of the shaft.

The shafts were typically 2 to 3 ft in diameter, and the free space between adjacent shafts was generally 4 to 6 ft. The shafts were designed to penetrate into the intact shale layer at a depth where the undrained strength of the shale was relatively high. To construct the shafts, holes were excavated through the slide material using conventional drilling, the reinforcing steel was placed, and the shaft was back-filled with concrete. After construction of the drilled-shaft walls, the slope was reconstructed to a specified inclination.

CASE HISTORY 1—WINDSOR DRIVE SLIDE 1

Slide Description

A plan view of the slide mass in relation to the house and Windsor Drive is shown in Figure 2. The house is on a hillside approximately 20 to 25 ft above the elevation of Windsor Drive. A steep slope extends from the front of the house to the east side of Windsor Drive. Above-normal precipitation and poor drainage allowed the subsurface soils to become wet, and a slide occurred in the slope immediately in front of the home. The head of the slide in front of the house was well defined and the toe of the slide intersected the asphalt paving on the east side of Windsor Drive. As a result of the slide, the southwest corner of the house settled several inches and caused a large crack in the basement floor. The outside edge of the front porch settled and pulled away from the house. The driveway, which extended diagonally up the hill in front of the house, was displaced and broken, and a cinder block retaining wall was sheared in two and carried down the hillside.

Subsurface Soil and Water Conditions

Four boreholes were drilled into the bedrock at locations shown in Figure 2. A cross section through Boreholes 1, 2 and 4 is shown in Figure 3. The subsurface profile generally consisted of a brown to black clay that graded into a dark brown to black Manning Canyon shale. The clay material above the shale has principally been derived from the weathering of the parent material. The clay classified as a CL material using the unified soil classification system, and the plastic index ranged from about 15 to 30 percent. No static water table was encountered in any of the test holes; however, the clays were very moist, and experience has shown that seeps frequently occur in the fractures of the Manning Canyon shale.

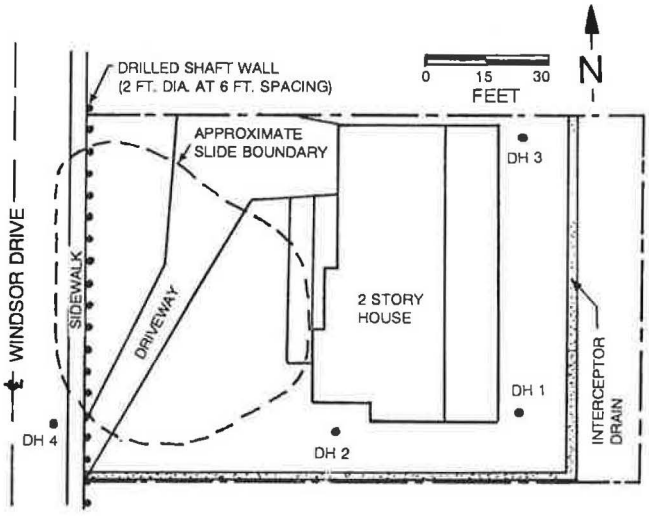

FIGURE 2 Plan view of Windsor Drive Slide 1 and drillhole locations.

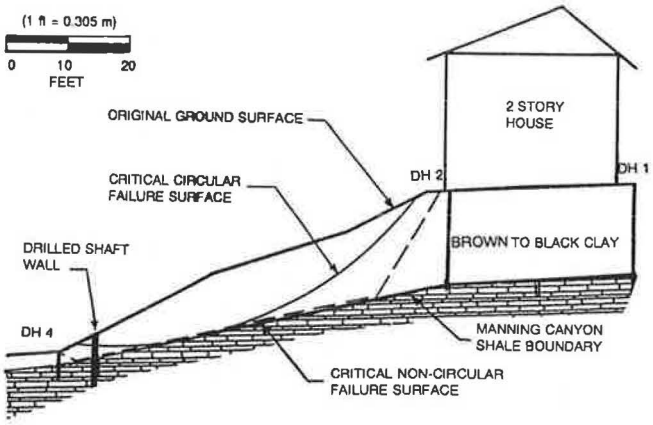

FIGURE 3 Profile through Windsor Drive Slide 1.

Stability Analyses

The shear strength of the shale layers consistently exceeded 2,500 psf, the strength of the clay was fairly erratic and varied from 200 to 2,000 psf. Because the failure surface was approximately known, it was possible to estimate the shear strength corresponding to a factor of safety of 1.0. For an assumed shear strength, the critical factor of safety was determined for potential circular surfaces passing through the toe of the slide. The safety factor became equal to 1.0 when an undrained shear strength of 270 psf was specified.

For the same strength values, a search was made for the critical noncircular failure surface, assuming that the failure occurred along the clay-shale interface. The search procedure employed the method proposed by Celestino and Duncan (*7*). The safety factor for the noncircular failure case was 20 percent higher than that for the circular failure case, so it was concluded that a circular failure mode was more critical. This finding also agrees with the shape of the slide.

Stabilization Measures

Additional stability analyses were conducted for potential failure surfaces through the reconstructed slope to determine the horizontal force necessary to stabilize the slope. It was determined that a horizontal force of 7,000 lb/ft of wall applied at the location shown in Figure 2 would bring the factor of safety up from 1.0 to 1.5. Based on Broms' method (*5,6*) it was determined that the shafts should extend to a depth of 15 ft in the intact shale a center-to-center spacing of 6 ft. On the basis of shear and moment requirements, 2-ft-diameter shafts and four #10 steel reinforcing bars were specified. The locations of the drilled-shafts in plan and profile are shown in Figures 2 and 3. The cost of the wall was estimated at about $160/ft of wall, a total cost of about $14,400. Because the cost of the wall was a small fraction of the total value of the house and few other alternatives for stabilization were available, the drilled-shaft wall was constructed.

After construction of the drilled-shaft walls, the slope was reconstructed to its original inclination and thin concrete panels were placed between the shafts above ground level. These panels, which did not exceed a height of about 4 ft, were

FIGURE 4 View of completed drilled-shaft wall with landslide developing immediately adjacent to it.

FIGURE 5 View of slide mass with drilled-shaft wall in background.

intended to prevent surface erosion that might not be controlled by soil arching. In addition to the shaft wall, a 10-ft-deep interceptor drain was constructed across the back side of the house as shown in Figure 2. A perforated 4-in. PVC drainpipe was placed at the bottom of the trench and extended to the roadway at the base of the slope. A photograph of the completed wall is shown in Figure 4.

The success of the stabilization procedure was recently proved when the slope behind the drilled-shaft wall became wet because of heavy spring rains and a leaky sewage line that had not been completely repaired in the reconstruction of the hillside. A slide similar in magnitude to the original slide developed in the slope immediately adjacent to the wall and moved onto the street. The stark contrast in the hillside performance at the interface between the slide mass and the wall is shown in Figure 5. Clearly, without the presence of the shaft wall, the slope in front of the home would have once again failed. Although the soil behind the wall became nearly saturated, the slope has remained stable and there are no signs of distress in the shafts. Structural damage to the home because of movement of the slide has been arrested since construction of the shafts.

CASE HISTORY 2—WINDSOR DRIVE SLIDE 2

Slide Description

Within a year of the original slide described in Case History 1, a similar slide began to move in front of another house several hundred ft away. A plan view of the slide mass in relation to the existing house is shown in Figure 6. The house consists of a basement and two levels above the ground surface. The topography in this area slopes steeply toward the west; a level site for the facility was developed by cutting into the hillside. A profile showing the original ground surface and the ground surface prior to slope failure is shown in Figure 7.

The intersection of the slip plane with the ground surface appears to be located a few feet east of the western side of the house. Slip plane traces could be seen on both the north and south side. A major north-south crack developed along the basement floor directly behind the western wall and exhibited considerable vertical displacement. Differential movement between the north and south corners at the first-floor level was more than 3 in., and cracking of the basement walls was also evident. Cracking of the brickwork was also observed in front of the house and on the north and south sides. Slide movements in front of the house had significantly disrupted sidewalks, steps, and a retaining wall made from wood railroad ties. Bulging of the asphalt pavement on Windsor Drive directly adjacent to the easterly curb of the street suggested that the slide terminated in this area.

Site Characterization and Stability

To evaluate the stability of the site, four test borings were drilled to depths between 20 and 60 ft, as shown in Figure 6. The locations of these holes in profile and the soil stratigraphy

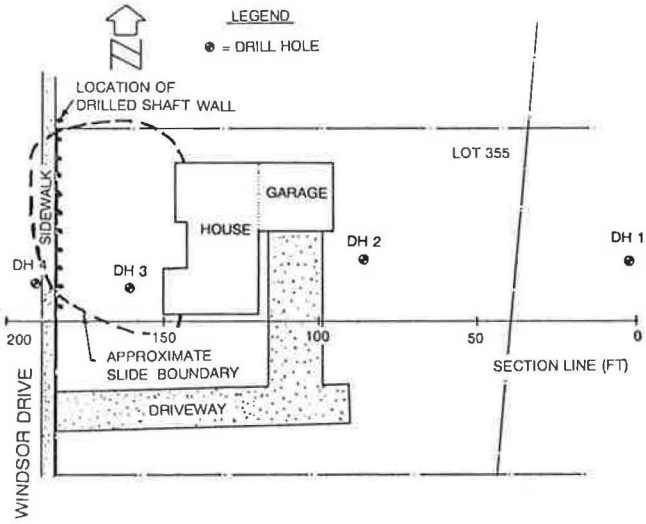

FIGURE 6 Plan view of Windsor Drive Slide 2 and drillhole locations.

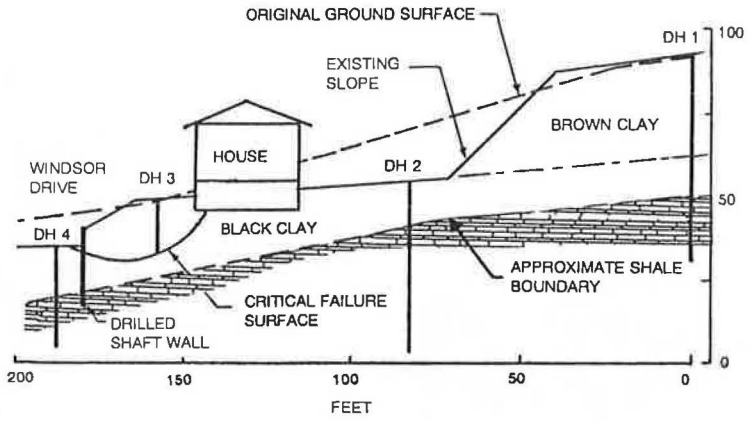

FIGURE 7 Profile through Windsor Drive Slide 2.

at the site are shown in Figure 7. The subsurface profile generally consisted of gray to black clay that graded into Manning Canyon shale. However, the steep slope behind the house was composed largely of a brown clay with a markedly lower plasticity index.

Although groundwater was not encountered in any of the boreholes, the black clay in the vicinity of the slide was 80 to 90 percent saturated. The undrained strength generally varied from around 400 psf near the ground surface to about 1,200 psf at a depth of 20 ft; however, samples obtained near the failure surface had undrained strengths of about 300 psf. Slope stability analyses determined that a factor of safety of 1.0 was obtained for an average shear strength of 300 psf. The location of the critical failure circle is shown in Figure 7; it may be seen that it closely approximates the observed failure surface. It is interesting to note that the undrained strength and failure mode in this case are very similar to the previous case history.

Stabilization Measures

The undrained cohesion of 300 psf was subsequently used in stability analyses to calculate the magnitude of the lateral force acting on the downhill face of the slide necessary to increase the factor of safety from 1.0 up to 1.5. It was determined that a force of 8,100 lb/linear-ft of wall would be required. On the basis of horizontal force, 2-ft-diameter shafts spaced at 6 ft on centers were specified. The shafts extended 12 ft into the subsurface profile at the location shown in Figure 7. This embedment depth was beyond the observed failure surface at the base of the slide. The investment in the drilled-shaft wall was considered worthwhile because it restored the original value of the property at a small fraction of the original cost of the structure.

In addition to the drilled-shaft wall, other measures to improve stability included channeling runoff from roof drains into pipes that were carried to the street level and the installation of a shallow interceptor drain along the front of the house. The house itself was then repaired, and no additional distress has been observed even though slides in the immediate vicinity of the house have occurred.

CASE HISTORY 3—MILE HIGH DRIVE–IMPERIAL WAY SLIDE

The previous case histories involved small shallow slides adjacent to structures, the following case histories involve somewhat larger landslides.

Slide Description

The general location of the slide area between Mile High Drive and Imperial Way is shown in Figure 8. The head of the slide intersects nearly all of Mile High Drive, and the toe of the slide is located on the easterly edge of Imperial Way. Both roadways were closed because of the slide. The topography of the slide area is also shown in Figure 8, and a profile through the center of the slide is shown in Figure 9. The location of two small drainage channels east of Mile High Drive, designated as "A" and "B," are also shown in Figure 8. Before construction of the roadway, water from these drainage channels flowed down a depressed area to the south of the slide and was carried downslope. With the construction of the roadway, the drainage path was interrupted and water from both drainages seeped into the subsurface material in the general slide area. Following heavy runoff the slide moved downslope about 15 ft.

Site Characterization and Stability

The characteristics of the subsurface material throughout the slide area were defined by drilling four test holes to depths varying from 14 to 40 ft as shown in Figures 8 and 9. It should be noted that the Manning Canyon shale was encountered in each of these test borings at depths varying from 9 to 36 ft below the ground surface. The location of the overburden and shale materials are shown in Figure 9. The overburden generally consisted of gravelly sand and clayey gravel overlying a 6- to 8-ft-thick layer of residual clay above the shale. Groundwater was encountered in every boring. The water table was typically 25 ft above the shale interface near the

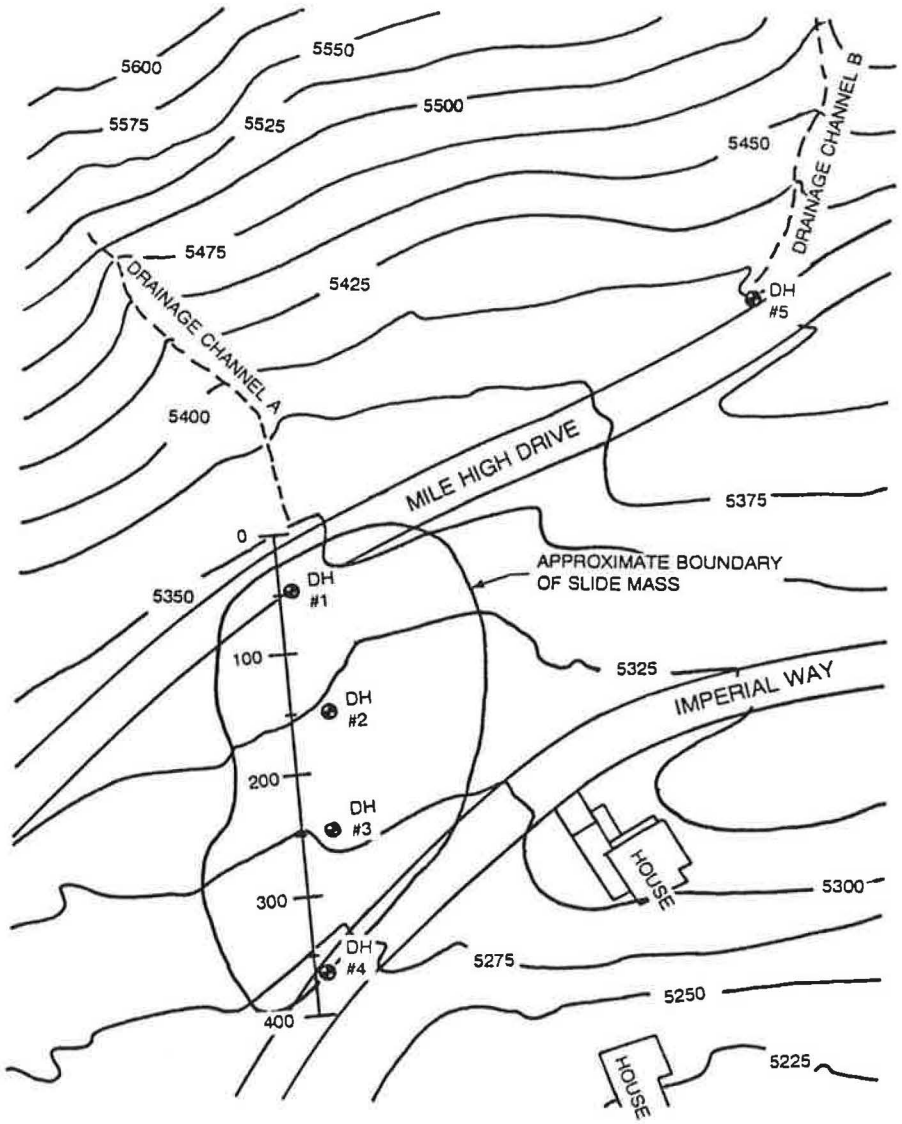

FIGURE 8 Plan view of Mile High Drive–Imperial Way landslide and drillhole locations.

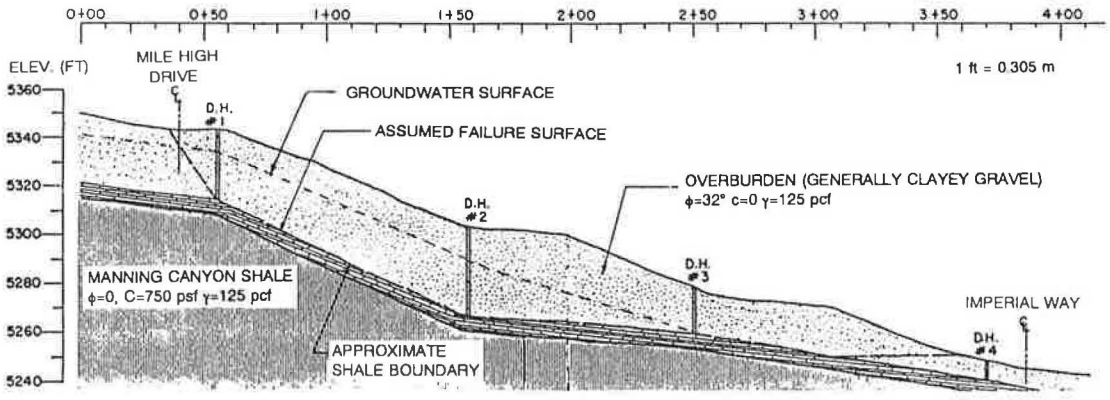

FIGURE 9 Profile through Mile High Drive–Imperial Way landslide.

head of the slide but just a few feet above the shale elevation at the base of the slide.

The location of the shale surface along with the groundwater conditions and the characteristics of the overburden material strongly suggest that the failure surface is in the vicinity of the interface between the overburden and the shale. Assuming that the failure surface lies near the clay-shale interface and that the factor of safety against sliding is equal to 1.0, a stability analysis was performed to determine the average shear strength along the failure surface. Assuming undrained conditions in the clay-shale, the results of the stability analyses indicate an undrained shear strength of about 750 psf. At the head and toe of the slide the failure surface passes through the overburden material. The groundwater level shown in Figure 9 was taken as the piezometric surface for the granular soils. The unit weight and strength parameters used for the overburden material are shown in Figure 9. The results were not highly sensitive to small variations in these properties.

Stabilization Measures

The stabilization measures for this slide called for (a) installation of a 24-in.-diameter storm drain to carry the flow from the drainage channels away from the slide, (b) a 3-ft-wide interceptor drain back-filled with coarse concrete aggregate to a depth of 10 ft, and (c) a line of drilled shafts extending across the slide zone on the west side of Mile High Drive. Stability analyses indicated that a drilled-shaft wall near the toe of the slide would produce an increase in the factor of safety of less than 10 percent for the entire slope; however, a drilled shaft wall at the top of the slope could provide significant resistance and protect the upper roadway from future sliding. Based on the back-calculated strength values, stability analyses indicated that the drilled shafts adjacent to the roadway would need to provide a resistance of 7,000 lb/linear-ft to provide a factor of safety of 1.5 against sliding of the upper wedge of the slide.

The shafts were designed to penetrate through approximately 30 ft of overburden and 15 ft into the shale itself. The concrete shafts were 2.5 ft in diameter and were spaced at 5 ft on centers. Reinforcing consisted of four #11 bars. Movements of the slide have been minor since the construction of the stabilization measures.

CASE HISTORY 4—OAK HILLS SLIDE

Slide Description

A plan view of the Oak Hills slide is shown in Figure 9. This slide is located at the toe of a large ancient landslide near the base of Provo Mountain. Although the topography next to the slide is shown in Figure 10, the topography of the slide zone immediately before the slide occurred is uncertain. Construction was under way to prepare a level pad for a house and an access road up to the house. On the basis of photographs, eyewitness accounts, and volume comparisons with the slide debris, the best estimate of the original profile through the slide is shown in Figure 11. The slide was about 400 ft long and 100 ft wide. The scarp formed by the slide was more than 40 ft high and the slide moved more than 70 ft laterally. The slide threatened to engulf an adjacent home before coming to equilibrium approximately 10 ft in front of it.

Site Characterization and Stability

To define the soil profile and the probable location of the failure surface, it was necessary to drill four borings at the locations shown in Figure 11. Three of the borings penetrated the intact Manning Canyon shale, and the fourth boring, located at the bottom of the slide, did not. On the basis of the borings, the approximate location of the shale boundary is shown in Figure 11. It should be noted that the shale boundary is not a simple linear feature because previous landslides have displaced the shale. The material above the shale generally consists of low-plasticity gravelly silt and silty gravel. In addition to the intact shale zone, photos taken by a geologists before the slide showed a mass of shale with granular material above and below it was exposed in one of the lower cuts. It is theorized that the failure surface followed this detached shale layer and then ran along the shale interface and finally ruptured through the overburden as shown in Figure 11. No groundwater was encountered in any of the holes, but the soils were approaching saturation.

An examination of the cores in the shale indicated that they were highly fractured with zones of relatively hard shale interbedded with relatively soft layers. The plastic index of the shale ranged from 5 to 18, and the unconfined compressive strength varied from 1,500 to 4,900 psf. Thus, if the failure plane moved through the weakest zones, the shear strength would be about 750 psf. Stability analyses were conducted to determine the strength of the shale interface that was required to produce a factor of safety of 1.0. Assuming a reasonable range of values for the strength and unit weight of the granular zones above the shale (see Figure 11), the back-calculated strength of the shale interface was found to be between 700 and 900 psf. This strength is in good agreement with laboratory results and the interface strength that was determined for the Mile High Drive slide.

Stabilization Measures

The stabilization evaluation assumed that the slide mass would be removed from the roadway and that the slope would be cut back from the edge of the roadway to provide a stable slope. A number of alternatives were investigated and stability evaluations made for both circular and noncircular failure surfaces. The strength of the shale interface was assumed to have a value of 800 psf, which was based on back calculations and laboratory test results. For the case with the slope cut back to an inclination of about 1.75 H to 1.0 V, the factor of safety was 1.35. The addition of a horizontal force of 10,000 lb/linear-ft increased the factor of safety to 1.5. This force could be provided by using 3-ft-diameter shafts spaced at 6 ft on centers. The shafts would need to extend to a depth of 15 ft into the shale at the base of the slide. An interceptor drain was also recommended for the uphill side of the slide. It should be noted that because of the volume of the slide mass involved, the drilled-shaft wall, in this case, produced

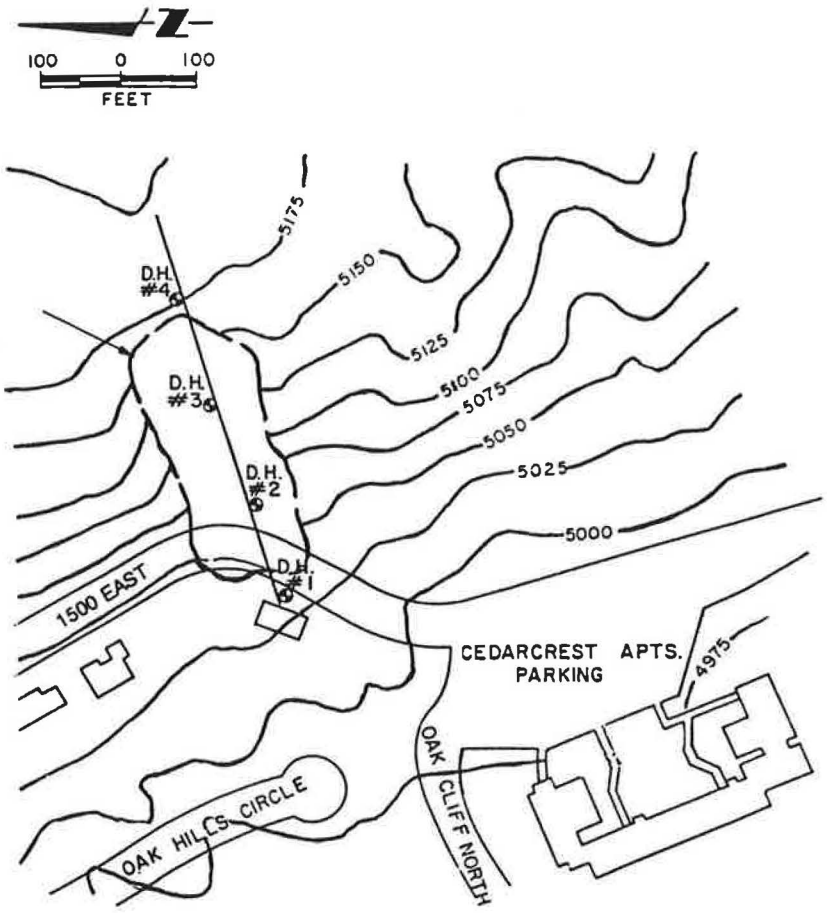

FIGURE 10 Plan view of Oak Hills slide and drillhole locations.

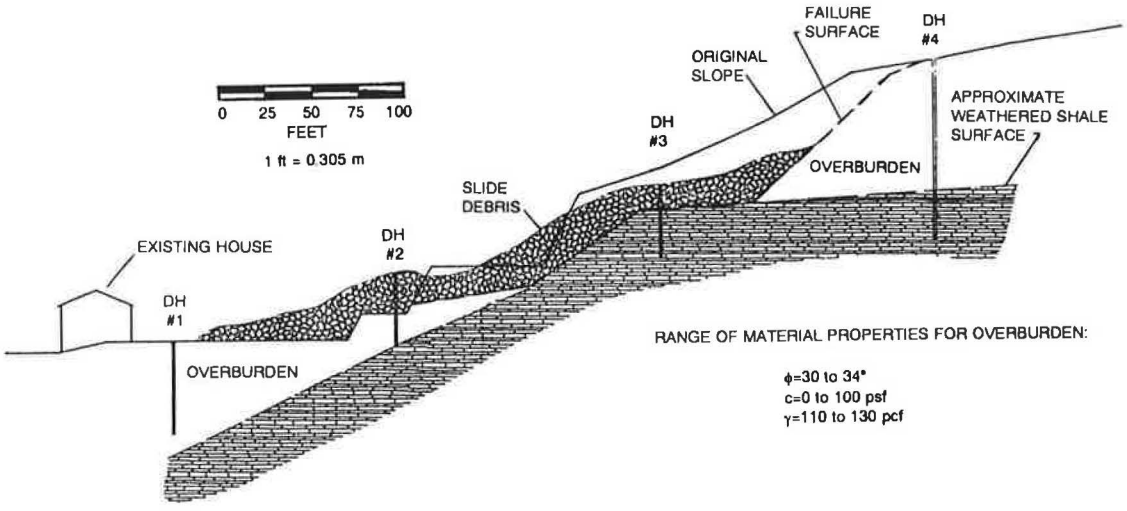

FIGURE 11 Profile through Oak Hills slide.

relatively small increases in the factor of safety against sliding even though the design forces were greater than in the first two cases. Legal issues concerning responsibility for the slide have delayed any actions regarding repair of the slide for more than 8 years, during which time the roadway has been blocked to traffic.

CONCLUSIONS

1. Drilled-shaft walls when used in combination with appropriate drainage provisions can be a practical, effective, and reasonably economical means of stabilizing small to medium-size landslides such as those discussed in the first two case histories—slope heights less than 30 ft and slope lengths less than 60 ft.
2. Significant increases in the factor of safety (from 1.0 to 1.5) are possible for small slides, but only moderate increases can be expected for larger slides such as those discussed in the next two case histories—slope heights of 80 ft and slope lengths of 200 ft.
3. The design of the shaft walls for landslide control requires a relatively good understanding of the mechanism controlling the slope failure, the strength of the soil, and the force distribution on the shaft.

REFERENCES

1. National Oceanic and Atmospheric Administration. *Climatalogical Data and Annual Summary for Utah*, Vol. 83–86, No. 13, 1981–1984.
2. M. F. Nethero. Slide Control by Drilled Pier Walls. *Application of Walls to Landslide Control Problems* (R. B. Reeves, ed.), ASCE, 1982, pp. 61–76.
3. N. R. Morgenstern. The Analysis of Wall Supports to Stabilize Slopes. *Application of Walls to Landslide Control Problems* (R. B. Reeves, ed.), ASCE, 1982, pp. 19–29.
4. S. G. Wright. *Documentation for SSTAB1: A General Computer Program for Slope Stability Analyses*. Geotechnical Engineering Software G-582-1. Geotechnical Engineering Center, University of Texas, Austin, 1982.
5. B. B. Broms. Lateral Resistance of Piles in Cohesive Soils. *Journal of the Soil Mechanics and Foundation Division*. ASCE, Vol. 90, SM2, 1964, pp. 27–63.
6. B. B. Broms. Lateral Resistance of Piles in Cohesionless Soil. *Journal of the Soil Mechanics and Foundation Division*, ASCE, Vol. 90, SM3, 1964, pp. 123–156.
7. T. B. Celestino and J. M. Duncan. Simplified Search for Non-Circular Slip Surfaces. *Proc., 10th International Conference on Soil Mechanics and Foundation Engineering*, Stockholm, Sweden, 1981.

Publication of this paper sponsored by Study Committee on Landslides: Analysis and Control.

Bud Peck Slide, Interstate 15 near Malad, Idaho

SUNIL SHARMA AND TRI BUU

In May 1983, the two northbound lanes on Interstate 15, approximately 8.6 mi north of Malad, Idaho, were destroyed; a case history of the embankment failure is described. Details about the site investigation, dewatering, and final permanent repair are discussed as is the monitoring program that has spanned 7 years. The failure, known as the Bud Peck slide, followed an abnormally wet season. The damaged highway slumped an average of about 20 ft over a 500-ft length. A temporary diversion allowed traffic to pass around the failed area while studies were being conducted to investigate the cause of the failure and possible remediation plans. A site investigation consisting of 17 borings and shallow test pits and the installation of five slope inclinometers, which also served as groundwater observation wells, was quickly performed to determine the mechanisms that might have caused the embankment failure. The data from the borings indicated that the embankment, constructed in 1970, was placed on a 2- to 3-ft sand blanket overlying a deep residual clay layer. The slope indicator data identified a slip plane 3 to 5 ft into the clay layer. It appears that the buildup of pore water pressures in the embankment, due to an inadequate drainage layer, may have caused failure of the slope. On the basis of the available information, several alternatives, including a rock buttress, a sand and gravel fill, and a lightweight fill, were considered as a permanent solution. To lower the groundwater levels, horizontal drains were installed in 1983, and the final repairs used a lightweight pumice fill for embankment reconstruction in 1985. The use of the pumice fill provides a calculated factor of safety against slope failure of 1.3.

In July 1982, cracking was noted in the pavement of a 500-ft section of the two northbound lanes of Interstate 15, 8 mi north of Malad, Idaho (see Figure 1). This distress occurred in 1982 after an unusually wet season in which precipitation amounts were about 100 percent above normal. The pavement continued to crack and slump during 1982 and after another abnormally wet spring in 1983, it collapsed in early May 1983. Figure 2 shows a view, looking to the south, of the failed section of the embankment, as observed near Station 297 + 00 in May 1983. After the failure, the pavement for the two lanes dropped approximately 15 and 25 ft at the north and south ends, respectively.

At this location, I-15 is at an elevation of about 5,430 ft and ascends gradually toward Malad Summit (Elevation 5576). The highway is constructed of an 8-in. layer of continuously reinforced concrete pavement overlying a 4-in.-thick layer of cement-treated base over an embankment of silty clay fill. The embankment averages a height of approximately 45 ft and has slopes angled at 2:1 (horizontal:vertical). The northbound lanes are located on the highest part of the embankment.

S. Sharma, Department of Civil Engineering, University of Idaho, Moscow, Idaho 83843. T. Buu, Idaho Transportation Department, P.O. Box 7129, Boise, Idaho 83707.

Because both northbound lanes of this vital link between Salt Lake City and Pocatello were disrupted by the cracking in 1982, the Idaho Transportation Department quickly prepared a plan for the design of remedial works. To allow northbound travel, a temporary paved roadway was quickly constructed in the central median area. At the same time a site investigation was being performed to determine the cause of the cracking and slumping.

SITE INVESTIGATIONS

The site investigation program was started in August 1982. It consisted of 17 borings and shallow test pits and the initial installation of five slope indicators to monitor the behavior of the embankment. The location of the test borings and slope indicator locations is shown in the sketches presented in Figures 3 and 4. Additionally, to investigate ground movements, three survey lines were established to supplement the slope indicator data. There was also some concern about the stability of the entire area and therefore eight additional slope indicators were installed to monitor the movement of a much larger portion of the hillside.

As part of the site investigation program, six siphon wells were also installed upslope from the distressed embankment to lower the groundwater levels. Such siphons, consisting of PVC pipe inserted into a shallow boring, provide an effective and economic method to lower the groundwater level 10 to 15 ft as long as there is an adequate elevational drop. However, these siphons must be initially primed to start the flow of water and do require regular monitoring to ensure that the exit pipes are operating properly. In order to monitor the operation of the siphons, two observation wells (OW-1 and OW-2) were drilled, west of the southbound lanes. All other borings were also used as open standpipes for monitoring groundwater levels at the site.

SOIL CONDITIONS

The site investigations provided information concerning the subsoil profile and the groundwater conditions. Representative soil samples were also tested in the laboratory to determine typical strength and compressibility parameters.

Subsoils

The subsoil at the site consists of silty clay fill material and the 2- to 3-ft-thick sand layer from the original embankment

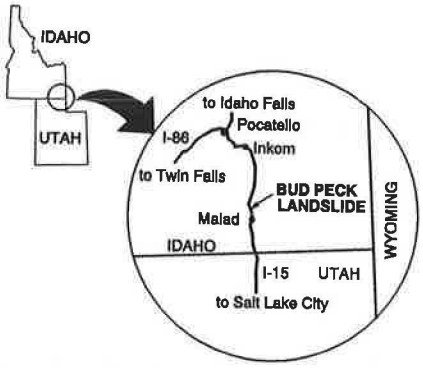

FIGURE 1 Site plan for Bud Peck slide, I-15, near Malad, Idaho.

FIGURE 2 View of failed embankment, near Station 297+00, May 1983.

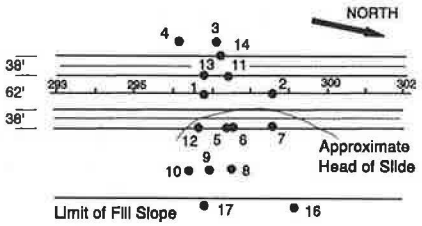

FIGURE 3 Location of test holes for site investigations.

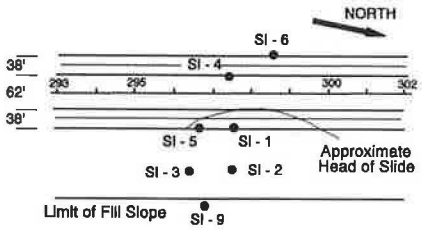

FIGURE 4 Location of slope indicators for site investigations.

overlying the natural clay soils as shown in Figure 5. The silty clay fill was used to construct the embankment in 1970 and had an approximate unit weight of 120 lb/ft^3 and estimated effective shear strength parameters of $\phi' = 25$ degrees and $c' = 0$.

The underlying natural material consists of weathered rhyolite that has decomposed to a gravelly clay residual soil near the surface. With increasing depth, these surface materials are less weathered and show consistent increases in strength and unit weights. The water content of the natural clayey soils in the upper 10 ft ranged between 27.7 and 32.4 percent. The Atterberg limits for the fine fraction of these soils generally ranged from 40 to 56 for the liquid limit, and the plasticity index varied between 22 and 33. Direct shear test revealed that the natural soils had the following range of shear strength parameters:

	ϕ' *(degrees)*	c' *(ksf)*
Peak strength	2–17	0.6–1.2
Residual strength	1–17	0.0–0.7

Groundwater Conditions

The groundwater measurements as expected, revealed the effects of the higher than normal precipitation. The groundwater levels measured at the end of September 1982, are shown in the subsurface profile shown in Figure 5. Some temporary artesian conditions were also encountered for wells in the sand blanket under the southbound lanes. This condition was probably due to the inability of the sand blanket to adequately drain the infiltrating water. Thus water backed up in the slope, and its presence was confirmed by the artesian conditions found at the end of September 1982.

Slope Indicator Data

For the locations shown in Figure 4, the slope indicator data for readings obtained during November 1982 are shown in Figures 6 and 7. The data for locations SI-1 and SI-5 at the crest of the slide (Figure 6) indicate the existence of a potential failure plane below the sand-fill blanket. It appears that there is considerable movement 50 to 60 ft below the surface, or 5 to 10 feet below the sand blanket. At location SI-1 and SI-5 movements of up to 2 in. were measured between November 17 and 26, 1982. The increasing rate of movement for SI-1 and SI-5, as shown in Figure 6, suggests that the slope mass was unstable and appeared to be moving rapidly. Supporting evidence regarding the location of the failure plane was also provided by the slope indicator data for SI-2 and SI-3, located near the toe of the embankment, as shown in Figure 7. Unfortunately, the observations made at slope indicator sites, SI-2 and SI-3, were small and generally inconsistent as the base of the slope indicator does not appear to have been anchored into a stable zone.

Two slope inclinometers, SI-4 and SI-6, were also installed to monitor movements below the southbound lanes. Data collected at these two locations are shown in Figures 8 and 9. The data from SI-4 (Figure 8) indicate small movements that suggest a sliding plane approximately 32 ft below the

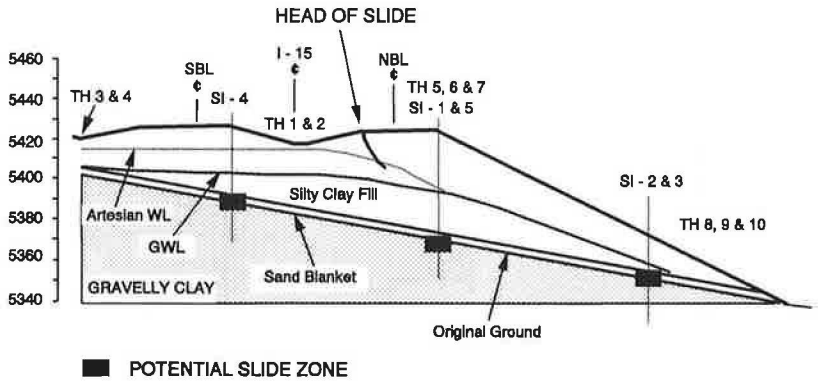

FIGURE 5 Subsoil profile at Station 297+00 (NBL = northbound lane; SBL = southbound lane; GWL = groundwater level; WL = water level; and TH = test hole).

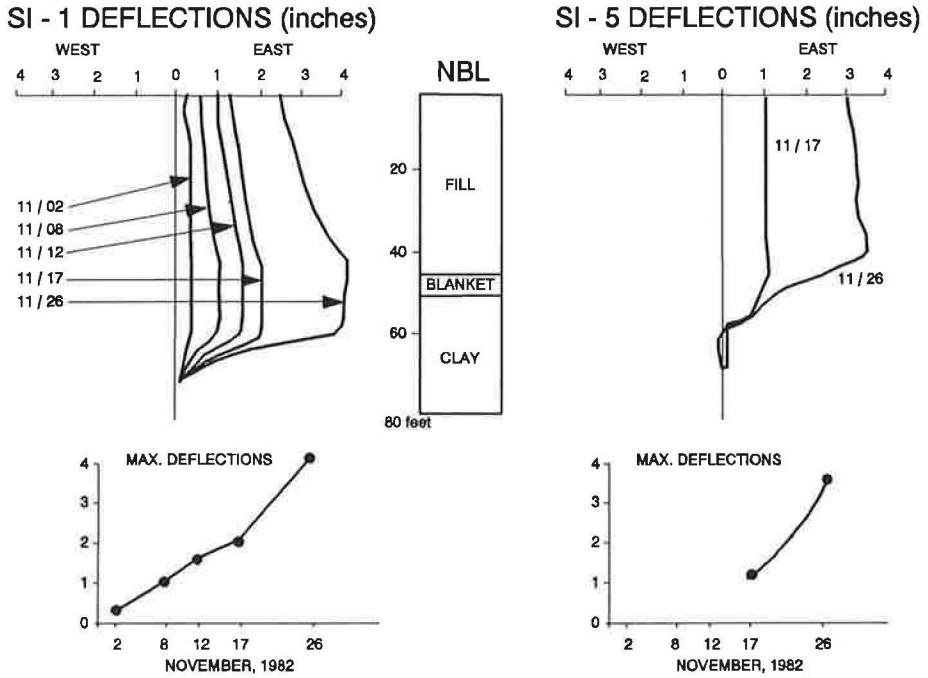

FIGURE 6 Slope indicator data for SI-1 and SI-5 at crest of embankment.

pavement surface. The data from SI-6 (Figure 9) indicated a movement of about 1.3 in. at the surface in early 1983, but the movement appeared to have stabilized after that initial slip. However, the actual movements at the slip plane are less than ½ in. because again, the slope indicators were not anchored in a stable zone. Overall, these movements were small and the southbound lanes were considered to be fairly stable.

The slope indicators were originally installed to monitor the movements of the highway embankment rather than the hillside slope. Unfortunately, the entire hillside slope was found to be actively moving, on the basis of the slope indicator data. This was confirmed by independent observations made using two survey lines. However, because a slip plane could be readily interpreted from the existing slope indicator data, additional slope indicators installed to a much greater depth were not used for studying the behavior of the hillside slope.

EMBANKMENT ANALYSIS

The stability of the embankment slope was investigated using the slope indicator and groundwater level data. With knowledge of the location of the slip plane and groundwater conditions, a limiting equilibrium analysis was used to find the failure mechanism and the residual shear strength along the potential failure plane. The results of the analysis are shown in Figure 10. By analyzing failure surfaces passing through the shear zone indicated by the slope indicator data, the shear strength parameters of the residual soil were back-calculated as $\phi' = 10.5$ degrees and $c' = 325$ psf for the critical surface shown in Figure 10. These parameters appear to be in reasonable agreement with the laboratory test results.

In reviewing the available data, it was apparent that the buildup of water within the embankment had led to exces-

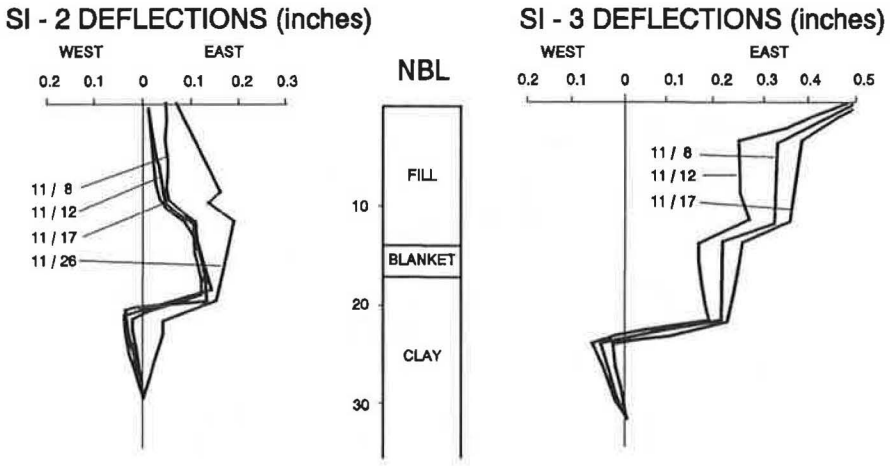

FIGURE 7 Slope indicator data for SI-2 and SI-3 at toe of embankment.

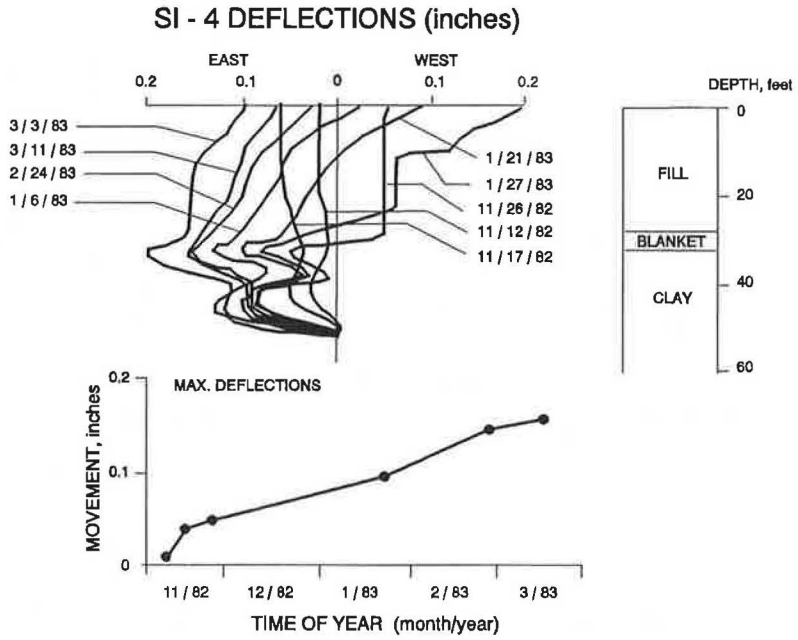

FIGURE 8 Slope indicator data for SI-4, southbound lane.

sively high pore water pressures that probably caused the failure. Thus, it was important that such high pore water pressures be reduced if the slope was to be effectively stabilized. The slope was found to have an adequate factor of safety (FS) against failure providing that the groundwater level could be maintained below the top of the underlying sand blanket. However, because the embankment also needed to be repaired, an additional increase in the FS of the newly constructed slope could be achieved using materials other than the displaced, original silty clay fill.

Two options were considered for repairing the failed embankment. The first option considered a granular-fill buttress at the toe of the existing embankment as shown in Figure 11. The second option required removal of the upper 20 ft of the existing, disturbed silty clay fill and restoration of the embankment to the original 2:1 slope with one of the following fill materials (a) sand and gravel, (b) pumice fill, and (c) wood fibers (Figure 12).

Stability calculations were performed for the three options, assuming that the groundwater level would be located in the sand blanket and strength parameters of $\phi' = 10.5$ degrees and $c' = 325$ psf for the underlying gravelly clay. The minimum FS for the buttress was estimated as 1.5. For the replacement fill alternatives, the following FS values were computed as

Material	ϕ' *(degrees)*	c' *(psf)*	*Compacted Unit Weight (pcf)*	*Factor of Safety*
Sand and gravel	39	0.0	130	1.14
Pumice	41	0.0	75	1.29
Wood fibers	37	0.0	55	1.35

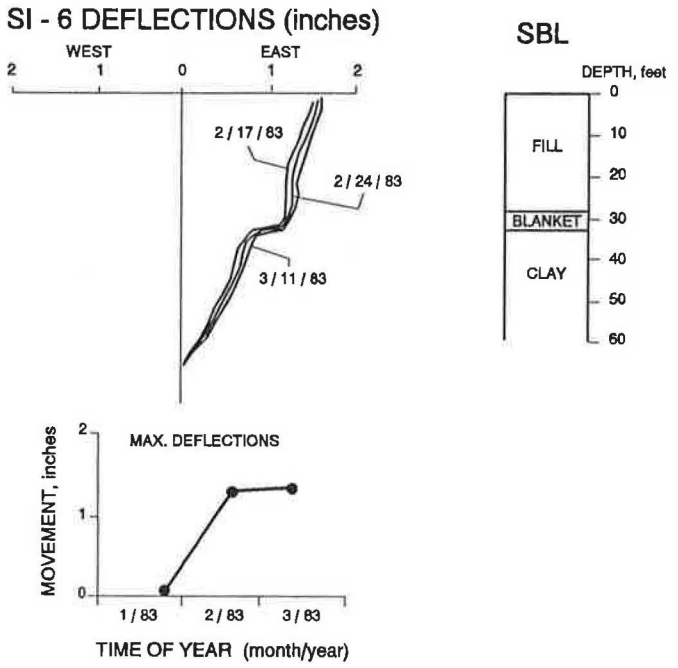

FIGURE 9 Slope indicator data for SI-6, southbound lane.

In reviewing the costs of construction, the buttress would have required at least 50 percent more material than the other alternatives, even though a higher FS would have been obtained for stability. However, after monitoring the site for about 12 months, there were signs that a much larger portion of the hillside was moving, perhaps because of a very deep seated failure plane. Thus the buttress option was discarded as a possible long-term solution in favor of extensive dewatering, to stabilize the hillside, and the use of a lightweight fill to repair the embankment. The lightweight fill would also have minimized the impact of an external load on a potential deep-seated failure surface.

In comparing the remaining options, the pumice fill was found to be the most desirable and could be readily obtained from a source 40 mi away. The strength of the compacted pumice at 95 percent of modified Proctor compaction was estimated as $\phi' = 41$ degrees from direct shear tests. The nearest source for the wood-fiber fill was about 60 mi from the site. However, the wood fibers would have required protection from water and air to avoid potential spontaneous combustion and decay. Also, concerns were expressed about the disposal of the slightly toxic and odorous leachate that would have drained from the wood-fiber fill. The sand and gravel fill would have been marginally cheaper, but the increased stability offered by the pumice fill was a deciding factor in the selection of the pumice for the restoration of the failed embankment.

Because the weight of pumice fill is considerably less than the original weight of the silty clay fill being replaced, the embankment was expected to experience negligible settle-

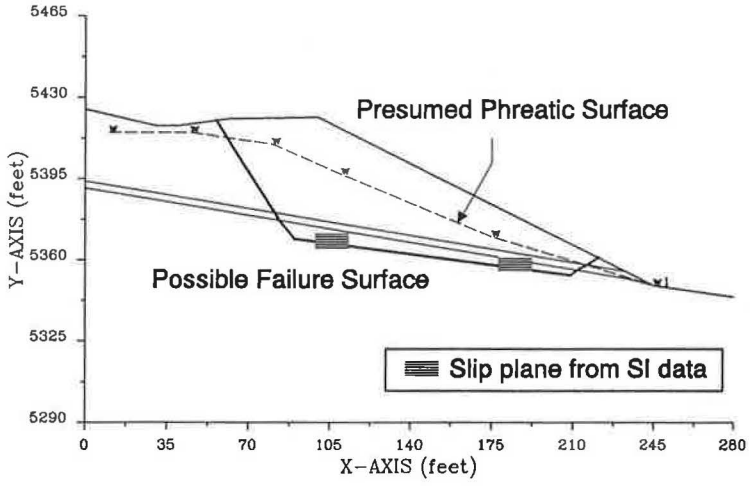

FIGURE 10 Potential failure surface for 1983 slide.

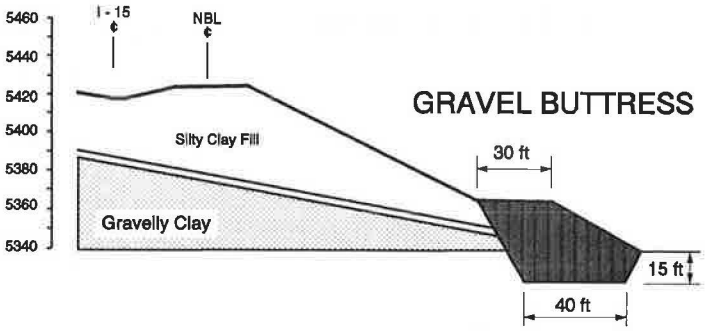

FIGURE 11 Repair of embankment with a granular buttress.

ments. Such settlements were expected to have occurred because of compaction of the pumice fill during construction.

CONSTRUCTION

The damaged embankment and northbound lanes were repaired between 1983 and 1985; work was done under two separate contracts. The initial contract concerned the dewatering of the affected embankment in order to prevent any further movement or failures. The second contract consisted of repairing the embankment and construction of the northbound lanes.

Horizontal Drains

The first contract was started in August 1983 and concentrated on dewatering the slope and embankment. This consisted of installing 42 horizontal drains from 4 separate pads near the toe of the embankment, as shown in Figure 13. Drainage was provided by slotted PVC pipe, 2 in. in inside diameter, laid at an approximate gradient of 5 percent in predrilled borings. The lengths of the drains ranged between 125 and 350 ft and were arranged to extensively penetrate the failed portion of the embankment. These drains were installed at a cost of $100,000.

Initial flows of about 200 gal/min quickly lowered the groundwater level approximately 20 ft below the southbound lanes to Elevation 5,388 ft. With groundwater levels at this depressed level, embankment movements were finally arrested as shown by the survey line data presented in Figure 14. These data clearly show the influence of the horizontal drainage in lowering the groundwater level at Observation Well OW-1 and the negligible movements measured from the two survey lines, SL-1 and SL-3.

Embankment

The embankment was repaired in the fall of 1985. The work consisted of removing the disturbed silty clay fill from the damaged embankment and replacing it with pumice. The slope was reconstructed to its original 2H:1V angle to match the adjacent surviving portions of the embankment. The pumice was placed in 8-in. lifts and compacted with a 12-ton single-drum vibratory roller to achieve a minimum 95 percent modified Proctor unit weight of 75 pcf at about 25 to 30 percent water content. The exposed slope was covered with a 12-in. layer of topsoil.

A considerable amount of water was exiting the embankment through the installed horizontal drains, so a French drain was constructed near the toe of the slope. This drain was intended to convey the exiting water away from the embankment and toward the natural drainage path of Devil Creek, about 750 ft to the east.

PERFORMANCE OF EMBANKMENT

The repaired embankment has performed satisfactorily since its reconstruction. The slope indicators and the groundwater observation wells are being monitored regularly. The slope indicators near the embankment have showed negligible

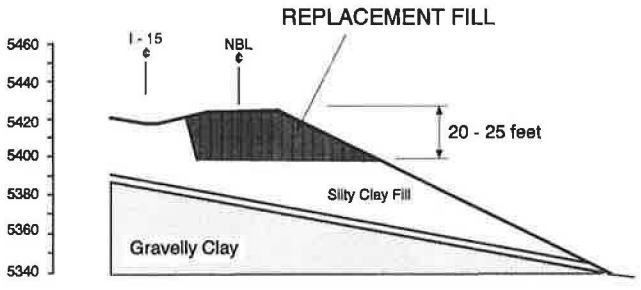

FIGURE 12 Repair of embankment with replacement fill.

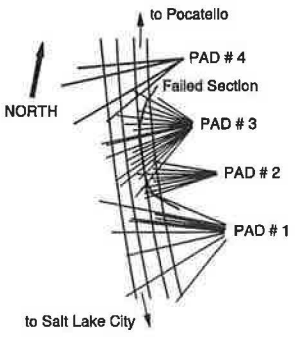

FIGURE 13 Location of horizontal drains.

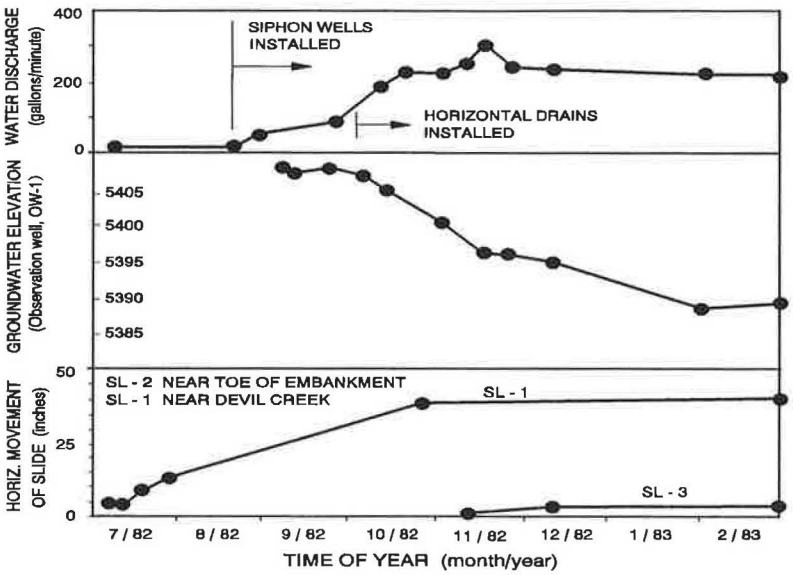

FIGURE 14 Slope monitoring data for seepage, groundwater levels, and movement.

movements, and the groundwater levels are currently at their lowest since 1983. However, some movement has been detected at slope indicators that were placed about 200 ft downslope (east) of the embankment. This movement is probably due to creep of the surficial soils over the entire hillside.

The seepage from the horizontal drains has been monitored to ensure proper operation. In September 1989, these drains were flowing at a rate of about 22 gal/min, which is considerably less than the 74 gal/min measured in April 1987 after the spring rains. The drains were cleaned and flushed in 1987 and 1988.

SUMMARY AND CONCLUSIONS

An embankment constructed in 1970 suffered a failure after two consecutive abnormally wet seasons in 1982 and 1983. The failure damaged a 500-ft section of the northbound lanes of I-15 near Malad, Idaho. Unfortunately, the 2- to 3-ft-thick sand blanket failed to discharge the large quantity of infiltrating groundwater, which resulted in a buildup of pore water pressures. In the opinion of the authors, this buildup of pore water pressures within the embankment was the primary cause of the failure.

While traffic was diverted over a temporary pavement installed in the central median, the slope was stabilized by dewatering in 1983 and final repairs were made to the embankment in 1985. The total cost for the installation of the horizontal drains and reconstruction of the damaged embankment was estimated at $770,000.

For future design and construction of silty clay embankments, the sand blanket should be designed as a positive drainage layer. This feature may be implemented by including slotted pipes within the sand blanket to provide a direct path for the flow of infiltrating groundwater. The relatively high permeability of the sand blanket cannot be relied on to prevent the buildup of high pore water pressures as encountered at the Bud Peck slide near Malad. Such a scheme can be specified at the construction stage for only a nominal increase in the overall costs. Also, a French drain should be used for all sideslope embankments to intercept groundwater flows above the embankment, thus limiting the chances of pore pressure buildup.

ACKNOWLEDGMENTS

This paper was made possible with the data collected and made available by the Idaho Transportation Department, Boise. Financial support for the preparation of this paper was provided by the University of Idaho, Moscow.

Publication of this paper sponsored by Study Committee on Landslides: Analysis and Control.